arXiv:0909.0354v1 [math.AG] 2 Sep 2009

The boundary of the Milnor fibre of a non–isolated hypersurface surface singularity

András Némethi

Ágnes Szilárd

Rényi Institute of Mathematics, Budapest, Reáltanoda u. 13–15, 1053, Hungary
E-mail address: `nemethi@renyi.hu`

Rényi Institute of Mathematics, Budapest, Reáltanoda u. 13–15, 1053, Hungary
E-mail address: `szilard@renyi.hu`

---

[0] The authors were partially supported by the EU grant Marie Curie TOK "BUDALGGEO"; Hungarian OTKA grants T049449, K61116; the first author by OTKA grant K67928; and both authors by NKTH-TÉT Austro-Hungarian, Spanish-Hungarian and French-Hungarian bilateral grants.

2000 *Mathematics Subject Classification.* Primary 32S25; Secondary 32S05, 32S22, 32S35, 32S40, 32S45, 32S55, 14J17, 14B05, 14P15, 57M27

Key words and phrases. Complex surface singularity, real singularities, non-isolated singularity, isolated complete intersection singularity, Milnor fiber, plumbed 3–manifolds, links of singularities, topological series of singularities, resolution, resolution graph, coverings of graphs, monodromy, vertical monodromy, characteristic polynomial, line arrangements, mixed Hodge structures

Abstract. Let $f:(\mathbb{C}^3,0)\to(\mathbb{C},0)$ be an analytic germ whose zero set has 1–dimensional singular locus. We develop an explicit procedure and algorithm that describes the boundary ∂F of the Milnor fibre of f as an oriented plumbed 3–manifold. The method provides the characteristic polynomial of the algebraic monodromy acting on $H_1(\partial F)$ as well. Moreover, for any analytic germ $g:(\mathbb{C}^3,0)\to(\mathbb{C},0)$ such that the pair (f,g) is an isolated complete intersection singularity, the (multiplicity system of the) open book decomposition of ∂F with binding $\partial F\cap\{g=0\}$ and pages determined by the argument of g is also computed. In order to do this, we have to establish crucial results regarding the horizontal and vertical monodromies of the transversal type singularities associated with the singular locus of f and of the ICIS (f,g).

The theory is supported by many examples. E.g. the case of homogeneous singularities (including the case of arrangements) is detailed completely. A list of especially peculiar examples, and also a list of related open problems is given.

The key starting point is the 'localization' of ∂F as the link of a *real* singular germ. Indeed, if (f,g) is an ICIS, k an even large integer, then ∂F coincides with the local link of the real analytic germ $\{f=|g|^k\}\subset(\mathbb{C}^3,0)$. Resolving this real singularity, the tubular neighbourhood of the exceptional set provides a plumbing representation.

In the case of 'composed singularities', the general method is compared and complemented by other geometric constructions as well.

Contents

Chapter I. Introduction 5
§ 1. Motivations, goals and results 5
§ 2. List of examples with special properties 9

Chapter II. Invariants of hypersurface singularities (preliminaries) 11
§ 3. The topology of a germ f 11
§ 4. The topology of a pair (f, g) 12

Chapter III. Plumbing graphs and their coverings (preliminaries) 15
§ 5. Plumbing graphs and oriented plumbed 3–manifolds. 15
§ 6. $\mathbb{Z}$–Coverings of graphs. 22

Chapter IV. The graph $\Gamma_{\mathcal{C}}$ of a pair (f, g) (preliminaries) 25
§ 7. The definition of the weighted graph $\Gamma_{\mathcal{C}}$ 25
§ 8. Properties of the graph $\Gamma_{\mathcal{C}}$. 28

Chapter V. Examples for $\Gamma_{\mathcal{C}}$ 33
§ 9. Singularities associated with plane curve singularities 33
§ 10. Homogeneous singularities 43
§ 11. Some sporadic cases 45

Chapter VI. Plumbing graphs from $\Gamma_{\mathcal{C}}$ 47
§ 12. The Main Algorithm 47
§ 13. Proof of the Main Algorithm 56
§ 14. The Collapsing Main Algorithm 65

Chapter VII. Homological properties of the monodromies. 73
§ 15. Vertical/horizontal monodromies. Generalities. 73
§ 16. Vertical/horizontal monodromies. Characters. 74

Chapter VIII. Homological invariants of ∂F and $\partial F \setminus V_g$ 83
§ 17. The characteristic polynomial of ∂F. Starting point. 83
§ 18. The ranks of $H_1(\partial F)$ and $H_1(\partial F \setminus V_g)$ via plumbing. 85
§ 19. The characteristic polynomial of ∂F via $P^{\#}$ and $P^{\#}_j$. 88
§ 20. The proof of the characteristic polynomial formulae. 92
§ 21. The mixed Hodge structure of $H_1(\partial F)$. 96

Chapter IX. The case of homogeneous singularities. 99
§ 22. The general case. 99
§ 23. Line arrangements. 110
§ 24. The weight filtration of the mixed Hodge structure. 112

Chapter X. More examples. 115
§ 25. Cylinders of plane curve singularities: $f = f'(x, y)$ 115
§ 26. f of type $zf'(x, y)$. 117
§ 27. The $T_{*,*,*}$–family. 119

§ 28. f of type $\tilde{f}(x^a y^b, z)$. Suspensions. 119

Chapter XI. Peculiar structures on ∂F. Open problems. 123
§ 29. Contact structures. Triple product. Resonance varieties 123
§ 30. Open Problems. 125

Bibliography 127

CHAPTER I

Introduction

§ 1. Motivations, goals and results

1.1. The origins of the present work go back to some milestones marking the birth of singularity theory (of complex dimension ≥ 2). They include the Thesis of Hirzebruch (1950) containing (among others) the (modern) theory of cyclic quotient singularities; the construction of Milnor in 1956 of the exotic 7–spheres (as plumbed manifolds associated with 'plumbing graphs'); Mumford's article about normal surface singularities [**39**] stressing for the first time the close relationship of the topology with the algebra; the treatment and classification of links of singularities by Hirzebruch and his students in the 60's (especially Brieskorn and Jänich, and later their students) based on famous results on classification of manifolds by Smale, Thom, Pontrjagin, Adams, Kervaire and Milnor, and the signature theorem of Hirzebruch. Since then, and since the appearance of the very influential book [**38**] of Milnor in 1968, the theory of normal surface singularities and isolated hypersurface singularities produced an enormous amount of significant results. In all of them, the link of an isolated singularity plays a central role.

In the presence of a smoothing, such as in the case of hypersurfaces, the link appears also as the boundary of the smoothing, the Milnor fiber. This interplay has enormous consequences: first, the link of a singularity is the boundary of an arbitrary small neighbourhood of the singular point, hence one can *localize* the link in *any arbitrarily small* representative. Hence, by resolving the singularity, the link appears as the boundary of a small tubular neighbourhood of the exceptional locus. In this way, e.g. for isolated surface singularities, one creates a bridge between the link and resolution: the resolution at topological level is codified in the resolution graph, which also serves as a plumbing graph for the link.

On the other hand, the same manifold is the boundary of the Milnor fiber, that 'nearby fiber' whose degeneration and monodromy measures the complexity of the singularity. This interplay between the two holomorphic fillings of the link, the resolution and the Milnor fiber, produces (perhaps) the nicest index–theoretical relations of hypersurface singularity theory (relations of Durfee [**21**] and Laufer [**29**] valid for hypersurfaces, generalizations of Looijenga, Wahl [**32, 73**], Seade [**58**] for more general smoothings, and culminating in deformation theory describing the miniversal deformation spaces in some cases).

Recently, the links of normal surface singularities, as special oriented 3–manifolds represented by negative definite plumbing graphs, started to have a significant role in low–dimensional topology as well: they not only provide crucial testing manifolds for the Seiberg–Witten, or Heegaard–Floer theory of 3–manifolds, and provide ground for surprising connections between these topological invariants and the algebraic/analytic invariants of the singularity germ (see e.g. [**45**] and [**46**] and the references therein), but they appear also as the outputs of natural topological classification results, as solutions of some universal topological properties — e.g. the rational singularities appear as L–spaces [**46**], i.e. 3–manifolds with vanishing reduced Heegaard–Floer homology. Similarly, the classification of symplectic fillings (or more particularly, the classification of rational ball fillings) of some 3–manifolds find their natural foreground in some singularity links, see [**47**] and [**68**] (and references therein).

1.2. Although the literature of isolated singularities is huge, surprisingly, the literature of non–isolated singularities, even the non–isolated hypersurface singularities, is rather restrictive. One of the main difficulties is generated by the fact that in this case the link is not smooth. On the other hand, the boundary of the Milnor fiber is smooth, but (till now) there was no construction which would guarantee that it also appears as the boundary (of any arbitrary small representative) of an isolated singular germ. Lacking such a result, it is hard to prove in a conceptual way that this manifold is a plumbed manifold, even in the case of surfaces.

The present work aims to fill in this existing gap: we provide a general procedure that may be used to attack and treat non–isolated hypersurface singularities. Although the whole presentation is for surface singularities, some results can definitely be extended to arbitrary dimensions too.

More precisely, some of the conceptual results of the present work are the following. Below $f:(\mathbb{C}^3,0)\to(\mathbb{C},0)$ is a hypersurface singularity with 1–dimensional singular locus Σ. Its zero set $\{f=0\}$ is denoted by V_f, and its Milnor fiber by F. Its oriented boundary ∂F is a connected oriented 3–manifold.

(1) The oriented 3–manifold has a plumbing representation. In fact, we not only prove this result, but we provide a concrete algorithm for the construction of the plumbing graph: given any germ f, anyone (with some experience in blowing ups, resolutions and involved equations) is able to determine the graph after some work. (For the algorithm, see § 12.) The output graphs, in general, are not irreducible, are not negative definite (see also some other peculiarities below), hence in their discussion the usual calculus (blowing up and down (-1)–rational curves) is not enough. In our graph–manipulations we will use the calculus of oriented 3–manifolds as it is described in Neumann's foundational article [**49**] (in fact, we will restrict ourself to a 'reduced class of graph–operations'). (The corresponding background material and preliminary discussions are presented in § 5.)

The fact that the boundary of the Milnor fiber is plumbed was announced by F. Michel and A. Pichon in [**33, 34**], and examples were provided in [**33, 35**] obtaining certain lens spaces and Seifert manifolds. The present work however uses a completely new different line of arguments to prove the existence of the plumbing representation. In addition, it is also completely new in the respect that we find the plumbing graph for arbitrary germs (even for which ad hoc methods are not available), and it points out for the first time in the literature that for these boundary manifolds one needs to use 'extended', general plumbing graphs — where the edges might have negative weights as well. Such graphs were not used in complex algebraic geometry before. The sign decorations of edges are irrelevant for trees, but are crucial in the presence of cycles in the plumbing graph, as it is shown in many examples in this work.

(2) Recall that for any germ $g:(\mathbb{C}^3,0)\to(\mathbb{C},0)$ such that the pair (f,g) forms an ICIS (isolated complete intersection singularity), by a result of Caubel [**10**], g determines an open book decomposition on ∂F (similarly as the classical Milnor fibration is cut out by the argument of g). Our method, for any such g, codifies (the 'multiplicity system' of) this open book decomposition in the plumbing graph (for definitions, see (5.1.3)).

(3) The boundary ∂F consists of two parts (a fact already proved by D. Siersma [**61, 60**] and used by F. Michel, A. Pichon and C. Weber in

[**33, 34, 35**] too): the first, $\partial_1 F$, is the link of the normalization of V_f (having inside it the 1–dimensional link–components cut out by the strict transforms of Σ). The second one, $\partial_2 F$, can be recovered from the (embedded resolution graphs of the) transversal plane curve singularity types of Σ together with the corresponding horizontal/vertical monodromy actions of them. Already determining these two independent pieces can be a non–trivial task, but the identification of their gluing can be incomparably harder. The present work clarifies this gluing completely (in fact, resolves it so automatically, that if one does not look for the phenomenon deliberately, one will not even see it).

We emphasize that both parts $\partial_1 F$ and $\partial_2 F$ can be represented by plumbing graphs with (only) positive edges, but their gluing, in general, *can not*. (In general, certain parts of the graph behave as 'usual graphs of complex algebraic geometry' but with opposite orientation. This fact is explained by the *real analytic* origin of the plumbing representation, see the next subsection (1.3).)

(4) The monodromy action on ∂F, in general, is not trivial. In fact, its restriction to the piece $\partial_1 F$ is trivial, but on $\partial_2 F$ can be rather involved. In order to understand $\partial_2 F$ we need the *vertical* monodromies of the transversal singularity types, and, in fact, via the Wang exact sequence, we need their Jordan block structure corresponding to eigenvalue one; on the other hand, the monodromy action on $\partial_2 F$ is induced by the *horizontal* monodromy of the transversal singularity types. In the body of the paper we determine these actions, and as a by–product, the homology of ∂F and the characteristic polynomial of the algebraic monodromy action on $H_1(\partial F)$ too (under certain assumptions).

1.3. The main algorithm is based on a special construction: we will take an arbitrary germ $g : (\mathbb{C}^3, 0) \to (\mathbb{C}, 0)$ such that $\Phi = (f, g)$ forms an ICIS. The topology of such a map is described in Looijenga's book [**31**], and it will be used intensively. We recall the necessary material in § 4.

In general, Φ provides a powerful tool to analyse the germ f or its g–polar properties. Usually, for an arbitrary germ f with 1–dimensional singular locus, one takes a plane curve singularity $P : (\mathbb{C}^2, 0) \to (\mathbb{C}, 0)$ and considers the composed function $P \circ \Phi$, which can be thought of as an approximation of f by isolated singularities. E.g., if $P(c, d) = c + d^k$, then $P \circ \Phi = f + g^k$ is one of the most studied test series, the Iomdin series of f associated with g.

If one wishes to understand the geometry of $P \circ \Phi$, e.g, its Milnor fiber, then one needs to analyse all the intersections of $\{P = \delta\}$ with the discriminant Δ of Φ, and one has to understand the whole monodromy representation of Φ (over the complement of Δ) — a very difficult task, in general. On the other hand, if one wishes to determine some 'correction terms' 'only'(e.g. $i(f) - i(f + g^k)$ for an invariant i), it is enough to study Φ only above the neighbourhood of the link of the distinguished discriminant component $\Delta_1 := \Phi(V_f)$.

This fact has been exploited in many different levels, and for several invariants, see e.g. the articles of Lê and Teissier initiating and developing the 'theory of discriminants' [**36, 37, 71**]; the article of Siersma [**62**] about the zeta function of the Iomdin series, or its generalizations by the first author, cf. [**41**] and the references therein.

Using this principle, in [**48**] we determined the *links* of members of the Iomdin series, i.e. the links of isolated singularities $f + g^k$ (where $k \gg 0$). In that work the key new ingredient was the construction of a special graph $\Gamma_{\mathcal{C}}$, dual to a curve configuration $\mathcal{C}$ in an embedded resolution of $V_{fg} \subset \mathbb{C}^3$ localized above a 'wedge neighbourhood' of Δ_1 (for the terminology and more comments see (8.5) as well).

The point is that the very same graph $\Gamma_{\mathcal{C}}$ not only contains all the information necessary to determine the links of the Iomdin series (and the correction terms $i(f) - i(f + g^k)$ for several invariants i), but it is the right object to determine ∂F as well.

The bridge that connects ∂F with the previous discussion (about series and discriminant of the ICIS (f, g)) is realized by the following fact. Let k be a sufficiently large even integer. Consider the local *real* analytic germ

$$\{f = |g|^k\} \subset (\mathbb{C}^3, 0).$$

Then its link (intersection with an arbitrary small sphere) is a smooth oriented 3–manifold, independent of the choice of k (for large k), which, most importantly, *is diffeomorphic with* ∂F (cf. § 13). In particular, it means that ∂F can be 'localized': it appears as the boundary of an arbitrary small neighbourhood of an analytic germ! But, in this (non–isolated) case, the corresponding space–germ is not complex, but real analytic.

As a consequence, after resolving this real analytic singularity, the tubular neighbourhood of the exceptional set provides a plumbing representation G of ∂F. The point is that the graph $\Gamma_{\mathcal{C}}$ (introduced in [**48**]) codifies all the necessary information to recover the topology of the resolution and of the plumbing: the plumbing graph G of ∂F appears as a 'graph covering' of $\Gamma_{\mathcal{C}}$. The Main Algorithm (cf. § 12) provides a pure combinatorial description of G derived from $\Gamma_{\mathcal{C}}$. (The abstract theory of coverings of graphs, developed in [**44**], is reviewed in § 6.)

The method emphasizes the importance of real analytic germs, and their necessity even in the study of complex geometry.

In Chapters VII and VIII we determine several related homological invariants from $\Gamma_{\mathcal{C}}$ (characteristic polynomials of horizontal/vertical monodromies, Jordan block structure, cf. below). In fact, we believe that $\Gamma_{\mathcal{C}}$ contains even more information than what was exploited in [**48**] or here, which can be the subject of future research. On the other hand, finding the graphs $\Gamma_{\mathcal{C}}$ can sometimes be a serious job. Therefore, we decided to provide examples for $\Gamma_{\mathcal{C}}$ in abundance in order to help the reader to understand the present work, and support possible future research as well.

Different embedded resolutions might produce different graphs $\Gamma_{\mathcal{C}}$, hence readers with more experience in resolutions might find even simpler graphs in some cases. Each $\Gamma_{\mathcal{C}}$ can equally be used for the theory worked out.

1.4. The above presentation already suggests that the geometry of Φ near Δ_1 is reflected in the topology of ∂F as well. Technically, this is described in the commuting actions of the horizontal and vertical monodromies on the fiber of Φ. Similarly, one can consider the horizontal/vertical monodromies of the local transversal types of Σ. The determination of these two pairs of representations is an important task (independently of the identification of ∂F), and it is crucial in many constructions about non-isolated singularities. We wish to stress that our method provides (besides the result regarding ∂F) a uniform discussion of these monodromy representations, provides a clear procedure how one can determine them (with precise closed formulas for the corresponding characters or characteristic polynomials). Moreover, we determine even the Jordan block structures in those cases which are needed for the homology of ∂F and its algebraic monodromy.

1.5. The material of the present work can be grouped into three parts. The first part (Chapters II, III, IV) contains results regarding the ICIS Φ and the graph $\Gamma_{\mathcal{C}}$ read from a resolution. The second one (Chapters VI, VII, VIII) contains the description of ∂F, its invariants, and establishes the main connections with other geometrical objects.

Finally, scattered throughout the text, there are many examples.

Any example is given in two steps: one has to first determine the graph $\Gamma_{\mathcal{C}}$, a more or less independent task. (This can be done in many different ways using one's preferred resolution tricks. Nevertheless, in most of the cases, it is not a trivial procedure, except special cases such as cylinders of composed germs.) Then, in the second step, we run the Main Algorithm to get the plumbing graph of ∂F or its monodromy (or the open book decomposition of g living on ∂F).

Our examples test and illustrate the theory, emphasizing the new aspects: the obtained graphs are not the usual negative definite graphs provided by resolutions of normal surface singularities, not even the dual graphs of complex curve configurations of a complex surface (where the intersections of curves are always positive). They contain pieces with 'opposite' orientation, so vertices can be connected by negative–edges (representing intersection of curves intersecting negatively). (They appear as follows: in the resolution of the real singularity $\{f = |g|^k\}$, some singularities are *orientation reversing* equivalent with complex Hirzebruch-Jung singularities; hence the corresponding Hirzebruch strings should be sewed in the final graph with opposite orientation.)

In Chapter X, for certain families (basically, for 'composed singularities') we also provide alternative, topological constructions of ∂F.

1.6. The titles of the chapters and sections already listed in the Contents (preceding this Introduction) were chosen so as that they would guide the reader easily through the sections.

1.7. Most of the theoretical results of the present work were obtained in 2004–2005; the Main Algorithm was presented at the Singularity Conference at Leuven, 2005. Since that time we added several examples and completed the theoretical part.

The authors are grateful to A. Parusinski for his advices regarding § 13.

§ 2. List of examples with special properties

In order to arouse the curiosity of the reader, and to exemplify the variety of 3–manifolds obtained as ∂F, we list some peculiar examples. (They are extracted from the body of the work where a lot more examples are found.)

In the sequel $\approx$ means orientation preserving diffeomorphism. $-\partial F$ is ∂F with opposite orientation.

2.1. For certain choices of f, the boundary ∂F might have one of the following peculiar properties:

2.1.1. ∂F cannot be represented by a negative definite plumbing, but $-\partial F$ admits such a representation (see e.g. example (12.5.12)).

2.1.2. Neither ∂F, nor $-\partial F$ can be represented by a negative definite plumbing (see e.g. (22.9)(4a)).

2.1.3. Although ∂F can be represented by a negative definite graph, it is not diffeomorphic with the link of the normalization of V_f. (Such examples can be realized even when ∂F is not a lens space, see e.g. examples (22.10)(e-f)).

2.1.4. In all examples, ∂F is not orientation preserving diffeomorphic with the link of the normalization of V_f (evidently, provided that $\Sigma \neq \{0\}$); a fact already noticed in [**33**].

2.1.5. There are examples when ∂F is orientation *reversing* diffeomorphic with the link of the normalization of V_f, see e.g. (22.10)(d).

2.1.6. There are examples when $\partial F \approx -\partial F$, even when ∂F is not a lens space, cf. (26.1.3).

2.1.7. It may happen that ∂F fibers over S^1, (even with $rank\, H_1(\partial F)$ large), cf. (26.1).

2.1.8. ∂F might be non–irreducible, cf. (25.1.7).

2.1.9. Any S^1–bundles with non–negative Euler number over any oriented surface can be realized as ∂F, cf. (28.1) and (23.2.4).

2.1.10. The monodromy on ∂F, in general, is not trivial, the algebraic monodromy might even have Jordan blocks of size two, cf. (25.2).

2.1.11. There exist pairs of singularity germs with diffeomorphic ∂F but different characteristic polynomials, and/or different (mixed Hodge) weight filtrations on $H_1(\partial F)$, and/or different multiplicites, cf. (24.1.2).

CHAPTER II

Invariants of hypersurface singularities (preliminaries)

§ 3. The topology of a germ f

3.1. The link and the Milnor fiber. Let $f : (\mathbb{C}^3, 0) \to (\mathbb{C}, 0)$ be the germ of an analytic function and set $(V_f, 0) = (f^{-1}(0), 0)$. Assume that its singular locus $(Sing(V_f), 0)$ is 1–dimensional, denote it by $(\Sigma, 0)$ and write $\Sigma = \cup_{j=1}^{s} \Sigma_j$ for its irreducible decomposition. Let $K := V_f \cap S^5_\epsilon$ be the *link* of $(V_f, 0)$ (with $0 < \epsilon \ll 1$). Under the above assumption K is singular too: its singular part is $L = \cup_j L_j$, where $L_j := K \cap \Sigma_j$.

Let $F_{\epsilon,\delta} := B_\epsilon \cap f^{-1}(\delta)$ be the Milnor fiber of f in a small closed Milnor ball B_ϵ (where $0 < \delta \ll \epsilon$). Sometimes, when ϵ and δ are irrelevant, it will be simply denoted by F.

The family $\{F_{\epsilon, e^{i\alpha}\delta}\}_{\alpha \in [0,2\pi]}$ is a locally trivial fibration (the so-called Milnor fibration, see [**38**]), whose monodromy (well defined up to an isotopy) is called the Milnor geometric monodromy of $F_{\epsilon,\delta}$. It induces a Milnor geometric monodromy action on the boundary $\partial F_{\epsilon,\delta}$ too (which is trivial if $\Sigma = \emptyset$, otherwise might be not).

For more details regarding this subsection, see [**38**].

3.2. Transversal type singularities. For any fixed $j \in \{1, \dots, s\}$, let $T\Sigma_j$ be the transversal singularity type of Σ_j; i.e. the equi–singularity type of the plane curve singularity $f|_{S_x} : (S_x, x) \to (\mathbb{C}, 0)$, where $x \in \Sigma_j \setminus \{0\}$, and (S_x, x) is a transversal smooth 2–dimensional slice-germ of Σ_j at x. Its Milnor fiber $(f|_{S_x})^{-1}(\delta) \subset S_x$ is independent of x and δ (for δ small), and it will be denoted by F'_j. The monodromy diffeomorphism of F'_j, induced by the family $[0, 2\pi] \ni \alpha \mapsto (f|_{S_x})^{-1}(\delta e^{i\alpha})$, is called the *horizontal monodromy of* F'_j, and is denoted by $m'_{j,hor}$. The diffeomorphism induced by the family $s \mapsto (f|_{S_{x(s)}})^{-1}(\delta)$, above an oriented simple loop $s \mapsto x(s) \in \Sigma_j \setminus \{0\}$, which generates $\pi_1(\Sigma_j \setminus \{0\}) = \mathbb{Z}$ (and with δ small and fixed), is called the *vertical monodromy*. It is denoted by $m'_{j,ver}$. Both monodromies are well-defined up to isotopy, and they commute (up to an isotopy).

3.3. The boundary of the Milnor fiber. Let ∂F denote the boundary of the Milnor fiber F of f, i.e. $\partial F = \partial F_{\epsilon,\delta} = S^5_\epsilon \cap f^{-1}(\delta)$. It is a connected and oriented 3-manifold, cf. [**38**]. By [**61**], it has a natural decomposition $\partial F = \partial_1 F \cup \partial_2 F$. Indeed, let $T(L_j)$ be a small closed tubular neighbourhood of L_j in S^5_ϵ, and denote by $T^\circ(L_j)$ its interior. Then $\partial_2 F = \cup_j \partial_{2,j} F$ with $\partial_{2,j} F = \partial F \cap T(L_j)$, and $\partial_1 F = \partial F \setminus \cup_j T^\circ(L_j)$. $\partial_1 F$ and $\partial_2 F$ are glued together along their boundaries, which is a union of tori. (For more details, see [**61**].)

Proposition 3.3.1. [**61**]

(1) For each j, the natural projection $T(L_j) \to L_j$ induces a locally trivial fibration of $\partial_{2,j} F$ over L_j with fiber F'_j (the Milnor fiber of $T\Sigma_j$) and monodromy $m'_{j,ver}$ of F'_j. This induces a fibration of $\partial(\partial_{2,j} F)$ over L_j with fiber $\partial F'_j$.

(2) *The Milnor monodromy of ∂F can be chosen in such a way that it preserves both $\partial_1 F$ and $\partial_2 F$. Moreover, its restriction on $\partial_1 F$ is trivial, and also on the gluing tori $\partial(\partial_1 F) = - \cup_j \partial(\partial_{2,j} F)$.*

(3) *The Milnor monodromy on $\partial_2 F$ might be nontrivial. This monodromy action on each $\partial_{2,j} F$ is induced by the horizontal monodromy $m'_{j,hor}$ acting on F'_j. (Since it commutes with $m'_{j,ver}$, it induces an action on the total space $\partial_{2,j} F$ of the bundle.)*

Notice that by (3.3.1)(1), since F'_j is connected, $\partial_{2,j} F$ is connected too.

REMARK 3.3.2. One has the following relationship connecting the boundary ∂F and the link K. Definitely, K has a similar decomposition $K = K_1 \cup K_2$, where $K_2 = \cup_j K_{2,j}$, $K_{2,j} := T(L_j) \cap K$, and $K_1 := K \setminus \cup_j T^\circ(L_j)$. Then $K_1 = \partial_1 F$, hence $\partial K_1 = \partial(\partial_1 F)$ as well. On the other hand, each $K_{2,j}$ has the homotopy type of L_j.

§ 4. The topology of a pair (f, g)

4.1. The ICIS–invariants. In many cases it is convenient to add to the germ f another one, say g, such that the pair (f, g) forms an *isolated complete intersection singularity* (ICIS in short). Traditionally, one studies in this way the *g−polar geometry* of f, or computes by induction on the dimension certain invariants of f. g might also serve as an auxiliary object in order to determine abstract g−independent invariants of f: in the present situation, we will describe ∂F with the help of (f, g).

For simplicity, we denote the ICIS $(f, g) : (\mathbb{C}^3, 0) \to (\mathbb{C}^2, 0)$ by Φ, and we fix a good representative as in [**31**]. More precisely, we consider a closed ball B_ϵ with sufficiently small radius ϵ around the origin of $\mathbb{C}^3$, and we assume that $\Phi : B_\epsilon \cap \Phi^{-1}(D^2_\eta) \to D^2_\eta$ is a locally trivial fibration with fiber F_Φ over the complement of the discriminant Δ_Φ of Φ (defined in a sufficiently small closed disc D^2_η around the origin), and Φ induces on $S^5_\epsilon \cap \Phi^{-1}(D^2_\eta)$ a trivial fibration with fiber ∂F_Φ above D^2_η.

We will denote the coordinates of $(\mathbb{C}^2, 0)$ by (c, d), hence $c \circ \Phi = f$. Obviously, Φ projects Σ onto $\{c = 0\}$, hence $\Delta_1 := \{c = 0\}$ is one of the components of Δ_Φ. We define d_j as the degree of the (finite) map $g|\Sigma_j : \Sigma_j \to \Delta_1$ $(1 \leq j \leq s)$.

For any fixed c_0, set $D_{c_0} := \{c = c_0\} \cap D^2_\eta$. Then, if $|c_0| \ll \eta$, the circle ∂D_{c_0} is disjoint from Δ_Φ. Consider the torus $T_\delta := \cup_{c_0} \partial D_{c_0}$, where the union is over c_0 with $|c_0| = \delta$. Hence, for $\delta \ll \eta$, the restriction of Φ on $\Phi^{-1}(T_\delta)$ is a fiber bundle with fiber F_Φ.

The monodromy above a circle in T_δ, consisting of points with fixed d–coordinates, is called the *horizontal monodromy* of Φ near Δ_1, and is denoted by $m_{\Phi,hor}$. Similarly, the monodromy above a circle in T_δ, consisting of points with fixed c–coordinates, (e.g., above ∂D_δ) is the *vertical monodromy* of Φ near Δ_1, denoted by $m_{\Phi,ver}$.

REMARK 4.1.1. Set $(V_g, 0) := g^{-1}(0)$ in $(\mathbb{C}^3, 0)$. Clearly, $F_{\epsilon,\delta}$ and $\Phi^{-1}(D_\delta)$ can be identified (after smoothing the boundary of the second one, which is a manifold with 'corners'). Under this identification, $F_{\epsilon,\delta} \cap V_g$ corresponds to $\Phi^{-1}(\delta, 0)$. Hence $\partial F_{\epsilon,\delta}$ and $\partial\Phi^{-1}(D_\delta)$ can also be identified in such a way that $\partial F_{\epsilon,\delta} \cap V_g$ corresponds to $\partial\Phi^{-1}(\delta, 0)$. Notice that $\partial\Phi^{-1}(D_\delta)$ consists of two parts, one of them being $\Phi^{-1}(\partial D_\delta)$, the other is the complement of its interior, defined as

$$\partial'\Phi^{-1}(D_\delta) := \cup_{(\delta,d) \in D_\delta} \partial(\Phi^{-1}(\delta, d)).$$

By (local) triviality over D_δ, $\partial'\Phi^{-1}(D_\delta)$ is diffeomorphic to the product $D_\delta \times \partial\Phi^{-1}(\delta, 0)$.

4.2. The open book decomposition of $\partial F_{\epsilon,\delta}$ with binding V_g induced by $g/|g|$. Besides the geometry of the ICIS, the germ g also provides a different package of invariants via the *generalized Milnor fibration* induced by $\arg(g)=g/|g|$ on ∂F. Indeed, with the above notations one has:

PROPOSITION 4.2.1. [**10**] *The argument of the restriction of g on $\partial F_{\epsilon,\delta}\setminus V_g$ defines an open book decomposition on $\partial F_{\epsilon,\delta}$ with binding V_g. The fibration $g/|g|:\partial F_{\epsilon,\delta}\setminus V_g\to S^1$ is equivalent to the fibration $\Phi:\Phi^{-1}(\partial D_\delta)\to\partial D_\delta$ with monodromy $m_{\Phi,ver}$.*

Moreover, this structure is compatible with the action of the Milnor monodromy on $\partial F_{\epsilon,\delta}$. Indeed, the restriction of the Milnor monodromy of $\partial F_{\epsilon,\delta}$ on a tubular neighbourhood of $\partial F_{\epsilon,\delta}\cap V_g$ is trivial, and its restriction on $\partial F_{\epsilon,\delta}\setminus V_g$ is equivalent with the horizontal monodromy of $\Phi^{-1}(\partial D_\delta)$ over the oriented circle $\{|c|=\delta\}$ (induced by the local trivial family $\{\Phi^{-1}(\partial D_c)\}_{|c|=\delta}$).

PROOF. The first sentence is stated and proved in Proposition 3.4 of [**10**]. Although the second sentence is not stated in [loc.cit.], it follows from the proof of Proposition 3.4. and by similar arguments as Theorem 5.11 of Milnor in [**38**]. The last monodromy statement is proved in the same way. □

4.3. The decomposition of ∂F. Next, we present how one can recover the decomposition $\partial F_{\epsilon,\delta}=\partial_1 F\cup\partial_2 F$, cf. (3.3), from the structure of Φ via the identification of $F_{\epsilon,\delta}$ with $\Phi^{-1}(D_\delta)$, cf. (4.1.1).

For any $j\in\{1,\dots,s\}$, let T_j^ϕ be a small closed tubular neighbourhood in $\mathbb{C}^3$ of $\Phi^{-1}(\partial D_0)\cap\Sigma_j$. Then, for δ sufficiently small, for any $(\delta,d)\in\partial D_\delta$, the fiber $\Phi^{-1}(\delta,d)$ intersects ∂T_j^ϕ transversally. In particular, $\Phi^{-1}(\partial D_\delta)\cap T_j^\phi$ and $\Phi^{-1}(\partial D_\delta)\setminus(\cup_j T_j^\phi)$ are fiber bundles over ∂D_δ.

PROPOSITION 4.3.1. *One has the following facts:*

1. *There is a (orientation preserving) homeomorphism from $\partial F_{\epsilon,\delta}$ to $\Phi^{-1}(\partial D_\delta)\cup\partial'\Phi^{-1}(D_\delta)$ which sends a tubular neighbourhood $T(V_g)$ of V_g onto $\partial'\Phi^{-1}(D_\delta)$ and $\partial F_{\epsilon,\delta}\setminus T^\circ(V_g)$ onto $\Phi^{-1}(\partial D_\delta)$ (identifying even their fiber structures, cf. (4.2.1)). Under this identification, $T(V_g)\subset\partial_1 F_{\epsilon,\delta}$, and the fibration $g/|g|:\partial_1 F_{\epsilon,\delta}\setminus T^\circ(V_g)\to S^1$ corresponds to $\Phi:\Phi^{-1}(\partial D_\delta)\setminus(\cup_j T_j^{\phi,\circ})\to\partial D_\delta$, while $g/|g|:\partial_{2,j}F_{\epsilon,\delta}\to S^1$ to $\Phi:\Phi^{-1}(\partial D_\delta)\cap T_j^\phi\to\partial D_\delta$.*

   The identifications are compatible with the action of the Milnor/horizontal monodromies (over the circle $|c|=\delta$).
2. *For each $j\in\{1,\dots,s\}$, the fibration $g/|g|:\partial_{2,j}F_{\epsilon,\delta}\to S^1$ can be identified with the pullback of the fibration $\partial_{2,j}F_{\epsilon,\delta}\to L_j$ (cf. (3.3.1)) under the map $\arg(g|L_j):L_j\to S^1$ (which is a regular cyclic covering of S^1 of degree d_j). Therefore, the fiber of $g/|g|:\partial_{2,j}F_{\epsilon,\delta}\to S^1$ is a disjoint union of d_j copies of F'_j and the monodromy of this fibration is*

   $$m^\Phi_{j,ver}(x_1,\dots,x_{d_j})=(m'_{j,ver}(x_{d_j}),x_1,\dots,x_{d_j-1}).$$

   The action of the Milnor monodromy on $\partial_{2,j}F_{\epsilon,\delta}$ restricted to the fiber of $g/|g|$ is the 'diagonal' action:

   $$m^\Phi_{j,hor}(x_1,\dots,x_{d_j})=(m'_{j,hor}(x_1),\dots,m'_{j,hor}(x_{d_j})).$$

PROOF. The first part follows by combining arguments of [**38**] and [**10**] again, as in the second part of (4.2.1). The point is that when we 'push out' $\Phi^{-1}(\partial D_\delta)$ along the level sets of $\arg(g)$ into $\partial F_{\epsilon,\delta}$, this can be done by a vector field which preserves a tubular neighbourhood of each Σ_j. The second part is standard, it reflects the fiber structure of Φ, see e.g. [**41**] or [**62**]. □

Above, by (4.2.1) and by the structure of open books, the fibrations $\partial F_{\epsilon,\delta}\setminus V_g$ and $\partial F_{\epsilon,\delta}\setminus T^\circ(V_g)$ over S^1 (and induced by $g/|g|$) are equivalent. A similar fact is true for the fibrations $\partial_1 F_{\epsilon,\delta}\setminus V_g$ and $\partial_1 F_{\epsilon,\delta}\setminus T^\circ(V_g)$.

4.4. Relation with the normalization. The space $\partial_1 F$ and fibration $g/|g|:\partial_1 F_{\epsilon,\delta}\setminus V_g\to S^1$ have another 'incarnation' as well.

In order to see this, let $n:(V_f^{norm},n^{-1}(0))\to(V_f,0)$ be the normalization of $(V_f,0)$. Notice that each local irreducible component of $(V_f,0)$ lifts to a connected component of the normalization, hence $(V_f^{norm},n^{-1}(0))$ stands here for a multi-germ of normal surface singularities. Consider the lifting $g\circ n:(V_f^{norm},n^{-1}(0))\to(\mathbb{C},0)$ of g, which determines on the boundary of a small representative ∂V_f^{norm} an open book decomposition with binding $V_{g\circ n}$ and Milnor fibration $\arg(g\circ n):\partial V_f^{norm}\setminus V_{g\circ n}\to S^1$.

Furthermore, let $St(\Sigma)\subset V_f^{norm}$ be the strict transform of $(\Sigma,0)\subset(V_f,0)$. Then, in fact, $\partial V_f^{norm}\cap V_{g\circ n}\cap St(\Sigma)=\emptyset$, and

$$\arg(g\circ n):(\partial V_f^{norm}\setminus V_{g\circ n},St(\Sigma))\to S^1$$

is a locally trivial fibration of a pair of spaces.

PROPOSITION 4.4.1. *Let $T_{St(\Sigma)}$ be a small closed tubular neighbourhood of $St(\Sigma)$ in ∂V_f^{norm}. Then the following facts fold:*

(a) $\partial_1 F\approx\partial V_f^{norm}\setminus T^\circ_{St(\Sigma)}$. In particular, the number of connected components of $\partial_1 F$ is the number of irreducible components of f.

(b) The fibrations of the pairs of spaces

$$\arg(g\circ n):(\partial V_f^{norm}\setminus(V_{g\circ n}\cup T^\circ_{St(\Sigma)}),\partial T_{St(\Sigma)})\to S^1$$

and

$$\arg(g):(\partial_1 F_{\epsilon,\delta}\setminus V_g,\partial(\partial_1 F_{\epsilon,\delta}))\to S^1$$

are equivalent.

PROOF. The normalization map is an isomorphism above the regular part of V_f. □

The above facts show clearly that $\partial_1 F$ is guided by the (link of the) normalization, while $\partial_2 F$ by the local behaviour near Σ.

CHAPTER III

Plumbing graphs and their coverings (preliminaries)

§ 5. Plumbing graphs and oriented plumbed 3–manifolds.

5.1. Oriented plumbed manifolds. Our goal is to provide for any hypersurface singularity f (with 1–dimensional Σ) a plumbing representations of the 3-manifold ∂F, respectively of the 3-manifolds with boundary $\partial_1 F$ and $\partial_2 F$ (cf. 3.3).

In fact, for any fixed g as in (4.1), we will also provide a plumbing representation of the pair $(\partial F, V_g)$ and (the multiplicity system of) the generalized Milnor fibrations $\partial F \setminus V_g$, $\partial_1 F \setminus V_g$ and $\partial_2 F$ over S^1 induced by $\arg(g)$ (for definitions and details, see below).

Regarding the definitions of plumbed 3-manifolds and plumbing calculus we follow W. Neumann's seminal article [**49**] (with small modifications, which will be clarified below).

For any graph Γ, we denote the set of vertices by $\mathcal{V}(\Gamma)$ and the set of edges by $\mathcal{E}(\Gamma)$. If there is no danger of confusion, we denote them simply by $\mathcal{V}$ and $\mathcal{E}$.

In the case of plumbing graphs of *closed* 3-manifolds, any vertex has two decorations, one of them is the Euler obstruction, or *'Euler number'* — this is an integer, while the second one is the *'genus'* (written as $[g_v]$, and omitted if it is zero), this is a non–negative integer. On the other hand, the edges also have two possible decorations $+$ or $-$. In most of the cases we omit the decoration $+$, nevertheless we prefer to emphasize the sign $-$ with the symbol $\ominus$.

Although, for plumbing representations of links of normal surface singularities we need only the sign $+$, and also the intersection form (associated with the graph) is always negative definite, in the present situation both restriction should be relieved. On the other hand, all our 3-manifolds are *oriented*, hence we restrict ourselves to *'oriented plumbing graphs'*, cf. [**49**, (3.2)(i)].

Oriented plumbed 3–manifolds are constructed using a set of S^1–bundles $\{\pi_v : B_v \to S_v\}_v$, whose total space B_v has a fixed orientation. They are indexed by the set of vertices $\mathcal{V}$ of the plumbing graph, such that the base–space S_v of B_v is a closed (orientable) real surface of genus g_v, and the Euler number of the bundle B_v is the Euler number decoration of the vertex v on the graph. Then one glues these bundles corresponding to the edges of Γ as follows. First, one chooses an orientation of S_v and of the fibers (compatible with the orientation of B_v). Then for each edge adjacent to v one fixes a point $p \in S_v$, a trivialization $D_p \times S^1 \to \pi_v^{-1}(D_p)$ above a small closed disc $D_p \ni p$, and one deletes its interior $D_p^\circ \times S^1$. (Here S^1 is the unit circle with its natural orientation). Then, any edge (v, w) of Γ determines $\partial D_p \times S^1$ in B_v and $\partial D_q \times S^1$ in B_w (both diffeomorphic to $S^1 \times S^1$), which are glued by an identification map $\epsilon\left(\begin{smallmatrix} 0 & 1 \\ 1 & 0 \end{smallmatrix}\right)$, where $\epsilon = \pm$ is the decoration of the edge (for more details, see [**49**], page 303).

In order to keep additional geometric information as well, e.g. information on links in the 3–manifold, or boundary components, we will in fact be working with plumbing graphs that have extra decorations — as made precise in the next subsections.

5.1.1. **Oriented links in oriented closed plumbed 3–manifolds** are represented on the graph by arrowhead vertices (the other, 'usual' vertices will be called non–arrowheads). Arrowhead vertices have no 'Euler number' or 'genus' decorations. Each arrowhead is connected by an edge to some non–arrowhead vertex v, and this edge has a sign–decoration $+$ or $\ominus$, similarly as any edge connecting two non–arrowhead vertices (whose significance was explained in the preceding subsection). Any arrowhead supported by a non–arrowhead v codifies a generic S^1–fiber of B_v, while the sign–decoration of the supporting edge determines an orientation on it. The correspondence is realized as follows. For each non–arrowhead vertex v choose an orientation of S_v (and of the fibers) as in the previous subsection. This is used in the gluing of the bundles too, but it also identifies the orientation of link–components: If an arrowhead is supported by a $+$–edge then the link components inherits the fiber–orientation, otherwise the orientation is reversed. Their union (over all arrowheads) of these oriented S^1–fibers constitute an oriented link K.

(There is an exception to the above description when the graph consists of a double arrow. In this case the 3–manifold is S^3, and the arrows represent two Hopf link–components. If the sign–decoration of the double–arrow is $+$ then both Hoph link–components inherit the orientation of the oriented Hopf S^1–fibration, otherwise the orientation of one of them is reversed.)

Usually we write $\mathcal{A}$ for the set of arrowheads, and $\mathcal{W}$ for the set of non–arrowheads, i.e. $\mathcal{V} = \mathcal{A} \cup \mathcal{W}$.

Plumbing graphs with arrowhead vertices, in general, might carry an extra set of decorations: each (arrowhead and non-arrowhead) vertex has an additional *'multiplicity weight'*, denoted by (m_v). The typical example of a graph with arrowheads and multiplicity system is provided by an embedded resolution graph of an analytic function defined on a normal surface singularity, where the arrowheads correspond to the strict transforms of the zero set of the analytic function, the non–arrowheads to irreducible exceptional divisors, and the multiplicities are the vanishing orders of the pull–back of the function along the exceptional divisors and strict transforms.

More generally, the set of multiplicities represent a relative 2–cycle in the corresponding plumbed 4-manifold, which in the relative homology class represents zero. The oriented plumbed 4–manifold $X = X(\Gamma)$ is constructed in a similar way as the plumbed 3–manifold $M = M(\Gamma)$: one replaces the S^1–bundles with the corresponding disc–bundles $\mathcal{D}_v$ and one glues them by a similar procedure. Then X is a 4–manifold with boundary such that $\partial X = M$. Each vertex v determines a 2–cycle C_v in X: If v is an arrowhead then C_v is an oriented generic disc–fiber of $\mathcal{D}_v$ — hence it is a relative cycle. If v is a non–arrowhead vertex then C_v is the oriented 'core' (i.e. the zero section) of $\mathcal{D}_v$, — hence this is an absolute cycle. (Their simultaneous orientations can be arranged compatibly with the graph).

A multiplicity system $\{m_v\}_v$ (we will deal with) always satisfies a set of compatibility relations, which is equivalent to the fact that the class of $C(\underline{m}) := \sum_{v\in\mathcal{V}} m_v C_v$ in $H_2(X, \partial X, \mathbb{Z})$ is zero. This fact can be rewritten as follows. Let w be a fixed non–arrowhead vertex with Euler number e_w. Let $\mathcal{E}_w$ be the set of all adjacent edges, excluding loops supported by w. For each $e \in \mathcal{E}_w$, connecting w to the vertex $v(e)$ (where $v(e)$ may be in arrowhead or not), let $\epsilon_e \in \{+, -\}$ be its sign–decoration. Then:

$$e_w m_w + \sum_{e\in\mathcal{E}_w} \epsilon_e m_{v(e)} = 0. \tag{5.1.2}$$

Indeed, this follows from the fact that $H_2(X,\mathbb{Z})$ is freely generated by the absolute classes of C_w ($w\in\mathcal{W}$), hence the intersection number $(C(\underline{m}),C_w)=0$ for all non-arrowhead vertices w if and only if $[C(\underline{m})]=0$ in $H_2(X,\partial X,\mathbb{Z})$.

5.1.3. **Multiplicity systems associated with an open book.** Consider a pair (M,K) as in (5.1.1). The case of a fibred link K in the 3–manifold M has a special interest. In this case the pair (M,K) has a plumbed representation provided by a graph (decorated with Euler numbers and genera) and arrows (representing K), and additionally $p: M\backslash K\to S^1$ is a locally trivial fibration with a trivialization in a neighbourhood of K; in particular, p sends any oriented meridian of any (oriented) component of K to the positive generator of $H_1(S^1)$. In such a situation, we do the following construction. First, we fix the link–components (fibers), and then, for each non–arrowhead vertex w, let γ_w be an oriented generic S^1–fibre situated in B_w, different from any fixed fiber corresponding to components of K. (Here we use that orientation of the S^1–bundle which was used in the plumbing construction).

Definition 5.1.4. *Set* $m_w:=p_*([\gamma_w])\in H_1(S^1,\mathbb{Z})=\mathbb{Z}$ *for any non–arrowhead vertex* w*, and define* $m_v=1$ *for all arrowheads. This is the multiplicity system associated with the fibration* p*.*

The fact that this is indeed a multiplicity system can be seen as follows. Let F be the oriented fiber of p (in M, with $\partial F=K$). By a homotopy one can push $F\setminus K$ inside X (keeping $K=\partial F$ fixed), and its relative homology class can also be represented by the relative cycle $C(\underline{m})$. On the other hand, the corresponding relative homology class is zero, since F sits in ∂X.

We wish to emphasize that if M is a rational homology sphere then the open book can be recovered from the pair (M,K) by a theorem of Stallings. ([**18**, page 34] provides two different arguments for this fact, one of them based on [**6**], the other on [**74**].) On the other hand, in the general case, the information codified in the plumbing data of the pair (M,K) together with the multiplicity system (i.e. the graph with arrows decorated with Euler numbers, genera and multiplicities) is weaker than the open book decomposition itself (see e.g. [**44**] for different examples).

The matrix of the linear system of equations (5.1.2) (in variables $\{m_w\}_{w\in\mathcal{W}}$) is the 'intersection matrix' A of the graph (or of $H_2(X,\mathbb{Z})$). If it is non–degenerate then by (5.1.2) the pair (M,K) determines uniquely all the multiplicities.

5.1.5. **Manifolds with boundary.** In a similar way, one can codify plumbed oriented 3-manifolds with boundary, where each boundary component is a torus. In general, one starts with an oriented closed 3–manifold M with some link–components, cf. (5.1.1). Then one fixes a closed tubular neighbourhood $T(K)$ of each link–component K, and then one deletes their interior $T^\circ(K)$ obtaining a manifold with boundary $M\setminus T^\circ(K)$.

At the level of plumbing graphs, in the present article, this will be codified as follows: Assume that the arrowhead representing a connected component of K is connected by an edge to the non–arrowhead vertex v. Then replace this supporting edge by a *dash–edge* (and delete its sign–decoration, or consider it irrelevant). I.e., the dash–arrows represent deleted solid tori around the components of the corresponding link-components.

Equivalently, if r_w is the number of dash–arrows supported by the non–arrowhead vertex w, then one can also get the plumbed manifold with boundary using the plumbing construction by deleting r_w solid tori (the inverse image of r_w small open discs of the base space of B_w) from B_w. (This is codified in [**49**] by the decoration $[r_w]$ of w, instead of the r_w dash-arrows of w.)

Notice that in this way, (i.e. by replacing an arrow supported by a usual edge by an arrow supported by a dash–edge) one looses some information (e.g. the Euler–number of supporting non–arrowhead w becomes irrelevant).

5.1.6. **Fibrations and multiplicities.** Additionally, if $M\setminus T^\circ(K)$ is a locally trivial fibration p over S_1, one can define again a multiplicity system: for each non–arrowhead w one takes $m_w:=p_*(\gamma_w)$ as above. Nevertheless, in this case the arrowheads supported by dash–arrows will carry no multiplicity decorations (or, equivalently, they will be disregarded). This system satisfies the compatibility relations (5.1.2) in the following modified way: if w is a non–arrowhead which supports no dash–arrow, then (5.1.2) is valid for that w. But, in general, no other relation holds. (I.e. (5.1.2) is valid for all non–arrowhead vertices w with the convention that the multiplicity of the dash–arrows 'can be anything'.)

Notice that if (M,K) has an open book decomposition, then the fibration of the complement of K contains less information than the original open book decomposition: in general, a fibration $K\setminus T^\circ(K)$ cannot be closed canonically to an open book decomposition. Similarly, the multiplicity system associated with a fibration $p: M\setminus T^\circ(K)\to S^1$ contains less information than the multiplicity system associated with the original open book decomposition.

5.1.7. **The plumbing calculus.** The plumbing calculus of graphs with (non–dashed) arrowheads is similar to the *calculus of oriented 3–manifolds* presented in [**49**, (3.2)(i)] (valid for graphs without arrows, or for graphs with dash-arrows). According to this, there are 9 permitted operations (and their inverses); in Neumann's notation they are: R0(a), R0(b)', R1, R3, R5, R6, R7, R8, R2/4.

Nevertheless, in the present article, guided by some results of the present work, we will consider a *reduced set of operations.* Our graphs will be constructed from a singularity theoretical viewpoint. We believe that using only the reduced set of operations, we preserve better some structure of these graphs (inherited by the algebro–geometric/analytic situation), which might be lost if we run all the operations of the C^∞–calculus. (A similar situation is the case of the plumbing calculus of negative definite resolution graphs of normal surface singularities, or the dual graph of any kind of complex curve configuration on a smooth complex surface, where one usually uses only (-1)–blow ups, instead of all the operations of the C^∞–calculus.)

The principle how we make the 'reduced list' of operations is the following. For any decorated plumbing graph G let $c(G)$ be the number of independent cycles in G (i.e. the rank of $H_1(|G|)$, where $|G|$ is the topological realization of G). Furthermore, let $g(G)$ be the sum of the genus decorations of G, i.e $g(G)=\sum_{w\in\mathcal{W}(G)}g_w$. The point is that all our graphs provided by our main construction, associated with a fixed geometrical object (singularity) — but depending essentially on the choice of an embedded resolution —, share two properties: all of them are connected, and $c(G)+g(G)$ is the same for all of them (describing a geometric entity independent of the construction, cf. (16.4.10)). We believe that all these graphs (associated with the same geometric object) should be connected by a calculus preserving these two properties. In particular, our 'reduced list' contains exactly those operations (of the oriented calculus) which *preserve connectedness and the integer* $c(G)+g(G)$.

This list (in Neumann's notation) (valid for graphs without any kind of arrows) is the following: R0(a) (reverse the sign–decoration on all edges other than loops adjacent to a vertex), R1 (blowing down ±1 vertices), R3 (0–chain absorption), R5 (oriented handle absorption). Additionally, in the presence of dash–arrows, one adds R8 (annulus absorption) as well.

For the convenience of the reader we list them in the subsections (5.1.10)–(5.1.12).

In this article we will manipulate only with these operations. Nevertheless, if the reader wishes to use some other operations of the (oriented) plumbing calculus, this is perfectly fine if she or he wished to focus only on ∂F, but some geometric information will be lost regarding other invariants). In fact, sometimes it is helpful to have in mind the 'splitting operation' R6 too, since it helps represent some of the manifolds as a connected sums.

Definition 5.1.8. *We write $G_1 \sim G_2$ if G_1 can be obtained from G_2 by the above* reduced plumbing calculus.

5.1.9. In fact, we conjecture that even the integers $c(G)$ and $g(G)$ are independent of the choice of G, and they are related with the weight filtration of the mixed Hodge structure on $H^1(\partial F)$, see § 21. (Since these numbers are modified under the usual calculus, we get that the weight filtration of the mixed Hodge structure is not topological invariant of ∂F, for concrete examples see (24.1.1) and (24.1.2).) This suggests, that if we would like to preserve this analytic information too, we have to exclude the oriented handle absorption R5 from the list of operations of the 'reduced calculus', and use a more restrictive set (which can be called 'strictly reduced oriented calculus').

5.1.10. **'Reduced' oriented plumbing calculus** of plumbing graphs (without any kind of arrows) consists of the following operations and their inverses. We deal with *connected graphs* only and non–negative genus decorations.

[R0](a). Reverse the signs on all edges other than loops adjacent to any fixed vertex.

[R1] (Blowing down). $\epsilon = \pm 1$ and the edge signs ϵ_0, ϵ_1, ϵ_2 are related by $\epsilon_0 = -\epsilon\epsilon_1\epsilon_2$.

a.)

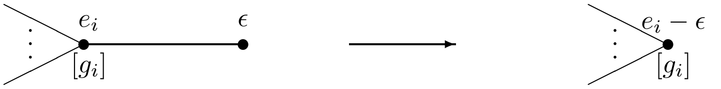

b.)

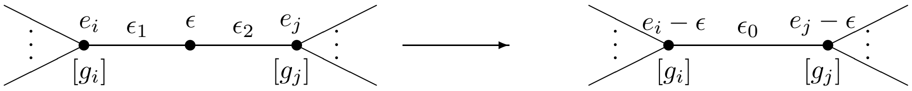

c.)

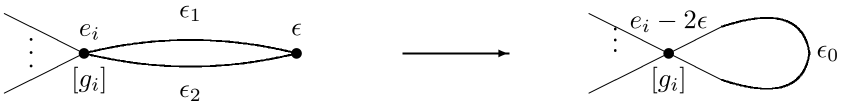

[R3] (0-chain absorption). The edge signs ϵ'_i ($i = 1, ..., s$) are related by $\epsilon'_i = -\epsilon\bar{\epsilon}\epsilon_i$ provided that the edge sign in question is not a loop, and $\epsilon'_i = \epsilon_i$, if it is a loop.

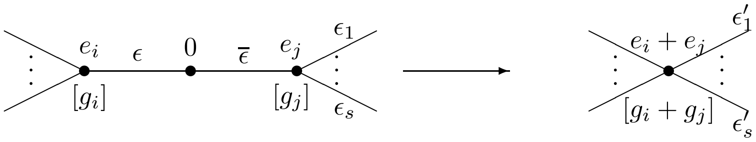

[R5] (Oriented handle absorption).

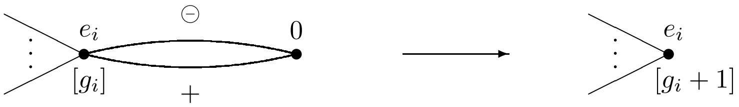

Remark 5.1.11. Usually, the operation R6 (splitting) of Neumann's article [**49**] replaces a connected graph by another one with several connected components. Nevertheless, if the starting graph is rather specific, then the output graph can be connected. This operation has the following form (where the two left–edges might have any sign–decorations) :

[R6^{naive}] ('Naive' splitting).

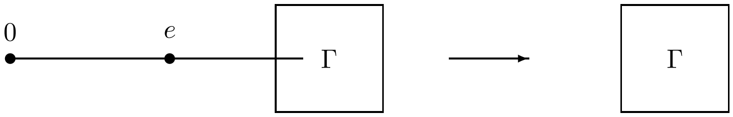

This operation can also be inserted in the list of (5.1.10); nevertheless, one can prove that it is a consequence of those already listed there. Indeed, blowing up the left–edge, and blowing down the strict transform of the 0–vertex, we realize that e can be replace by $e \pm 1$. Hence by repeating this pair of operations, we can replace e by 0. Then a 0–chain absorption of this newly created 0–vertex finishes the argument.

5.1.12. **'Reduced' oriented plumbing calculus of graphs with arrows.** If the graph has some arrows and/or dash–arrows, then all the above moves have their natural analogs, complemented with some additional rules:

1. the vertex involved in R0(a) (and, obviously, the ±1–vertex in R1 and the 0–vertex in R3 and R5) should be a non–arrowhead;
2. the (±1)–vertex blown down in R1 can have at most two edges (which might support even arrowheads); if the vertex has exactly one edge supporting an arrowhead, then we do not blow down;
3. the 0–vertex absorbed in R3 and R5, cannot support any kind of arrow;
4. by these operations, the arrows of the other vertices are naturally kept, and in the case of R3 the vertices supported by vertices i and j are summed;
5. if a vertex supports a dash–arrow then its Euler number is irrelevant.

Additionally, one has the following operation as well:

[R8] (Annulus absorption for dash–arrows).

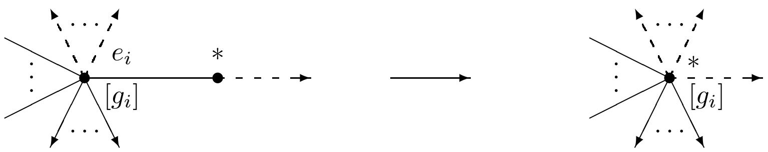

Here, if on the left hand side the vertex supports s arrows and t dash–arrows, then on the right hand side it supports s arrows and $t+1$ dash–arrows. The Euler number $*$ can be anything.

A special, 'degenerate' version of this is the operation

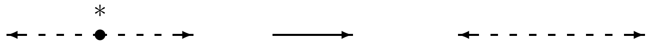

where both graphs represent a manifold with boundary obtained from S^3 by removing the tubular neighbourhoods of two Hopf link–components.

In the presence of a multiplicity system, all the above operations can be extended with the corresponding multiplicities too in a natural and unique way such that the formulae (5.1.2) stay stable under the operation. We emphasize again, that if a non–arrowhead vertex supports a dash–arrow, then its multiplicity is irrelevant.

5.2. Example. — Hirzebruch–Jung strings. [5, 25, 28]
For any three *strict positive* integers a, b and c, with $\gcd(a,b,c)=1$, let (X,x) be the normalization of $(\{x^ay^b+z^c=0\},0)\subset(\mathbb{C}^3,0)$. Let $z:(X,x)\to(\mathbb{C},0)$ be induced by $(x,y,z)\mapsto z$. Then the minimal embedded resolution graph of z is the following. First, consider the unique $0\leq\lambda<c/(a,c)$ and $m_1\in\mathbb{N}$ with:

$$b+\lambda\cdot\frac{a}{(a,c)}=m_1\cdot\frac{c}{(a,c)}. \tag{5.2.1}$$

(Here $(a,c)=\gcd(a,c)$.) If $\lambda\neq 0$, then consider the continuous fraction:

$$\frac{c/(a,c)}{\lambda}=k_1-\cfrac{1}{k_2-\cfrac{1}{\ddots-\cfrac{1}{k_s}}},\quad k_1,\dots,k_s\geq 2.$$

Then the next string is the embedded resolution graph of z:

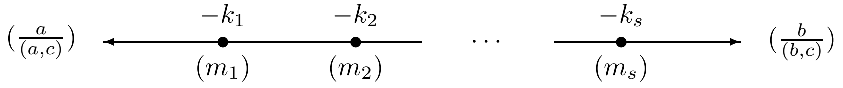

The arrow at the left (resp. right) hand side codifies the strict transform of $\{x=0\}$ (resp. of $\{y=0\}$). The first vertex has multiplicity m_1 given by (5.2.1); while $m_2,\dots,m_s$ can be computed by (5.1.2) with all edge–signs $\epsilon=+$, namely:

$$-k_1m_1+\frac{a}{(a,c)}+m_2=0, \text{ and } -k_im_i+m_{i-1}+m_{i+1}=0 \text{ for } i\geq 2.$$

This graph might also serve as the resolution graph of the germ x (induced by the projection $(x,y,z)\mapsto x$). The multiplicities of x are given in the next graph (where the arrows codify the same strict transforms):

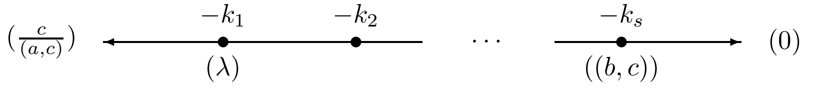

The other multiplicities can again be computed by (5.1.2) (with all $\epsilon=+$). Symmetrically, the graph of y is:

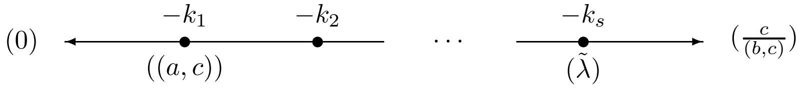

where $0\leq\tilde{\lambda}<c/(c,b)$ and

$$a+\tilde{\lambda}\cdot\frac{b}{(b,c)}=m_s\cdot\frac{c}{(b,c)}.$$

Hence, the embedded resolution graph $\Gamma(X,x^iy^jz^k)$ of the germ $x^iy^jz^k$ defined on X is the graph with the same shape, same Euler numbers and genera, and the multiplicity m_v (for any vertex v) satisfies:

$$m_v(x^iy^jz^k)=i\cdot m_v(x)+j\cdot m_v(y)+k\cdot m_v(z).$$

5.2.2. Next, we wish to define a string which will be used systematically in the main result. Strangely enough, its Euler numbers will be deleted. Before providing the precise definition, let us give a reason for it.

Clearly, once we know all the multiplicities and the edge–decorations, all the Euler numbers can be recovered by (5.1.2). In the main construction, we will glue together graphs whose multiplicity systems on common parts agree, but under the gluings the Euler numbers might change. In particular, as 'elementary blocks' of the gluing construction we consider graphs with multiplicity decorations, but no Euler numbers: their 'correct' Euler numbers will be determined last after the gluing has been done and after deciding the edge–decorations.

Definition 5.2.3. *In the sequel, for positive integers a, b and c, $Str(a,b;c\,|\,i,j;k)$ denotes the string $\Gamma(X,x^iy^jz^k)$, together with its two arrowheads, all vertices (arrowheads or not) weighted with multiplicities as above, and with all edge decorations $+$, but with all Euler numbers deleted. Moreover, $Str^{\ominus}(a,b;c\,|\,i,j;k)$ is the same string but with all edges (connecting arrowheads and non-arrowheads) decorated with $\ominus$.*

In particular, if $\lambda=0$, then the corresponding string $Str^{\pm}(a,b;c\,|\,i,j;k)$ is a double arrow (decorated with $+$ or $\ominus$) having no non-arrowhead vertex.

The same $\pm$-double-arrow will be used for the string $Str^{\pm}(a,b;c\,|\,i,j;k)$ even if $a=0$ or $b=0$ (with the convention $a/(a,b)=0$ whenever $a=0$).

§ 6. ℤ–Coverings of graphs.

6.1. In this subsection we review a graph–theoretical constructions from [**44**].

Definition 6.1.1. *A morphism of graphs $p:\Gamma_1\to\Gamma_2$ consists of two maps $p_{\mathcal V}:\mathcal V(\Gamma_1)\to\mathcal V(\Gamma_2)$ and $p_{\mathcal E}:\mathcal E(\Gamma_1)\to\mathcal E(\Gamma_2)$, such that if $e\in\mathcal E(\Gamma_1)$ has end–points v_1 and v_2, then $p_{\mathcal V}(v_1)$ and $p_{\mathcal V}(v_2)$ are the end–points of $p_{\mathcal E}(e)$. If $p_{\mathcal V}$ and $p_{\mathcal E}$ are isomorphisms of sets, then we say that p is an isomorphism of graphs.*

If Γ is a graph, we say that $\mathbb Z$ acts on Γ, if there are group–actions $a_{\mathcal V}:\mathbb Z\times\mathcal V\to\mathcal V$ and $a_{\mathcal E}:\mathbb Z\times\mathcal E\to\mathcal E$ of $\mathbb Z$ with the following compatibility property: if $e\in\mathcal E$ has end–points v_1 and v_2, then $a_{\mathcal E}(h,e)$ has end–points $a_{\mathcal V}(h,v_1)$ and $a_{\mathcal V}(h,v_2)$. The action is trivial if $a_{\mathcal V}$ and $a_{\mathcal E}$ are trivial actions.

If $\mathbb Z$ acts on both Γ_1 and Γ_2, then a morphism $p:\Gamma_1\to\Gamma_2$ is equivariant if the maps $p_{\mathcal V}$ and $p_{\mathcal E}$ are equivariant with respect to the actions of $\mathbb Z$. If additionally p is an isomorphism then it is called an equivariant isomorphism of graphs.

Fix a finite graph Γ, and assume that $\mathbb Z$ acts on it in a trivial way.

Definition 6.1.2. *A $\mathbb Z$–covering, or cyclic covering, of Γ consists of a finite graph G, that carries a $\mathbb Z$–action, together with an equivariant morphism $p:G\to\Gamma$ such that the restriction of the $\mathbb Z$–action on any set of type $p^{-1}(v)$ ($v\in\mathcal V(\Gamma)$), respectively $p^{-1}(e)$ ($e\in\mathcal E(\Gamma)$), is transitive.*

For any $v\in\mathcal V(\Gamma)$ (respectively $e\in\mathcal E(\Gamma)$ with end–points $\{v_1,v_2\}$), let $\mathfrak n_v\mathbb Z$ (respectively $\mathfrak d_e\cdot lcm(\mathfrak n_{v_1},\mathfrak n_{v_2})\mathbb Z$) be the maximal subgroup of $\mathbb Z$ which acts trivially on $p^{-1}(v)$ (respectively on $p^{-1}(e)$). This defines a system of strictly positive integers $(\mathbf n,\mathbf d)=\big\{\{\mathfrak n_v\}_{v\in\mathcal V(\Gamma)};\{\mathfrak d_e\}_{e\in\mathcal E(\Gamma)}\big\}$. It is called the *covering data of the covering.*

Sometimes we write $\mathfrak n_e$ for $\mathfrak d_e\cdot lcm(\mathfrak n_{v_1},\mathfrak n_{v_2})$.

Definition 6.1.3. *Two cyclic coverings $p_i:G_i\to\Gamma$ ($i=1,2$) are equivalent ($G_1\sim G_2$) if there is an equivariant isomorphism $q:G_1\to G_2$ such that $p_2\circ q=p_1$.*

The set of equivalence classes of cyclic coverings of Γ*, all of them associated with a fixed covering data* $(\mathbf{n},\mathbf{d})$*, is denoted by* $\mathcal{G}(\Gamma,(\mathbf{n},\mathbf{d}))$.

It turns out (cf. [**44**, (1.15)]) that $\mathcal{G}(\Gamma,(\mathbf{n},\mathbf{d}))$ is independent of $\mathbf{d}$, and it contains a distinguished element (the so-called 'trivial covering') T. T is characterized by the existence of a (non-equivariant) morphism of graphs $s:\Gamma\to T$ with $p\circ s=id_\Gamma$. Moreover, $\mathcal{G}(\Gamma,(\mathbf{n},\mathbf{d}))$ has an abelian group structure, where T plays the role of the zero-element.

In general, $\mathcal{G}(\Gamma,(\mathbf{n},\mathbf{d}))$ is non-trivial. E.g., if (the topological realization of) Γ consists of a single cycle, i.e. $\mathcal{V}(\Gamma)=\{v_1,v_2,\ldots,v_k\}$, $\mathcal{E}(\Gamma)=\{(v_1,v_2),(v_2,v_3),\ldots,(v_k,v_1)\}$ with $k\geq 3$), and $n:=\gcd\{\mathfrak{n}_v : v\in\mathcal{V}(\Gamma)\}$, then $\mathcal{G}(\Gamma,(\mathbf{n},\mathbf{d}))=\mathbb{Z}_n$. On the other hand, one has:

THEOREM 6.1.4. [**44**, (1.20)] *Fix* Γ *and* $(\mathbf{n},\mathbf{d})$ *as above. Set* $\mathcal{V}^1:=\{v\in\mathcal{V}(\Gamma):\mathfrak{n}_v=1\}$*. Let* $\Gamma_{\neq 1}$ *be the subgraph of* Γ *obtained from* Γ *by deleting the vertices* $\mathcal{V}^1$ *and their adjacent edges. If each connected component of* $\Gamma_{\neq 1}$ *is a tree, then* $\mathcal{G}(\Gamma,(\mathbf{n},\mathbf{d}))=0$.

6.1.5. In particular, if Γ is a tree, then with any fixed covering data $(\mathbf{n},\mathbf{d})$ there is only one covering G. It is not hard to show that G has exactly $\gcd\{\mathfrak{n}_v\}_{v\in\mathcal{V}(\Gamma)}$ connected components.

6.1.6. The graphs above might also have loops — as special edges: in the definitions and statements above the end–vertices v_1 and v_2 of a loop should be identified.

6.2. Variations. One extends the set of coverings as follows (cf. [**44**, 1.25]).

(1) Assume that we have two types of vertices: arrowheads $\mathcal{A}$ and non–arrowheads $\mathcal{W}$, i.e. $\mathcal{V}=\mathcal{A}\coprod\mathcal{W}$. Then in the definition of the coverings $p:G\to\Gamma$ we add the following axiom: $\mathcal{A}(G)=p^{-1}(\mathcal{A}(\Gamma))$.

(2) Assume that our graphs have some decorations. Then for coverings $p:G\to\Gamma$ we also require that the decoration of G must be equivariant.

(3) Change (in an equivariant way) any edge of G into a string. More precisely, one starts with the following data:
   (a) a graph Γ and a system $(\mathbf{n},\mathbf{d})$ as above;
   (b) a covering $p:G\to\Gamma$, as an element of $\mathcal{G}(\Gamma,(\mathbf{n},\mathbf{d}))$;
   (c) for any edge e of Γ, we fix a string $Str^{\pm}(e)$ (with decorations):

$Str^{\pm}(e)$:

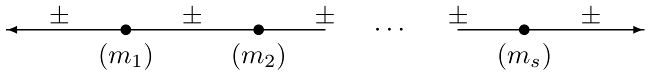

Then the new graph $G(\{Str^{\pm}(e)\}_e)$ is constructed as follows: we replace any edge $\tilde{e}\in p_{\mathcal{E}}^{-1}(e)$ (with end–points $\tilde{v}_1$ and $\tilde{v}_2$ and decoration ±) of G as it is shown below:

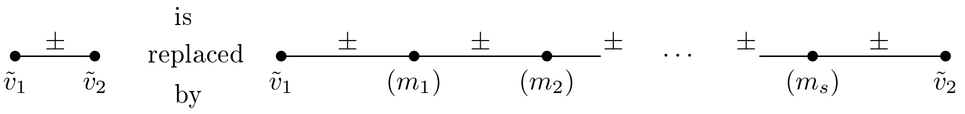

CHAPTER IV

The graph $\Gamma_{\mathcal{C}}$ of a pair (f,g) (preliminaries)

§ 7. The definition of the weighted graph $\Gamma_{\mathcal{C}}$

7.1. Introductory words. The main tool of the present work is the weighted graph $\Gamma_{\mathcal{C}}$ introduced and studied in [**48**]. It has two types of vertices, non-arrowheads and arrowheads. The non-arrowhead vertices have two types of decorations, the first one is an ordered triple $(m;n,\nu)$ for some integers $m,\nu>0$ and $n\geq 0$, the second (the 'genus') is denoted by $[g]$ for a non-negative integer g. If $g=0$ then this decoration might be omitted. The arrowheads have only one decoration, namely the ordered triple $(1;0,1)$. The edges are not directed, and loops are accepted. Each edge has a decoration $\in\{1,2\}$ (which in some situations might be omitted, cf. (7.2.1)).

The graph $\Gamma_{\mathcal{C}}$ was introduced in [**48**] to study a hypersurface singularity f with 1–dimensional singular locus, and the 'generalized Iomdin series' associated with f.

More precisely, in [**48**] we have considered an additional germ $g:(\mathbb{C}^3,0)\to(\mathbb{C},0)$ such that the pair (f,g) forms an ICIS, and we determined the resolution graph of each normal surface singularity $f+g^k$, for k large, in terms of $\Gamma_{\mathcal{C}}$. Motivated by the fact that $\Gamma_{\mathcal{C}}$ contains all the information needed to treat 'almost all' the correction terms of the invariants of the series, cf. [**48**] and (1.3), we used to call $\Gamma_{\mathcal{C}}$ 'universal'. Its power is reinforced by the present work as well.

Nevertheless, perhaps, the name *bi–colored relative graph associated with the pair* (f,g) tells more about the geometry encoded in the graph. Here, the first attribute points out that the edges have bi–colored decorations (a key fact which has enormous geometrical effects), while by 'relative' we wish to stress, that the graph codifies the g–polar geometry of f concentrated near the singular locus of V_f (in particular, in $\Gamma_{\mathcal{C}}$ the functions f and g do not have a symmetric role). For more motivation and supporting intuitive arguments regarding $\Gamma_{\mathcal{C}}$, see (8.5) too.

In short, the graph $\Gamma_{\mathcal{C}}$ is the decorated dual graph of some curve configuration $\mathcal{C}$ in the embedded resolution of the pair $(\mathbb{C}^3,V_f\cup V_g)$, see below.

7.1.1. **Short review of the construction of $\Gamma_{\mathcal{C}}$.** (For more details, see [**48**].)

Consider an ICIS $(f,g):(\mathbb{C}^3,0)\to(\mathbb{C}^2,0)$ and the local divisor $(D,0):=(V_f\cup V_g,0)\subset(\mathbb{C}^3,0)$. Let Φ denote a fixed good representative as in (4.1).

Take an embedded resolution

$$r:V^{emb}\to U$$

of $(D,0)\subset(\mathbb{C}^3,0)$. Here V^{emb} is smooth, r is proper, U is a small representative of $(\mathbb{C}^3,0)$ of type $U=\Phi^{-1}(D^2_\eta)\cap B_\epsilon$, and the total transform $\mathbf{D}:=r^{-1}(D)$ is a normal crossing divisor. Moreover, we assume that the restriction of r on $V^{emb}\setminus r^{-1}(Sing(V_f)\cup Sing(V_g))$ is a biholomorphic isomorphism. (Notice that $Sing(V_f)\cup Sing(V_g)$ is a smaller set than the 'usual' $Sing(D)$, but since the intersection $V_f\cap V_g$ is already transversal off the origin, the above assumption can always be satisfied for a convenient resolution.) In particular,

$$\widetilde{\Phi}=\Phi\circ r:\big(r^{-1}(\Phi^{-1}(D^2_\eta\setminus\Delta_\Phi)\cap B_\epsilon),r^{-1}(\Phi^{-1}(D^2_\eta\setminus\Delta_\Phi)\cap S^5_\epsilon\big)\to D^2_\eta\setminus\Delta_\Phi$$

is a locally trivial C^∞-fibration of a pair of spaces (here $S^5_\epsilon = \partial B_\epsilon$).

Consider a special curve configuration determined by the vanishing behaviour of the pullbacks of f and g on $\mathbf{D}$. Denote by $\mathbf{D}_c$ those irreducible components of the total transform $\mathbf{D}$ where only $f\circ r$ vanishes, i.e. $\mathbf{D}_c = \overline{r^{-1}(V_f \setminus V_g)}$. Similarly, consider $\mathbf{D}_d = \overline{r^{-1}(V_g \setminus V_f)}$ and $\mathbf{D}_0 = r^{-1}(V_f \cap V_g)$.

Definition 7.1.2. *The curve configuration $\mathcal{C}$ is defined by*

$$\mathcal{C} = (\mathbf{D}_c \cap \mathbf{D}_0) \cup (\mathbf{D}_c \cap \mathbf{D}_d).$$

Thus, for each irreducible component C of $\mathcal{C}$, there are exactly two irreducible components B_1 and B_2 of $\mathbf{D}$ for which C is a component of $B_1 \cap B_2$. By the definition of $\mathcal{C}$, we can assume that B_1 is such that *only* $f\circ r$ vanishes on it, and B_2 is such that either only $g\circ r$ vanishes on it, or both $f\circ r$ and $g \circ r$.

Let m_{f,B_i} (respectively m_{g,B_i}) be the vanishing order of $f\circ r$ (respectively of $g\circ r$) along B_i ($i=1,2$). Then $m_{f,B_1}>0$, $m_{g,B_1}=0$, $m_{f,B_2}\geq 0$, and $m_{g,B_2}>0$. To the component C we assign the triple $(m_{f,B_1}; m_{f,B_2}, m_{g,B_2})$.

A component C of $\mathcal{C}$ is either compact (projective) or non-compact (isomorphic to a disc). The non-compact components consist of the strict transform of $V_f\cap V_g$. Therefore, $(m_{f,B_1}; m_{f,B_2}, m_{g,B_2}) = (1;0,1)$ for them. The compact components are exactly those which are contained in $r^{-1}(0)$.

7.1.3. **The graph** $\Gamma_{\mathcal{C}}$ is the dual graph of the curve configuration $\mathcal{C}$.

The set of vertices $\mathcal{V}$ consists of non-arrowheads $\mathcal{W}$ and arrowheads $\mathcal{A}$. The non-arrowhead vertices correspond to the compact irreducible curves of $\mathcal{C}$ while the arrowhead vertices to the non-compact ones.

In $\Gamma_{\mathcal{C}}$, one connects the vertices v_i and v_j by l edges $\{(v_i,v_j)_k\}_{k=1,\dots,l}$ if the corresponding curves $C_i, C_j \subset \mathcal{C}$ intersect in l points. Moreover, if a compact component $C_i\subset\mathcal{C}$, corresponding to a vertex $v_i\in\mathcal{W}$, intersects itself then each self-intersection point determines a loop (v_i,v_i) in the graph $\Gamma_{\mathcal{C}}$. The edges are not directed, i.e. $(v_i,v_j)_k = (v_j,v_i)_k$.

One decorates the graph $\Gamma_{\mathcal{C}}$ as follows:

(1) Each non-arrowhead vertex $v\in\mathcal{W}$ has two weights: the ordered triple of integers $(m_{f,B_1}; m_{f,B_2}, m_{g,B_2})$ assigned to the irreducible component C corresponding to v, and the genus g of (the normalization of) C.

(2) Each arrowhead vertex has a single weight: the ordered triple $(1;0,1)$.

(3) Each edge has a weight $\in\{1,2\}$ determined as follows. By construction, any edge corresponds to the intersection point of three local irreducible components of $\mathbf{D}$. Among them either one or two local components belong to $\mathbf{D}_c$. Correspondingly, in the first case let the weight on the edge be 1, in the second case 2.

7.2. Summary of notation for $\Gamma_{\mathcal{C}}$, and local equations. The next table and local coordinate realizations will be helpful in the further discussions and proofs.

Vertices:

The vertex $\overset{(m;n,\nu)}{\underset{[g]}{\bullet}}$ codifies a compact irreducible component C of $\mathcal{C}$ of genus g.

There is a local neighbourhood U_p of any generic point $p\in C$ with local coordinates (u,v,w) such that $U_p\cap\mathbf{D} = B^l_1\cup B^l_2$, $B^l_1=\{u=0\}$, $B^l_2=\{v=0\}$, $f\circ r|_{U_p} = u^m v^n$, and $g\circ r|_{U_p} = v^\nu$ with $m,\nu>0$; $n\geq 0$. (Here B^l_i are *local* components of $\mathbf{D}$ at p.)

The arrowhead vertex $\longrightarrow (1;0,1)$ codifies a non-compact component. The local description goes by the same principle as above.

Edges: An edge corresponds to an intersection point $p \in C_i \cap C_j$ (or a self-intersection of C_i if $i = j$). There is a local neighbourhood U_p of p with local coordinates (u, v, w) such that $U_p \cap \mathbf{D} = B_1^l \cup B_2^l \cup B_3^l$, and $B_1^l = \{u = 0\}$, $B_2^l = \{v = 0\}$, $B_3^l = \{w = 0\}$. Moreover, the local equations of f and g are as follows:

An edge with decoration 1:

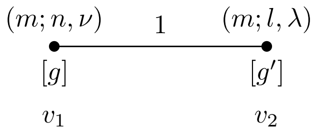

corresponds to local equations:

$$f \circ r|_{U_p} = u^m v^n w^l, \ g \circ r|_{U_p} = v^\nu w^\lambda,$$

where $m, \nu, \lambda > 0$ and $n, l \geq 0$.

One has similar equations with $m =, \lambda = 1$, $l = 0$, $\nu > 0$, $n \geq 0$ if v_2 is an arrowhead:

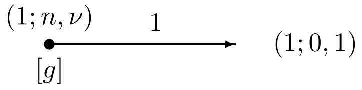

An edge with decoration 2:

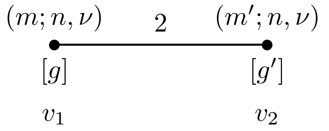

provides local equations:

$$f \circ r|_{U_p} = u^m v^{m'} w^n, \quad g \circ r|_{U_p} = w^\nu$$

with $m, m', \nu > 0$ and $n \geq 0$.

One has similar equations with $m' =$, $\nu = 1$, $n = 0$ and $m > 0$ if v_2 is an arrowhead:

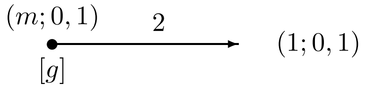

Remark 7.2.1. There is a compatibility between the weights that simplifies decorations. Indeed, consider the following edge:

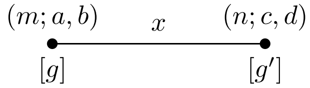

(a) if $m \neq n$, then $(a, b) = (c, d)$ and $x = 2$;
(b) if $(a, b) \neq (c, d)$, then $m = n$ and $x = 1$.

In particular, in the cases (a)–(b) above, the weight of the edge is determined by the weights of the vertices, hence (in some cases) it will be omitted.

Remark 7.2.2. Clearly, different resolutions r provide different curve configurations $\mathcal{C}$. In particular, the graph $\Gamma_{\mathcal{C}}$ is not unique. (We believe that there is a 'calculus' of such graphs connecting different graphs $\Gamma_{\mathcal{C}}$ coming from different embedded resolutions of $(D, 0) \subset (\mathbb{C}^3, 0)$, but this was not yet developed with all the details; we will return to it in a forthcoming work.)

7.3. Assumption A. In the graph $\Gamma_{\mathcal{C}}$ a special attention is needed for edges of weight 2 with both end–vertices having first multiplicity $m = 1$ (including the case of loops too, when the two end-vertices coincide). Such an edge corresponds to a point p which lies at the intersection of three locally irreducible components on exactly two of which only $f \circ r$ vanishes and that happens with multiplicity one. Thus the intersection of these two locally irreducible components is the strict transform of a component of $Sing(V_f)$ with transversal type A_1, which has *not* been blown up during the resolution procedure r.

Performing an additional blow-up along this intersection, we obtain a new embedded resolution r', whose special curve configuration $\mathcal{C}'$ will have an additional rational curve. The relevant edge of the dual graph $\Gamma_{\mathcal{C}}$ is changed to the dual graph $\Gamma_{\mathcal{C}'}$ with a new part via the transformation as:

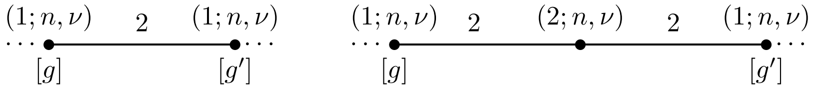

In order to avoid some pathological cases in the discussion, and to have a uniform treatment of the properties of $\Gamma_{\mathcal{C}}$ (e.g. of the 'cutting edges' and subgraphs $\Gamma^1_{\mathcal{C}}$ and $\Gamma^2_{\mathcal{C}}$, see the next section), we will assume that $\Gamma_{\mathcal{C}}$ has no such edges (i.e. that we already performed the extra blow-ups, if it was necessary). The same discussion/assumption is valid for loops and for the situation when one of the ends above is replaced by an arrowhead.

This assumption is not crucial at all, the interested reader might eliminate it with the price of having to slightly modify the statements of the forthcoming subsections (8.2) and (8.3). (In fact, in the algorithm which provides ∂F, Assumption A is irrelevant.)

§ 8. Properties of the graph $\Gamma_{\mathcal{C}}$.

8.1. We review those properties of $\Gamma_{\mathcal{C}}$ that are needed in the sequel. For a more complete discussion, see [**48**].

PROPOSITION 8.1.1. [**48**, (5.23)] $\Gamma_{\mathcal{C}}$ *is connected.*

8.1.2. **A partition of $\Gamma_{\mathcal{C}}$ and 'cutting edges'.** The vertices of the graph $\Gamma_{\mathcal{C}}$ can be divided into two disjoint sets $\mathcal{V}(\Gamma_{\mathcal{C}}) = \mathcal{V}^1(\Gamma_{\mathcal{C}}) \cup \mathcal{V}^2(\Gamma_{\mathcal{C}})$, where $\mathcal{V}^1(\Gamma_{\mathcal{C}})$ (respectively $\mathcal{V}^2(\Gamma_{\mathcal{C}})$) consists of the vertices decorated by $(m; n, \nu)$ with $m = 1$ (respectively $m \geq 2$). We will use similar notations for $\mathcal{W}(\Gamma_{\mathcal{C}})$ and $\mathcal{A}(\Gamma_{\mathcal{C}})$.

The set of edges (v_1, v_2) with ends $v_1 \in \mathcal{V}^1(\Gamma_{\mathcal{C}})$ and $v_2 \in \mathcal{W}^2(\Gamma_{\mathcal{C}})$ will be called *cutting edges*. Their edge–decoration is always 2. We denote their index set by $\mathcal{E}_{cut}$.

According to the decomposition $\mathcal{V} = \mathcal{V}^1 \cup \mathcal{V}^2$, we partition $\Gamma_{\mathcal{C}}$ into two graphs $\Gamma^1_{\mathcal{C}}$ and $\Gamma^2_{\mathcal{C}}$ as follows.

8.2. The graph $\Gamma^1_{\mathcal{C}}$. It is constructed in two steps. First, consider the maximal subgraph $\Gamma^1_{\mathcal{C}}$ of $\Gamma_{\mathcal{C}}$ which is spanned by the vertices $v \in \mathcal{V}^1(\Gamma_{\mathcal{C}})$ and has no edges of weight 2. Then, corresponding to each cutting edge — whose end-vertices v_1, respectively v_2, carry weights $(1; n, \nu)$ and $(m; n, \nu)$, $m > 1$ —, add an arrowhead decorated with the weight $(m; n, \nu)$, and connect it to v_1 by an edge. In particular, $\Gamma^1_{\mathcal{C}}$ has two types of arrowheads: first, all the arrowheads of $\Gamma_{\mathcal{C}}$ are arrowheads of $\Gamma^1_{\mathcal{C}}$ (all with weight $(1; 0, 1)$), then all the cutting edges provide arrowheads, the first entry of the weight of such an arrowhead satisfies $m > 1$.

If an edge of $\Gamma_{\mathcal{C}}$ with decoration 2 supports an arrowhead v (and the other vertex has weight $(m; 0, 1)$, where $m > 1$ automatically because of Assumption A, cf. (7.3)), then this edge becomes a double arrowhead of $\Gamma^1_{\mathcal{C}}$: an edge supporting two arrowheads (one with weight $(1; 0, 1)$, the other with $(m; 0, 1)$). This double arrowhead forms a connected component of $\Gamma^1_{\mathcal{C}}$.

8.2.1. Deleting some of the information of $\Gamma^1_{\mathcal{C}}$, we obtain another graph $G^1_{\mathcal{C}}$ (which looks like the weighted embedded resolution graph of a germ of an analytic function defined on a normal surface singularity): For any non-arrowhead vertex, or for any arrowhead with decoration $(1;0,1)$, replace the weight $(1;n,\nu)$ by (ν), and keep the genus-decorations of non-arrowheads. The weight $(m;n,\nu)$ of an arrowhead vertex with $m>1$ is replaced by weight (0). Notice also that all the decorations of the edges are 1; they can be replaced by $+$ (hence, they can be deleted by our convention). Finally, we determine the Euler numbers via (5.1.2) using edge–decorations $\epsilon_e=+$.

PROPOSITION 8.2.2. [**48**, (5.27)] *$G^1_{\mathcal{C}}$ is an embedded resolution graph of*

$$V_f^{norm}\xrightarrow{g\circ n}(\mathbb{C},0),$$

where $n:(V_f^{norm},n^{-1}(0))\to(V_f,0)$ is the normalization. In particular, the number of connected components of $\Gamma^1_{\mathcal{C}}$ coincides with the number of irreducible components of the germ $(V_f,0)$. (Here, a connected component of $\Gamma^1_{\mathcal{C}}$ which consists of a double arrowhead, corresponds to a smooth component of V_f^{norm} on which $g\circ n$ is smooth, and which has not been modified during the resolution.)

The arrowheads with multiplicity (0) represent the strict transforms of the singular locus Σ_f.

8.3. The graph $\Gamma^2_{\mathcal{C}}$. Similarly, the 'complementary' subgraph $\Gamma^2_{\mathcal{C}}$ is constructed in two steps as well. First, consider the maximal subgraph of $\Gamma_{\mathcal{C}}$ spanned by the vertices $v\in\mathcal{V}^2(\Gamma_{\mathcal{C}})$. Then, corresponding to each cutting edge (cf. (8.1.2)), whose end-vertices v_1, respectively v_2 carry weights $(1;n,\nu)$ respectively $(m;n,\nu)$, $m>1$, regardless of v_1 being an arrowhead or not, add an arrowhead (and a supporting edge glued to v_2 and decorated by 2). Moreover, decorate this arrowhead with weight $(1;n,\nu)$.

PROPOSITION 8.3.1. [**48**, (5.32)] *There is a one-to-one correspondence between the connected components of $\Gamma^2_{\mathcal{C}}$ and the irreducible components of $(Sing(V_f),0)$.*

Fix an irreducible component Σ_j of $Sing(V_f)$. Define $\mathcal{C}_{\Sigma_j}\subset\mathcal{C}$ as the union of those irreducible components C of $\mathcal{C}$ weighted $(m;n,\nu)$ with $m>1$, for which $C\subset B$ for some component $B\subset\mathbf{D}_c$, such that B is projected via r onto *Σ_j.*

Then $\mathcal{C}_{\Sigma_j}$ is connected and its irreducible components correspond to the non–arrowhead vertices of one of the connected components $\Gamma^2_{\mathcal{C},j}$ of $\Gamma^2_{\mathcal{C}}$.

In fact, besides other data, $\Gamma^2_{\mathcal{C},j}$ contains all the information about the equisingularity type of the transversal singularity $T\Sigma_j$ of Σ_j. In order to formulate this, we need some preparation.

We define on $\mathcal{W}(\Gamma^2_{\mathcal{C},j})$ the following equivalence relation. First, we say that $w_1\sim w_2$ if w_1 and w_2 are connected by an edge of weight 1, then we extend $\sim$ to an equivalence relation. If $K=\{w_{i_1},\dots,w_{i_t}\}$ is an equivalence class (with decorations $(m;n_{i_l},\nu_{i_l})$) then set $\nu(K):=\gcd(\nu_{i_1},\dots,\nu_{i_t})$ and $m(K):=m$. Each class K defines a connected subgraph $G(K)$ of $\Gamma^2_{\mathcal{C},j}$ with vertices from K and 1-edges connecting them.

A new (connected) graph $\Gamma^2_{\mathcal{C},j}/\sim$ is obtained from $\Gamma^2_{\mathcal{C},j}$ by collapsing it along edges of weight 1. More precisely, each subgraph $\Gamma(K)$ is replaced by a non-arrowhead vertex. If two subgraphs $\Gamma(K)$ and $\Gamma(K')$ are connected by k 2-edges in $\Gamma^2_{\mathcal{C},j}$, then the corresponding vertices of $\Gamma^2_{\mathcal{C},j}/\sim$ are connected by k edges. (In fact, it turns out that $k\leq 1$.) If the non-arrowhead vertices of $\Gamma(K)$ support k arrowheads altogether, then on the corresponding non-arrowhead vertex of $\Gamma^2_{\mathcal{C},j}/\sim$ one puts exactly k arrowheads.

PROPOSITION 8.3.2. [**48**, (5.43)] *Let d_j be the degree of the finite map $g|\Sigma_j$. Then there exists an embedded resolution graph $G(T\Sigma_j)$ of the transversal type $T\Sigma_j$ and a cyclic graph covering $p:d_j\cdot G(T\Sigma_j)\to\Gamma^2_{\mathcal{C},j}/\sim$. (Here, $d\cdot G$ means d disjoint copies of G.) Therefore, $\Gamma^2_{\mathcal{C},j}$ is a tree, with all genus decorations zero.*

The covering data is the following. For any non-arrowhead vertex w of $\Gamma^2_{\mathcal{C},j}/\sim$, which corresponds to K, set $\mathfrak{n}_w := \nu(K)$. For any arrowhead vertex v of $\Gamma^2_{\mathcal{C},j}/\sim$, which corresponds to an arrowhead of $\Gamma^2_{\mathcal{C},j}$ with weight $(1;n,\nu)$, set $\mathfrak{n}_v := \nu$. For any edge of $\Gamma^2_{\mathcal{C},j}/\sim$, which comes from a 2-edge e of $\Gamma^2_{\mathcal{C},j}$ with endpoints with weights $(*;n,\nu)$, set $\mathfrak{n}_e := \nu$.

In this way (since $G(T\Sigma_j)$ is connected) one recovers from $\Gamma^2_{\mathcal{C},j}$ the shape of $G(T\Sigma_j)$ and the integer d_j (see also (8.3.3)). The decorations of $\Gamma^2_{\mathcal{C},j}$ (which are the same as the decorations of the embedded resolution graph $G(T\Sigma_j)$, cf. (6.2)) can be obtained as follows. The multiplicity of any vertex in $p^{-1}(w)$, where w corresponds to K, is $m(K)$, while the multiplicities of arrowheads are 1. Finally, the Euler number can be computed via (5.1.2) (with all $\epsilon = +$).

REMARK 8.3.3. In fact, using (6.1.5), we get for any $j \in \{1,\dots,s\}$ that

$$d_j = \gcd(\nu_v)_{v\in\mathcal{W}(\Gamma^2_{\mathcal{C},j})}.$$

Hence, (8.3.2) guarantees that there is a graph covering of connected graphs

$$G(T\Sigma_j) \to \Gamma^2_{\mathcal{C},j}/\sim$$

whose covering data are those presented in (8.3.2) divided by d_j.

8.4. Cutting edges revisited. Consider a *cutting edge* e of $\Gamma_{\mathcal{C}}$, cf. (8.1.2); let the weights of the end–vertices have the form $(\,\cdot\,;n,\nu)$. Fix local coordinates as in (7.2), and set $C^*_e := B^l_1 \cap B^l_2$. Then $r|C^*_e : C^*_e \to \Sigma_j$ is finite. Denote its degree by $d(e)$. Obviously $deg(r|C^*_e)\cdot deg(g|\Sigma_j) = deg(g\circ r|C^*_e) = \nu$, hence $d(e)\cdot d_j = \nu$.

Since d_j and ν can be obtained from $\Gamma_{\mathcal{C}}$ (cf. (8.3)), the degree $d(e)$ can also be recovered from $\Gamma_{\mathcal{C}}$.

For every fixed j, let $\mathcal{E}_{cut,j}$ be the set of cutting edges connecting $\Gamma^2_{\mathcal{C},j}$ with $\Gamma^1_{\mathcal{C}}$. Also, write $\#T\Sigma_j$ for the number of local irreducible components of $T\Sigma_j$, which coincides with the number of connected components of $\partial F'_j$.

The point is that $\#(T\Sigma_j) \geq |\mathcal{E}_{cut,j}|$, and, in general, the equality does not hold. Indeed, each $e \in \mathcal{E}_{cut,j}$ is 'responsible' for $d(e)$ local irreducible component of $T\Sigma_j$, and

$$\#T\Sigma_j = \sum_{e\in\mathcal{E}_{cut,j}} d(e). \tag{8.4.1}$$

The above identity can also be interpreted as follows. The vertical (transversal type) monodromy $m'_{j,ver}$ permutes the connected components of $\partial F'_j$; each orbit corresponds to a cutting edge $e \in \mathcal{E}_{cut,j}$, and the length (cardinality) of the corresponding orbit is $d(e)$.

8.5. Why work with $\mathcal{C}$? Let $\Phi : U \to \mathbb{C}^2$, $\Phi(\Sigma_f) = \Delta_1 = \{c = 0\}$ be as in (4.1). Similarly as above, (c,d) are the coordinates of the target. For any integer $M > 0$, we define the 'wedge set' of Δ_1 by

$$\mathsf{W}_{\eta,M} = \{(c,d) \in D^2_\eta \mid 0 < |c| < |d|^M\}.$$

One verifies that $\mathsf{W}_{\eta,M} \subset D^2_\eta \setminus \Delta_\Phi$ for $M \gg 0$. Moreover (cf. [**48**, (5.5)]),

$$\overline{\widetilde{\Phi}^{-1}(\mathsf{W}_{\eta,M})} \cap \widetilde{\Phi}^{-1}(0) = \mathcal{C}. \tag{8.5.1}$$

Therefore, one expects, that from the dual graph $\Gamma_{\mathcal{C}}$ of the special curve configuration $\mathcal{C}$ (endowed with all the necessary multiplicity data), one is able to extract topological information about $r^{-1}(S)$ for all sets $\mathcal{S} \subset (\mathbb{C}^3,0)$ with $\Phi(\mathcal{S}) \subset \mathsf{W}_{\eta,M}$.

Notice that $\Phi^{-1}(\partial D_\delta)$, or even $\Phi^{-1}(T_\delta)$ (cf. (4.1)), is such a space! Hence, $\mathsf{W}_{\eta,M}$ should contain crucial information regarding ∂F and its Milnor monodromy too. This fact is exploited in the present article.

The identity (8.5.1) has the following consequence:

COROLLARY 8.5.2.

a) For any open (tubular) neighbourhood $T(\mathcal{C}) \subset V^{emb}$*, there exist a sufficiently large* M *and a sufficiently small* η *such that for any* $(c,d) \in \mathsf{W}_{\eta,M}$ *the "lifted Milnor fibre"* $\widetilde{\Phi}^{-1}(c,d)$ *is in* $T(\mathcal{C})$*.*

b) For any $p \in \mathcal{C}$ *and local neighbourhood* U_p *of* p*, there exist a sufficiently large* M *and a sufficiently small* η *such that for any* $(c,d) \in \mathsf{W}_{\eta,M}$ *one has* $U_p \cap \widetilde{\Phi}^{-1}(c,d) \neq \emptyset$*.*

8.5.3. In this way, the curve $\mathcal{C}$ as a 'limit of the lifted Milnor fiber', provides a natural decomposition of $\widetilde{F}_\Phi := r^{-1}(F_\Phi)$, or of F_Φ.

Indeed, for each edge e of $\Gamma_{\mathcal{C}}$, let P_e be the corresponding intersection point of two components of $\mathcal{C}$. Let U_{P_e} be a small neighbourhood of P_e. Then the lifted Milnor fiber $\widetilde{F}_\Phi = \widetilde{\Phi}^{-1}(c,d)$ (with (c,d) as in (8.5.2)(b)) intersects U_{P_e} in a tubular neighbourhood of some embedded circles of $\widetilde{F}_\Phi$. Consider the collection E of all these type of circles. Then $\widetilde{F}_\Phi$ is a union of type

$$\bigcup_{v \in \mathcal{V}(\Gamma_{\mathcal{C}})} \widetilde{F}_v, \tag{8.5.4}$$

where each $\widetilde{F}_v$ is sitting in a tubular neighbourhood of the corresponding component C_v of $\mathcal{C}$. Moreover, both horizontal and vertical monodromy actions over the torus T_δ (cf. (4.1)) may be chosen in such a way that they preserve the cutting circles E and their restrictions on each $\widetilde{F}_v$ are isotopic to a pair of finite actions which commute. (This last fact follows from the fact that any S^1–bundle over a non-closed Riemann surface is trivial, and from the form of the local equations of f and g near C_v, cf. (7.2).)

CHAPTER V

Examples for $\Gamma_{\mathcal{C}}$

§ 9. Singularities associated with plane curve singularities

9.1. Cylinders of plane curve singularities. Consider $f(x, y, z) = f'(x, y)$ and $g(x, y, z) = z$, where $f' : (\mathbb{C}^2, 0) \to (\mathbb{C}, 0)$ is an isolated plane curve singularity. Replacing the quadratic transformations of the infinitely near points of $0 \in \mathbb{C}^2$ by blowing ups along the 1–dimensional axis (namely, the corresponding local z–axis), one obtains the following. Let $\Gamma(\mathbb{C}^2, f')$ denote the minimal embedded resolution graph of the plane curve singularity $f' : (\mathbb{C}^2, 0) \to (\mathbb{C}, 0)$. Recall that (besides the Euler numbers and genera of the non–arrowheads) each vertex has a multiplicity decoration (m), the vanishing order of the pull-back of f' along the corresponding irreducible curve.

Then, one can get a possible dual graph $\Gamma_{\mathcal{C}}$ from $\Gamma(\mathbb{C}^2, f')$ via the following conversion:

The shape of $\Gamma_{\mathcal{C}}$ is the same, only the decorations are modified: the Euler numbers are deleted, while for each vertex the multiplicity (m) is replaced by $(m; 0, 1)$. The genus decorations in $\Gamma_{\mathcal{C}}$ (similarly as in $\Gamma(\mathbb{C}^2, f')$) of all non-arrowheads are zero. Moreover, all edges in $\Gamma_{\mathcal{C}}$ have weight 2.

Example 9.1.1. Let $f(x, y, z) = f'(x, y) = (x^2 - y^3)(y^2 - x^3)$. Then $\Gamma(\mathbb{C}^2, f')$ is:

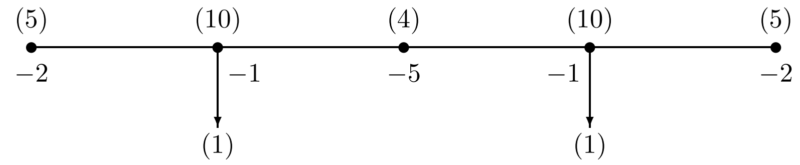

which is transformed into $\Gamma_{\mathcal{C}}$:

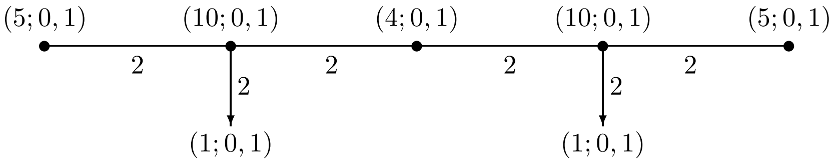

9.1.2. It is easy to verify that $\Gamma^2_{\mathcal{C}} = \Gamma_{\mathcal{C}}$, and $\Gamma^1_{\mathcal{C}}$ consists of $\#\mathcal{A}$ double arrows, where $\#\mathcal{A}$ is the number of irreducible components of f'. The statements of (8.2) and (8.3) can easily be verified.

9.2. Germs of type $f = zf'(x, y)$**.** Here $f' : (\mathbb{C}^2, 0) \to (\mathbb{C}, 0)$ is an isolated plane curve singularity as above, $f(x, y, z) := zf'(x, y)$ and g is a generic linear form in (x, y, z).

For this family we found no nice uniform presentation of $\Gamma_{\mathcal{C}}$ (with similar simplicity and conceptual conciseness as in (9.1)) (compare also with the second paragraph of (9.3.1)). Since the boundary 3–manifold ∂F can be determined completely and rather easily for any $f = zf'(x, y)$ by another method, see § 26, we decided to omit general technical graph–presentations here. Nevertheless, particular testing examples can be determined without big difficulty, e.g. we will provide $\Gamma_{\mathcal{C}}$ for $f' = x^{d-1} + y^{d-1}$ (when f becomes homogeneous, a case which is treated in § 10 uniformly with highest generality), or for $f' = x^2 + y^3$ below. For more comments (and mysteries) regarding the possible graphs $\Gamma_{\mathcal{C}}$, see (26.1.7).

EXAMPLE 9.2.1. Assume that $f = z(x^2 + y^3)$ and take g to be a generic linear form. The 'ad hoc blowing up procedure' (using the 'naive' principle to blow up the 'worst singular locus') provides the following $\Gamma_{\mathcal{C}}$ (where we marked the 2–edges, all the others are 1–edges):

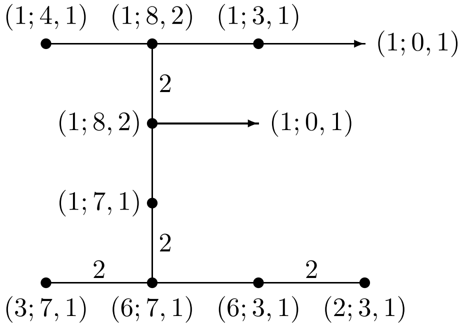

9.3. (Double) suspensions. Suspension singularities have the form $f(x, y, z) = f'(x, y) + z^d$, where $f' : (\mathbb{C}^2, 0) \to (\mathbb{C}, 0)$ is a *non–isolated* plane curve singularity. When $d = 2$ the germ is called double–suspension. When f' is not very complicated, one might find a convenient resolution by 'ad hoc' blow ups, such as in the following case:

EXAMPLE 9.3.1. Assume that $f = x^2y + z^2$ and $g = x + y$. Then a possible $\Gamma_{\mathcal{C}}$ is:

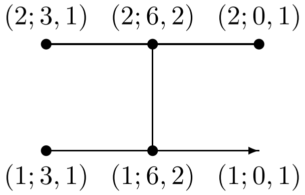

Of course, for the general family, we need a more conceptual and uniform procedure. In general, when determining $\Gamma_{\mathcal{C}}$, the construction of an embedded resolution r (cf. (7.1.1)) is not always simple, and it might depend essentially on the choice of the germ g as well. Ideally, for any f it would be nice to find a germ g such that the pair (f, g) would admit a resolution r which reflects *only* the geometry of f (e.g. it is a 'canonical', or 'minimal' embedded resolution of V_f; but unfortunately, in general, such a resolution does not work since the strict transform of g may still have 'bad contacts' with the created exceptional divisors).

Nevertheless, for double suspensions $f = f' + z^2$, if one constructs a 'canonical' resolution using the classical Abhyankar–Jung construction fitting with the shape of f (i.e. based on the projection on the (x, y)–plane, and used in the construction of suspension isolated singularities in [**44**] as well), the obtained embedded resolution will be compatible with g too, provided that we take for g the generic linear form. We expect that a similar phenomenon is valid for arbitrary suspensions as well.

Since the embedded resolution of double suspensions is already present in the literature, cf. [**4**], this case can be exemplified without too much extra work (nevertheless, the computations are not trivial, and their verification will require some effort from the reader, and familiarity with [**4**]). In the sequel we present the main steps needed to understand the procedure, we provide some examples, and we let the reader explore his/her favourite example. To the general case ($d > 2$) we will return back later in a forthcoming work.

We prefer to write g as $g'(x,y) + z$, where g' is a generic linear form (with respect to f') in variables (x, y).

The embedded resolution of $(fg)^{-1}(0) \subset (\mathbb{C}^3, 0)$ is constructed in several steps, which are summarized in the following diagram:

$$\begin{tikzcd}
\tilde{X} \arrow[r, "r"] & X \arrow[r, "\Phi'"] \arrow[d, "p'"'] & U^3 \arrow[d, "p"] & \supset (fg)^{-1}(0) \\
 & Z \arrow[r, "\Phi"] & U^2 & \supset (f'g')^{-1}(0)
\end{tikzcd}$$

where

1. U^3 is a small representative of $(\mathbb{C}^3, 0)$ and $p : U^3 \to U^2$ is induced by the projection $(x, y, z) \to (x, y)$.
2. $\Phi : Z \to U^2$ is a 'good' embedded resolution of $((f'g')^{-1}(0), 0) \subset (\mathbb{C}^2, 0)$. Each irreducible component D of the exceptional divisor and of the strict transform has two nonnegative integers attached to it: the multiplicity (vanishing order) $m(f')$, respectively $m(g')$ of f', respectively g', along that component.

   We take the minimal good embedded resolution modified as in [**4**, (3.1)]: we assume that there are no pairs of irreducible components D_i, D_j with $(D_i, D_j) \neq 0$ and both multiplicities $m_i(f), m_j(f)$ odd. (This can always be achieved by an additional blow up.)
3. $p' : X \to Z$ is the pull-back of $p : U^3 \to U^2$ via Φ. Note that X is smooth. Let $T = (\Phi')^{-1}((fg)^{-1}(0))$ be the total transform of $(fg)^{-1}(0)$ in X. In fact, by construction, both strict transforms of V_f and V_g are smooth (but the transversality of the components might not be satisfied).
4. r is the 'embedded resolution' of $(\Phi')^{-1}(V_f) \subset X$ as described in [**4**, (3.4)] (which associates 'towers' of exceptional — ruled — surfaces over each exceptional divisor in Z).

The point is that if we follow the convention of [**4**, (3.4)], namely that one constructs *first* the 'towers' above irreducible curves of the exceptional divisor in Z with *even* multiplicity $m(f)$, then r automatically provides an 'embedded resolution' of the total transform $T = (\Phi')^{-1}(V_f \cup V_g) \subset X$ as well.

It is important to note that, as explained in the Introduction of [**4**], $\Phi' \circ r : \tilde{X} \to U^3$ obtained this way is only an isomorphism above $U^3 - \{x = y = 0\}$, and not above $U^3 - \{0\}$. In particular, the Milnor fiber of f is not lifted diffeomorphically under this modification (it is blown up in the intersection points of $F_{\epsilon,\delta}$ with the z–axis). Nevertheless, as the boundary $\partial F_{\epsilon,\delta}$ has no intersection points with the z–axis provided that $\delta \ll \epsilon$, this modification serves in this procedure as a genuine embedded resolution.

The above strategy leads to a combinatorial algorithm in two steps. In *Step 1* one determines the embedded resolution graph $\Gamma_{f'g'}$ (weighted with both multiplicities of f' and g') of the plane curve singularity $(f'g')^{-1}(0) \subset (\mathbb{C}^2, 0)$; and in *Step 2* one reads from the 'towers' provided by [**4**] the graph $\Gamma_{\mathcal{C}}$ of (f, g), which appears as a 'modified covering' of $\Gamma_{f'g'}$. (However, one needs to carry in all the towers the multiplicities of g as well. Also, in certain cases, the genera of the projective irreducible components C of the special curve configuration $\mathcal{C}$ may be difficult to determine from the *local* equations of C. However, if the link of the normalization of V_f is a rational homology sphere, then we can be sure that in $\Gamma_{\mathcal{C}}$ all the genus decorations are zero, cf. (8.2.2) and (8.3.2) — as it happens in all the examples worked out in this section.)

EXAMPLE 9.3.2. Assume that $f'(x,y)=x^ay^b$. There are three cases that need to be distinguished, depending on the parity of a and b.

CASE 1. If both a and b are even, that is $f(x,y)=x^{2n}y^{2m}$, and $g'=x+y$, then by *Step 1* the dual graph of the minimal good embedded resolution of the plain curve singularity $\{f'g'=0\}\subset(\mathbb{C}^2,0)$ (with weights as above) is

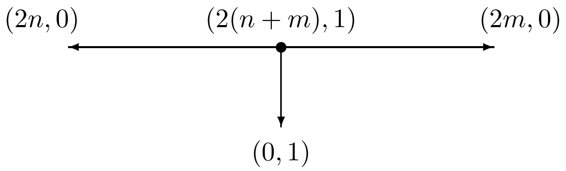

By *Step 2*, a possible graph $\Gamma_{\mathcal{C}}$ of (f,g) is:

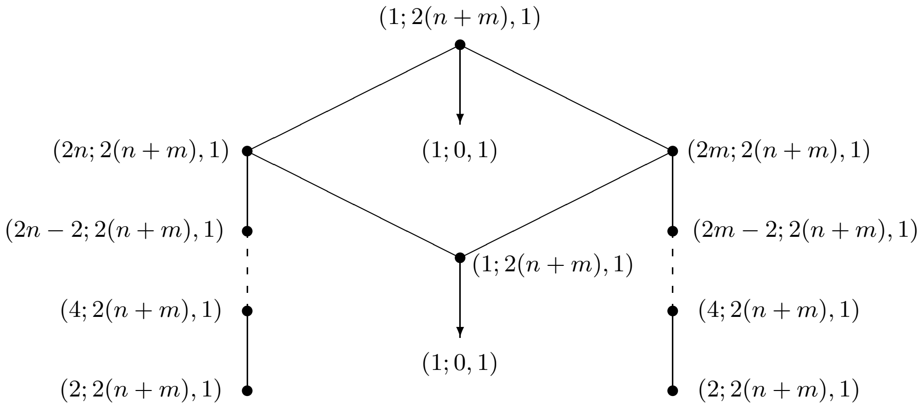

CASE 2. If a is even and b is odd, that is $f(x,y)=x^{2n}y^{2m+1}$, and $g'=x+y$, then by *Step 1* one gets the graph:

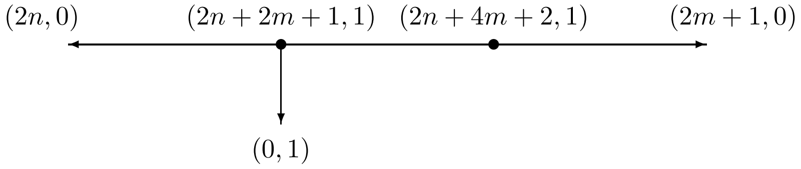

(Here the assumption of not having adjacent irreducible components with both multiplicities $m_i(f), m_j(f)$ odd is taken into account.)

By *Step 2*, a possible universal graph $\Gamma_{\mathcal{C}}$ of (h,g) is:

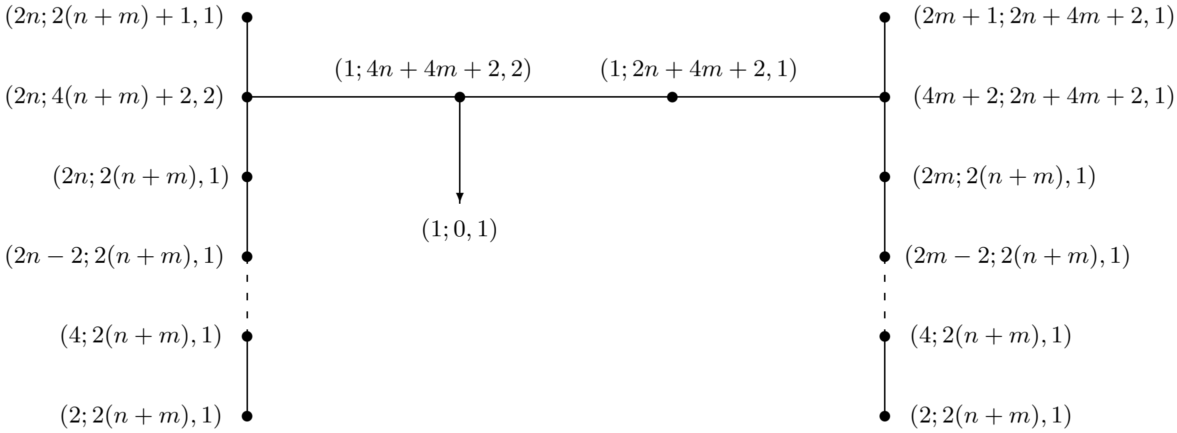

CASE 3. Finally, if both a and b are odd, that is $f(x,y) = x^{2n+1}y^{2m+1}$, and $g' = x + y$, then *Step 1* produces the graph:

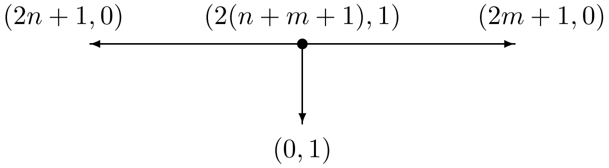

While a possible graph $\Gamma_{\mathcal{C}}$ is:

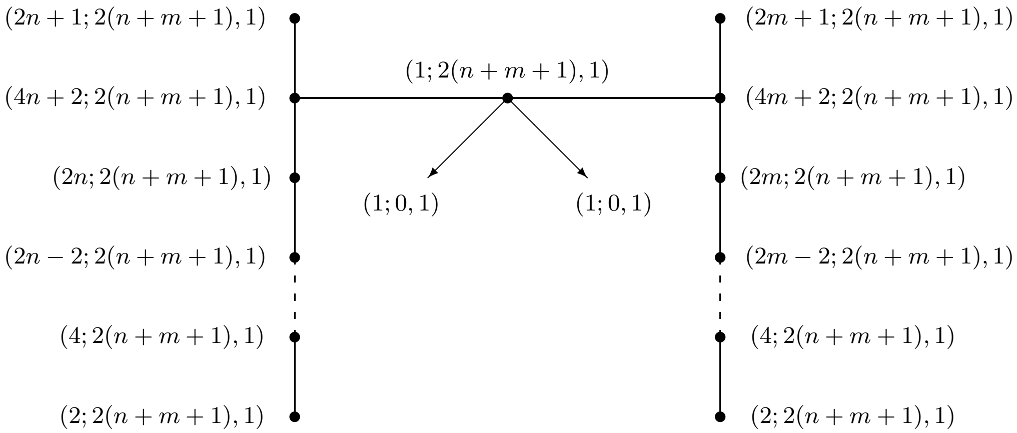

Example 9.3.3. Consider the infinite family $T_{a,2,\infty}$, i.e. $f(x,y,z) = x^a + y^2 + xyz$ with $a \geq 3$. This expression, by completing the square and renaming variables, can be brought to the form $f(x,y,z) = x^2(x^{a-2} + y^2) + z^2$. In particular, the previous method can be used with $g(x,y,z) = x + y + z$.

Step 1: The dual graph of the minimal good embedded resolution of the plain curve singularity $\{f'g' = 0\} \subset (\mathbb{C}^2, 0)$ with $f' = x^2(x^{a-2} + y^2)$ and $g' = x + y$, for $a = 2k + 3$, $k \geq 1$ is

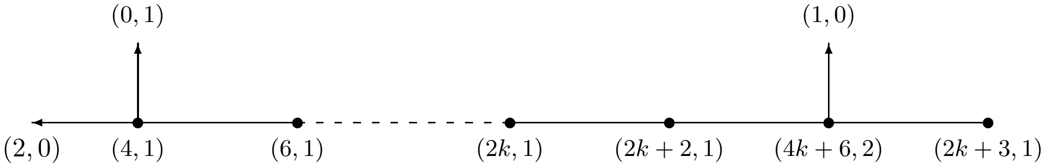

Step 2: A possible $\Gamma_{\mathcal{C}}$ for (f, g) is:

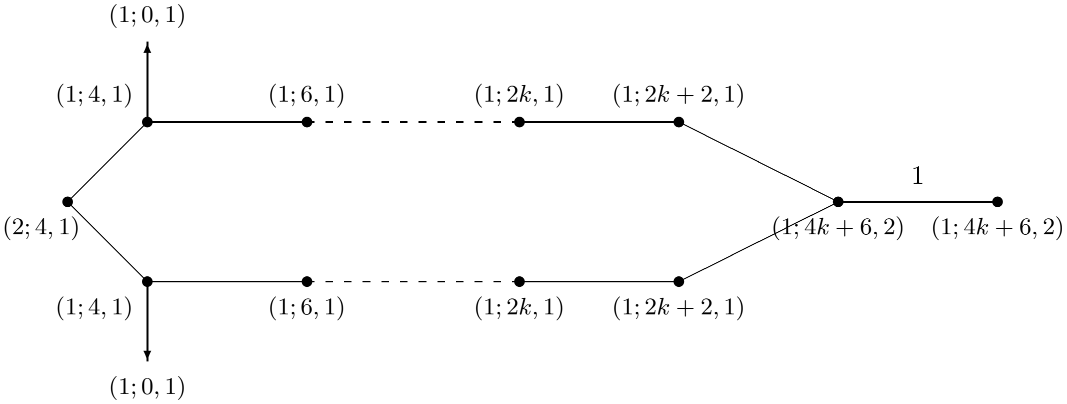

For $k = 0$ (i.e. for $a = 3$), *Step 1* of the Abhyankar-Jung method provides

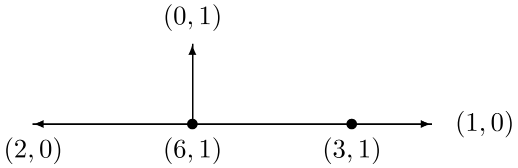

'covered' by the graph $\Gamma_{\mathcal{C}}$:

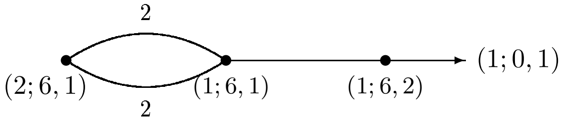

(For an alternative universal graph with different g, see (9.4.3).)

In case $a = 2k$, $k \geq 3$, *Step 1* provides

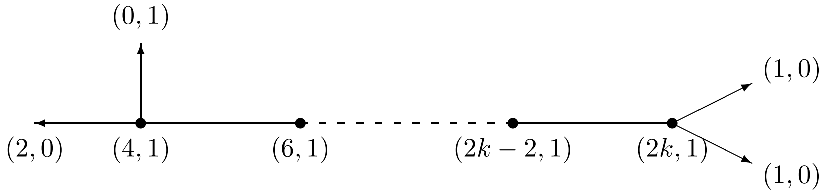

and a possible universal graph $\Gamma_{\mathcal{C}}$ is the 'covering'

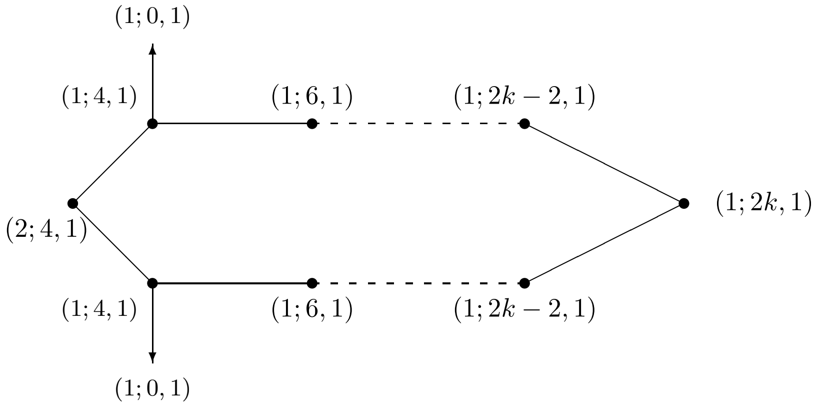

For $k = 2$ (that is $a = 4$) *Step 1* gives

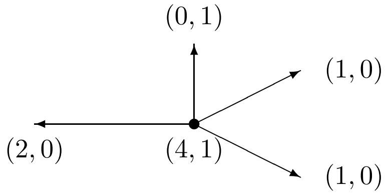

while *Step 2* provides

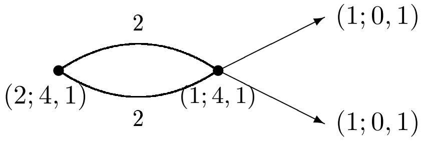

EXAMPLE 9.3.4. Consider the family $f(x, y, z) = x^a y(x^2 + y^3) + z^2$ with $a \geq 2$ and $g = x + y + z$. Again, we need to consider two cases depending on parity of a.

When a is even, and taking into account, that no neighbouring vertices can have both multiplicities of f' to be odd, *Step 1* gives for $f'g'$:

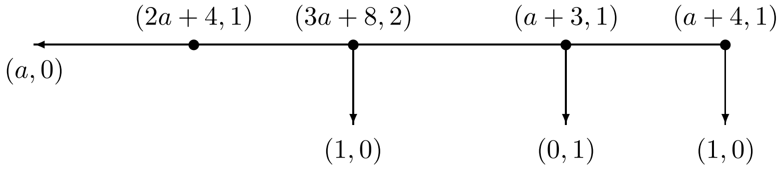

Step 2 provides

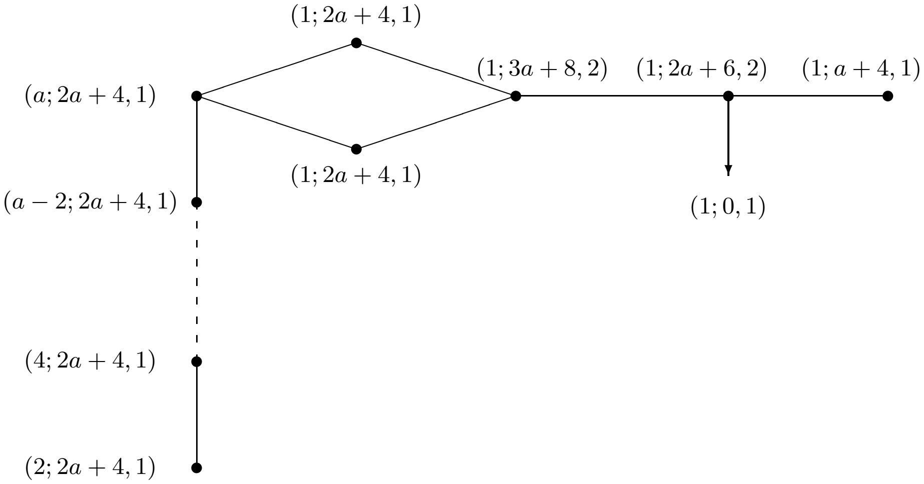

When a is odd, and again taking into account, that no neighbouring vertices can have both multiplicities of f' to be odd, *Step 1* gives for $f'g'$:

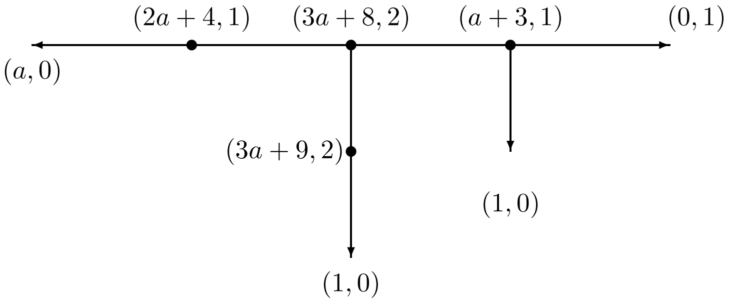

while *Step 2* provides

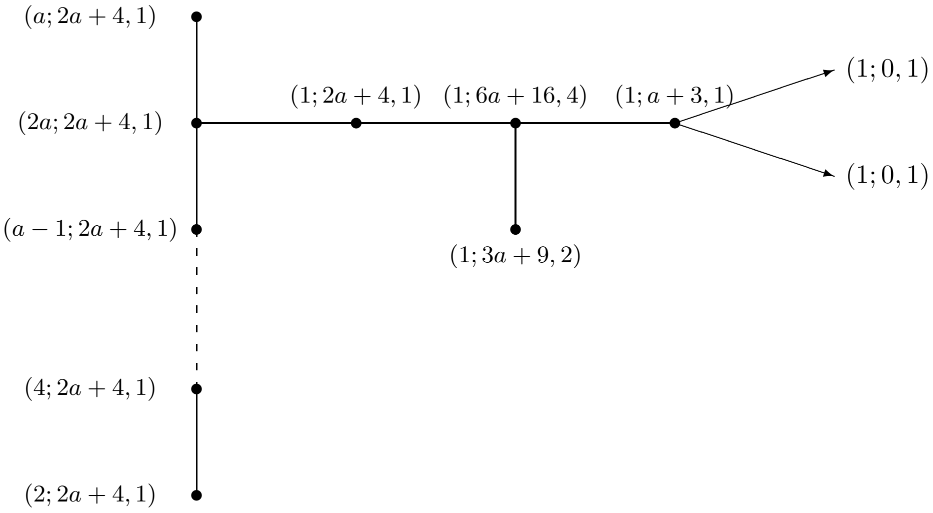

Example 9.3.5. The procedure (9.3.2) has a natural generalization for certain suspensions. E.g., consider $f(x,y,z)=x^{md}y^{nd}+z^d$, $g(x,y,z)=x+y+z$, hence $f'(x,y)=x^{dn}y^{dm}$, and $g'=x+y$. By *Step 1* the dual graph of the minimal good embedded resolution of the plain curve singularity $\{f'g'=0\}\subset(\mathbb{C}^2,0)$ (and 'double-multiplicity' weights as above) is

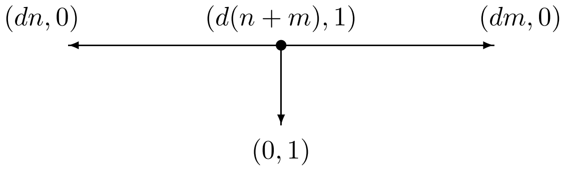

Finally, by *Step 2*, a possible graph $\Gamma_{\mathcal{C}}$ of (f,g) is:

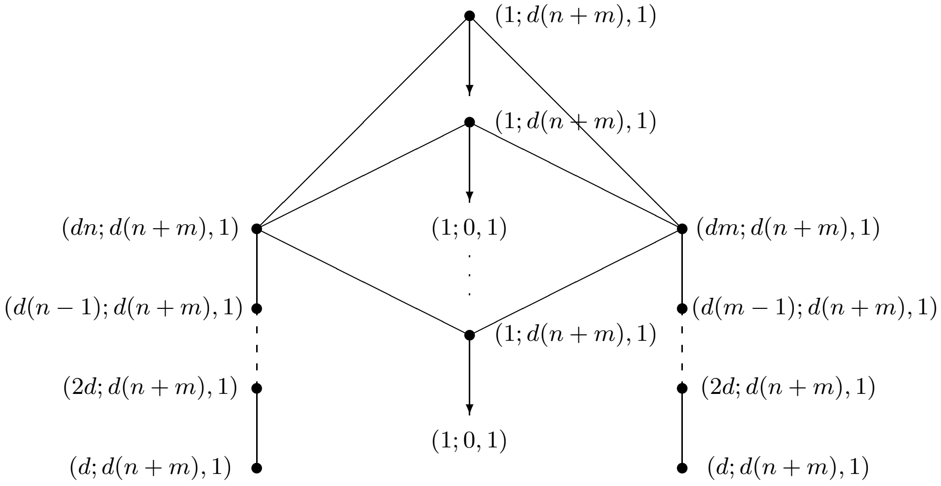

where in the middle column there are d vertices.

For another suspension case, see (11.1.1).

9.4. The $T_{a,*,*}$–family.

9.4.1. **The $T_{a,\infty,\infty}$–family.** Let $f=x^a+xyz$ and set $g=x+y+z$.

If $a=2k+1$, $k>1$, then a possible universal graph is:

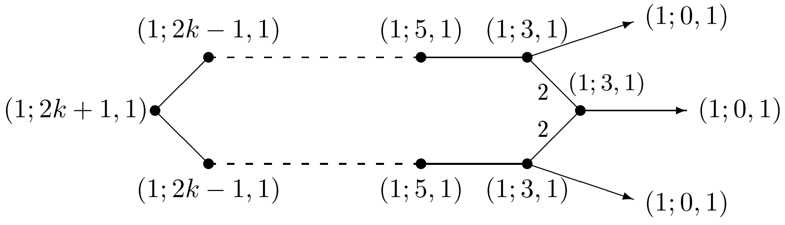

Above, all unmarked edges have weight 1.

The resolution process was started by a blow-up at the origin. Since $f=x^{2k+1}+xyz=x(x^{2k}+yz)$, there is only one singularity remaining, of the form $\{t^{2k-2}+sr=0\}$. It is resolved by a series of blow-ups at infinitely near points, resulting in the above graph.

When $a = 3$ (homogeneous case) a single blow-up at the origin suffices and we get

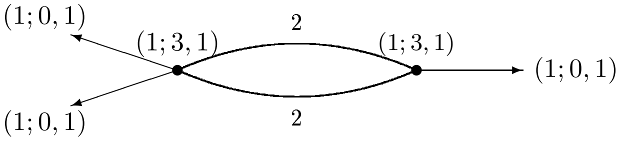

Set now $a = 2k$, $k > 2$. The same strategy for the resolution as above can be followed. However, when the strict transform of f becomes smooth, it is not in normal crossing with the exceptional divisors. Additional two blow-ups along singular axes lead to the following universal graph:

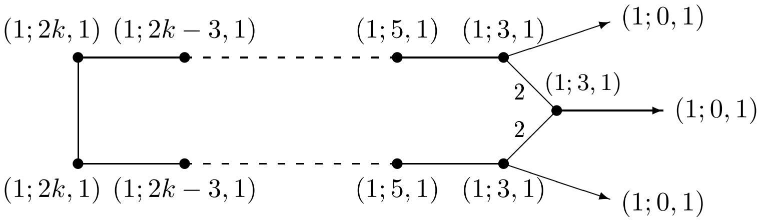

(All unmarked edges have weight 1, as before.)

Finally, in case $a = 4$ the previous resolution 'strategy' leads to

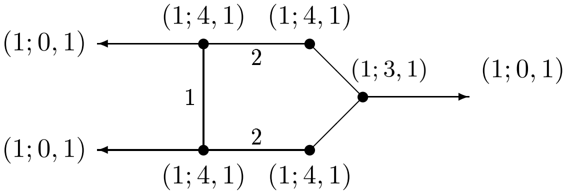

9.4.2. **The $T_{a,2,\infty}$–family (again).** Set $f(x, y, z) = x^a + y^2 + xyz$.

The cases $a = 3$ and $a = 5$ (with $g = z$) already were considered in [**48**], where $\Gamma_{\mathcal{C}}$ was obtained using alternative/ad hoc resolution. The graphs $\Gamma_{\mathcal{C}}$ thus obtained will serve as clarifying examples for several geometric discussions in this work as well. Their graphs are the following:

Example 9.4.3. If $f = x^3 + y^2 + xyz$ and $g = z$ then a possible $\Gamma_{\mathcal{C}}$ is:

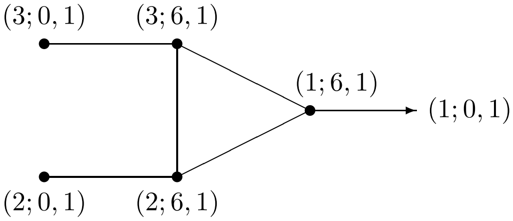

Example 9.4.4. If $f = x^5 + y^2 + xyz$ and $g = z$ then a possible $\Gamma_{\mathcal{C}}$ is:

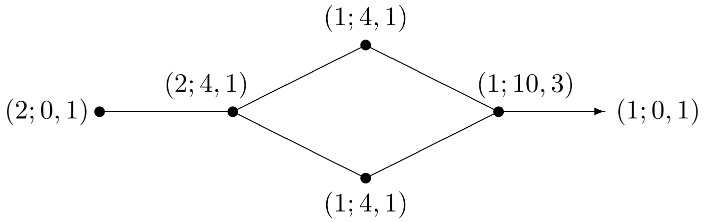

The general case (i.e. arbitrary $a \geq 3$), with $g = x+y+z$, is clarified in (9.3.3). (Notice that in the above two examples and in (9.3.3) we used different g's and different sequences of blow ups; in particular, the output graphs are also different.)

§ 10. Homogeneous singularities

10.1. The general case. Assume that f is a homogeneous polynomial of degree d, and we choose g to be a generic linear function (with respect to f).

Let $C \subset \mathbb{CP}^2$ be the projective plane curve $\{f = 0\}$. We show that a possible graph $\Gamma_{\mathcal{C}}$ can easily be determined from the combinatorics of the components of C and the topological types of its local singularities.

Let $C = \cup_{\lambda \in \Lambda} C_\lambda$ be the irreducible decomposition of C, and set $d_\lambda := \deg(C_\lambda)$ (hence $\sum_\lambda d_\lambda = d$). Furthermore, let g_λ be the genus of (the normalization of) C_λ.

Let $\{P_j\}_{j \in \Pi}$ be the set of singular points of C. (Following notations of (3.2), $\Pi = \{1, \ldots, s\}$). Assume that the local irreducible components of (C, P_j) are $(C_{j,i}, P_j)_{i \in I_j}$. Clearly, there is an 'identification map' of global/local components $c : \cup_j I_j \to \Lambda$ which sends the index of a local component $C_{j,i}$ into the index λ whenever $C_{j,i} \subset C_\lambda$.

Let Γ_j be the minimal embedded resolution graph of the local plane curve singularity $(C, P_j) \subset (\mathbb{C}^2, P_j)$. (This is the same as $G(T\Sigma_j)$ of (8.3.2).) It has $|I_j|$ arrowheads (each with multiplicity (1)).

PROPOSITION 10.1.1. *A possible* $\Gamma_{\mathcal{C}}$ *is constructed from the dual graphs* $\{\Gamma_j\}_{j \in \Pi}$ *and* $|\Lambda|$ *additional non–arrowhead vertex as follows:*

First, for each $\lambda \in \Lambda$ *put a non–arrowhead vertex* v_λ *in* $\Gamma_{\mathcal{C}}$ *and decorate it with* $(1; d, 1)$ *and* $[g_\lambda]$*. Moreover, put* d_λ *edges supported by* v_λ*, each of them decorated by 1 and supporting an arrowhead weighted by* $(1; 0, 1)$.

Then, consider each graph Γ_j*, keep its shape, but replace the decoration of each non–arrowhead with multiplicity* (m) *by the new decoration* $(m; d, 1)$*, and decorate all edges by 2. Furthermore, each arrowhead of* Γ_j*, corresponding to the local component* $C_{j,i}$*, is identified with* $v_{c(j,i)}$.

PROOF. One performs the following sequence of blow ups. First one blows up the origin of $\mathbb{C}^3$. This creates an exceptional divisor $E = \mathbb{CP}^2$ which intersects the strict transform $St(V_f)$ of V_f along C. Moreover, the strict transform of the generic linear function intersects the strict transform of each irreducible component $V(f)_\lambda$ in d_λ discs.

The singular part of $St(V_f)$ consists of discs meeting E in the singular points P_j of C. Then we blow up these infinitely near discs following the blowing up procedure of the corresponding plane curve singularity (such as in the cylinder case). □

REMARK 10.1.2. Notice that if a local graph Γ_j is a double–arrow (representing a local singularity of type A_1) and both local irreducible components sit on the same global component C_λ, then by the above procedure the double arrow transforms into a loop supported on v_λ decorated by 2. If the two local irreducible components sit on two different global components, then it becomes a 2–edge. In both cases, the corresponding edge will not satisfy Assumption A (7.3).

Nevertheless, if we consider embedded resolution graphs Γ_j with at least one non-arrowhead vertex (e.g. the graphs of A_1 singularities will have one (-1)-vertex), then the graph $\Gamma_{\mathcal{C}}$ obtained in this way will satisfy Assumption A (and will be related with the previous one by the moves of (7.3)).

Example 10.1.3. If $f = z^d - xy^{d-1}$ with $d \geq 3$, then $\Gamma_{\mathcal{C}}$ is the following:

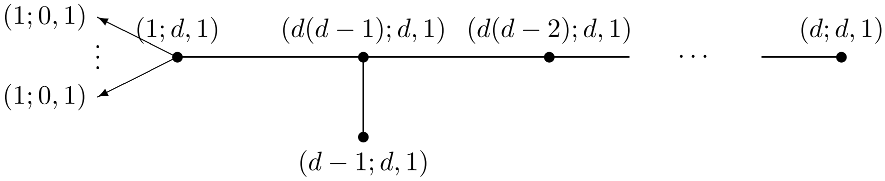

where there are d arrowheads, and all the edges connecting non–arrowheads have decoration 2.

Example 10.1.4. Assume that $f = x^2y^2 + y^2z^2 + z^2x^2 - 2xyz(x+y+z)$. Then C is an irreducible rational curve with three A_2 singularities. Therefore, $\Gamma_{\mathcal{C}}$ is:

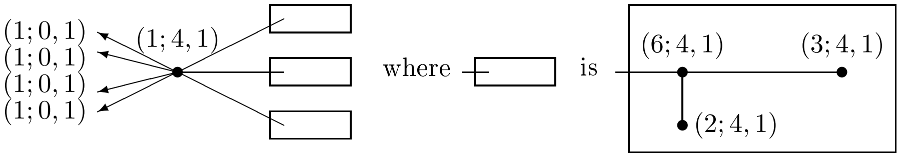

Example 10.1.5. Let $f = x^d + y^d + xyz^{d-2}$, where $d \geq 3$. Then (a possible) $\Gamma_{\mathcal{C}}$ (which does not satisfy Assumption A) is:

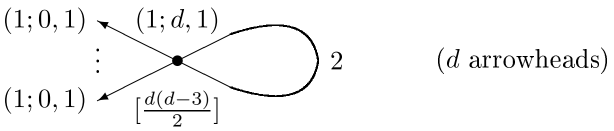

Its modification (cf. (7.3) and (10.1.2)) which satisfies Assumption A is:

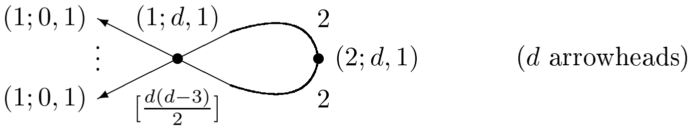

Remark 10.1.6. Consider a Zariski pair (C_1, C_2). This means that the two irreducible projective curves C_1 and C_2 have the same degree and the topological type of their *local* singularities are the same, while their embeddings in the projective plane are topologically different. Then the two graphs $\Gamma_{\mathcal{C}}(C_1)$ and $\Gamma_{\mathcal{C}}(C_2)$ provided by the above algorithm will be the same. In particular, any invariant derived from $\Gamma_{\mathcal{C}}$ (e.g., invariants of ∂F) will not differentiate Zariski pairs.

10.2. Line arrangements. A special case of (10.1) is the case of line arrangements in $\mathbb{CP}^2$, when each connected component of C is a line. For such an arrangement, let $\{L_\lambda\}_{\lambda\in\Lambda}$ be the set of lines, and $\{P_j\}_{j\in\Pi}$ the set of intersection points. Write $|\Lambda| = d$, and for each j set $m_j := \#\{L_\lambda : L_\lambda \ni P_j\}$. Then $\Gamma_{\mathcal{C}}$ can be constructed as follows:

For each $\lambda \in \Lambda$ put a non–arrowhead vertex v_λ with weight $(1;d,1)$. For each $j \in \Pi$ put a non–arrowhead vertex v_j with weight $(m_j;d,1)$. Join the vertices v_λ

and v_j with a 2–edge whenever $P_j \in L_\lambda$. Finally, put on each vertex v_λ an edge with decoration 1, which supports an arrowhead with weight $(1;0,1)$.

Notice that v_j is connected with m_j vertices of type v_λ. Clearly, v_j corresponds to the exceptional divisor obtained by blowing up an intersection point of m_j lines. (Notice that if in the special case of $m_j = 2$ — i.e. when P_j sits only on L_{λ_1} and L_{λ_2} —, this blow up is imposed by Assumption A, cf. (7.3). Nevertheless, if we wish to neglect Assumption A, then this vertex v_j can be deleted together with the two adjacent edges, and one can put only one 2–edge connecting v_{λ_1} with v_{λ_2}).

Example 10.2.1. In the case of the A_3 arrangement $f = xyz(x-y)(y-z)(z-x)$, the two graphs $\Gamma_{\mathcal{C}}$ (satisfying Assumption A or not) are:

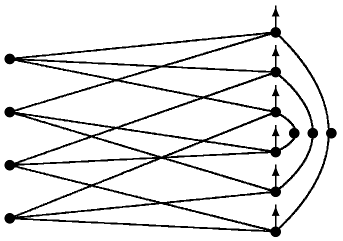

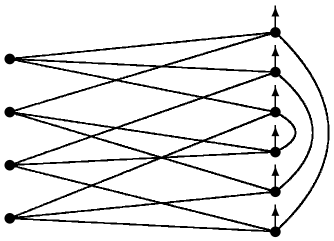

where in the left hand graph the four left-vertices are weighted by $(3;6,1)$, the next six by $(1;6,1)$, the remaining three by $(2;6,1)$, and the arrowheads by $(1;0,1)$. The edges supporting arrowheads are decorated by 1, the others by 2.

Example 10.2.2. The (simplified) graph $\Gamma_{\mathcal{C}}$ (which does not satisfy Assumption A) for the generic arrangement with d lines consists of d vertices v_λ, each decorated with $(1;d,0)$, each supporting an arrow $(1;0,1)$, and any pair of non–arrowheads is connected by a 2–edge.

§ 11. Some sporadic cases

11.1. In this section we list some additional examples, which will be used in the sequel in order to exemplify specific questions, problems as part of the theory.

Example 11.1.1. By similar way, one gets for $f = x^3y^7 - z^4$ and $g = x + y + z$ the following graph $\Gamma_{\mathcal{C}}$:

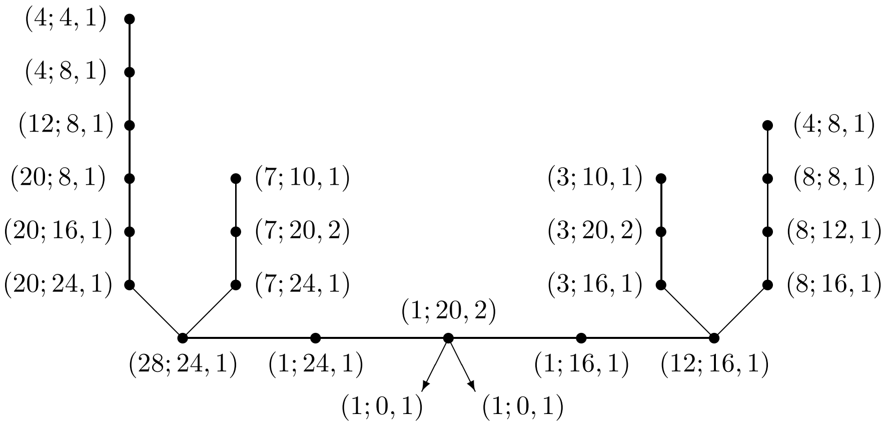

Example 11.1.2. Assume that $f = x^2y^2 + z^2(x + y)$ and take $g = x + y + z$. Then a possible $\Gamma_{\mathcal{C}}$ is:

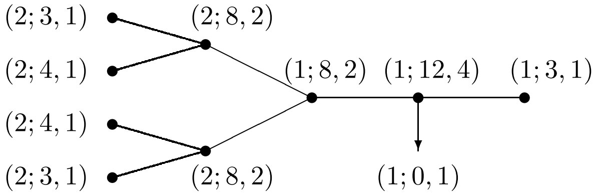

EXAMPLE 11.1.3. Assume that $f = y^3 + (x^2 - z^4)^2$ and $g = z$. Then a possible $\Gamma_{\mathcal{C}}$ is:

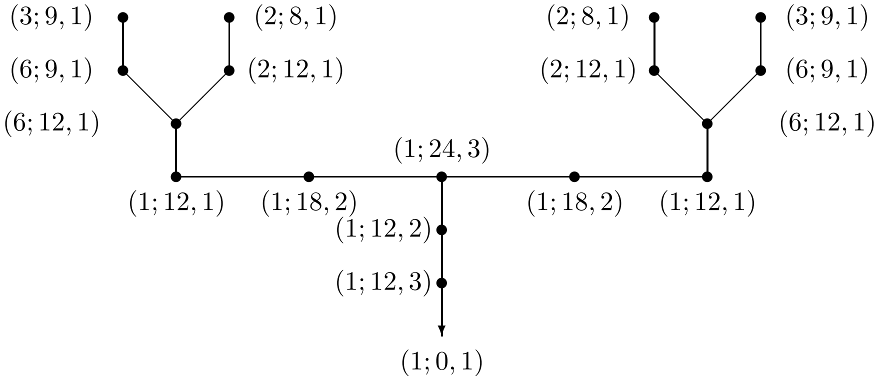

CHAPTER VI

Plumbing graphs from $\Gamma_{\mathcal{C}}$

§ 12. The Main Algorithm

12.1. The goal of the section. The algorithm presented in this section provides the plumbing representations of the 3–manifolds ∂F, $\partial_1 F$ and $\partial_2 F$, and the multiplicity systems of the open book decomposition of $(\partial F, V_g)$ and the generalized Milnor fibrations $\partial F \setminus V_g$, $\partial_1 F \setminus V_g$ and $\partial_2 F$ over S^1 induced by $\arg(g)$.

12.1.1. **Assumptions.** In (7.3) we imposed Assumption A for $\Gamma_{\mathcal{C}}$, which can always be realized by an additional blow up. Although in the Main Algorithm (12.3) of the next section it is irrelevant, in the geometric interpretations (8.2)–(8.3)–(8.4) it simplified (unified) the presentation substantially.

In the next paragraph we introduce another restriction, Assumption B. This plays a relevant role in the formulation of algorithm and in its proof as well. Nevertheless, this also will be removed later in section § 14

12.1.2. **Assumption B.** In sections § 12 and § 13 we will assume that $\Gamma_{\mathcal{C}}$ has no edge of weight 2 (regardless of type of the end-vertices) such that the middle weights of the end-vertices of that edge are zero. In the sequel, we call such an edge '*vanishing 2–edge*'. Their absence can be assumed, since if $\Gamma_{\mathcal{C}}$ has such a 2–edge e:

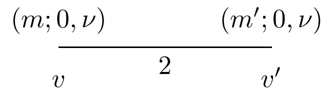

then the embedded resolution r (from (7.1.1)) modified by an additional blow–up with centre $p \in C_v \cap C_{v'}$, provides a new graph $\Gamma'_{\mathcal{C}}$ where e is replaced by

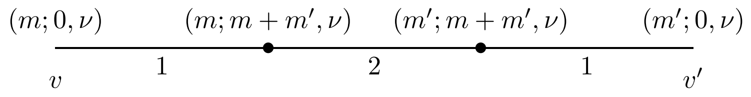

(In the figures above the vertices v and v' might either be arrowheads or not. In the case of non–arrowheads, they might have genus decorations as well.)

12.2. Terminology — 'legs' and 'stars'. In the description of the algorithm we use the following expressions.

Fix a non–arrowhead vertex v of $\Gamma_{\mathcal{C}}$ with weights $(m; n, \nu)$ and $[g]$. Then v determines a 'star' in $\Gamma_{\mathcal{C}}$, which intuitively keeps track of all the edges adjacent to v along with their decorations and the weights $(k; l, \nu)$ of the vertex at the other end of the edges, but disregards the type of these vertices. The aim is to unify the different cases represented by loops and edges connecting non–arrowheads or arrowheads. In order to define it precisely, we start as follows.

A *leg supported by the vertex* v has the form:

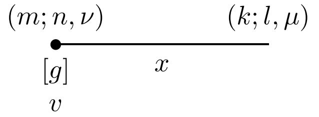

where $x \in \{1,2\}$ and the decorations satisfy the same compatibility conditions as the edges in (7.2.1). Then, *a star*, by definition, consists of a vertex v (together with its decorations) and a collection of legs supported by v.

Once $\Gamma_{\mathcal{C}}$ and v are fixed, *the star of v in $\Gamma_{\mathcal{C}}$* is constructed as follows: Its 'center' will have the decorations $(m;n,\nu)$ and $[g]$ of the vertex v. Furthermore, any edge with decoration x, with end-vertices v and v' (where $v' \neq v$, and v' is either an arrowhead or not) provides a leg with decorations x and the weight (the ordered triple) of v'. (In particular, if v' is a non–arrowhead, and it is connected to v by more than one edge, then each edge contributes a leg.) Moreover, any loop supported by v and weighted by x, provides *two* legs supported by v, both decorated by the same x and (their 'free ends' by) $(k;l,\mu)=(m;n,\nu)$.

(One has the following geometrical interpretation: regard $\Gamma_{\mathcal{C}}$ as the dual graph of the curve configuration $\mathcal{C}$, and let v correspond to the component C. Then the legs of the star of v correspond to the inverse images of the double points of $\mathcal{C}$ sitting on C by the normalization map $C^{norm} \to C$.)

12.3. The Main Algorithm: the construction of the plumbing graph of ∂F.

Recall that in this section we assume that the graph $\Gamma_{\mathcal{C}}$ satisfies Assumption B. First, we construct the plumbing graph of the open book of ∂F with binding V_g and fibration $\arg(g): \partial F \setminus V_g \to S^1$ (cf. (4.2.1)). Hence, we have to determine the shape of the graph together with its arrows, and endow it by the genus and Euler number decorations and a multiplicity system (cf. (5.1.4)). The graph will be determined as a covering graph G of $\Gamma_{\mathcal{C}}$, modified with strings, cf. (6.1)–(6.2). In order to do this, we have to provide the *covering data of the graph–covering* (cf. (6.1.2)).

12.3.1. Step 1. — The covering data of the vertices $\{\mathfrak{n}_v\}_{v\in\mathcal{V}(\Gamma_{\mathcal{C}})}$.

Case 1. Consider a non-arrowhead vertex w of $\Gamma_{\mathcal{C}}$ decorated by $(m;n,\nu)$ and $[g]$. (In fact, by (8.3.2), $g=0$ whenever $m>1$.) Consider its star (see (12.2))

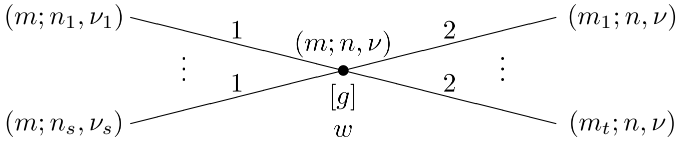

Let s (respectively t) be the number of legs weighted by $x=1$ (respectively by $x=2$). Then, in the covering procedure, above the vertex w of $\Gamma_{\mathcal{C}}$ put $\mathfrak{n}_w$ non-arrowhead vertices, where

(12.3.2) $$\mathfrak{n}_w = \gcd(m,n,n_1,...,n_s,m_1,...,m_t).$$

Furthermore, put on each of these non–arrowhead vertices the same 'multiplicity' decoration $(\tilde{m})$, where

(12.3.3) $$\tilde{m} = \frac{m\nu}{\gcd(m,n)}\,,$$

and the genus decoration $[\tilde{g_w}]$ determined by the formula:

$$\mathfrak{n}_w \cdot (2-2\tilde{g_w}) = (2-2g-s-t)\cdot \gcd(m,n) + \sum_{i=1}^{s} \gcd(m,n,n_i) + \sum_{j=1}^{t} \gcd(m,n,m_j). \tag{12.3.4}$$

(In Step 3, the Euler–number of each vertex will also be provided.)

Case 2. Consider an arrowhead vertex v (i.e. $\rightarrow (1;0,1)$ of $\Gamma_{\mathcal{C}}$. Above the vertex v, in the covering graph G, put exactly one arrowhead vertex; i.e. set $\mathfrak{n}_v = 1$. Let the 'multiplicity' of this arrowhead be 1. In particular, all the arrowheads of G are: $\rightarrow (1)$.

12.3.5. **Step 2. — The covering data of edges $\{\mathfrak{n}_e\}_{e\in\mathcal{E}(\Gamma_{\mathcal{C}})}$ and the types of the inserted strings.**

Case 1. Consider an edge e in $\Gamma_{\mathcal{C}}$, with decoration 1 (cf. 7.2):

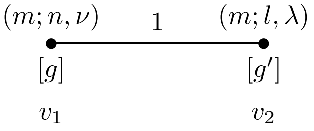

Define:

$$\mathfrak{n}_e = \gcd(m,n,l).$$

Notice that Step 1 guarantees that both $\mathfrak{n}_{v_1}$ and $\mathfrak{n}_{v_2}$ divide $\mathfrak{n}_e$.

Then, above the edge e insert (cyclically) in G exactly $\mathfrak{n}_e$ strings of type

$$Str\left(\frac{n}{\mathfrak{n}_e}, \frac{l}{\mathfrak{n}_e}; \frac{m}{\mathfrak{n}_e} \;\Big|\; \nu, \lambda; 0\right).$$

If the edge e is a loop (i.e. if $v_1 = v_2$), then the procedure is the same with the only modification that the end–vertices of the $\mathfrak{n}_e$ strings are identified (cyclically) with the $\mathfrak{n}_{v_1}$ vertices above v_1, hence they will form 1–cycles in the graph. (In other words, on each vertex above v_1 one puts $\mathfrak{n}_e/\mathfrak{n}_{v_1}$ 'closed' strings.)

If the right vertex v_2 is replaced by an arrowhead, i.e. the edge e is

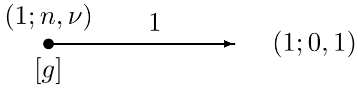

then complete the same procedure as above with $m = 1$ and $\mathfrak{n}_e = 1$: above such an edge e put a single edge decorated by + (which supports that arrowhead of G which covers the corresponding arrowhead of $\Gamma_{\mathcal{C}}$).

Case 2. Consider an edge e in $\Gamma_{\mathcal{C}}$, with decoration 2 (cf. 7.2):

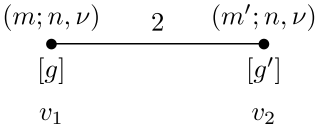

Notice that, by Assumption B (12.1.2), $n \neq 0$. For such an edge, define:

$$\mathfrak{n}_e = \gcd(m,m',n). \tag{12.3.6}$$

Notice again that both $\mathfrak{n}_{v_1}$ and $\mathfrak{n}_{v_2}$ divide $\mathfrak{n}_e$.

Then, above the edge e insert (cyclically) in G exactly $\mathfrak{n}_e$ strings of type

$$Str^{\ominus}\left(\frac{m}{\mathfrak{n}_e}, \frac{m'}{\mathfrak{n}_e}; \frac{n}{\mathfrak{n}_e} \;\Big|\; 0,0;\nu\right).$$

If the edge is a loop, then we modify the procedure as in the case of 1–loops. Notice that by Assumption B, there are no 2-edges supporting arrowheads.

(Also notice that above $\Gamma^1_{\mathcal{C}}$ and above the cutting edges the 'covering degree' is always one.)

12.3.7. **Step 3. — Determination of the missing Euler numbers.** The decorations provided by the first two steps are: the multiplicities of all the vertices, all the genera, *some* of the Euler numbers, and all the sign–decorations of the edges (those without $\ominus$ have decoration $+$). Then, finally, the missing Euler numbers are determined by formula (5.1.2).

12.4. The output of the algorithm. Corollary of (6.1.4). Notice that the set of integers $\{\mathfrak{n}_v\}_{v\in\mathcal{V}(\Gamma_{\mathcal{C}})}$ and $\{\mathfrak{n}_e\}_{e\in\mathcal{E}(\Gamma_{\mathcal{C}})}$ satisfy the axioms of a covering data. Furthermore, if $v\in\mathcal{V}^1(\Gamma_{\mathcal{C}})$ then $m=1$ hence $\mathfrak{n}_v=1$. Moreover, by (8.3.2), each $\Gamma^2_{\mathcal{C},j}$ is a tree. Therefore, by Proposition (6.1.4), we get that

> *there is only one cyclic graph–covering of* $\Gamma_{\mathcal{C}}$ *with this covering data (up to a graph–isomorphism).*

The graphs obtained by the above algorithm (12.3), in general, can be simplified by the operations of the oriented plumbing calculus (or their inverses). If we are interested only in the output oriented 3–manifold, one can apply this freely without any restriction. Nevertheless, if we wish to keep some information from the (analytic) construction which provides the graph (e.g., if we wish to apply the results of Chapters VII and VIII regarding different horizontal and vertical monodromies), then it is better to apply only the *reduced plumbing calculus* of oriented 3–manifolds (with arrows), cf. (5.1.10)–(5.1.12). This is what we do in this article.

Nevertheless, even if we rely only on the reduced calculus, during the plumbing calculus, some invariants still might change. E.g., the operation R5 modifies the sum $g(Gr)$ of the genus decorations and the number $c(Gr)$ of independent 1–cycles of a graph Gr. Since, in the sequel in some discussions these numbers will also be involved, we will adopt the following notation: we write G, G_1 and G_2 for the graphs obtained by the original algorithm (12.3); while the general notation for a *modified graphs* (under the reduced list of operations, cf. (5.1.7)) is G^m, G^m_1, $G^m_{2,j}$.

THEOREM 12.4.1. *The oriented 3–manifold ∂F and the link $V_g\cap\partial F$ in it can be represented by an (oriented) plumbing graph (see (5.1) for the terminology).*

More precisely, let (f,g) as in (4.1). Then, the decorated graph G constructed in (12.3) is a possible plumbing graph of the pair $(\partial F,\partial F\cap V_g)$, which carries the multiplicity system of the open book decomposition $\arg(g):\partial F\setminus V_g\to S^1$. *If one deletes the arrowheads and the multiplicities, one obtains a possible plumbing graph of the boundary of the Milnor fiber ∂F of f.*

The proof of (12.4.1) will be given in section § 13. Nevertheless, we wish to stress here the main geometric idea of the proof.

If f is an *isolated* hypersurface singularity, then the link $K=V_f\cap S^5_\epsilon$ is smooth, and there exists an orientation preserving diffeomorphism $\partial F\approx K$. Hence, ∂F can be 'localized', i.e. can be represented as a boundary of an arbitrary small representative of a (singular) germ. If that germ is resolved by a modification (whose existence is guaranteed by the existence of resolution of singularities), then K appears as the boundary of the exceptional locus, hence automatically one gets a plumbing representation for K. Its plumbing data can be read from the combinatorics of the exceptional set (and the multiplicity system from the corresponding vanishing orders).

If f is not isolated then K is not smooth, and the above argument does not work, and even the fact that ∂F has any kind of plumbing representation is not automatic at all. Guided by the above case of isolated singularities, definitely, if we would be able to 'localize' ∂F, as a link of a singular germ, then we would be able to extend all the theory valid for isolated hypersurfaces (or even for normal surface singularities). *This realization is the main point in the proof* of (12.4.1), but with the difference that the germ whose local link is ∂F is *not holomorphic* (complex analytic), but it is *real analytic.* One has the following surprising result:

PROPOSITION 12.4.2. *(See (13.3.3).) Let f be a hypersurface singularity with a 1–dimensional singular locus. Take another germ g such that (f,g) forms an ICIS, cf. (4.1). For a sufficiently large even integer k consider the real analytic germ*

$$\mathcal{S}_k := \{ z \in (\mathbb{C}^3, 0) \, : \, f(z) = |g(z)|^k \}.$$

Then the link of $\mathcal{S}_k$ is independent of the choice of g and k, and, in fact, it is (orientation preserving) diffeomorphic to ∂F.

The proof of (12.4.1), in fact, describes (the topology of) a resolution of $\mathcal{S}_k$ 'guided' by $\Gamma_{\mathcal{C}}$, and the algorithm (12.3) extracts from this the combinatorics of the exceptional locus and its tubular neighbourhood.

Notice that the above proposition is true for k odd too, nevertheless, $\mathcal{S}_k$ for k even has nicer analytic properties; e.g. if f and g are polynomials, then $\mathcal{S}_k$ is a real algebraic variety. (Moreover, the above result (12.4.2) is true for any germ $f : (\mathbb{C}^n, 0) \to (\mathbb{C}, 0)$ with 1–dimensional singular locus — the only modification in the statement and its proof is the replacement of $\mathbb{C}^3$ with $\mathbb{C}^n$.)

12.5. The graphs of $\partial_1 F$ and $\partial_2 F$. The above algorithm, which provides ∂F, is compatible with the decomposition of this space into its parts $\partial_1 F$ and $\partial_2 F$. In this subsection we make this statement more precise.

12.5.1. **The graphs of $(V_f^{norm}, g \circ n)$ and $\partial_1 F$.** Repeat the steps 1 and 2 from the Main Algorithm (12.3), but only for the vertices and edges sitting in $\Gamma^1_{\mathcal{C}}$ (including the cutting edges too). Replace each cutting edge by an edge (connected to $v_1 \in \mathcal{V}(\Gamma^1_{\mathcal{C}})$) supporting an arrowhead with multiplicity (0). In this way we get a graph with all the multiplicities determined (and in fact, with all edge–decorations +). Calculate the Euler numbers by (5.1.2). This graph will be denoted by G_1.

(Notice that in the two graphs G and G_1, the corresponding Euler numbers of the end–vertex v_1 of a cutting edge are not the same; the other Euler numbers evidently coincide.)

THEOREM 12.5.2. *G_1 is a possible embedded resolution graph of $(V_f^{norm}, g \circ n)$, where the arrows with multiplicity (0) represent the link–components determined by the strict transforms of $Sing(V_f)$. If we delete these 0–multiplicity arrows, we get a possible embedded resolution graph of $(V_f^{norm}, g \circ n)$. Furthermore, if we delete all the arrowheads and all the multiplicities, we get a possible resolution graph of the normalization of V_f^{norm}.*

If in G_1 we replace the 0–multiplicity arrows by dash-arrows we get the plumbing representation of the pair $(\partial_1 F, V_g \cap \partial F)$, where the remaining arrows represent the link $V_g \cap \partial F$, and the multiplicities are the multiplicities of the local trivial fibration $arg(g) : \partial_1 F \setminus V_g \to S^1$. In particular, if we delete all these remaining non–dash–arrows and all the multiplicities too, we get the plumbing graph of the 3–manifold with boundary $\partial_1 F$.

If we replace in G_1 all the arrows by dash–arrows and we delete the multiplicities, we get the plumbing graph of the manifold with boundary $\partial_1 F \setminus T^\circ(V_g)$.

12.5.3. **The graph of $\partial_2 F$.** Let G_2 be the graph obtained from G as follows. Delete all vertices and edges of G sitting above the vertices and edges of $\Gamma^1_{\mathcal{C}}$, and replace the (unique) string above any cutting edge by a dash–arrow (putting no multiplicity–decoration on it). Obviously, G_2 has s connected components $\{G_{2,j}\}_{1\leq j\leq s}$; $G_{2,j}$ being related with Σ_j (cf. (8.3)).

THEOREM 12.5.4. *For each* $j = 1, \dots, s$, $G_{2,j}$ *is a possible plumbing graph for the 3–manifold with boundary* $\partial_{2,j}F$, *where the set of multiplicities consists of the multiplicity system associated with the fibration* $\arg(g) : \partial_{2,j}F \to S^1$. *If we delete all the multiplicities, we get a plumbing graph of the 3–manifold with boundary* $\partial_{2,j}F$.

REMARK 12.5.5. From the plumbing graphs of $\partial_1 F$ and $\partial_2 F$ it is impossible to recover the graph of ∂F, since the *gluing* information (an automorphism of the gluing tori) cannot be read from the partial information contained in the graphs of $\partial_1 F$ and $\partial_2 F$. (See e.g. the next examples (12.5.8) and (12.5.9).) This gluing information is exactly one of the main advantages of the graph $\Gamma_{\mathcal{C}}$ and of the main algorithm, which provides the full ∂F.

REMARK 12.5.6. In fact, on $G_{2,j}$ one can put even more information/decoration inherited from G. If one introduces a 'canonical' framing (closed simple curve) of the boundary components of $\partial_{2,j}F$, then one can define a well–defined multiplicity of the dash–arrows as well (inherited from G). Usually, such an information is needed when one wishes to glue two manifolds with (several tori boundary components) along their boundaries: this information is part of the gluing data. Since here we have the complete description of ∂F (namely, the 3–manifold, which might be the aim of the gluing), we will not consider framed boundaries. But, definitely, the interested reader might consider and add to the picture these data as well.

12.5.7. **The gluing tori.** Each connected component $\partial_{2,j}F$ $(j = 1, \dots, s)$ is glued to $\partial_1 F$ along $\partial\partial_{2,j}F$, which is a union of tori. Since for each cutting edge e one has $\mathfrak{n}_e = 1$ (i.e. in the main algorithm one inserts exactly one string above e), the number of these tori is exactly the cardinality of $\mathcal{E}_{cut,j}$, the number of cutting edges adjacent to $\Gamma^2_{\mathcal{C},j}$.

Let e be such a cutting edge, and we will use the notations of (8.4) regarding this edge. Let T_e be the torus component of $\partial(\partial_{2,j}F)$ corresponding to e. Furthermore, consider the fibration $T_e \to L_j$ from (3.3.1). Then the fiber of this projection consists of $d(e)$ circles, the corresponding orbit of the (permutation) action of $m'_{j,ver}$ on $\partial F'_j$. (Recall that $m'_{j,hor}$ acts on T_e trivially, cf. (3.3.1)(2).)

These gluing tori appear in the link K of V_f as well. Indeed, consider $L_j = K \cap \Sigma_j$ as in (3.1). Let $T(L_j)$ a tubular neighbourhood of L_j in S^5_ϵ as in (3.3). Then $\partial T(L_j)$ intersects K in $\#\mathcal{E}_{cut,j}$ tori, which can be identified by the gluing tori of ∂F, see also (3.3.2).

EXAMPLE 12.5.8. Assume that $f = x^3 + y^2 + xyz$ and $g = z$ as in (9.4.3). Then the output of the Main Algorithm is the following graph G:

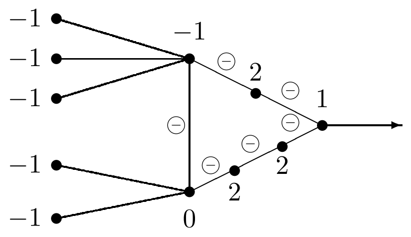

(and all the multiplicities are (1)).

There is only one non–arrowhead vertex in G with multiplicity 1. Therefore, one has the following graphs for $(V_f^{norm}, g \circ n)$, $\partial_1 F \setminus T(V_g)$, and $\partial_1 F$:

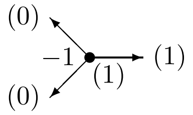

G_1

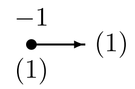

$(V_f^{norm}, g\circ n)$

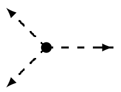

$\partial_1 F \setminus T(V_g)$

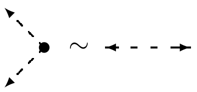

$\partial_1 F$

Moreover, by plumbing calculus, the graph of $\partial_2 F$ is also the double dash–arrow ← - - → . Notice that both parts $\partial_1 F$ and $\partial_2 F$ are extremely simple 3–manifolds with boundary (namely, $S^1\times S^1\times[0,1]$); the main information in ∂F is exactly how these parts are glued. By calculus starting from G, ∂F is represented by the graph:

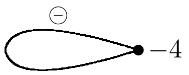

The multiplicity system of the open book decomposition $(\partial F, V_g)$ is given by:

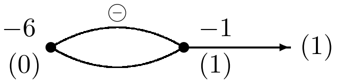

EXAMPLE 12.5.9. Assume that $f = x^2y + z^2$ and $g = x + y$, cf. (9.3.1). Then, by the main algorithm and plumbing calculus we get that the (minimal) plumbing graph of ∂F consists of a unique vertex with genus zero and Euler number -4, i.e. ∂F is the lens space $L(4, 1)$. Moreover,

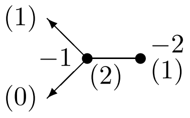

G_1

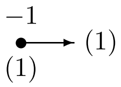

$(V_f^{norm}, g\circ n)$

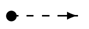

$\partial_1 F$

and

$\partial_2 F$:

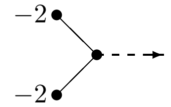

Notice that for the unique cutting 2-edge e in (9.3.1) one has $d_1 = 1$, hence $\nu = d(e) = 2$. Therefore, although the transversal singularity has two local irreducible components, $\partial_1 F$ and $\partial_2 F$ are glued by only one torus. The point is that the transversal type is A_1, and the two local irreducible components of the transversal type are permuted by the vertical monodromy, see (8.4) and (12.5.7) (and compare also with the next example and Example (3.1) of [**60**]).

The open book decomposition of $(\partial F, V_g)$ is given by:

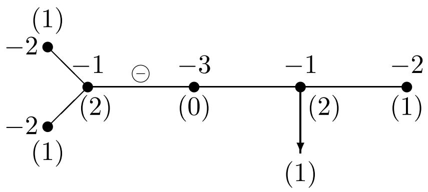

Example 12.5.10. In both cases of (9.4.3) and (9.4.4), the singular locus Σ of V_f is irreducible and consists of the z–coordinate axis. The transversal type is an A_1 singularity, hence $\#T(\Sigma) = 2$. Furthermore, $\#\mathcal{E}_{cut,1} = 2$ and for both cutting edges $d(e) = 1$. Therefore (see (8.4) and (12.5.7)), the action of the vertical monodromy does not permute the two local components, and in both cases (9.4.3) and (9.4.4), there are two gluing tori.

On the other hand, it might happen that the two local components of a transversal A_1 singularity are permuted by the vertical monodromy, see e.g. (12.5.9). Similarly, in the case of (11.1.2), $\Sigma = \Sigma_1 \cup \Sigma_2$, and for both Σ_j the transversal type is A_1, hence $\#T(\Sigma_j) = 2$ $(j = 1, 2)$. Moreover, for both j, $\mathcal{E}_{cut,j} = 1$, $d_j = 1$, and $d(e) = 2$; hence $\partial_{2,j}F$ is glued to $\partial_1 F$ by exactly one torus.

Example 12.5.11. Assume that $f = x^d + y^d + xyz^{d-2}$, $d \geq 3$. For $\Gamma_{\mathcal{C}}$ see the second graph of (10.1.5) (which satisfies Assumption A). In this case Σ is irreducible with transversal type A_1. The gluing data are $\#\mathcal{E}_{cut,1} = 2$ and $d_1 = 1$. For both cutting edges $d(e) = 1$, hence one has two gluing tori. The graph of ∂F is:

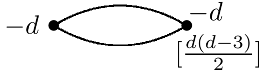

Example 12.5.12. For $f = x^3y^7 - z^4$ the graph $\Gamma_{\mathcal{C}}$ is given in (11.1.1). After a computation, we get for G^m the graphs:

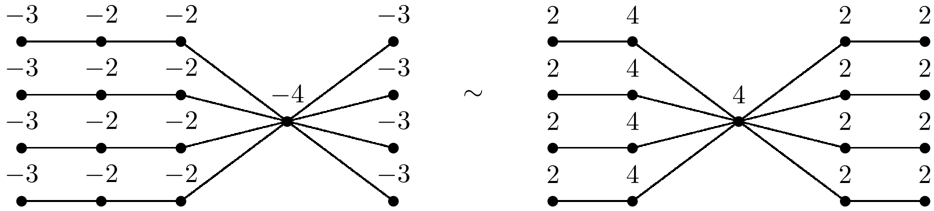

The graph at the left–hand side is the 'normal form' (cf. [**18**]). Its central vertex has self–intersection $b = -4$, while the eight pairs of normalized Seifert invariants (α_i, ω_i), $(1 \leq i \leq 8)$, associated with the eight legs, are determined as Hirzebruch continued fractions associated with the entries of the corresponding legs: α_i/ω_i for $1 \leq i \leq 4$ is $[2, 2, 3] = 7/4$, while the other four are $[3] = 3/1$. Recall that the orbifold Euler number of the Seifert 3–manifold is defined as $e := b + \sum_i \omega_i/\alpha_i$, and the normal form graph is negative definite if and only if $e < 0$. In this case $e = 4/21 > 0$, hence the graph from the left–hand side is *not* negative definite. (The rational number e is also called 'virtual degree', see [**72**].)

Example 12.5.13. For $f = x^2y^2 + z^2(x + y)$ a possible graph $\Gamma_{\mathcal{C}}$ is given in (11.1.2). For a possible G^m we get:

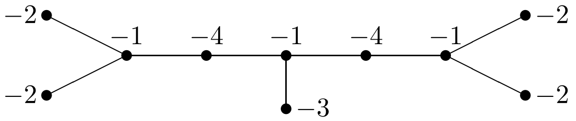

(Notice that for this graph it would be possible to use the $\mathbb{RP}^2$–absorption of the *non–orientable* calculus, but we do not do that.)

Example 12.5.14. Assume that $f = y^3 + (x^2 - z^4)^2$. Then using (11.1.3) we get for G^m:

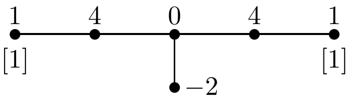

EXAMPLE 12.5.15. Finally, the next example is a 1–parameter infinite family. In general, in order to treat such a family uniformly for all the values of the parameter, one needs some ingenuity, or familiarity with the algorithm (and/or familiarity with some other algorithms as well, e.g. with that one which determines the resolution graph of cyclic coverings).

Here we will exemplify the case of $f = x^a y(x^2 + y^3) + z^2$ with $a \geq 2$. The reader may consider this as a model for other infinite families.

The graph $\Gamma_{\mathcal{C}}$ with $g = x + y + z$ is given in (9.3.4).

Case 1. Assume that a is even. We will determine G is several steps.

First, the graph G_1 can be determined easily (in particular, the normalization of V_f is the D_5 singularity):

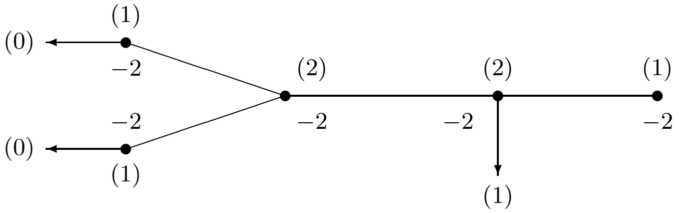

Clearly, we have two gluing tori. Let v_1 and v_2 be the vertices of G_1 which support the (0)–arrows. Next, we wish to determine the multiplicity m_1 of the vertex v_1' of G, which is not in G_1 and is a neighbour of v_1. For this we have to analyze the cutting edge with weights $(a; 2a + 4, 1)$ and $(1; 2a + 4, 1)$. By (5.2.1), m_1 satisfies $a + \lambda = m_1(2a + 4)$ for some λ with $0 \leq \lambda < 2a + 4$. Hence $m_1 = 1$. In G the vertex v_1' is glued to v_1 by a $\ominus$–edge, hence the Euler number of v_1 in G is -1.

Finally, we analyze the graph $\Gamma^2_{\mathcal{C}}$. Its shape and the first entries of the weights of the vertices coincide with the minimal embedded resolution graph of the (transversal type) plane curve singularity $u^2 + v^a$, provided that we replace v_1 and v_2 by arrowheads with multiplicity 1 (see (8.3.2) too). Comparing the main algorithm and the algorithm which provides the graph of suspension singularities (cf. [**42**]), we realize that the part of G above $\Gamma^2_{\mathcal{C}}$ is exactly the resolution graph of $u^2 + v^a + w^{2a+4} = 0$ with opposite orientation. More precisely, let

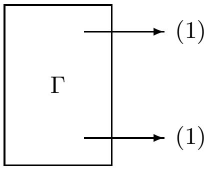

be the minimal embedded resolution graph of the germ $w : (\{u^2 + v^a + w^{2a+4} = 0\}, 0) \to (\mathbb{C}, 0)$, induced by the projection $(u, v, w) \mapsto w$. Let $-\Gamma$ be this graph with opposite orientation (in which one changes the sign of all Euler numbers and edge–decorations, and keeps the multiplicities). Then the graph of the open book decomposition of $(\partial F, V_g)$ is obtained by gluing $-\Gamma$ with G_1 such that the arrows of $-\Gamma$ are identified with v_1 and v_2:

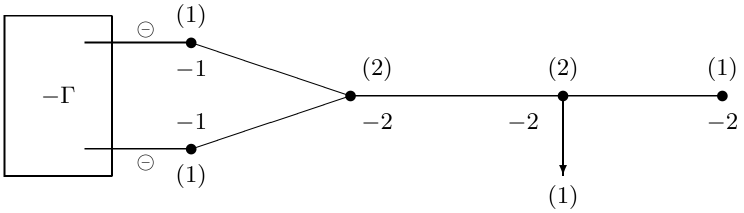

This graph has a cycle. Moreover, Γ is a star–shaped graph whose central vertex has genus $\frac{gcd(a,4)}{2}-1$. The determination of Γ is standard (see [**44**] or [**52**]).

Case 2. Assume that a is odd, $a\geq 3$. We proceed as above. The graph G_1 is the following:

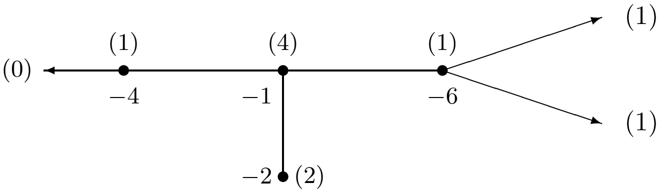

There is only one gluing torus. Let v be the (-4)–vertex, and v' its adjacent vertex of G which is not in G_1. Then the multiplicity of v' is again 1. Hence, the Euler number of v in G is -3. Therefore, the graph of $(\partial F, V_g)$ is

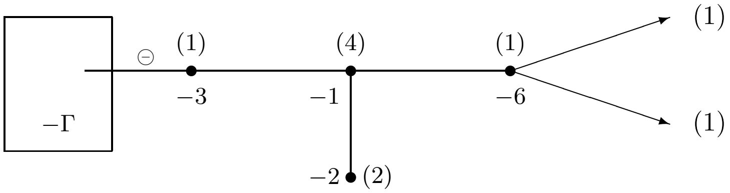

where Γ is the minimal embedded resolution graph of the germ $w:(\{u^2+v^a+w^{2a+4}=0\},0)\to(\mathbb{C},0)$, as above (and the unique arrow–head of $-\Gamma$ is identified with the (-3)–vertex). Note that ∂F is a rational homology sphere.

§ 13. Proof of the Main Algorithm

13.1. Preliminary (historical) remarks. The algorithm (and its proof) is a highly generalized version of the algorithm which determines the resolution graph of cyclic coverings. Its origin goes back to the case of suspensions: there one determines the resolution graph of the hypersurface singularity $\{f'(x,y)+z^n=0\}$ from the embedded resolution graph of f' and the integer n (where f' is an isolated plane curve singularity). For this algorithm see [**42**] (for older treatments of particular cases see also [**28, 50, 52, 3**]). The general case of cyclic coverings is given in [**44**]. The aim of this article is to compute the resolution graph of the normalization of $\{(x,z)\in(X,0)\times(\mathbb{C},0)\,:\,f(x)=z^n\}$, where $(X,0)$ is a normal complex surface singularity and $f:(X,0)\to(\mathbb{C},0)$ is a complex analytic isolated germ. All the geometrical constructions behind these algorithms, targeting cyclic coverings, are realized within the framework of the complex analytic/algebraic geometry; in particular, all the graphs involved are negative definite graphs (and the plumbing calculus reduces to blowing up/down (-1)–rational curves). (Recall also that for normal surface singularities the resolution graph is a possible plumbing graph for the link, which is diffeomorphic with the boundary of the Milnor fiber of any smoothing.)

The first case when a more complicated 'aid–graph' was used in a construction is in [**48**]. Here the starting situation was the following: having a germ f with 1–dimensional singular locus, and another germ g such that the pair (f, g) forms an ICIS, one wished to determine the resolution graph of the hypersurface singularities of type $f + g^n$, $n \gg 0$, (members of the so–called 'generalized Iomdin series'). In [loc.cit.], in order to find this ('usual', i.e. negative definite) graph, all the necessary information about the ICIS (f, g) was stored in the 'non-usual' decorations of the 'non–usual' graph $\Gamma_{\mathcal{C}}$.

This construction serves as a model for the present proof as well. We will start again with the very same graph $\Gamma_{\mathcal{C}}$, but rather significant differences will appear. Although, in [loc.cit.], all the procedure was within realm the complex analytic geometry (similarly as in the case of cyclic coverings), the present case grows out of the complex analytic world: we glue together real analytic spaces with singularities (sometimes with gluing maps which reverse the 'canonical' orientations of the regular parts). This generates some additional difficulties, which should be handled during the proof. The output plumbing graphs will be 'general plumbing graphs' (which may not be definite, or not even non–degenerate), and we have to consider a larger set of moves of the C^∞ plumbing calculus (not really standard in algebraic geometry) in order to simplify them (and to reduce them to their 'normal forms').

The explanation of the fact/idea that the graph $\Gamma_{\mathcal{C}}$ contains all the information needed to describe ∂F is given in (8.5). In fact, this is the main starting point of the whole construction. In the next subsection, we will stress again this point and we outline the main steps of the proof.

13.2. The guiding principle and the outline of the proof. Consider an ICIS $\Phi = (f, g)$ as in (4.1), an embedded resolution $r : V^{emb} \to (\mathbb{C}^3, 0)$ of the divisor $V_f \cup V_g$ as in (7.1.1), and a 'wedge' $\mathsf{W}_{\eta,M}$ of Δ_1 for some $M \gg 0$ as in (8.5).

If one has a complex analytic isolated singularity $(\mathcal{S}, 0) \subset (\mathbb{C}^3, 0)$ for which $\Phi(\mathcal{S}) \setminus \{0\} \subset \mathsf{W}_{\eta,M}$ then one can construct a resolution of $\mathcal{S}$ in three steps.

First, consider the strict transform $\widetilde{\mathcal{S}} \subset V^{emb}$ of $\mathcal{S}$ (by r). It sits in a tubular neighbourhood of $\mathcal{C}$ (cf. (8.5.1)), and its singular locus sits in $\mathcal{C}$. Then this can be resolved in two further steps: first taking the normalization $\mathcal{S}^{norm}$ of $\widetilde{\mathcal{S}}$, then resolving the isolated normal surface singularities of $\mathcal{S}^{norm}$. The point is that if $\mathcal{S}$ is determined by f and g, then $\widetilde{\mathcal{S}}$ has some nice local equations near any point of $\mathcal{C}$ (which can be recovered from the decorations of $\Gamma_{\mathcal{C}}$). E.g., $\widetilde{\mathcal{S}}$ is an equisingular family of curves along the regular part of $\mathcal{C}$; in particular, the singular locus of $\mathcal{S}^{norm}$ will sit in the double points of $\mathcal{C}$. Moreover, all these singular points will be of Hirzebruch–Jung type. In particular, the last step is the resolution of these HJ–singularities (whose combinatorial data again is codified in $\Gamma_{\mathcal{C}}$). Summing up we get the diagram:

$$\begin{tikzcd}
\overline{\mathcal{S}} \arrow[r, "\text{HJ}"] & \mathcal{S}^{norm} \arrow[r] & \widetilde{\mathcal{S}} \arrow[r, "r"] \arrow[d, phantom, "\cap"] & \mathcal{S} \arrow[d, phantom, "\cap"] \\
 & & V^{emb} & (\mathbb{C}^3, 0)
\end{tikzcd}$$

According to the above, we have the following steps at the level of graphs:

- start with the graph $\Gamma_{\mathcal{C}}$ (which stores all the local information about $\tilde{\mathcal{S}}$);
- provide a cyclic covering-graph (in the sense of §6) corresponding to the normalization step;
- modify this graph by 'Hirzebruch–Jung strings' (see 'variation' (6.2)).

A key additional argument is a consequence of Theorem (6.1.4), which guarantees the uniqueness of the cyclic covering graph (and the inserted strings).

It is exactly this guiding principle that was used in [**48**] to determine the resolution graph (equivalently, the plumbing graph of the link) of any member of the generalized Iomdin–series $\mathcal{S} = \{f + g^n = 0\}$ $(n \gg 0)$.

Now we want to obtain the plumbing-graph of the boundary ∂F of the Milnor fibre of a non–isolated f. We show in (13.3.3) that ∂F is the boundary (link) of the *real* analytic germ

$$\mathcal{S}_k = \{f = |g|^k\} \subset (\mathbb{C}^3, 0),$$

and $\Phi(\mathcal{S}_k) \setminus \{0\} \subset \mathsf{W}_{\eta,M}$, provided that $k \gg 0$. Hence, we will run the same algorithm (with some modifications) in the world of real analytic geometry.

A final remark: the Euler number of an S^1-bundle over a curve is a 'global object', its computation in a resolution can be rather involved (one needs more charts and gluing information connecting them). Therefore, we will determine the Euler numbers of our graphs by an indirect way: we consider the open book decomposition (induced by g) and determine the associated multiplicity system (this can easily be determined from local data!), then we apply (5.1.2).

13.3. The first step. The real varieties $\mathcal{S}_k$. We fix a pair $\Phi = (f, g)$ as in (4.1), and we use all the notations and results of that section. In particular, we fix a good representative of Φ whose discriminant is Δ_Φ. Similarly as above, we write (c, d) for the coordinates of $(\mathbb{C}^2, 0)$.

For any *even* integer k (see also (13.3.2) for more comments) we set

$$Z_k := \{(c, d) \in (\mathbb{C}^2, 0) \,:\, c = |d|^k\}.$$

The next lemma is elementary and its proof is left to the reader.

LEMMA 13.3.1. *Z_k is a C^∞ real analytic (even algebraic) surface. For k sufficiently large $Z_k \cap \Delta_\Phi = \{0\}$. In fact, $Z_k \setminus \{0\} \subset \mathsf{W}_{\eta,M}$ if $k > M$.*

REMARK 13.3.2. As mentioned before, all the important facts regarding Z_k (and the space $\mathcal{S}_k$ which will be defined next) are valid for k odd too (recall that the classification of oriented 2– and 3–dimensional topological manifolds agrees with the classification of C^∞ ones); nevertheless it is more convenient to use even integers k, since for them $|d|^k$ becomes real algebraic. In fact, later we will impose even more divisibility assumptions for k.

The point is that k has only an auxiliary role and carries no geometric meaning (e.g., it will not appear in any 'final' formula of ∂F), hence its value (as soon as it is sufficiently large) is completely unimportant.

Next, define the real analytic variety $\mathcal{S}_k$ of real dimension 4 by

$$\mathcal{S}_k := \Phi^{-1}(Z_k) = \{z \in (\mathbb{C}^3, 0) \,:\, f(z) = |g(z)|^k\}.$$

LEMMA 13.3.3. *For k sufficiently large, the real variety $\mathcal{S}_k \setminus \{0\}$ is regular, hence it is a C^∞ oriented 4–dimensional manifold. Moreover, for $\epsilon > 0$ sufficiently small, the sphere S^5_ϵ intersects $\mathcal{S}_k$ transversally. The intersection $\mathcal{S}_k \cap S^5_\epsilon$ is an oriented 3–manifold, which is diffeomorphic (by an orientation preserving diffeomorphism) to ∂F. In particular, the link of $\mathcal{S}_k$ (i.e. $\mathcal{S}_k \cap S^5_\epsilon$) is independent of the choice of k.*

PROOF. The first sentence follows from (13.3.1) and from the properties of the ICIS Φ (or by a computation). The second one is standard, using e.g. the 'curve selection lemma', see [**38**]. Next, we will prove the diffeomorphism $\mathcal{S}_k \cap S^5_\epsilon \simeq \partial F$.

First recall that in most of the topological arguments regarding the Milnor fiber of f, the sphere $S^5_\epsilon = \partial B_\epsilon$ can be replaced by (the 5–manifold with corners) $\partial(\Phi^{-1}(D^2_\eta) \cap B_\epsilon)$, the Milnor fiber $F = \{f = \delta\} \cap B_\epsilon$ by $F^\circ := \{f = \delta\} \cap \Phi^{-1}(D^2_\eta) \cap$

B_ϵ, or the boundary ∂F by the boundary (with corners) ∂F°. For details, see e.g. [**31**], see also (4.1.1). By a similar argument one shows the equivalence of $\Phi^{-1}(Z_k)\cap B_\epsilon$ with $\mathcal{S}_k^\circ := \Phi^{-1}(Z_k\cap D^2_\eta)\cap B_\epsilon$, and $\Phi^{-1}(Z_k)\cap S^5_\epsilon$ with the 3–manifold with corners $\partial\mathcal{S}_k^\circ$. Hence, we need only to show the equivalence of ∂F° and $\partial\mathcal{S}_k^\circ$.

Consider the intersection $Z_k\cap\partial D^2_\eta$, i.e., the solution of the system $\{|c|^2+|d|^2=\eta^2;\ c=|d|^k\}$. It is a circle along which c is constant; let this value of c (determined by η and k) be denoted by c_0. Set (as in (4.1)) $D_{c_0}=\{c=c_0\}\cap D^2_\eta$. Then

$$\partial D_{c_0}=\partial(Z_k\cap D^2_\eta), \tag{13.3.4}$$

and $\partial F^\circ=\partial(\Phi^{-1}(D_{c_0}))$ has a decomposition:

$$\partial F^\circ=\Phi^{-1}(\partial D_{c_0})\cap B_\epsilon\bigcup_{\Phi^{-1}(\partial D_{c_0})\cap S^5_\epsilon}\Phi^{-1}(D_{c_0})\cap S^5_\epsilon.$$

Via (13.3.4), $\partial\mathcal{S}_k^\circ$ has a decomposition

$$\partial\mathcal{S}_k^\circ=\Phi^{-1}(\partial D_{c_0})\cap B_\epsilon\bigcup_{\Phi^{-1}(\partial D_{c_0})\cap S^5_\epsilon}\Phi^{-1}(Z_k\cap B^2_\eta)\cap S^5_\epsilon.$$

Notice that there is an isotopy of D^2_η, preserving ∂D^2_η, which sends D_{c_0} into $Z_k\cap D^2_\eta$. Since the restriction of Φ on $\Phi^{-1}(D^2_\eta)\cap S^5_\epsilon$ is a trivial fibration over D^2_η, this isotopy can be lifted. This identifies the pairs

$$(\Phi^{-1}(D_{c_0})\cap S^5_\epsilon,\Phi^{-1}(\partial D_{c_0})\cap S^5_\epsilon)\simeq(\Phi^{-1}(Z_k\cap B^2_\eta)\cap S^5_\epsilon,\Phi^{-1}(\partial D_{c_0})\cap S^5_\epsilon).$$

□

13.4. The strict transform $\widetilde{\mathcal{S}}_k$ of $\mathcal{S}_k$ via r. Consider the resolution $r: V^{emb}\to U$ as in (7.1.1). Let $\widetilde{\mathcal{S}}_k$ be the strict transform of $\mathcal{S}_k$ by r, i.e. $\widetilde{\mathcal{S}}_k$ is the closure (in eucleidian topology) of $r^{-1}(\mathcal{S}_k\setminus\{0\})$.

Lemma 13.4.1.

$$\widetilde{\mathcal{S}}_k\cap r^{-1}(0)=\mathcal{C}.$$

Proof. The proof is similar to the proof of (8.5.1) (see [**48**, (5.5)] for its source), and it is left to the reader. □

Since the restriction of r induces a diffeomorphism $\widetilde{\mathcal{S}}_k\setminus\mathcal{C}\to\mathcal{S}_k\setminus\{0\}$, we get that the singular locus of $\widetilde{\mathcal{S}}_k$ satisfies

$$Sing(\widetilde{\mathcal{S}}_k)\subset\mathcal{C}.$$

Moreover, r induces a diffeomorphism between $\partial\mathcal{S}_k$ (the subject of our interest) and $\partial\widetilde{\mathcal{S}}_k$. Since $\widetilde{\mathcal{S}}_k$ can be replaced by its intersection with an arbitrarily small tubular neighbourhood of $\mathcal{C}$, the boundary $\partial\widetilde{\mathcal{S}}_k$ can be localized totally near $\mathcal{C}$. (In fact, this is the main advantage of the space $\mathcal{S}_k$, in this way the wanted 3–manifold appears as a local link, or, after a resolution, as the boundary of a tubular neighbourhood of a curve configuration).

Next, we analyze the local equations of $\widetilde{\mathcal{S}}_k$ in the neighbourhood of any point of $\mathcal{C}$. For this we use the notations of (7.2). In all the cases, U_p is a complex 3-ball around the point $p\in\mathcal{C}$ with three complex local coordinates (u,v,w).

It is convenient to use the following notation. If $H=\{(u,v,w)\in U_p : h(u,v,w)=0\}$ is a real analytic variety in U_p, then we denote by H^+ the closure of $H\setminus\{uvw=0\}$ (in this way we neglect those components of H which sit in one of the coordinate planes). Using this notation, the local equations of $\widetilde{\mathcal{S}}_k$ are as follows.

If p is a generic point of a component C of $\mathcal{C}$ with decoration $(m;n,\nu)$, then

$$\widetilde{\mathcal{S}}_k \cap U_p = \{(u,v,w)\,:\,u^m v^n = |v|^{\nu k}\}^+ = \{(u,v,w)\,:\,u^m = v^{\frac{\nu k}{2}-n}\overline{v}^{\frac{\nu k}{2}}\} \tag{13.4.2}$$

with $m,\nu > 0$. If p is an intersection (singular) point of $\mathcal{C}$ of type 1 (i.e. if the corresponding edge has decoration 1), then

$$\widetilde{\mathcal{S}}_k \cap U_p = \{(u,v,w)\,:\,u^m v^n w^l = |v|^{\nu k}|w|^{\lambda k}\}^+ \tag{13.4.3}$$

with $m,\nu,\lambda > 0$. Finally, if p is an intersection (singular) point of $\mathcal{C}$ of type 2, then

$$\widetilde{\mathcal{S}}_k \cap U_p = \{(u,v,w)\,:\,u^m v^{m'} w^n = |w|^{\nu k}\}^+ \tag{13.4.4}$$

with $m,m',\nu > 0$.

13.5. Local complex analytic/algebraic models for the points of $\widetilde{\mathcal{S}}_k$. Notice that for $k \gg 0$ and for p as in (13.4.2)–(13.4.3)–(13.4.4), $\widetilde{\mathcal{S}}_k \cap U_p$ is a *real* algebraic variety. We will show that any such germ is homeomorphic with the germ of certain *complex* algebraic hypersurface. In these computations we will assume that $k/2$ is multiple of all the integers appearing in the decorations of $\Gamma_{\mathcal{C}}$; more precisely: whenever in the next discussion a fraction k/l appears for some l, then we will assume that k/l is, in fact, an even integer.

In the next paragraphs U will denote a local neighbourhood of the origin in $\mathbb{C}^3$.

13.5.1. Assume that p **is a generic point of** $\mathcal{C}$ as in (13.4.2). Consider the map

$$\psi_p : \{(x,y,z)\in U\,:\,x^m = y^n\} \longrightarrow \{(u,v,w)\in U_p\,:\,u^m v^n = |v|^{\nu k}\}^+$$

given by the correspondences

$$\left\{\begin{array}{rcl} u &=& x^{-1}|y|^{\nu k/m}\\ v &=& y\\ w &=& z \end{array}\right. \qquad\qquad \left\{\begin{array}{rcl} x &=& u^{-1}|v|^{\nu k/m}\\ y &=& v\\ z &=& w. \end{array}\right. \tag{13.5.2}$$

Then ψ_p is regular real algebraic (i.e. it extends over $x=0$ too), it is birational and a homeomorphism. Moreover, it is a partial normalization of $\widetilde{\mathcal{S}}_k \cap U_p$, i.e. the coordinates x,y,z of $\{x^m = y^n\}\cap U$ are integral over the regular functions of $\widetilde{\mathcal{S}}_k \cap U_p$. Indeed, birationality follows from the fact that the second set of equations provides the inverse of the first one, regularity follows from a limit computation, or by rewriting the first equation into $u = x^{-1}|x|^{\nu k/n}$. This formula also shows that ψ_p is bijective and a homeomorphism. Moreover, since $x^m = v^n$, x is integral over the ring of regular functions of $\widetilde{\mathcal{S}}_k \cap U_p$ (a similar statement for y and z is trivial).

In particular, the normalizations of the source and the target of ψ_p canonically coincide.

13.5.3. Assume that p **is a singular point of** $\mathcal{C}$ **of type 1** as in (13.4.3). Consider the map

$$\psi_p : \{(\alpha,\beta,\gamma)\in U\,:\,\alpha^m = \beta^n\gamma^l\} \longrightarrow \{(u,v,w)\in U_p\,:\,u^m v^n w^l = |v|^{\nu k}|w|^{\lambda k}\}^+$$

given by

$$\left\{\begin{array}{rcl} u &=& \alpha^{-1}|\beta|^{\nu k/m}|\gamma|^{\lambda k/m}\\ v &=& \beta\\ w &=& \gamma \end{array}\right. \qquad\qquad \left\{\begin{array}{rcl} \alpha &=& u^{-1}|v|^{\nu k/m}|w|^{\lambda k/m}\\ \beta &=& v\\ \gamma &=& w. \end{array}\right. \tag{13.5.4}$$

Then, again ψ_p is regular real algebraic, birational, and additionally, it is a homeomorphism. Moreover, it is a partial normalization of $\widetilde{\mathcal{S}}_k \cap U_p$, i.e. the coordinates α,β,γ are integral over the regular functions of $\widetilde{\mathcal{S}}_k \cap U_p$. Indeed, the regularity follows from

$$u = \alpha^{m-1}\overline{\alpha}^m|\beta|^{\nu k/m-2n}|\gamma|^{\lambda k/m-2l},$$

where $k \gg 0$ and $m > 0$. Moreover, α is integral over the ring of $\widetilde{\mathcal{S}}_k \cap U_p$ since $\alpha^m = v^n w^l$.

Hence again, the normalizations of the source and the target of ψ_p canonically coincide.

13.5.5. Assume that p **is a singular point of $\mathcal{C}$ of type 2** as in (13.4.4). In this case we can prove considerably less (from the analytic point of view). We will consider the map

$$\psi_p : \{(\alpha,\beta,\gamma) \in U \,:\, \alpha^n = \beta^m\gamma^{m'}\} \longrightarrow \{(u,v,w) \in U_p \,:\, u^m v^{m'} w^n = |w|^{\nu k}\}^+$$

given by

$$\left\{\begin{array}{lcl} u & = & \beta^{-1}|\beta|^{\nu k/n} \\ v & = & \gamma^{-1}|\gamma|^{\nu k/n} \\ w & = & \alpha. \end{array}\right. \tag{13.5.6}$$

It is regular real algebraic and an homeomorphism, but it is *not* birational.

Notice also that the above maps (in all three cases) preserve the coordinate axes.

13.6. The normalization $\mathcal{S}_k^{norm}$ of $\widetilde{\mathcal{S}}_k$.

13.6.1. Let $n_{\mathcal{S}} : \mathcal{S}_k^{norm} \to \widetilde{\mathcal{S}}_k$ be the normalization of $\widetilde{\mathcal{S}}_k$; for its existence, see [**9**]. Since the normalization is compatible with restrictions on smaller open sets, we get the globally defined $\mathcal{S}_k^{norm}$ whose restrictions above an open set of type $\widetilde{\mathcal{S}}_k \cap U_p$ are the normalization of that $\widetilde{\mathcal{S}}_k \cap U_p$. In particular, the local behaviour of the normalization $\mathcal{S}_k^{norm}$ over the different open neighbourhoods $\widetilde{\mathcal{S}}_k \cap U_p$ can be tested in the charts considered in the previous subsections.

E.g., if p **is a generic point** of $\mathcal{C}$, and ψ_p is the 'partial normalization' from (13.5.1), then it induces an isomorphism of normalizations:

$$\psi_p^{norm} : \{(x,y,z) \in U \,:\, x^m = y^n\}^{norm} \longrightarrow \{(u,v,w) \in U_p \,:\, u^m v^n = |v|^{\nu k}\}^{+,norm}.$$

Since the left hand side is smooth, we get that $\mathcal{S}_k^{norm}$ is smooth over the regular points of $\mathcal{C}$, hence after normalization only finitely many singular points will survive in $\mathcal{S}_k^{norm}$, and they are sitting over the double points of $\mathcal{C}$.

If p **is a double point of $\mathcal{C}$ of type 1**, then ψ_p from (13.5.3) induces again an isomorphism at the level of normalizations:

$$\psi_p^{norm} : \{(\alpha,\beta,\gamma) \,:\, \alpha^m = \beta^n\gamma^l\}^{norm} \longrightarrow \{(u,v,w) \,:\, u^m v^n w^l = |v|^{\nu k}|w|^{\lambda k}\}^{+,norm}.$$

Hence, after normalization, the singular points above the double points of $\mathcal{C}$ of type 1 are equivalent with complex analytic singularities of Hirzebruch-Jung type. Recall that these singularities are determined completely combinatorially (e.g. by the integers m, n, l above), and by the above representations (charts) the needed combinatorial data is also recovered from $\Gamma_{\mathcal{C}}$.

13.6.2. We emphasize that the above two types of charts from (13.6.1) are compatible. By this we mean the following: consider a double point p of $\mathcal{C}$ of type 1, and a neighbourhood U_p as above. Then $\mathcal{C} \cap U_p$ is the union of the v and w axis. Let q be a generic point of $\mathcal{C} \cap U_p$ and consider a sufficiently small local neighbourhood $U_q \subset U_p$ (where we denote this inclusion by j) and the chart ψ_p over $\widetilde{\mathcal{S}}_k \cap U_p$ as in (13.5.1), respectively ψ_q over $\widetilde{\mathcal{S}}_k \cap U_q$ as in (13.5.3). Then $\psi_p^{-1} \circ j \circ \psi_q$ is a complex analytic isomorphism (onto its image) which at the level of normalization induces an isomorphism of complex analytic smooth germs. Indeed, if q is a generic point of the w–axis (with non–zero w–coordinate) and the inclusion

$$\{(u',v',w') \in U_q \,:\, (u')^m(v')^n = |v'|^{\nu k}\}^+ \xrightarrow{j} \{(u,v,w) \,:\, u^m v^n w^l = |v|^{\nu k}|w|^{\lambda k}\}^+$$

is given by $u = u'(w')^{-l/m}|w'|^{\lambda k/m}$, $v = v'$ and $w = w'$, then $\psi_p^{-1} \circ j \circ \psi_q$ is given by $\alpha = xz^{l/m}$, $\beta = y$ and $\gamma = z$. Then the normalizations tautologically coincide. E.g., assume $\gcd(m,n) = 1$ and take the free variables (t, γ) normalizing $\{\alpha^m = \beta^n \gamma^l\}$ by $\alpha = t^n \gamma^{l/m}$, $\beta = t^m$ and $\gamma = \gamma$. Similarly, consider the free variables (s, z) normalizing $\{x^m = y^n\}$ by $x = s^n$, $y = s^m$ and $z = z$. Then $(\psi_p^{-1} \circ j \circ \psi_q)^{norm}$ is $t = s$ and $\gamma = z$.

In particular, *the two complex charts ψ_p^{norm} and ψ_q^{norm} of (13.6.1) induce the same orientation on their images, they identify the strict transform of $\mathcal{C}$ by the same orientation and induce on a normal slice of $\mathcal{C}$ the same orientation* (these are the key gluing–data for a plumbing construction).

13.6.3. On the other hand, **if p is a singular point of $\mathcal{C}$ of type 2**, then ψ_p from (13.5.5) will *not* induce an analytic isomorphism (since ψ_p itself is not birational). In this case, (13.5.5) implies that at the level of normalizations the induced map

$$\psi_p^{norm} : \{(\alpha, \beta, \gamma) \,:\, \alpha^n = \beta^m \gamma^{m'}\}^{norm} \longrightarrow \{(u, v, w) \,:\, u^m v^{m'} w^n = |w|^{\nu k}\}^{+,norm}$$

is regular and a homeomorphism. Nevertheless, one can prove slightly more:

LEMMA 13.6.4. *ψ_p^{norm} from (13.6.3) induces a diffeomorphism over $U_p \setminus \{0\}$.*

PROOF. Let p be a double point of $\mathcal{C}$ of type 2 as in (13.5.5). Then $\mathcal{C} \cap U_p$ is the union of the u and v axes. Let q be a generic point on the v axis, — the other case is completely symmetric. Then q is in the image of the following map

$$\begin{aligned} \varphi_{p,v} : \{(x, y, z) \in U' \setminus \{z = 0\} \,:\, x^n = y^m z^{m'}\} \longrightarrow & \\ \{(u, v, w) \in U_p \setminus \{v = 0\} \,:\, u^m v^{m'} w^n &= |w|^{\nu k}\}^+ \end{aligned}$$

given by the correspondences

$$(13.6.5) \qquad \left\{ \begin{array}{lcl} u & = & y^{-1}|x|^{\nu k/m} \\ v & = & z^{-1} \\ w & = & x \end{array} \right. \qquad\qquad \left\{ \begin{array}{lcl} y & = & u^{-1}|w|^{\nu k/m} \\ z & = & v^{-1} \\ x & = & w. \end{array} \right.$$

Then $\varphi_{p,v}$ is regular on $U_p \setminus \{z = 0\}$, since

$$u = |x|^{\nu k/m - 2n} y^{m-1} \overline{y}^m |z|^{2m'},$$

it is birational (its inverse is given by the second set of equations of (13.6.5)), and it is a partial normalization, since $y^m = w^n v^{m'}$. Therefore,

$$\varphi_{p,v}^{norm} : \{(x, y, z) \in U' \setminus \{z = 0\} \,:\, x^n = y^m z^{m'}\}^{norm} \longrightarrow n_{\mathcal{S}}^{-1}(\widetilde{\mathcal{S}}_k \cap U_p \setminus \{v = 0\})$$

is an isomorphism. Using this isomorphism, the restriction of ψ_p^{norm} from (13.6.3),

$$\psi_p^{norm} : \{(\alpha, \beta, \gamma) \in U \setminus \{\gamma = 0\} \,:\, \alpha^n = \beta^m \gamma^{m'}\}^{norm} \longrightarrow n_{\mathcal{S}}^{-1}(\widetilde{\mathcal{S}}_k \cap U_p \setminus \{v = 0\})$$

can be understood explicitly. Indeed, the map

$$\begin{aligned} (13.6.6) \quad \varphi_{p,v}^{-1} \circ \psi_p : \{(\alpha, \beta, \gamma) \in U \setminus \{\gamma = 0\} \,:\, \alpha^n = \beta^m \gamma^{m'}\} \longrightarrow & \\ \{(x, y, z) \in U' \setminus \{z = 0\} \,:\, x^n &= y^m z^{m'}\} \end{aligned}$$

is given by

$$(13.6.7) \qquad \left\{ \begin{array}{lcl} x & = & \alpha \\ y & = & \beta|\gamma|^{\nu k m'/mn} \\ z & = & \gamma|\gamma|^{-\nu k/n}. \end{array} \right.$$

We claim that this induces a diffeomorphism at the level of normalization. In order to verify this, we make two reductions. First, by a cyclic covering argument, we may assume that $m' = 1$. Second, we will also assume that $\gcd(m, n) = 1$ (otherwise the normalization will have $\gcd(m,n)$ components, and the normalization maps below must be modified slightly; the details are left to the reader). We fix two integers a and b such that $an-bm=1$. Then the left hand side of (13.6.6) is normalized by $(t,\gamma)\in(\mathbb{C}^2,0)\setminus\{\gamma=0\}$, $\alpha=t^m\gamma^a$, $\beta=t^n\gamma^b$, $\gamma=\gamma$; while the right hand side is normalized by $(s,z)\in(\mathbb{C}^2,0)\setminus\{z=0\}$, $x=s^mz^a$, $y=s^nz^b$ and $z=z$. Hence, at the normalization level

$$(\varphi_{p,v}^{-1}\circ\psi_p)^{norm}:(\mathbb{C}^2,0)\setminus\{\gamma=0\}\to(\mathbb{C}^2,0)\setminus\{z=0\}$$

is given by the diffeomorphism

$$\left\{\begin{array}{lcl} s & = & t|\gamma|^{a\nu k/mn} \\ z & = & \gamma|\gamma|^{-\nu k/n}. \end{array}\right. \tag{13.6.8}$$

□

13.6.9. By the results of (13.6.3), in $\mathcal{S}_k^{norm}$ and above a double point of $\mathcal{C}$ of type 2, say p, the type of the singularity can again be identified with a (complex analytic) Hirzebruch–Jung singularity, identified via the homeomorphism ψ_p^{norm}. In particular, corresponding to that point, in the plumbing graph we have to insert an appropriate HJ–string. In order to do this we need to clarify orientation–compatibilities at the intersection points of this string with the strict transforms of $\mathcal{C}$. More precisely, we have to clarify the compatibility of the chart ψ_p with 'nearby' charts of type (13.5.1).

Let p be as in the previous paragraph, fix one of its neighbourhoods $\widetilde{\mathcal{S}}_k\cap U_p$ as in (13.6.3), and a generic point q on the v–axis with small neighbourhood $\widetilde{\mathcal{S}}_k\cap U_q$ and chart $\psi_q:\{(x')^n=(y')^m\}\to\{(u')^m(w')^n=|w'|^{\nu k}\}=\widetilde{\mathcal{S}}_k\cap U_q$ given by $u'=y'^{-1}|x'|^{\nu k/m}$, $w'=x'$ and $v'=z'$, cf. (13.5.1). The inclusion $j:\widetilde{\mathcal{S}}_k\cap U_q\longrightarrow\widetilde{\mathcal{S}}_k\cap U_p$ is given by the equations $u=u'(v')^{-m'/m}$, $v=v'$ and $w=w'$. Hence $\varphi_{p,v}^{-1}\circ j\circ\psi_q$ is given by $x=x'$, $y=y'(z')^{m'/m}$ and $z=(z')^{-1}$. This combined with (13.6.7), the map $\psi_p^{-1}\circ j\circ\psi_q:\{x'^n=y'^m,\ z'\neq 0\}\to\{\alpha^n=\beta^m\gamma^{m'},\ \gamma\neq 0\}$ is given by (the inverse) of

$$\left\{\begin{array}{lcl} x' & = & \alpha \\ y' & = & \beta\gamma^{m'/m} \\ z' & = & \gamma^{-1}|\gamma|^{\nu k/n}. \end{array}\right. \tag{13.6.10}$$

For simplicity assume again that $\gcd(m,n)=1$ (the interested reader can reproduce the general case). We take integers a and b with $an-bm=m'$ as above. Then the free coordinates (t,γ) normalize $\{\alpha^n=\beta^m\gamma^{m'}\}$ by $\alpha=t^m\gamma^a$, $\beta=t^n\gamma^b$ and $\gamma=\gamma$, while the free coordinates (s,z') normalize $\{x'^n=y'^m\}$ by $x'=s^m$, $y'=s^n$ and $z'=z'$. In particular, the isomorphism $(\varphi_{p,v}^{-1}\circ j\circ\psi_q)^{norm}$ is given by the correspondence $(\mathbb{C}^2,0)\setminus\{\gamma=0\}\leftrightarrow(\mathbb{C}^2,0)\setminus\{z'=0\}$:

$$\left\{\begin{array}{lcl} s & = & t\gamma^{a/m} \\ z' & = & \gamma^{-1}|\gamma|^{\nu k/n}. \end{array}\right. \tag{13.6.11}$$

Notice that the strict transform of $\mathcal{C}$ (in the two charts) is given by $t=0$, respectively by $s=0$.

Now, consider the natural orientations of $n_{\mathcal{S}}^{-1}(\widetilde{\mathcal{S}}_k\cap U_p)$ provided via ψ_p by the complex structure of the source of ψ_p, and also the orientation of $n_{\mathcal{S}}^{-1}(\mathcal{C}\cap U_p)$ via the same procedure. In a similar way, consider the orientations of $n_{\mathcal{S}}^{-1}(\widetilde{\mathcal{S}}_k\cap U_q)$ and $n_{\mathcal{S}}^{-1}(\mathcal{C}\cap U_q)$ induced by ψ_q and the complex structure of its source. Then (13.6.11) shows the following fact:

LEMMA 13.6.12. *$(\varphi_{p,v}^{-1} \circ j \circ \psi_q)^{norm}$ is a diffeomorphism which reverses the orientations. Moreover, its restriction on the strict transforms of $\mathcal{C}$ reverses the orientation of these Riemann surfaces as well. On the other hand, the orientation of the transversal slices to the strict transforms of $\mathcal{C}$ are preserved.*

13.7. The 'resolution' $\overline{\mathcal{S}}_k$ of $\widetilde{\mathcal{S}}_k$. The singularities of $\mathcal{S}_k^{norm}$ are sitting above the double points of $\mathcal{C}$. Above a double point of type 1 they are isomorphic with complex analytic Hirzebruch–Jung singularities, hence their resolution follows the resolution procedure of these germs, cf. (13.6.2).

Above double points of type 2 the real analytic type of the singularity and their resolution is not determined here. Nevertheless, these singularities are also identified, up to an orientation reversing homeomorphism, with complex analytic Hirzebruch–Jung singularities, cf. (13.6.12). This is enough to determine the topology of $\mathcal{S}_k^{norm}$ and to describe the plumbing representation of its boundary. This will be done in the next subsection.

Although, for the purpose of the present work the above topological representation is enough, if we would like to handle real analytic invariants read from the (structure sheaf of the) resolution (like, say, the geometric genus is read from the resolution of a normal surface singularity), then an explicit description of this variety would be more than necessary. Though this type of analytic questions are beyond the aims of the present work, we formulate this as an important goal for further research.

13.7.1. **Problem.** Find an explicit description of the real analytic/algebraic resolution of the singularity

$$\{(u,v,w)\in(\mathbb{C}^3,0)\,:\,u^m v^{m'} w^n = |w|^k\}^+,$$

where m, $m'>0$ and k is a sufficiently large (even) integer (which might satisfy some other divisibility assumptions as well, if it is necessary).

13.8. The plumbing graph. The end of the proof of (12.4.1). Once the geometry of the tubular neighbourhood of the divisor $\mathcal{C}$ is clarified, it is standard to describe the plumbing representation of the boundary of this neighbourhood. We follow the strategy of [**48**] (with slight modification above the double points of type 2).

13.8.1. Consider a component C of $\mathcal{C}$ with decoration $(m;n,\nu)$. By (13.5.1), the local equation of $\widetilde{\mathcal{S}}_k$ in a neighbourhood of a generic point of C is $x^m=y^n$, hence $n_{\mathcal{S}}^{-1}(C)\to C$ is a regular covering of degree $\gcd(m,n)$ over the regular part of C. Let C^{norm} be the normalization of C, i.e. the curve obtained by separating the self–intersection points of C (which are codified by loops of $\Gamma_{\mathcal{C}}$ attached to the vertex v_C which corresponds to C). Then $q: n_{\mathcal{S}}^{-1}(C)\to C^{norm}$ is a cyclic branched covering whose branch points B sit above the double points of $\mathcal{C}$. They correspond bijectively to the legs of the star of v_C, cf. (12.3.1). Notice that if $v_C\in\mathcal{V}^1(\Gamma_{\mathcal{C}})$ (see (8.1.2) for notation) then $m=1$, hence the covering is trivial. Otherwise C^{norm} is rational by (8.3.2).

Fix a branch point $b\in B$ whose neighbourhood has local equation is of type $z^c=x^ay^b$. Then $q^{-1}(b)$ has exactly $\gcd(a,b,c)$ points; this number automatically divides $\gcd(m,n)$ for any choice of b. The number $\mathfrak{n}_{v_C}$ of connected components of $n_{\mathcal{S}}^{-1}C$ is the order of $\operatorname{coker}(\pi_1(C^{norm}\setminus B)\to\mathbb{Z}_{gcd(m,n)})$, where a small loop around b is sent to the class of $\gcd(a,b,c)$. Hence the formula (12.3.2) for $\mathfrak{n}_{v_C}$ follows, and (12.3.4) follows too by an Euler–characteristic argument.

In the local charts of (13.5.1) $g=v^\nu=y^\nu$. Since by normalization $y=t^{m/gcd(m,n)}$, and $t=0$ is the local equation of the strict transform of C, the vanishing order of y^ν along the strict transform of C (i.e. the multiplicity of the open book decomposition of $\arg(g)$) is $m\nu/\gcd(m,n)$, proving (12.3.3). This ends the proof of Step 1 of the main algorithm and (12.4.1).

13.8.2. Next, one has to insert the Hirzebruch–Jung strings corresponding to the singularities of $\mathcal{S}_k^{norm}$. Type 1 singular points behave similarly as those appearing in the case of cyclic coverings [**44**] or in the case of Iomdin series [**48**] (or anywhere in complex analytic geometry). In particular, the orientation compatibilities imply (cf. (13.6.2)) that they are glued in by edges with decorations + (as usual for dual graphs of complex analytic curve configurations).

One the other hand, the way how the Hirzebruch–Jung strings of type 2 are inserted is dictated by Lemma (13.6.12). Assume that the singularity is (above) the intersection point $C_1 \cap C_2$ of two components of $\mathcal{C}$. Then, in the plumbing representation we have to connect their strict transforms (denoted by the same symbols) by a string $E_1, \ldots, E_s$. By (13.6.12), when C_1 is glued to the HJ–string, its orientation is reversed. In order to keep the ambient orientation, we have to change the orientation of its transversal slice too. But this is identified with the first curve E_1 of the string. If the orientation of E_1 is changed, then, similarly as above, we have to change the orientation of its transversal slice, which is identified with E_2. By this iteration, we see, that all the decorations of all the edges of the string (inserted by Step 2, Case 2 in (12.3.5)) should be $\ominus$.

The multiplicity decorations are given by the vanishing orders of g, and are computed by the usual procedures, cf. (5.2). This proves Step 2 of the Main Algorithm. Finally, Step 3 does not require any further explanation (see (5.1.2)). This ends the proof of Theorem (12.4.1).

Theorems (12.5.2) and (12.5.4) are particular cases, they are obtained by forgetting some information from the graph of ∂F.

13.9. The 'extended' monodromy action. Usually, when one has a plumbing graph G, besides the 3–manifold (constructed by gluing S^1–bundles), one can consider the plumbed 4–manifold too (constructed by gluing disc–bundles). This is the case here as well; in fact, as it is clear from the constructions of this section, the plumbed 4–manifold associated with G is exactly the manifold $\overline{\mathcal{S}}_k$ (cf. (13.7)).

The point we wish to stress in this subsection is that there is a natural monodromy action on the pair $(\overline{\mathcal{S}}_k, \partial\overline{\mathcal{S}}_k)$ such that the induced action on $\partial\overline{\mathcal{S}}_k$ coincides with the (Milnor) monodromy action of ∂F.

Indeed, instead of only defining the space $Z_k = \{c = |d|^k\}$, cf. (13.3), one can take all the family of spaces $Z_k(t) := \{c = |d|^k e^{it}\}$ for all values $t \in [0, 2\pi]$, and repeat the constructions of § 13. In particular, one can define in a natural way $\mathcal{S}_k(t)$, $\widetilde{\mathcal{S}}_k(t)$ and $\overline{\mathcal{S}}_k(t)$ for all t. This is a locally trivial bundle over the parameter t, hence moving t from 0 to 2π, we get the wished action on the pair $(\overline{\mathcal{S}}_k, \partial\overline{\mathcal{S}}_k)$.

At homological level, by a covering argument, the generalized 1–eigenspace $H_1(\overline{\mathcal{S}}_k)_1$ equals $H_1(\mathcal{S}_k)$, hence

$$\begin{aligned} &rank\, H_1(\overline{\mathcal{S}}_k) = 2g(G) + c(G);\\ &rank\, H_1(\overline{\mathcal{S}}_k)_1 = rank\, H_1(\mathcal{S}_k) = 2g(\Gamma_{\mathcal{C}}) + c(\Gamma_{\mathcal{C}}).\end{aligned} \tag{13.9.1}$$

The monodromy action on the cohomology long exact sequence of $(\overline{\mathcal{S}}_k, \partial\overline{\mathcal{S}}_k)$ will have some important consequences later (see e.g. the proof of (19.2.10)).

§ 14. The Collapsing Main Algorithm

14.1. Elimination of Assumption B. In the formulation and the proof of the Main Algorithm (12.3) it is essential the absence of 'vanishing 2–edges' in $\Gamma_{\mathcal{C}}$. If a certain $\Gamma_{\mathcal{C}}$ has such an edge, it can be modified by a blow up, which replaces the unwanted edge by three 'acceptable' edges, see (12.1.2). Therefore, in any situation, it is easy to assure the condition of Assumption B, and the Main Algorithm serves as a complete algorithm for ∂F, $\partial F_1 F$, $\partial_2 F$ and for the different multiplicity systems.

Nevertheless, if the graph $\Gamma_{\mathcal{C}}$ is constructed by a canonical geometric procedure, and it has vanishing 2–cycles, the above method of the Main Algorithm (i.e., which starts with the blowing up of these edges) has some inconveniences.

First of all, in the new graph $\Gamma_{\mathcal{C}}$ we create several new vertices and edges; on the other hand, it turns out that in the output final graph G all these extra vertices/edges can be eliminated, collapsed (see e.g. (14.1.1)). Hence, this indicates that blowing up $\Gamma_{\mathcal{C}}$ might be unnecessary, and there should be another method to eliminate these edges, in such a way that the new graph is not 'increasing'.

But, in fact, the main reason to search for another approach/solution is dictated by a more serious reason: in the next section we will see that 'unicolored' graphs/subgraphs (i.e. those for which the edge decorations are the same) have big advantages in the determination of the geometrical structure (e.g. Jordan blocks, monodromy operators). On the other hand, by the elimination procedure (12.1.2) we might destroy such a property. E.g., for cylinders, the graph $\Gamma_{\mathcal{C}}$ (as it is constructed in (9.1), i.e. before applying the elimination procedure), is unicolored (all the edge–decorations are 2), a property which is not preserved after the extra blow ups (of (12.1.2)).

Moreover, we will see in (20.1.6) that the 'twist' (local variation map) associated with a *vanishing* 2–edge is *vanishing*. Hence, the separating annulus (in the fiber of the open book) codified by such an edge is 'rigid', hence it should be glued rigidly with its neighbourhood. Hence, in the language of the graph, such an edge should be rather collapsed than blown up!

This can also be reinterpreted in the following way. We will prove (see (20.1.6)) that the twist of a 1–edge is negative, of a non–vanishing 2–edge is positive, while, as we already said, of a vanishing 2–edge, is zero. Since by blowing up a vanishing 2–edge we create two new 1–edges and one new 2–edge, we replace the zero–twist–contribution by two contributions of different signs. Nevertheless, handling operators (see a concrete situation in subsections (20.1.7)–(20.1.10)), sometimes it is more convenient to have a semi–definite matrix rather than a non–degenerate one, which is not definite.

In this subsection we will present an alternative way to modify $\Gamma_{\mathcal{C}}$ and the Main Algorithm in the presence of vanishing 2–edges. In fact, this second method is also based on the algorithm just proved: we blow up such an edge, we run the Main Algorithm (12.3), then we apply the plumbing calculus for that part of the graph whose ancestor is that vanishing 2–edge and its adjacent vertices, and we show that that part collapses into a single vertex. Moreover, any connected subgraph whose edges are vanishing 2–edges, by this procedure collapses into a single vertex.

We keep the output of all these steps as a shortcut, which will be built in the new version of the Main Algorithm, called 'Collapsing Main Algorithm'. (Obviously, if the original graph has no vanishing 2–edges, then the two algorithms are the same.)

14.1.1. Consider a vanishing 2–edge e as in (12.1.2):

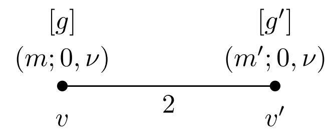

For simplicity assume that $v, v' \in \mathcal{W}$ and $v \neq v'$. Assume that the 1–legs (cf. (12.2)) of v have weights $\{(m;n_i,\nu_i)\}_{i=1}^{s}$, and the 2–legs of v, other than e, are decorated by $\{(m_j;0,\nu)\}_{j=1}^t$. Set $N:=\gcd(m,n_1,\dots,n_s,m_1,\dots,m_t)$. We will have similar notations s', t', n'_i, ν'_i, m'_j, N' for v' too. In (12.1.2) we have replaced e by the string $Str(e)$:

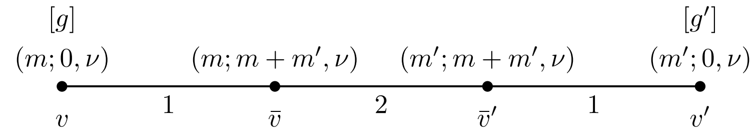

Then let us run the Main Algorithm for this part of the graph. In the covering graph G the number of vertices over v is $\mathfrak{n}_v:=\gcd(N,m')$, over v' is $\mathfrak{n}_{v'}:=\gcd(N',m)$, and over the new vertices $\bar v$ and $\bar v'$ their number is $\mathfrak{n}_e:=\gcd(m,m')$. Moreover, over all the edges we have to put $\mathfrak{n}_e$ edges, they form $\mathfrak{n}_e$ strings, containing the $\mathfrak{n}_e$ vertices sitting above the new vertices, and the ends of these strings are cyclically identified with the vertices sitting over v and v' respectively. The vertices over v have multiplicity decoration (ν) and genus decoration $\tilde g$ determined by (12.3.4):

$$\mathfrak{n}_v\cdot(2-2\tilde g)=(2-2g-s-t-1)\cdot m+\sum_{i=1}^{s}\gcd(m,n_i)+\sum_{j=1}^{t}\gcd(m,m_j)+\mathfrak{n}_e. \tag{14.1.2}$$

There is a similar statement for vertices over v' too. The vertices of G over the new vertices v and v' have zero genera and multiplicity decorations $(m\nu/\mathfrak{n}_e)$ and $(m'\nu/\mathfrak{n}_e)$ respectively. Furthermore, if we apply Step 2 of the algorithm (12.3.5), then we realize that above the 1–edges the corresponding strings are degenerate (hence we insert $+$–edges only), while above the 2–edge of $Str(e)$ any inserted string $Str^{\ominus}$ has only one vertex with multiplicity (ν) and Euler decoration $(m+m')/\mathfrak{n}_e$. In particular, all the $\mathfrak{n}_e$ strings above $Str(e)$ have the form

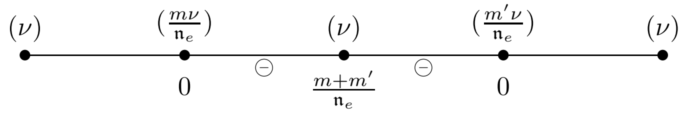
(ν)
$(\frac{m\nu}{\mathfrak{n}_e})$
(ν)
$(\frac{m'\nu}{\mathfrak{n}_e})$
(ν)
$\ominus$
$\ominus$
0
$\frac{m+m'}{\mathfrak{n}_e}$
0

The configuration of all the vertices and edges sitting above e and its end–vertices form $\mathfrak{n}:=\gcd(\mathfrak{n}_v,\mathfrak{n}_{v'})$ connected components.

Now, we run the plumbing calculus of oriented plumbed 3–manifolds, cf. (5.1). Notice that by two 0–chain absorptions the above string can be collapsed. In particular, by *0–chain absorptions* and *oriented handle absorptions* all these strings can be collapsed identifying their end–vertices as well. Hence, after 0–chain and oriented handle absorptions each connected component collapses into a single vertex. Their number will be $\mathfrak{n}$ and all of them will carry multiplicity (ν). The genus decoration g_e of such a vertex can be computed as follows: First we have a contribution from 0–chain absorptions, namely the sum of all the genera of the vertices in that component, namely $(\mathfrak{n}_v\tilde g+\mathfrak{n}_{v'}\tilde g')/\mathfrak{n}$. Then, corresponding to oriented handle absorptions, we have to add one for each 1–cycle of that component. This, by an Euler–characteristic argument is $(\mathfrak{n}_e-\mathfrak{n}_v-\mathfrak{n}_{v'}+\mathfrak{n})/\mathfrak{n}$. Hence $\mathfrak{n}(1-g_e)=\mathfrak{n}_v(1-\tilde g)+n_{v'}(1-\tilde g')-\mathfrak{n}_e$, or, this combined with (14.1.2), gives

$$\begin{aligned}\mathfrak{n}\cdot(2-2g_e)&=(2-2g-s-t-1)\cdot m+\sum_i\gcd(m,n_i)+\sum_j\gcd(m,m_j)\\&\quad+(2-2g'-s'-t'-1)\cdot m'+\sum_i\gcd(m',n'_i)+\sum_j\gcd(m',m'_j).\end{aligned}$$

14.1.3. The point is that it might happen that a vertex of $\Gamma_{\mathcal{C}}$ is the end–vertex of more than one vanishing 2–edge. Hence, if we run the above procedure (14.1.1) for all the vanishing 2–edges simultaneously, a bigger part of the graph will be collapsed. We make this fact more precise in this subsection.

Consider the graph $\Gamma_{\mathcal{C}}$ (as it is given by a resolution procedure, or by a geometric construction, *unmodified* by Assumption B), which satisfies Assumption A.

We start with the claim that $\Gamma_{\mathcal{C}}$ has no *vanishing 2–loops.* Indeed, such a loop can be supported neither by a vertex of $\Gamma^1_{\mathcal{C}}$ (because of Assumption A (7.3)), nor by a vertex of $\Gamma^2_{\mathcal{C},j}$, because $\Gamma_{\mathcal{C},j}$ is a tree by (8.3.2).

The same argument shows that any connected subgraph of $\Gamma_{\mathcal{C}}$, with the property that all its edges are *vanishing 2–edges*, is a *tree.*

Let Γ_{van} be a maximal connected subgraph of $\Gamma_{\mathcal{C}}$ with only non–arowhead vertices and vanishing 2–edges connecting them. (In particular, Γ_{van} has no edges supporting arrowheads). As we already proved, it is a tree.

This subgraph might have only one vertex w with decoration, say $(m; n, \nu)$. In this case define $\mathfrak{n}_{\Gamma_{van}} = \mathfrak{n}_w$ (given by (12.3.2)), $m_{\Gamma_{van}} = m\nu/\gcd(m, n)$ (cf. (12.3.3)), and $g_{\Gamma_{van}} = \tilde{g}_w$ given by (12.3.4).

Next, assume that Γ_{van} contains several vertices. For any vertex w of Γ_{van}, consider its star in $\Gamma_{\mathcal{C}}$:

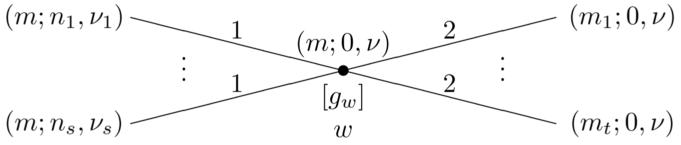

Notice that the 2–legs of this star come from two sources: either are associated with the edges of Γ_{van}, or are 2–edges supporting arrowheads. Let $\hat{t}_w$ be the number of this second group. (The end decorations of these legs are $(1; 0, 1)$, hence if there is a vertex w of Γ_{van} with $\hat{t}_w > 1$, then $\nu = 1$ automatically.)

Associated with the star of w we consider the integers n_w, $\tilde{g}_w$ and $\hat{g}_w$ as follows:

- $n_w := \gcd(m, n_1, \ldots, n_s, m_1, \ldots, m_t)$, cf. (12.3.2);
- $\mathfrak{n}_w(2 - 2\tilde{g}_w) = (2 - 2g_w - s - t)m + \sum_{i=1}^{s} \gcd(m, n_i) + \sum_{j=1}^{t} \gcd(m, m_j)$, cf. (12.3.4);
- $\mathfrak{n}_w(2 - 2\hat{g}_w) = (2 - 2g_w - s - t)m + \sum_{i=1}^{s} \gcd(m, n_i) + \hat{t}_w$.

Furthermore, for any edge $e \in \mathcal{E}(\Gamma_{van})$ (with decorations as in (14.1.1)) define

- $\mathfrak{n}_e := \gcd(m, m')$, cf. (14.1.1).

Then, similarly as in (14.1.1), if we eliminate all the vanishing 2–edges of Γ_{van} by blow ups (12.1.2), and we run the Main Algorithm (12.3), after 0–chain and oriented handle absorptions, the whole subgraph above Γ_{van} will collapse into

$$\mathfrak{n}_{\Gamma_{van}} := \gcd\{\, n_w \,:\, w \in \mathcal{V}(\Gamma_{van})\} \tag{14.1.4}$$

vertices, all with multiplicity

$$m_{\Gamma_{van}} = \nu, \tag{14.1.5}$$

and genus decoration $g_{\Gamma_{van}}$, which is determined similarly as in (14.1.1): the contribution from the genera of the vertices is $\sum_w \mathfrak{n}_w \tilde{g}_w / \mathfrak{n}_{\Gamma_{van}}$, while the contribution from the cycles is

$$(14.1.6)\qquad \Big(\sum_{e\in\mathcal{E}(\Gamma_{van})}\mathfrak{n}_e-\sum_{w\in\mathcal{V}(\Gamma_{van})}\mathfrak{n}_w+\mathfrak{n}_{\Gamma_{van}}\Big)/\mathfrak{n}_{\Gamma_{van}}.$$

In particular, for $g_{\Gamma_{van}}$ we get:

$$(14.1.7)\qquad \mathfrak{n}_{\Gamma_{van}}(2-2g_{\Gamma_{van}})=\sum_{w\in\mathcal{V}(\Gamma_{van})}\mathfrak{n}_w(2-2\hat{g}_w).$$

14.1.8. Consider a (vanishing) 2–edge e of $\Gamma_{\mathcal{C}}$ which supports an arrowhead, whose non–arrowhead vertex w has weight $(m;0,1)$. Let Γ_{van} be the subgraph (as in (14.1.3)) which contains w. Clearly, $\mathfrak{n}_{\Gamma_{van}}=1$, hence Γ_{van} can be collapsed to a point as in (14.1.3).

Regarding e, by similar steps as in (14.1.1) and (14.1.3), we get in G, above e, exactly $\mathfrak{n}_e=1$ string, whose shape is:

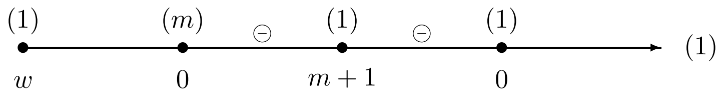

Obviously, the first 0–vertex can be eliminated by 0–chain absorption. This modified shorter string is glued to the unique vertex constructed in (14.1.3) corresponding to Γ_{van}.

Now we are able to formulate the new version of the Main Algorithm.

14.2. The Collapsing Main Algorithm.

14.2.1. Start again with the graph $\Gamma_{\mathcal{C}}$ read from a resolution (cf. 7.1.1)). If it has vanishing 2–edges, we will not blow them up, as in (12.1.2). Instead, we will 'collapse' them by the procedure described in the previous subsection (14.1).

Denote by $\widehat{\Gamma_{\mathcal{C}}}$ the (undecorated) graph obtained from $\Gamma_{\mathcal{C}}$ by contracting (independently) each subgraphs of type Γ_{van} into a unique vertex. All 1–edges, non–vanishing 2–edges, arrowhead vertices and vanishing 2–edges supporting arrowhead vertices naturally survive inheriting the natural adjacency relations.

Then, we construct a plumbing graph $\widehat{G}$ of the open book of ∂F with binding V_g and fibration $\arg(g):\partial F\setminus V_g\to S^1$ as follows. It will be determined as a covering graph of $\widehat{\Gamma_{\mathcal{C}}}$, modified with strings, cf. (6.1)–(6.2). In order to identify it, we have to provide the covering data of the covering $\widehat{G}\to\widehat{\Gamma_{\mathcal{C}}}$ (cf. (6.1.2)).

14.2.2. **Step 1. — The covering data of the vertices of $\widehat{\Gamma_{\mathcal{C}}}$.**

Over a vertex of $\widehat{\Gamma_{\mathcal{C}}}$, obtained by the contraction of the subgraph Γ_{van} of $\Gamma_{\mathcal{C}}$, we insert $\mathfrak{n}_{\Gamma_{van}}$ vertices in $\widehat{G}$ (cf. (14.1.4)), all of them with genus decoration $g_{\Gamma_{van}}$ (cf. (14.1.7)), and multiplicity $m_{\Gamma_{van}}$ (cf. (14.1.5)).

Any arrowhead vertex of $\widehat{\Gamma_{\mathcal{C}}}$ is covered by one arrowhead vertex of $\widehat{G}$, decorated by multiplicity decoration (1), similarly as in the original version (12.3.1).

14.2.3. **Step 2. — The covering data of edges and the types of the inserted strings.**

Case 1. The case of 1–edges is the same as in the original version (12.3.5). Over such an edge e, which in $\Gamma_{\mathcal{C}}$ had the form

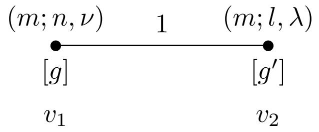

insert (cyclically) in $\widehat{G}$ exactly $\mathfrak{n}_e = \gcd(m,n,l)$ strings of type

$$Str\left(\frac{n}{\mathfrak{n}_e},\frac{l}{\mathfrak{n}_e};\frac{m}{\mathfrak{n}_e}\;\Big|\;\nu,\lambda;0\right).$$

If the edge e is a loop, then the procedure is the same with the only modification that the end–vertices of the strings are identified. If the right vertex v_2 is an arrowhead, then complete again the same procedure with $m=1$ and $\mathfrak{n}_e=1$, namely: above such an edge e put a single edge decorated by $+$ (which supports that arrowhead of $\widehat{G}$ which covers the corresponding arrowhead of $\widehat{\Gamma_{\mathcal{C}}}$).

Case 2. The case of *non–vanishing* 2–edges is again unmodified. Above such an edge e, which in $\Gamma_{\mathcal{C}}$ had the form (with $n>0$)

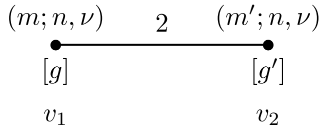

insert (cyclically) in G exactly $\mathfrak{n}_e=\gcd(m,m',n)$ strings of type

$$Str^{\ominus}\left(\frac{m}{\mathfrak{n}_e},\frac{m'}{\mathfrak{n}_e};\frac{n}{\mathfrak{n}_e}\;\Big|\;0,0;\nu\right).$$

If the edge is a loop, then we modify the procedure as in the case of 1–loops.

Case 3. Finally, we have to consider the case of those *vanishing* 2-edges which support arrowheads (the others have been collapsed).

Above such an edge we insert in $\widehat{G}$ one string of type

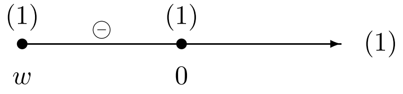

If the 2–edge was supported in $\Gamma_{\mathcal{C}}$ by a vertex which belonged to Γ_{van}, then the end–vertex w of the above string should be identified with the unique vertex of $\widehat{G}$ corresponding to that subgraph Γ_{van}.

14.2.4. **Step 3. — Determination of the missing Euler numbers.** The first two steps provide a graph with the next decorations: the multiplicities of all the vertices, all the genera, some of the Euler numbers and all the sign–decorations of the edges. The missing Euler numbers are determined by the formula (5.1.2).

14.3. The output of the 'collapsing algorithm'. Similarly as in the first case, Proposition (6.1.4) guarantees that *there is only one cyclic graph–covering of* $\Gamma_{\mathcal{C}}$ *with this covering data (up to a graph–isomorphism).*

In fact, by (14.1.3), the output $\widehat{G}$ of the 'improved algorithm' and the output G of the original algorithm are connected by the 'reduced oriented plumbing calculus': $\widehat{G}\sim G$. Hence, Theorem (12.4.1) is valid for $\widehat{G}$ as well: $\widehat{G}$ *is a possible plumbing graph of the pair* $(\partial F, \partial F\cap V_g)$*, which carries the multiplicity system of the open book decomposition* $\arg(g):\partial F\setminus V_g\to S^1$.

The algorithm is again compatible with the decomposition of ∂F into $\partial_1 F$ and $\partial_2 F$. The part regarding $\partial_1 F$ is unmodified (since $\Gamma^1_{\mathcal{C}}$ has no 2–edges). The graph G_2 transforms into $\widehat{G_2}$ similarly as G transforms into $\widehat{G}$. Moreover, all the statements of (12.5) regarding G_1 and G_2 are valid for $\widehat{G_1}=G_1$ and $\widehat{G_2}$ with the natural modifications; the details are left to the reader.

14.3.1. On the other hand, the difference between G and $\widehat{G}$, the outputs of the original and the new algorithms, both *unmodified by plumbing calculus*, can be substantial, sometimes even spectacular. See e.g. the complete computation in the case of cylinders in section § 25.

For example, the difference $c(G) - c(\widehat{G})$ is the sum over all subgraphs Γ_{van} of the expression appearing in (14.1.6), which can be a rather large number. This will have a crucial consequences in the discussion of the Jordan blocks of the vertical monodromies (showing, in fact, the incontestable advantage of $\widehat{G}$ versus G).

Similarly as in (12.4), we will use the notation $\widehat{G}$ for the output graph obtained by the Collapsing Main Algorithm described above, and which is unmodified by any operation of the calculus. We adopt the same notation for the graphs of $\partial_1 F$ and $\partial_2 F$, namely $\widehat{G_1}$ and $\widehat{G_2}$. (Recall that $G \sim \widehat{G}$. Hence there is no need to consider the 'modified $\widehat{G}$', since for that we can use the old notation G^m, cf. (12.4)).

CHAPTER VII

Homological properties of the monodromies.

§ 15. Vertical/horizontal monodromies. Generalities.

15.1. The monodromy operators. Let f be a hypersurface singularity with a 1–dimensional singular locus. In general, it is rather difficult to determine the horizontal and vertical monodromies $\{m'_{j,hor}\}_{i=1}^{s}$ and $\{m'_{j,ver}\}_{i=1}^{s}$ of $Sing(V_f)$, especially the vertical one. (For the terminology, see (3.2).) It is even more difficult to identify the two commuting actions simultaneously.

This difficulty survives at the homological level too: in the literature there is no general treatment of the corresponding two commuting operators. In lack of general theory, the existing literature is limited to few sporadic examples, which are obtained by ad hoc methods (for relatively simple situations when such methods are sufficient to produce the answer).

Our goal here is to provide a general procedure to treat these homological objects and to produce (in principle without any obstruction) examples as complicated as we wish.

Similarly, if we fix another germ g such that $\Phi = (f, g)$ is an ICIS, then one of the most important tasks is the computation of the algebraic monodromy representation of $\mathbb{Z}^2$ induced by $m_{\Phi,hor}$ and $m_{\Phi,ver}$ (for their definition, see (4.1)). Our treatment will include the determination of these objects as well.

In fact, we target the following algebraic monodromy operators:

- the commuting pair $M'_{j,hor}$ and $M'_{j,ver}$, acting on $H_1(F'_j)$, induced by $m'_{j,hor}$ and $m'_{j,ver}$ $(1 \leq j \leq s)$,
- the commuting pair $M^{\Phi}_{j,hor}$ and $M^{\Phi}_{j,ver}$, acting on $H_1(F_\Phi \cap T_j) = H_1(F'_j)^{\oplus d_j}$ (cf. (4.3.1)), induced by $m^{\Phi}_{j,hor}$ and $m^{\Phi}_{j,ver}$ $(1 \leq j \leq s)$,
- the commuting pair $M_{\Phi,hor}$ and $M_{\Phi,ver}$, acting on $H_1(F_\Phi)$, induced by $m_{\Phi,hor}$ and $m_{\phi,ver}$, cf. (4.1).

Here, usually, we considered homology with complex coefficients, but obviously, one might also consider the integral case. In fact, in some of our examples, occasionally, the additional $\mathbb{Z}$–invariants will be treated as well.

We separate our discussion into two parts. In this chapter we determine completely (via $\Gamma_{\mathcal{C}}$) the character decomposition (i.e. the semi–simple part) of the relevant $\mathbb{Z}^2$–representations. This includes all the characteristic polynomials of all the monodromy operators. Moreover, we connect the ranks of some generalized eigenspaces with the combinatorics of the plumbing graph G as well. We wish to emphasize that, although we get all our results rather automatically from the graph $\Gamma_{\mathcal{C}}$, all these results are new, and were out of reach (in this generality) with previous techniques. This shows once more the power of $\Gamma_{\mathcal{C}}$.

The second part treats the structure of the Jordan blocks. This is considerably harder. Our main motivation in this part is the computation of the homology of ∂F and its algebraic monodromy action. Since the homology of ∂F will be determined via the homology of $\partial F \setminus V_g$, hence by the Wang exact sequence in which the operator $M_{\Phi,ver} - I$ appears, the determination of the 2–Jordan blocks of $M_{\Phi,ver}$ with eigenvalue one is a crucial ingredient.

Therefore, in this work we will concentrate only on the computation of these Jordan blocks, although for some cases we will provide the complete picture. This second part (including the discussion regarding the Jordan blocks of the vertical monodromies for eigenvalue one, and the computation of homology and algebraic monodromy of ∂F) constitutes the next chapter.

REMARK 15.1.1. Although F_Φ is not the local Milnor fiber of a hypersurface singularity, a convenient restriction of Φ provides a map over a sufficiently small disc (a transversal slice of the d–axis at one of its generic points) with generic fiber F_Φ such that the horizontal monodromy $M_{\Phi,hor}$ is the monodromy over the small punctured disc (in other words, the horizontal monodromy $M_{\Phi,hor}$ can be 'localized', it can be represented as the monodromy of a family of curves over a small punctured disc). On the other hand, the vertical monodromy $M_{\Phi,ver}$ *cannot* be localized in this sense. In particular, general results about the monodromy of families over a punctured disc cannot be applied for the vertical monodromies. (This is one of the reasons why their computation is so difficult. This difficulty will be overcome here using the graph $\Gamma_{\mathcal{C}}$.)

15.2. General facts. The statements of the next lemma are well–known for the horizontal monodromies (by the celebrated 'Monodromy Theorem', see e.g. [**13, 30**] for the global case, [**12, 31**] for the local case, or [**27**] for a recent monograph), and may be known for the vertical monodromies as well, although we were not able to find a reference for them:

LEMMA 15.2.1. *The eigenvalues of the operators $M'_{j,hor}$, $M'_{j,hor}$, $M^{\Phi}_{j,hor}$, $M^{\Phi}_{j,ver}$ ($1\leq j\leq s$), respectively $M_{\Phi,hor}$ and $M_{\phi,ver}$, are roots of unity. Moreover, the size of the Jordan blocks cannot be larger than two.*

PROOF. For the operators acting on $H_1(F_\Phi)$ use the decomposition (8.5.3) of F_Φ, and the fact that the restriction of the geometric actions on each subset $\widetilde{F}_v$ is isotopic to a finite action. (As a model of the proof, see e.g. [**18**, §13].) The same is true for the operators acting on $H_1(F_\Phi\cap T_j)$. (In this case only those subsets $\widetilde{F}_v$ appear which are indexed by the non–arrowhead vertices of $\Gamma^2_{\mathcal{C},j}$.) Finally, the operators $M^{\Phi}_{j,*}$ and $M'_{j,*}$ are connected by a simple algebraic operation, see (4.3.1)(2). Compare with the proofs of (16.2.6) and (19.2.2) as well. □

REMARK 15.2.2. By the 'Monodromy Theorem' valid for isolated hypersurface singularities, the Jordan blocks of $M'_{j,hor}$ with eigenvalue one must have size one (see e.g. [**27**, (3.5.9)]). By the correspondence (4.3.1)(2), this fact is true for $M^{\Phi}_{j,hor}$ as well. Nevertheless, for the other four operators, such a restriction is *not* true anymore: In (22.6.2) we provide an example when all $M'_{j,ver}$, $M^{\Phi}_{j,ver}$ $M_{\phi,hor}$ and $M_{\phi,ver}$ have Jordan blocks of size 2 with eigenvalue one.

In fact, examples with $M'_{j,ver}$ having such a Jordan block can be constructed as follows: Fix a topological/equisingularity type of isolated plane curve singularity S whose monodromy has a 2–Jordan block. Let o be the order of the eigenvalue of this block. Then one can construct a projective plane curve C of degree d (sufficiently large), which is a multiple of o, and such that C has a local singularity of type S. Let V_f be the cone over C. By a result of Steenbrink [**63**] $M'_{j,ver}=(M'_{j,hor})^{-d}$, hence $M'_{j,ver}$ has a Jordan block with eigenvalue one and size two.

§ 16. Vertical/horizontal monodromies. Characters.

16.1. Definitions. Algebraic preliminaries. Let H be a finite dimensional $\mathbb{C}$–vector space, and assume that $M\in Aut(H)$. Let $P_M(t)$ (or $P_{H,M}(t)$) be the characteristic polynomial $\det(tI-M)$ of M. For each eigenvalue λ, let $H_{M,\lambda}=$

$\ker((\lambda I-M)^N)$ (for N large) be the generalized λ–eigenspace of M. Obviously, the multiplicity of $t-\lambda$ in $P_M(t)$ is exactly $\dim H_{M,\lambda}$. Sometimes it is more convenient to replace $P_M(t)$ by its 'divisor'

$$Div(H;M) := \sum_{\lambda} \dim H_{M,\lambda}\cdot(\lambda)\in \mathbb{N}[\mathbb{C}^*]. \tag{16.1.1}$$

More generally, assume that two commuting automorphisms M_1 and M_2 act on H. Then, for each pair $(\lambda,\xi)\in\mathbb{C}^*\times\mathbb{C}^*$, set $H_{(\lambda,\xi)} := H_{M_1,\lambda}\cap H_{M_2,\xi}$ and

$$Div(H;M_1,M_2) := \sum_{(\lambda,\xi)} \dim(H_{(\lambda,\xi)})\cdot(\lambda,\xi)\in \mathbb{N}[\mathbb{C}^*\times\mathbb{C}^*]. \tag{16.1.2}$$

16.1.3. **Key Example.** Fix a triple of integers $(m;n,\nu)$ with m, $\nu>0$ and $n\geq 0$. Let $\mathcal{P}$ be the set of points

$$\mathcal{P} := \{(u,v)\in\mathbb{C}^*\times\mathbb{C}^*\,|\,v^\nu=1,\ u^mv^n=1\}.$$

In fact, $\mathcal{P}$ is a finite subgroup of $\mathbb{C}^*\times\mathbb{C}^*$ of order $m\nu$. On this set of points we define two commuting permutations: For each pair of real numbers (t_{hor},t_{ver}), consider the set of points

$$\mathcal{P}(t_{hor},t_{ver}) := \{(u,v)\in\mathbb{C}^*\times\mathbb{C}^*\,|\,v^\nu=e^{it_{ver}},\ u^mv^n=e^{it_{hor}}\}.$$

Fixing $t_{ver}=0$ and moving t_{hor} from 0 to 2π, we get a locally trivial family of $m\nu$ points, which defines a permutation σ_{hor} of $\mathcal{P}$. Similarly, fixing $t_{hor}=0$ and moving t_{ver} from 0 to 2π, we get the permutation σ_{ver} of $\mathcal{P}$. One can verify that the two permutations commute (since, e.g., the torus $\{|u|=|v|=1\}$ has abelian fundamental group).

Let $H:=H_0(\mathcal{P},\mathbb{C})$ be the vector space with base elements indexed by the points from $\mathcal{P}$, i.e. the vector space of elements of type $\sum_{p\in\mathcal{P}}c_p\cdot p$, where $c_p\in\mathbb{C}$. For any permutation σ of $\mathcal{P}$, define $\sigma_*\in Aut(H)$ by

$$\sigma_*(\textstyle\sum_p c_p\cdot p) := \sum_p c_p\cdot\sigma(p).$$

Our goal is to determine

$$\Lambda(m;n,\nu) := Div(H;\sigma_{hor,*},\sigma_{ver,*})\in\mathbb{N}[\mathbb{C}^*\times\mathbb{C}^*].$$

Consider the elements $\mathfrak{h}:=(e^{2\pi i/m},1)$ and $\mathfrak{v}:=(e^{-2\pi in/m\nu},e^{2\pi i/\nu})$ of $\mathcal{P}$. Then, by a computation one can verify that σ_{hor} (respectively σ_{ver}) can be obtained by multiplication in $\mathcal{P}$ by $\mathfrak{h}$ (respectively by $\mathfrak{v}$). Let $\widetilde{\mathcal{P}}$ be the subgroup of the permutation group of $\mathcal{P}$ generated by σ_{hor} and σ_{ver}. Having the forms of $\mathfrak{h}$ and $\mathfrak{v}$, one can verify easily that $\mathfrak{h}$ and $\mathfrak{v}$ (hence σ_{hor} and σ_{ver} in $\widetilde{\mathcal{P}}$ too) satisfy the relation $\mathfrak{h}^m=\mathfrak{v}^{m\nu/(m,n)}=\mathfrak{h}^n\mathfrak{v}^\nu=1$, and that $\widetilde{\mathcal{P}}$ acts transitively on $\mathcal{P}$. (Here $(m,n)=\gcd(m,n)$.) Define the group

$$G(m;n,\nu) := \{(\lambda,\xi)\in\mathbb{C}^*\times\mathbb{C}^*\ :\ \lambda^m=\lambda^n\xi^\nu=1\}. \tag{16.1.4}$$

(Notice that for $(\lambda,\xi)\in G(m;n,\nu)$, one has automatically $\xi^{m\nu/(m,n)}=1$.) Then $G(m;n,\nu)$ is isomorphic to $\widetilde{\mathcal{P}}$, both have order $m\nu$, and since $\widetilde{\mathcal{P}}$ acts transitively on $\mathcal{P}$ (which has the same order) both are isomorphic to $\mathcal{P}$ (by a morphism generated by $\sigma_{hor}\mapsto\mathfrak{h}$ and $\sigma_{ver}\mapsto\mathfrak{v}$). Therefore, for any $(\lambda,\xi)\in G(m;n,\nu)$ there is a (λ,ξ)–eigenvector of the action $(\sigma_{hor},\sigma_{ver})$ which has the form:

$$\sum_{k,l}\lambda^k\xi^l\cdot\sigma_{hor}^{-k}\sigma_{ver}^{-l}(p_0),$$

where $p_0 = (1,1) \in \mathcal{P}$, and the index set k,l is taken in such a way that the set $\{\sigma_{hor}^k \sigma_{ver}^l\}_{k,l}$ is exactly $\widetilde{\mathcal{P}}$, and each element is represented once. Therefore

$$\Lambda(m;n,\nu) = \sum_{(\lambda,\xi)\in G(m;n,\nu)} (\lambda,\xi). \tag{16.1.5}$$

As a particular example, assume that in (16.1.3) one has $\nu = 1$. Then $G(m;n,1) = \{\lambda : \lambda^m = 1\}$ and $\xi = \lambda^{-n}$. Hence

$$\Lambda(m;n,1) = \sum_{\lambda^m=1} (\lambda, \lambda^{-n}). \tag{16.1.6}$$

From (16.1.5) it also follows that the characteristic polynomials of $\sigma_{hor,*}$, respectively of $\sigma_{ver,*}$ acting on H are the following:

$$P_{\sigma_{hor,*}}(t) = (t^m - 1)^\nu, \quad P_{\sigma_{ver,*}}(t) = (t^{m\nu/(m,n)} - 1)^{(m,n)}. \tag{16.1.7}$$

Moreover, the characteristic polynomial of $\sigma_{hor,*}$ restricted on the generalized 1–eigenspace $H_{\sigma_{ver,*},1}$ of $\sigma_{ver,*}$ is

$$P_{\sigma_{hor,*}|H_{\sigma_{ver,*},1}}(t) = t^{(m,n)} - 1. \tag{16.1.8}$$

16.1.9. **The 'd–covering'.** Let H be a finite dimensional vector space with two commuting automorphisms M_1 and M_2. Furthermore, fix a positive integer d. We define $H^{(d)} := H^{\oplus d}$ and its automorphisms $M_1^{(d)}$ and $M_2^{(d)}$ by

$$M_1^{(d)}(x_1,\dots,x_d) = (M_1(x_1),\dots,M_1(x_d)),$$

and

$$M_2^{(d)}(x_1,\dots,x_d) = (M_2(x_d),x_1,\dots,x_{d-1}).$$

It is not hard to see that $Div(H^{(d)}; M_1^{(d)}, M_2^{(d)})$ can be recovered from $Div(H; M_1, M_2)$ and the integer d. Indeed, consider the morphism

$$\Xi^{(d)} : \mathbb{N}[\mathbb{C}^*\times\mathbb{C}^*] \to \mathbb{N}[\mathbb{C}^*\times\mathbb{C}^*], \quad \text{where } \Xi^{(d)}((\lambda,\xi)) := \sum_{\alpha^d=\xi} (\lambda,\alpha).$$

Then, one shows that

$$\Xi^{(d)}(Div(H; M_1, M_2)) = Div(H^{(d)}; M_1^{(d)}, M_2^{(d)}).$$

Lemma 16.1.10. *For any fixed positive integer d one has:*

(a) $\Xi^{(d)}$ is injective.

(b) $\Xi^{(d)}(\Lambda(m;n,\nu)) = \Lambda(m;n,d\nu)$.

Proof. (a) If one takes $\Omega^{(d)} : \mathbb{N}[\mathbb{C}^*\times\mathbb{C}^*] \to \mathbb{Q}[\mathbb{C}^*\times\mathbb{C}^*]$, defined by $\Omega^{(d)}(\lambda,\alpha) = \frac{1}{d}(\lambda,\alpha^d)$, then $\Omega^{(d)} \circ \Xi^{(d)}$ is the inclusion $\mathbb{N}[\mathbb{C}^*\times\mathbb{C}^*] \hookrightarrow \mathbb{Q}[\mathbb{C}^*\times\mathbb{C}^*]$. For (b) notice that the system $\{\lambda^m = \lambda^n\xi^\nu = 1,\ \alpha^d = \xi\}$ is equivalent to $\{\lambda^m = \lambda^n\alpha^{d\nu} = 1\}$. □

16.2. The divisors Div_Φ, Div_j^Φ and Div'_j in terms of $\Gamma_{\mathcal{C}}$.

Definition 16.2.1. *Using the monodromy operators introduced in (15.1), we set*

$$Div'_j := Div(H_1(F'_j); M'_{j,hor}, M'_{j,ver}) \qquad (1 \le j \le s), \tag{16.2.2}$$

$$Div_j^\Phi := Div(H_1(F'_j)^{\oplus d_j}; M^\Phi_{j,hor}, M^\Phi_{j,ver}), \quad (1 \le j \le s), \tag{16.2.3}$$

and

$$Div_\Phi := Div(H_1(F_\Phi); M_{\Phi,hor}, M_{\Phi,ver}). \tag{16.2.4}$$

16.2.5. **Further notations.** Recall that $\mathcal{W}(\Gamma_{\mathcal{C}})$ (respectively $\mathcal{W}(\Gamma^2_{\mathcal{C},j})$) denote the set of non–arrowhead vertices of $\Gamma_{\mathcal{C}}$ (respectively of $\Gamma^2_{\mathcal{C},j}$, for any $j=1,\dots,s$). For each $w\in\mathcal{W}(\Gamma_{\mathcal{C}})$, let C_w be the corresponding irreducible curve in $\mathcal{C}$, g_w its genus, and δ_w the number of legs associated with the star of v (cf. 12.2), i.e. the number of edges in $\Gamma_{\mathcal{C}}$ adjacent to w, where each loop contributes twice. Moreover, assume that the decoration of w in $\Gamma_{\mathcal{C}}$ is $(m_w;n_w,\nu_w)$.

THEOREM 16.2.6.

$$Div_\Phi-(1,1)=\sum_{w\in\mathcal{W}(\Gamma_{\mathcal{C}})}(2g_w+\delta_w-2)\cdot\Lambda(m_w;n_w,\nu_w). \tag{16.2.7}$$

Moreover, for any $j=1,\dots,s$,

$$Div^\Phi_j-\sum_{\xi^{d_j}=1}(1,\xi)=\sum_{w\in\mathcal{W}(\Gamma^2_{\mathcal{C},j})}(\delta_w-2)\cdot\Lambda(m_w;n_w,\nu_w), \tag{16.2.8}$$

$$Div'_j-(1,1)=\sum_{w\in\mathcal{W}(\Gamma^2_{\mathcal{C},j})}(\delta_w-2)\cdot\Lambda(m_w;n_w,\nu_w/d_j), \tag{16.2.9}$$

where $d_j=\deg(g|\Sigma_j)$, or by (8.3.3), $d_j=gcd(\nu_w)_{w\in\mathcal{W}(\Gamma^2_{\mathcal{C},j})}$.

In particular, the above formulae provide the ranks of $H_1(F_\Phi)$ and $H_1(F'_j)$ as well.

PROOF. As in any 'A'Campo type' formula (cf. [**1**]), it is more convenient to work with a zeta–function of an action instead of its characteristic polynomial. In the present case also, we will determine first the element

$$D(F_\Phi):=Div(H_0(F_\Phi);M^0_{\Phi,hor},M^0_{\Phi,ver})-Div(H_1(F_\Phi);M_{\Phi,hor},M_{\Phi,ver})$$

in $\mathbb{Z}[\mathbb{C}^*\times\mathbb{C}^*]$. Above, $M^0_{\Phi,hor}$ and $M^0_{\Phi,ver}$ are the horizontal and the vertical monodromies acting on $H_0(F_\Phi)$. Since F_Φ is connected, this space is $\mathbb{C}$, and $M^0_{\Phi,hor}=M^0_{\Phi,ver}=Id_{\mathbb{C}}$, hence $Div(H_0(F_\Phi);M^0_{\Phi,hor},M^0_{\Phi,ver})=(1,1)$. Hence, the left hand side of (16.2.7) is $-D(F_\Phi)$.

The point is that $D(F_\Phi)$ is additive with respect to a Mayer–Vietoris exact sequence. More precisely, if we consider the decomposition (8.5.3), then

$$D(F_\Phi)=\sum_{w\in\mathcal{W}(\Gamma_{\mathcal{C}})}D(\widetilde{F}_w)-D(E),$$

where E is the union of 'cutting circles'. Since $H_0(E)=H_1(E)$ and the monodromy actions on them can also be identified, $D(E)=0$. On the other hand, $\widetilde{F}_w$ is a regular covering over the regular part C^{reg}_w of the curve C_w with a finite fiber which can be identified with $\mathcal{P}$ in the Key Example (16.1.3). Moreover, the horizontal and vertical actions on $\widetilde{F}_w$ are induced by the corresponding actions on $\mathcal{P}$. Hence $D(\widetilde{F}_w)=\chi(C^{reg}_w)\cdot D(\mathcal{P})=\chi(C^{reg}_w)\cdot\Lambda(m_w;n_w,\nu_w)$, where $\chi(C^{reg}_w)$ stands for the Euler–characteristic of C^{reg}_w, and equals $2-2g_w-\delta_w$.

The proof of (16.2.8) is similar. Using the results and notations of (4.3.1), one gets that $F_\Phi\cap T_j$ is cut by 'cutting circles' into the pieces $\{\widetilde{F}_w\}_{w\in\Gamma^2_{\mathcal{C},j}}$. But $F_\Phi\cap T_j$ consists of d_j copies of F'_j. Hence, with the additional fact that $g_w=0$ for all $w\in\mathcal{W}(\Gamma^2_{\mathcal{C},j})$, we get

$$-D(\cup_{d_j}F'_j;m^\Phi_{j,hor},m^\Phi_{j,hor})=\sum_{w\in\mathcal{W}(\Gamma^2_{\mathcal{C},j})}(\delta_w-2)\cdot\Lambda(m_w;n_w,\nu_w).$$

On the other hand, in this case, the 0–homology is different: $H_0(\cup_{d_j}F'_j,\mathbb{C})=\mathbb{C}^{d_j}$ on which the horizontal monodromy acts by identity and the vertical one by cyclic permutation —, hence its contribution is $\sum_{\xi^{d_j}=1}(1,\xi)$.

Now, using the special forms of $m^\Phi_{j,hor}$ and $m^\Phi_{j,hor}$ from (4.3.1)(2), by (16.1.9) and (16.1.10) one gets that $\Omega^{(d_j)}(Div^\Phi_j)=Div'_j$, hence (16.2.8) follows. □

(16.2.6), (16.1.7) and (16.1.8) imply:

COROLLARY 16.2.10.

(a) The characteristic polynomial of $M_{\Phi,hor}$ and $M_{\Phi,ver}$, acting on $H=H_1(F_\Phi,\mathbb{C})$, are

$$P_{M_{\Phi,hor}}(t)=(t-1)\cdot\prod_{w\in\mathcal{W}(\Gamma_{\mathcal{C}})}(t^{m_w}-1)^{\nu_w(2g_w+\delta_w-2)},$$

$$P_{M_{\Phi,ver}}(t)=(t-1)\cdot\prod_{w\in\mathcal{W}(\Gamma_{\mathcal{C}})}(t^{m_w\nu_w/(m_w,n_w)}-1)^{(m_w,n_w)(2g_w+\delta_w-2)}.$$

The characteristic polynomial of the restriction of $M_{\Phi,hor}$ on the generalized eigenspace $H_1(F_\Phi,\mathbb{C})_{M_{\Phi,ver},1}$ is

$$P_{M_{\Phi,hor}|H_{M_{\Phi,ver},1}}(t)=(t-1)\cdot\prod_{w\in\mathcal{W}(\Gamma_{\mathcal{C}})}(t^{(m_w,n_w)}-1)^{2g_w+\delta_w-2}.$$

(b) There are similar formulae for the operators acting on $H=H_1(F_\Phi\cap T_j)$:

$$P_{M^\Phi_{j,hor}}(t)=(t-1)^{d_j}\cdot\prod_{w\in\mathcal{W}(\Gamma^2_{\mathcal{C},j})}(t^{m_w}-1)^{\nu_w(\delta_w-2)},$$

$$P_{M^\Phi_{j,ver}}(t)=(t^{d_j}-1)\cdot\prod_{w\in\mathcal{W}(\Gamma^2_{\mathcal{C},j})}(t^{m_w\nu_w/(m_w,n_w)}-1)^{(m_w,n_w)(\delta_w-2)},$$

$$P_{M^\Phi_{j,hor}|H_{M^\Phi_{j,ver},1}}(t)=(t-1)\cdot\prod_{w\in\mathcal{W}(\Gamma^2_{\mathcal{C},j})}(t^{(m_w,n_w)}-1)^{\delta_w-2}.$$

(c) Finally, the characteristic polynomials of the local horizontal/vertical monodromies acting on $H=H_1(F'_j,\mathbb{C})$ are

$$P_{M'_{j,hor}}(t)=(t-1)\cdot\prod_{w\in\mathcal{W}(\Gamma^2_{\mathcal{C},j})}(t^{m_w}-1)^{\nu_w(\delta_w-2)/d_j},$$

$$P_{M'_{j,ver}}(t)=(t-1)\cdot\prod_{w\in\mathcal{W}(\Gamma^2_{\mathcal{C},j})}(t^{m_w\nu_w/d_j(m_w,n_w)}-1)^{(m_w,n_w)(\delta_w-2)},$$

$$P_{M'_{j,hor}|H_{M'_{j,ver},1}}(t)=(t-1)\cdot\prod_{w\in\mathcal{W}(\Gamma^2_{\mathcal{C},j})}(t^{(m_w,n_w)}-1)^{\delta_w-2}.$$

Notice that the output of the right hand sides of the formulae in (c) (a posteriori) should be independent of the choice of the germ g, since the left hand sides depend only on the germ f.

Notice also that $P_{M^\Phi_{j,hor}|H_{M^\Phi_{j,ver},1}}(t)=P_{M'_{j,hor}|H_{M'_{j,ver},1}}(t)$.

REMARK 16.2.11. The above formulas (16.2.6) and (16.2.10) are valid even if $\Gamma_{\mathcal{C}}$ does not satisfy Assumption A. In this case, it might happen that $\mathcal{W}(\Gamma^2_{\mathcal{C},j})=\emptyset$, see e.g. (10.1.5). In such a situation, by convention, $\sum_{\mathcal{W}(\Gamma^2_{\mathcal{C},j})}=0$ and $\prod_{\mathcal{W}(\Gamma^2_{\mathcal{C},j})}=1$.

16.3. Examples.

16.3.1. Assume that $f = x^3y^7 - z^4$; see (11.1.1) for the graph $\Gamma_{\mathcal{C}}$ (with $g = x+y+z$). Then, by (16.2.10)(c), the characteristic polynomials of the two vertical monodromies $M'_{j,ver}$ $(j = 1, 2)$ are $(t^7-1)^3/(t-1)^3$ (corresponding to the transversal type $y^7 - z^4$), respectively $(t^3-1)^3/(t-1)^3$ (corresponding to the transversal type $x^3 - z^4$). This can also be verified geometrically in an elementary way: by the Thom–Sebastiani theorem (see [**69**]), in the first case F'_j homotopically is the joint of 7 points with 4 points. Analyzing the equation of f we get that the vertical monodromy is the joint of the cyclic permutation of the 7 points with the trivial permutation of the 4 points. A similar geometric description is valid for the second case too.

In particular, in this case, these vertical operators have no eigenvalue 1.

16.3.2. If $f = y^3 + (x^2 - z^4)^2$ (see (11.1.3) for $\Gamma_{\mathcal{C}}$), then the transversal type is A_2 and $M'_{1,ver}$ has characteristic polynomial $(t-1)^2$. Since the eigenvalues of the commuting operator $M'_{1,hor}$ are distinct, $M'_{1,ver}$ is the identity.

16.3.3. If $f = x^a + y^2 + xyz$ $(a = 3$ or $5)$, cf. (9.4.3) and (9.4.4), then $s = 1$, the transversal type is A_1, and $Div'_1 = (1, 1)$.

16.3.4. If $f = x^2y^2 + z^2(x+y)$, or $f = x^2y + z^2$, cf. (11.1.2)) and (9.3.1), then again each transversal type is A_1, but $Div'_j = (1, -1)$.

Remark 16.3.5. Assume that f is homogeneous of degree d. For g a generic linear function, $\Gamma_{\mathcal{C}}$ was constructed in section §10. This says that any vertex has a decoration of type $(m; d, 1)$. Moreover, by (16.1.6),

$$\Lambda(m; d, 1) = \sum_{\lambda^m=1} (\lambda, \lambda^{-d}).$$

Therefore, the statement of (16.2.6) is compatible with $M_{\Phi,ver} = (M_{\Phi,hor})^{-d}$, or $M^{\Phi}_{j,ver} = (M^{\Phi}_{j,hor})^{-d}$ already mentioned (see also (22.2) for more details).

16.4. Vertical monodromies and the graph G.

16.4.1. As we already explained, we are primarily interested in the generalized eigenspaces of the vertical monodromies corresponding to eigenvalue one. Subsection (16.2) provides their ranks in terms of $\Gamma_{\mathcal{C}}$. In this subsection we compute them in terms of the combinatorics of the plumbing graph G.

The reader is invited to recall the definition of the graphs G and $G_{2,j}$, the plumbing graphs of $(\partial F, V_g)$ and $\partial_{2,j}F$, which were introduced in (12.4.1) and (12.5.3)), and are kept *unmodified by plumbing calculus*.

For any graph Gr whose vertices are arrowheads $\mathcal{A}(Gr)$ and non–arrowheads $\mathcal{W}(Gr)$ (and where the arrowheads are supported by usual or dash–edges), we also define $\mathcal{E}_{\mathcal{W}}(Gr)$ as the set of edges connecting non–arrowhead vertices. Recall that $c(Gr)$ denotes the number of independent cycles in Gr and $g(Gr)$ the sum of the genus decorations of Gr. These numbers, clearly, are not independent. E.g., if Gr is connected, then by an Euler–characteristic argument:

$$1 - c(Gr) = \#\mathcal{W}(Gr) - \#\mathcal{E}_w(Gr). \tag{16.4.2}$$

Example 16.4.3. Let G be one of the output graphs of the Main Algorithm (12.3). In order to determine $c(G)$ and $g(G)$, for each $w \in \mathcal{W}(\Gamma_{\mathcal{C}})$ we will rewrite the decorations $m, n, n_1, \ldots, n_s, m_1, \ldots, m_t$ used in the Main Algorithm as $m_w, n_w, n_{w,1}, \ldots, n_{w,s}, m_{w,1}, \ldots, m_{w,t}$. Then, using the formulae of (12.3), we have the following expressions in terms of $\Gamma_{\mathcal{C}}$ for the cardinalities $\#\mathcal{A}(G)$, $\#\mathcal{W}(G)$, and $\#\mathcal{E}_{\mathcal{W}}(G)$ of the corresponding sets associated with G:

$$\#\mathcal{A}(G) = \#\mathcal{A}(\Gamma_{\mathcal{C}});$$

$$\#\mathcal{W}(G)=\sum_{w\in\mathcal{W}(\Gamma_{\mathcal{C}})}\gcd(m_w,n_w,n_{w,1},\dots,n_{w,s},m_{w,1},\dots,m_{w,t});$$

$$2\#\mathcal{E}_{\mathcal{W}}(G)+\#\mathcal{A}(G)=\sum_{w\in\mathcal{W}(\Gamma_{\mathcal{C}})}\Big(\ \sum_i\gcd(m_w,n_w,n_{w,i})+\sum_j\gcd(m_w,n_w,m_{w,j})\ \Big);$$

Moreover,

$$2g(G)=\sum_{w\in\mathcal{W}(\Gamma_{\mathcal{C}})}(2g_w+\delta_w-2)\gcd(m_w,n_w)+2\#\mathcal{W}(G)-2\#\mathcal{E}_w(G)-\#\mathcal{A}(G);$$

and, obviously, $c(G)$ also follows via (16.4.2).

REMARK 16.4.4. One can verify that, in general, $g(G)\geq g(\Gamma_{\mathcal{C}})$ and $c(G)\geq c(\Gamma_{\mathcal{C}})$. (Compare with [**44**, (3.11)].)

PROPOSITION 16.4.5. *The ranks of the generalized eigenspaces $H_1(F_\Phi,\mathbb{C})_{M_{\Phi,ver},1}$ and $H_1(F'_j,\mathbb{C})_{M'_{j,ver},1}$ satisfy the following identities:*

$$\dim\, H_1(F_\Phi,\mathbb{C})_{M_{\Phi,ver},1}=2g(G)+2c(G)+\#\mathcal{A}(G)-1. \tag{16.4.6}$$

$$\dim\, H_1(F'_j,\mathbb{C})_{M'_{j,ver},1}=2g(G_{2,j})+2c(G_{2,j})+\#\mathcal{A}(G_{2,j})-1. \tag{16.4.7}$$

Notice also that by (16.2.10), one also has the identity

$$\dim H_1(F_\Phi\cap T_j,\mathbb{C})_{M^{\Phi}_{j,ver},1}=\dim H_1(F'_j,\mathbb{C})_{M'_{j,ver},1}. \tag{16.4.8}$$

Above, $\#\mathcal{A}(G_{2,j})$ is the number of arrowheads of $G_{2,j}$, which, in fact, are all dash–arrows. Their number is equal to $\#\mathcal{E}_{cut,j}$, the number of 'cutting edges' adjacent to $\Gamma^2_{\mathcal{C},j}$.

PROOF. By the third formula of (16.2.10)(a) one has

$$\dim\, H_1(F_\Phi)_{M_{\Phi,ver},1}=1+\sum_{w\in\mathcal{W}(\Gamma_{\mathcal{C}})}\gcd(m_w,n_w)\cdot(2g_w+\delta_w-2).$$

Then use (16.4.3) and (16.4.2). The proof of the second identity is similar. □

REMARK 16.4.9. Although, the graph $\Gamma^2_{\mathcal{C},j}$ is a tree whose vertices have zero genus–decorations (cf. (8.3.2)), in general, both $g(G_{2,j})$ and $c(G_{2,j})$ can be non–zero.

Consider for example a line arrangement with d lines and its graph $\Gamma_{\mathcal{C}}$ as in (10.2). Fix an intersection point $j\in\Pi$ contained in m_j lines, and consider its corresponding vertex v_j in $\Gamma_{\mathcal{C}}$. Above v_j there is only one vertex in G, whose genus $\widetilde{g}_j$ via (12.3.4) is

$$2-2\widetilde{g}_j=(2-m_j)\cdot\gcd(m_j,d)+m_j.$$

Therefore, $\widetilde{g}_j=0$ if and only if $(m_j-2)\cdot(\gcd(m_j,d)-1)=0$; hence $\widetilde{g}_j$ typically is not zero.

An example when $c(G_{2,j})\neq 0$ is (22.5.5) with d even.

It might happen that G_1 and G_2 have no cycles, while G does; see e.g. (9.4.3) or (9.4.4).

16.4.10. Proposition (16.4.5) points out an important fact: although the graph $\Gamma_{\mathcal{C}}$ depends on the choice of the resolution r in (7.1.1), hence the graphs G and $G_{2,j}$ inherit this dependency as well, certain numerical invariants of them, describing geometrical invariants of the original germ f or of the pair (f,g), are independent of this ambiguity. Sometimes, even more surprisingly, the role of g is irrelevant too. Here is the start of the list of such numerical invariants:

- $\#\mathcal{A}(G)=$ number of irreducible components of $V_f\cap V_g$;
- $\#\mathcal{A}(G_{2,j})=$ number of gluing tori of $\partial_{2,j}F$, see (12.5.7) (independent of g);
- $g(G)+c(G)$ is an invariant of (f,g) by (16.4.6);

- $g(G_{2,j})+c(G_{2,j})$ is an invariant of f (independent of g) by (16.4.7).

For the continuation of the list and more comments on $g(G)$ and $c(G)$, see (18.1.7) and (18.2).

Note that all these invariants are stable with respect to the *reduced* oriented plumbing calculus (in fact, the definition of the reduced set of operations relies exactly on this observation). In particular, we also have:

COROLLARY 16.4.11. *The statements of (16.4.5) are valid for any graph* G^m *(respectively* $G^m_{2,j}$*) with* $G^m\sim G$ *(respectively* $G^m_{2,j}\sim G_{2,j}$*). E.g., for* $\widehat{G}$ *too.*

CHAPTER VIII

Homological invariants of ∂F and $\partial F \setminus V_g$

§ 17. The characteristic polynomial of ∂F. Starting point.

In order to determine the characteristic polynomial of the Milnor monodromy acting on $H_1(\partial F)$ we need to understand two key geometrical objects: the pair $(\partial F, \partial F \setminus V_g)$ and the fibration $\arg(g) : \partial F \setminus V_g \to S^1$. In the next paragraphs we discuss both of them and we indicate those data which remain undetermined after this discussion. In the next sections we will determine these data, at least in the most significant cases.

[The main reason for the lack of a complete description lies in the fact that for the variation map involved, the 'uniform twist property' (usually valid in situations in complex geometry) is not satisfied. This is happening because for edges with different decorations we glue together subspaces with different orientations; for more technical details see (20.1).]

17.1. The pair $(\partial F, \partial F \setminus V_g)$. From the long homological exact sequence of the pair $(\partial F, \partial F \setminus V_g)$ we get

$$\longrightarrow H_2(\partial F, \partial F \setminus V_g) \xrightarrow{\partial} H_1(\partial F \setminus V_g) \longrightarrow H_1(\partial F) \to 0.$$

By excision, $H_2(\partial F, \partial F \setminus V_g)$ equals $H_0(\partial F \cap V_g) \otimes H_2(D, \partial D))$, where D is a real 2–disc, hence it is free of rank $\#\mathcal{A}(G) = \#\mathcal{A}(\Gamma_\mathcal{C})$, the number of components of $\partial F \cap V_g$. Since the monodromy is trivial in a neighbourhood of $\partial F \cap V_g$, we get:

Lemma 17.1.1. *The characteristic polynomials of the restriction of the Milnor monodromy action of F on ∂F and on $\partial F \setminus V_g$ satisfy*

$$P_{H_1(\partial F),M}(t) = P_{H_1(\partial F \setminus V_g),M}(t) \cdot (t-1)^{-rank\, im\, \partial},$$

where

$$1 \leq rank\, im\, \partial \leq \#\mathcal{A}(G). \tag{17.1.2}$$

Here, the first inequality follows from the fact that $H_1(\partial F) \neq H_1(\partial F \setminus V_g)$. Indeed, consider a component of $\partial F \cap V_g$ and a small loop around it in ∂F. Then its homology class in $H_1(\partial F)$ is zero, but it is sent into $\pm 1 \in H_1(S^1)$ by $\arg(g)_*$, hence it is non–zero in $H_1(\partial F \setminus V_g)$.

At this generality, it is impossible to say more about $rank\, im\, \partial$: both bounds in (17.1.2) are sharp. E.g., one can prove (see section § 22), that if f is homogeneous of degree d, and the projective curve $C = \{f = 0\}$ has $|\Lambda|$ irreducible components, then $rank\, im\, \partial = d - |\Lambda| + 1$ (and $d = \#\mathcal{A}(G)$). Therefore, in the case of arrangements $rank\, im\, \partial = 1$, and if C is irreducible then $rank\, im\, \partial = d = \#\mathcal{A}(G)$.

17.2. The fibrations $\arg(g)$. By (4.2.1), the fibration $\arg(g) : \partial F \setminus V_g \to S^1$ is equivalent to the fibration $\Phi^{-1}(\partial D_\delta) \to \partial D_\delta$ with fiber F_Φ and monodromy $m_{\Phi,ver}$, the Milnor monodromy being identified with the induced monodromy by $m_{\Phi,hor}$. Therefore, from the Wang exact sequence of this second fibration we get

$$P_{H_1(\partial F \setminus V_g),M}(t) = (t-1) \cdot P_{M_{\Phi,hor}|coker(M_{\Phi,ver}-I)}(t). \tag{17.2.1}$$

This formula can be 'localized' (around the singular locus): the Wang exact sequence of the fibration $\partial_{2,j}F\to S^1$ provides

$$P_{H_1(\partial_{2,j}F),M}(t)=(t-1)\cdot P_{M^{\Phi}_{j,hor}|coker(M^{\Phi}_{j,ver}-I)}(t). \tag{17.2.2}$$

Since the horizontal (Milnor) monodromy on ∂_1F is trivial, the left hand side of (17.2.1) differs from the product (over j) of the left hand side of (17.2.2) only by a factor of type $(t-1)^N$. This, of course, is true for the right hand sides too.

On the other hand, by (4.3.1), $(H_1(\partial_{2,j}F),M^{\Phi}_{j,hor},M^{\Phi}_{j,ver})$ is the 'd–covering' of $(H_1(F'_j),M'_{j,hor},M'_{j,ver})$ (cf. (16.1.9)). Therefore, the generalized 1–eigenspace of their vertical monodromies can be identified:

$$(H_1(\partial_{2,j}F)_{M^{\Phi}_{j,ver},1},M^{\Phi}_{j,hor},M^{\Phi}_{j,ver})=(H_1(F'_j)_{M'_{j,ver},1},M'_{j,hor},M'_{j,ver}). \tag{17.2.3}$$

In particular,

$$P_{M^{\Phi}_{j,hor}|coker(M^{\Phi}_{j,ver}-I)}(t)=P_{M'_{j,hor}|coker(M'_{j,ver}-I)}(t), \tag{17.2.4}$$

the second polynomial being computed at the level of the homology of the local transversal fiber $H_1(F'_j)$. Summing up, we get that

$$P_{H_1(\partial F),M}(t)=(t-1)^N\cdot\prod_j P_{M'_{j,hor}|coker(M'_{j,ver}-I)}(t), \tag{17.2.5}$$

for some integer N. This shows clearly, that in order to determine the characteristic polynomial $P_{H_1(\partial F),M}$, we need to clarify the Jordan blocks of $M'_{j,ver}$ with eigenvalue 1 (or, more precisely, the triplet $(H_1(F'_j)_{M'_{j,ver},1},M'_{j,hor},M'_{j,ver})$, and additionally, the rank of $H_1(\partial F)$ which will take care of the integer N in (17.2.5).

For the number of Jordan blocks we will use the following notation:

DEFINITION 17.2.6. *Let $\#^k_\lambda M$ be the number of Jordan blocks of the operator M of size k and with eigenvalue λ.*

17.2.7. In fact, it is useful (and instructive) to study in parallel both 'local' (i.e. the right hand side of (17.2.5)) and 'global' (the right hand side of (17.2.1)) expressions.

Accordingly, it is convenient to introduce the following polynomials:

DEFINITION 17.2.8. *Let $P^{\#}(t)$ be the characteristic polynomial of $M_{\Phi,hor}$ induced on the image of $(M_{\Phi,ver}-I)$ on the generalized 1–eigenspace $H_1(F_\Phi)_{M_{\Phi,ver},1}$.*

Similarly, for any $1\leq j\leq s$, let $P^{\#}_j(t)$ be the characteristic polynomial of $M'_{j,hor}$ induced on the image of $(M'_{j,ver}-I)$ on the generalized 1–eigenspace $H_1(F'_j)_{M'_{j,ver},1}$.

Clearly, $P^{\#}(t)$ has degree $\#^2_1M_{\Phi,ver}$ while the degree of $P^{\#}_j(t)$ is $\#^2_1M'_{j,ver}$.

Since the characteristic polynomials of the horizontal monodromies acting on $H_1(F_\Phi)_{M_{\Phi,ver},1}$ and $H_1(F'_j)_{M'_{j,ver},1}$ are determined in (16.2.10), the above facts give

LEMMA 17.2.9.

$$P_{M_{\Phi,hor}|H_1(\partial F\setminus V_g)}(t)=\frac{(t-1)^2}{P^{\#}(t)}\cdot\prod_{w\in\mathcal{W}(\Gamma_{\mathcal{C}})}(t^{(m_w,n_w)}-1)^{2g_w+\delta_w-2}.$$

Moreover, for any j

$$P_{M_{\Phi,hor}|H_1(\partial_{2,j}F)}(t)=\frac{(t-1)^2}{P^{\#}_j(t)}\cdot\prod_{w\in\mathcal{W}(\Gamma^2_{\mathcal{C},j})}(t^{(m_w,n_w)}-1)^{\delta_w-2}.$$

Since $m_w=1$ for $w\notin\cup_j\mathcal{W}(\Gamma^2_{\mathcal{C},j})$, $P^{\#}(t)=\prod_j P^{\#}_j(t)$ up to a factor $(t-1)^N$.

Therefore, if one combines (17.2.9) and (17.1.1), one gets that in order to determine $P_{H_1(\partial F),M}(t)$ one needs to find $P^{\#}(t)$ (or, equivalently, all $P^{\#}_j(t)$) and the rank of $H_1(\partial F)$. In the next sections we will treat these missing terms by different geometric methods.

17.2.10. **Final remark.** In order to understand the homology of ∂F, one does not need any information regarding the generalized $(\lambda\neq 1)$–eigenspaces of $M_{\Phi,ver}$ and $\oplus_j M^{\Phi}_{j,ver}$, although they codify important information about the ICIS Φ. This will be the subject of a forthcoming research. Nevertheless, for f homogeneous, we will determine the complete Jordan–block structure via the identities (22.2), see (22.6).

§ 18. The ranks of $H_1(\partial F)$ and $H_1(\partial F\setminus V_g)$ via plumbing.

18.1. Plumbing homology and Jordan blocks. We start with some general facts regarding the rank of the first homology group of plumbed 3–manifolds. The statements are known (at least) for negative definite graphs (see e.g. [**44**] and the cited references in it); here we will consider the general case.

For simplicity, we will state the results for the 3–manifolds ∂F, $\partial F\setminus V_g$ and $\partial_{2,j}F$ (hence for graphs $G^m\sim G$ and $G^m_{2,j}\sim G_{2,j}$, cf. (12.4.1) and (12.5.3)), although they are valid for any plumbed 3–manifold.

In the next definition, Gr denotes either the graph G^m or $G^m_{2,j}$ (or any other graph with similar decoration, and with non–arrowheads $\mathcal{W}$ and arrowheads $\mathcal{A}$).

DEFINITION 18.1.1. *Let A be the 'intersection matrix' of Gr, i.e. the symmetric matrix of size $\#\mathcal{W}\times\#\mathcal{W}$ whose entry a_{wv} is the Euler number of w if $w=v$, while for $w\neq v$ it is $\sum_e\epsilon_e$, where the sum is over all edges e connecting w and v, and $\epsilon_e\in\{+,-\}$ is the edge–decoration of e.*

Furthermore, let I be the 'incidence matrix' of the arrows of Gr, defined as follows. It is a matrix of size $\#\mathcal{W}\times\#\mathcal{A}$. For any $a\in\mathcal{A}$ let w_a be that non–arrowhead vertex which supports the arrow of a. Then, for each $a\in\mathcal{A}$, the entry (a,w_a) is 1, all the other entries are zero.

The matrix (A,I) of size $\#\mathcal{W}\times(\#\mathcal{W}+\#\mathcal{A})$ consists of the blocks A and I.

Set $corank(A)_{Gr}:=\#\mathcal{W}-rank(A)$ and $corank(A,I)_{Gr}:=\#\mathcal{W}+\#\mathcal{A}-rank(A,I)$.

LEMMA 18.1.2. *For any $G^m\sim G$ and $G^m_{2,j}\sim G_{2,j}$ one has*

$$rank\,H_1(\partial F)=2g(G^m)+c(G^m)+corank(A)_{G^m},$$

$$rank\,H_1(\partial F\setminus V_g)=2g(G^m)+c(G^m)+corank(A,I)_{G^m},$$

$$rank\,H_1(\partial_{2,j}F)=2g(G^m_{2,j})+c(G^m_{2,j})+corank((A,I)_{G^m_{2,j}})\quad(1\leq j\leq s).$$

In particular, for $rank\,im\,\partial$ from (17.1.1) one has

$$rank\,im\,\partial=corank(A,I)_{G^m}-corank(A)_{G^m}.$$

PROOF. Let X be the plumbed 4–manifold associated with a plumbing graph Gr obtained by plumbing disc–bundles. Assume that the arrowheads of Gr represent the link $K\subset\partial X$. Consider the homology exact sequence of the pair $(X,\partial X\setminus K)$:

$$H_2(X)\xrightarrow{i}H_2(X,\partial X\setminus K)\longrightarrow H_1(\partial X\setminus K)\longrightarrow H_1(X)\longrightarrow H_1(X,\partial X\setminus K)$$

Notice that $H_1(X,\partial X\setminus K)=H^3(X,K)=0$, while $H_2(X,\partial X\setminus K)=H^2(X,K)=H^2(X)\oplus H^1(K)$ (since $K\hookrightarrow X$ is homotopically trivial). Moreover, the morphism i can be identified with (A,I). Since the rank of $H_1(X)$ is $2g(Gr)+c(Gr)$, the second identity follows. Taking $K = \mathcal{A} = \emptyset$ above gives the first identity. The last one follows similarly. $\square$

Remark 18.1.3. Since $H_1(X, \mathbb{Z})$ is free, the same argument over $\mathbb{Z}$ shows that $H_1(\partial X, \mathbb{Z}) = \mathbb{Z}^{2g+c} \oplus coker(A)$. The point is that $coker(A)$ might have a torsion summand, see e.g. (22.3.1).

(18.1.2) via (17.2.1) and (17.2.2) reads as

Corollary 18.1.4.

$$\dim coker(M_{\Phi,ver} - I) = 2g(G^m) + c(G^m) + corank(A, I)_{G^m} - 1,$$

$$\dim coker(M'_{j,ver} - I) = 2g(G^m_{2,j}) + c(G^m_{2,j}) + corank((A, I)_{G^m_{2,j}}) - 1 \quad (1 \leq j \leq s).$$

This combined with (16.4.5) gives

Corollary 18.1.5.

$$\#^2_1 M_{\Phi,ver} = c(G^m) - corank(A, I)_{G^m} + \#\mathcal{A}(G),$$

$$\#^2_1 M'_{j,ver} = c(G^m_{2,j}) - corank((A, I)_{G^m_{2,j}}) + \#\mathcal{E}_{cut,j} \quad (1 \leq j \leq s).$$

Remark 18.1.6. Although $c(G)$ and $g(G)$ can be computed easily from the graphs $\Gamma_{\mathcal{C}}$ or G, for the ranks of the matrices A and (A, I) the authors found no 'easy' formula. Even in case of particular concrete examples their direct computation can be a challenge. These 'global data' of the graphs resonates with the 'global information' codified in the Jordan block structure of the vertical monodromies.

Remark 18.1.7. Clearly, the integers $g(Gr)$, $c(Gr)$ and $corank(A)_{Gr}$ might change under the reduced calculus (namely, under R4), see e.g. the construction of the 'improved' algorithm (14.2), or the next typical example (from (22.9)(3c)):

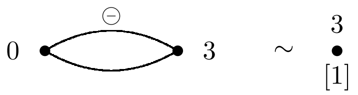

(oriented handle absorption)

For the first graph $A = \begin{bmatrix} 0 & 0 \\ 0 & 3 \end{bmatrix}$, hence $corank(A) = c = 1$ and $g = 0$, while for the second one $corank(A) = c = 0$ and $g = 1$.

On the other hand, the following graph–expressions are independent of the construction of G and they are also *stable under the reduced plumbed calculus* (in fact, the expressions $2g(G) + c(G) + corank(A)_G$ and $2g(G) + c(G) + corank(A, I)_G$ are stable even under all the operations of the oriented plumbed calculus):

- $\#\mathcal{A}(G)$, $g(G) + c(G)$, cf. (16.4.10);
- $g(G) + corank(A)_G$ and $g(G) + corank(A, I)_G$, cf. (18.1.2); in particular, $corank(A, I)_G - corank(A)_G$ and $c(G) - corank(A)$ as well;
- and all these expressions with $G_{2,j}$ instead of G.

18.2. Bounds for *corank*(A) and *corank*(A, I). Remarks.

18.2.1. (a) **Bounds for** $corank(A, I)_{G^m}$**.** From (18.1.5) and $\#\mathcal{W} \geq rank(A, I)$, we get

$$\#\mathcal{A}(G) \leq corank(A, I)_{G^m} \leq c(G^m) + \#\mathcal{A}(G). \tag{18.2.2}$$

These inequalities are sharp: the lower bound is realized e.g. when f is homogeneous (see (22.3.3)), while the upper bound by cylinders (see (25.1.5)). Decreasing $c(G^m)$ by (reduced) calculus, we decrease the difference between the two bounds as well.

(b) **Bounds for** $corank(A)_{G^m}$**.** By (18.1.2) and the left inequality of (17.1.2)

$$corank(A)_{G^m} \leq corank(A, I)_{G^m} - 1. \tag{18.2.3}$$

This and (18.2.2) imply

(18.2.4) $$0\leq corank(A)_{G^m}\leq c(G^m)+\#\mathcal{A}(G)-1.$$

Here again both bounds can be realized, the lower bound for f irreducible homogeneous, cf. (22.4.7), while the upper bound for cylinders, see (25.1.5).

REMARK 18.2.5. Finally, since $corank(A,I)_{G^m}\geq \#\mathcal{A}(G)$, (18.1.5) implies

(18.2.6) $$\#_1^2 M_{\Phi,ver}\leq c(G^m),$$

and, similarly, for any j

(18.2.7) $$\#_1^2 M'_{j,ver}\leq c(G^m_{2,j}).$$

In particular, if we succeed to decrease $c(G^m)$ by reduced calculus, we get a better estimate for the number of Jordan blocks. In particular, $c(\widehat{G})$, in general, is a much better estimate than $c(G)$.

In light of (4.2.1), the global inequality (18.2.6) reads as follows: Fix a germ f with 1–dimensional singular locus, and choose g such that $\Phi=(f,g)$ forms an ICIS. Consider the fibration $\arg(g):\partial F\setminus V_g\to S^1$. Then (18.2.6) says that the number of 2–Jordan blocks with eigenvalue 1 of the algebraic monodromy of the fibration $\arg(g)$, *for any germ g*, is dominated by $c(G^m)$. The surprising factor here is that G^m is a possible plumbing graph of ∂F, and ∂F is definitely independent of g. (Nevertheless, G^m is constructed via the pair (f,g), and it is not clear for the authors what kind of information it still keeps in it about g.)

It is instructive to compare the above identities with inequalities with similar statements valid in the world of complex geometry:

REMARK 18.2.8.

(a) Assume that (X,o) is a normal surface singularity. Let G_X be (one of its) dual resolution graphs; it is known that its intersection matrix A is negative definite.

Let $g:(X,0)\to(\mathbb{C},0)$ be the germ of an analytic function which defines an isolated singularity on (X,o), and consider the (generalized) Milnor fibration $\arg(g):\partial X\setminus V_g\to S^1$ (here ∂X is the boundary of a small Stein representative). Let F_g be the Milnor fiber and M_g the algebraic monodromy acting on $H_1(F_g,\mathbb{C})$. Then, e.g. by [**44**, (3.18)], one has

(18.2.9) $$rank\, H_1(F_g)=2g(G_X)+2c(G_X)+\#\mathcal{A}(G_X)-1,$$

(18.2.10) $$\dim ker(M_g-I)=2g(G_X)+c(G_X)+\#\mathcal{A}(G_X)-1.$$

(Notice that (16.4.6) and (18.1.4) are the generalizations of the above identities.)

In particular, $\#_1^2(M_g)=c(G_X)$. Moreover, $c(G_X)$ is independent of the choice of the resolution graph G_X (recall that in this case we only use the blowing up/down operations). I.e. $c(G_X)$ depends only on the 3–manifold ∂X, the link of X, and it is definitely independent of the choice of g. Therefore, $\#_1^2(M_g)$ is also independent of the choice of the germ g. (Notice the similarities with (18.2.6).)

(b) Furthermore, in the situation of (a) (compare with (18.1.2) too), $\dim H_1(\partial X)=2g(G_X)+c(G_X)$. In this case both $g(G_X)$ and $c(G_X)$ are graph–independent, and they have the following Hodge theoretical interpretation. If W denotes the weight filtration of $H_1(\partial X)$ (induced by the analytical structure of $(X,0)$), then $\dim Gr^W_{-1}H_1(\partial X)=2g(G_X)$ and $\dim Gr^W_0 H_1(\partial X)=c(G_X)$ (and all the other graded components are zero). Hence, in this situation, $Gr^W_{\cdot}H_1(\partial X)$ is topological.

(c) Let us analyze how the facts from (b) are modified if we consider more general situations. Assume that V is a smooth complex surface and $C\subset V$ a normal crossing divisor (with all irreducible components compact). We will denote by (the same) V a small tubular neighbourhood of C. Then the oriented 3–manifold ∂V can be represented by a plumbing graph — the dual graph of the configuration C; let we denote it by G_C. Similarly as above, A denotes the associated intersection matrix of G_C (equivalently, the intersection matrix of the curve–configuration C). Again (as in (18.1.2)), $\dim H_1(\partial V) = 2g(G_C) + c(G_C) + corank(A)$. Moreover, $H_1(\partial V)$ admits a mixed Hodge structure with weight filtration W, and $\dim Gr^W_{-2}H_1(\partial V) = corank(A)$, $\dim Gr^W_{-1}H_1(\partial V) = 2g(G_C)$ and $\dim Gr^W_0 H_1(\partial V) = c(G_C)$ (and all the other graded components are zero), cf. [**20**, (6.9)].

The point is that now this decomposition depends essentially on C and the analytic embedding of C into V, and, in general, cannot be deduced from the topology of ∂V alone. (Compare e.g. when C is the union of three generic lines in the projective plane with the case when C is a smooth elliptic curve with self–intersection zero). This discussion shows that in this situation, in order to keep the information regarding the weight filtration in ∂V, we are allowed to use only those calculus–operations which preserve $c(G_C)$, $g(G_C)$, respectively $corank(A)$. In particular, the oriented handle absorption should not be allowed.

§ 19. The characteristic polynomial of ∂F via $P^{\#}$ and $P^{\#}_j$.

19.1. The characteristic polynomial of coverings $G \to \Gamma_{\mathcal{C}}$ and $\widehat{G} \to \widehat{\Gamma_{\mathcal{C}}}$. In order to continue our discussion regarding the polynomials $P^{\#}$ and $P^{\#}_j$, $1 \le j \le s$ (cf. (17.2.8)–(17.2.9)), we have to introduce and discuss some natural 'combinatorial' characteristic polynomials associated with the involved graph coverings.

Consider the cyclic graph covering $G \to \Gamma_{\mathcal{C}}$, cf. (12.3). Recall that above a vertex $w \in \mathcal{W}(\Gamma_{\mathcal{C}})$ there are $\mathfrak{n}_w$ vertices, while above $e \in \mathcal{E}_w(\Gamma_{\mathcal{C}})$ exactly $\mathfrak{n}_e$ edges of G, where the integers $\mathfrak{n}_w$ and $\mathfrak{n}_e$ are given in (12.3.2) and (12.3.6) of the main algorithm. In particular, they can be read easily from the decorations of $\Gamma_{\mathcal{C}}$. The cyclic action on G permutes the vertices, respectively edges of the covering cyclically. Let $|G|$ be the topological realization (as a topological connected 1–complex) of the graph G. Then the action induces an operator, say $\mathfrak{h}(|G|)$, on $H_1(|G|, \mathbb{C})$.

Similarly, we consider the covering $\widehat{G} \to \widehat{\Gamma_{\mathcal{C}}}$ from (14.2). The vertices of $\widehat{\Gamma_{\mathcal{C}}}$ are the contracted subtrees $[\Gamma_{van}]$; and above $[\Gamma_{van}]$, in $\widehat{G}$ there sit exactly $\mathfrak{n}_{\Gamma_{van}}$ vertices. Those edges of $\widehat{\Gamma_{\mathcal{C}}}$ which do not support arrowheads are inherited from those edges $\mathcal{E}^*_{\mathcal{W}}$ of $\Gamma_{\mathcal{C}}$ which connect non–arrowheads and are not vanishing 2–edges. Each of them is covered by $\mathfrak{n}_e$ edges. The cyclic action induces the operator $\mathfrak{h}(|\widehat{G}|)$ on $H_1(|\widehat{G}|, \mathbb{C})$.

Definition 19.1.1. *We denote the characteristic polynomial of* $\mathfrak{h}(|G|)$ *(respectively of* $\mathfrak{h}(|\widehat{G}|)$*) by* $P_{\mathfrak{h}(|G|)}(t)$ *(resp. by* $P_{\mathfrak{h}(|\widehat{G}|)}(t)$*).*

By the connectivity of G and $\widehat{G}$, and by the fact that the cyclic action acts trivially on $H_0(|G|) = H_0(|\widehat{G}|)$, we get

Lemma 19.1.2.

$$P_{\mathfrak{h}(|G|)}(t) = (t-1)\cdot\frac{\prod_{e\in\mathcal{E}_{\mathcal{W}}(\Gamma_{\mathcal{C}})}(t^{\mathfrak{n}_e}-1)}{\prod_{w\in\mathcal{W}(\Gamma_{\mathcal{C}})}(t^{\mathfrak{n}_w}-1)},$$

$$P_{\mathfrak{h}(|\widehat{G}|)}(t) = (t-1)\cdot\frac{\prod_{e\in\mathcal{E}^*_{\mathcal{W}}(\Gamma_{\mathcal{C}})}(t^{\mathfrak{n}_e}-1)}{\prod_{\Gamma_{van}}(t^{\mathfrak{n}_{\Gamma_{van}}}-1)}.$$

19.1.3. We list some other properties of these polynomials:

(a) Their degrees are $rank\, H_1(|G|) = c(G)$ and $rank\, H_1(|\widehat{G}|) = c(\widehat{G})$.

(b) Analyzing (14.1.3), one sees the divisibility $P_{\mathfrak{h}(|\widehat{G}|)} \mid P_{\mathfrak{h}(|G|)}$.

(c) By (19.1.2), the multiplicity of the factor $(t-1)$ in $P_{\mathfrak{h}(|G|)}(t)$ is exactly $c(\Gamma_{\mathcal{C}})$. This fact remains true for $P_{\mathfrak{h}(|\widehat{G}|)}$ too, since each Γ_{van} is a tree and $c(\Gamma_{\mathcal{C}}) = c(\widehat{\Gamma_{\mathcal{C}}})$. Hence 1 is not a root of the polynomial $P_{\mathfrak{h}(|G|)}/P_{\mathfrak{h}(|\widehat{G}|)}$.

(d) It might happen that $c(\widehat{G}) > c(\Gamma_{\mathcal{C}})$, see e.g. (22.6.2), hence $\mathfrak{h}(|\widehat{G}|)$ might have non–trivial eigenvalues.

19.1.4. Obviously, all the above discussion can be 'localized' above the graph $\Gamma^2_{\mathcal{C}}$. With the natural notations, we set

$$P_{\mathfrak{h}(|G_{2,j}|)}(t) = (t-1)\cdot\frac{\prod_{e\in\mathcal{E}_{\mathcal{W}}(\Gamma^2_{\mathcal{C},j})}(t^{\mathfrak{n}_e}-1)}{\prod_{w\in\mathcal{W}(\Gamma^2_{\mathcal{C},j})}(t^{\mathfrak{n}_w}-1)},$$

$$P_{\mathfrak{h}(|\widehat{G_{2,j}}|)}(t) = (t-1)\cdot\frac{\prod_{e\in\mathcal{E}^*_{\mathcal{W}}(\Gamma^2_{2,j})}(t^{\mathfrak{n}_e}-1)}{\prod_{\Gamma_{van}\subset\Gamma^2_{2,j}}(t^{\mathfrak{n}_{\Gamma_{van}}}-1)}.$$

In fact, (the product over j of) these localized polynomials contain *all the non–trivial eigenvalues* of $P_{\mathfrak{h}(|G|)}$ and $P_{\mathfrak{h}(|\widehat{G}|)}$ respectively. Indeed, in the formulae of (19.1.2), if w is a vertex of $\Gamma^1_{\mathcal{C}}$ then $\mathfrak{n}_w = 1$. Similarly, if e is an edge with at least one of its end–vertices in $\Gamma^1_{\mathcal{C}}$, then $\mathfrak{n}_e = 1$ as well.

19.2. The characteristic polynomial of ∂F. In this subsection we compute the polynomials $P^{\#}$ and $P^{\#}_j$ under some additional assumptions. Via (17.2.9) and (17.1.1) this is enough (together with $rank\, H_1(\partial F)$) to determine the characteristic polynomial of the horizontal/Milnor monodromy of $H_1(\partial F)$.

Let $\Gamma_{\mathcal{C}}$ be the graph read from the resolution as in (7.1.3), it might have some vanishing 2–edges (which are not eliminated by blow ups considered in (12.1.2)).

DEFINITION 19.2.1. *Let Gr be either the graph $\Gamma_{\mathcal{C}}$, or $\Gamma^2_{\mathcal{C},j}$ for some j. We say that Gr is* 'unicolored', *if all its edges connecting non–arrowheads have the same sign–decoration and there are no vanishing 2–edges among them. We say that Gr is* almost unicolored, *if those edges which connect non–arrowheads and are not vanishing 2–edges, have the same sign–decoration.*

Consider the polynomials $P_{\mathfrak{h}(|G|)}(t)$ and $P_{\mathfrak{h}(|G_{2,j}|)}(t)$ introduced in (19.1). Recall that their degrees are $c(G)$ and $c(G_{2,j})$ respectively.

THEOREM 19.2.2.
(I) For any fixed j, the polynomial $P^{\#}_j(t)$ divides the polynomial $P_{\mathfrak{h}(|G_{2,j}|)}(t)$.
Moreover, the following statements are equivalent:

$$(19.2.3)\qquad \begin{array}{ll} (a) & P^{\#}_j(t) = P_{\mathfrak{h}(|G_{2,j}|)}(t) \\ (b) & \#^2_1 M'_{j,ver} = c(G_{2,j}) \\ (c) & corank(A,I)_{G_{2,j}} = \#\mathcal{E}_{cut,j}. \end{array}$$

These equalities hold in the following situations: either (i) $\Gamma^2_{\mathcal{C},j}$ is unicolored, or after determining the graph G via the Main Algorithm (12.3), it is such that either (ii) $c(G_{2,j}) = 0$, or (iii) $corank(A,I)_{G_{2,j}} = \#\mathcal{E}_{cut,j}$ holds.

(II) The polynomial $P^{\#}(t)$ divides the polynomial $P_{\mathfrak{h}(|G|)}(t)$.
Moreover, the following statements are equivalent:

$$(19.2.4)\qquad \begin{array}{ll} (a) & P^{\#}(t) = P_{\mathfrak{h}(|G|)}(t) \\ (b) & \#^2_1 M_{\Phi,ver} = c(G) \\ (c) & corank(A,I)_G = \#\mathcal{A}(G). \end{array}$$

These equalities hold in the following situations: either (i) $\Gamma_{\mathcal{C}}$ is unicolored, or after finding the graph G, it turns out to have either (ii) $c(G) = 0$ or (iii) $corank(A,I) = \#\mathcal{A}(G)$.

But, even if (19.2.4) does not hold, one has

$$P^{\#}(t) = P_{\mathfrak{h}(|G|)}(t) \quad \textit{up to a multiplicative factor of type } (t-1)^N \tag{19.2.5}$$

whenever (19.2.3) holds for all j.

REMARK 19.2.6. The equivalent statements (19.2.4) are satisfied e.g. by all homogeneous singularities (by (22.3.3)), or by all cylinders, provided that the algebraic monodormy of the corresponding plane curve singularity is finite (cf. (25.1.5)). Nevertheless, they are not satisfied by cylinders, which do not satisfies the above monodromy restriction. Nevertheless, their case will be covered by the 'improved' version (19.2.11).

The proof of (19.2.2) is given in § 20. The major application targets the characteristic polynomials of the monodromy acting on $H_1(\partial F)$:

THEOREM 19.2.7. *Assume that (19.2.3) holds for all j, or (19.2.4) holds. Then*

$$P_{H_1(\partial F),M}(t) = \frac{(t-1)^{2+corank(A)_G - \#\mathcal{A}(G)}}{P_{\mathfrak{h}(|G|)}(t)} \cdot \prod_{w \in \mathcal{W}(\Gamma_{\mathcal{C}})} (t^{(m_w,n_w)} - 1)^{2g_w+\delta_w-2}.$$

In particular, one has the following formulae for the ranks of eigenspaces:

$$rank\, H_1(\partial F)_1 = 2g(\Gamma_{\mathcal{C}}) + c(\Gamma_{\mathcal{C}}) + corank(A)_G, \tag{19.2.8}$$

$$rank\, H_1(\partial F)_{\neq 1} = 2g(G) + c(G) - 2g(\Gamma_{\mathcal{C}}) - c(\Gamma_{\mathcal{C}}). \tag{19.2.9}$$

More generally, in any situation (i.e. even if the above assumptions are not satisfied), there exists a polynomial Q with $Q(1) \neq 0$, which divides both $P_{\mathfrak{h}(|G|)}$ and $\prod_{w \in \mathcal{W}(\Gamma_{\mathcal{C}})} (t^{(m_w,n_w)} - 1)^{2g_w+\delta_w-2}$, such that

$$P_{H_1(\partial F),M}(t) = \frac{(t-1)^N}{Q(t)} \cdot \prod_{w \in \mathcal{W}(\Gamma_{\mathcal{C}})} (t^{(m_w,n_w)} - 1)^{2g_w+\delta_w-2},$$

where $N = 2 + corank(A)_G - \#\mathcal{A}(G) - c(G) + \deg(Q)$.

PROOF. Use (16.2.10), (18.1.2), (18.1.4) and (19.2.2). □

COROLLARY 19.2.10. *Assume that (19.2.3) holds for all j, or (19.2.4) holds. Then the following facts (over coefficients in $\mathbb{C}$) hold:*

(a) A_G has a (generalized) eigen–decomposition $(A_G)_{\lambda=1} \oplus (A_G)_{\lambda\neq 1}$, and $(A_G)_{\lambda \neq 1}$ is non–degenerate;

(b) Consider the subspaces $K^i := im[H^i(X)_1 \to H^i(\partial X)_1] \subset H^i(\partial X)_1$ for $i = 1, 2$. Then $\operatorname{codim} K^1 = \dim K^2 = corank(A)_G$. Moreover, the cup–product $H^1(\partial F)_\lambda \cup H^1(\partial F)_\mu \to H^2(\partial F)_{\lambda\mu}$ has the following properties:

(1) $H^1(\partial F)_\lambda \cup H^1(\partial F)\mu = 0$ for $1 \neq \lambda \neq \overline{\mu} \neq 1$;
(2) $\oplus_{\lambda \neq 1} H^1(\partial F)_\lambda \cup H^1(\partial F)_{\overline{\lambda}} \subset K^2$;
(3) $(\oplus_{\lambda \neq 1} H^1(\partial F)_\lambda) \cup K^1 = 0$;
(4) $K^1 \cup K^1 \subset K^2$;
(5) $K^1 \cup K^2 = 0$.

PROOF. We combine the proof of (18.1.2) with (13.9). Write $X := \overline{\mathcal{S}}_k$, and consider the cohomological long exact sequence associated with the pair $(X, \partial X)$. The map $H^2(X, \partial X) \to H^2(X)$ can be identified with A_G. The sequence has a generalized eigenspace decomposition. For eigenspace $\lambda \neq 1$, via (19.2.9) and (13.9.1), we get that the natural inclusion $H^1(X)_{\lambda\neq 1} \to H^1(\partial X)_{\lambda \neq 1}$ is an isomorphism. Hence $(A_G)_{\lambda\neq 1}$ is non–degenerate.

For the second part, lift the classes of $H^1(\partial X)$ to $H^1(X)$ before multiplying them. (5) follows from $H^3(X) = 0$. (Cf. also with **[70]**.) □

Such a result, in general, is the by–product of the structure–theorem regarding the mixed Hodge structure of the cohomology ring (i.e., it is the consequence of the fact that H^2 has no such weight where the product would sit). Compare also with (18.2.8) and the open problem (30.1.5) from § 30.

The next theorem, based on the 'Collapsing Main Algorithm' and the corresponding improved version of the proof of (19.2.2), provides a better 'estimate' in the general case and in the special (almost unicolored) cases handles the presence of vanishing 2–edges too. Consider the polynomials $P_{\mathfrak{h}(|\widehat{G}|)}(t)$ and $P_{\mathfrak{h}(|\widehat{G_{2,j}}|)}(t)$ introduced in (19.1). Recall that their degrees are $c(\widehat{G})$ and $c(\widehat{G_{2,j}})$ respectively.

Theorem 19.2.11.
(I) For any fixed j, the polynomial $P_j^{\#}(t)$ divides the polynomial $P_{\mathfrak{h}(|\widehat{G_{2,j}}|)}(t)$.
Moreover, the following statements are equivalent:

$$\begin{array}{ll} (a) & P_j^{\#}(t)=P_{\mathfrak{h}(|\widehat{G_{2,j}}|)}(t)\\ (b) & \#_1^2M'_{j,ver}=c(\widehat{G_{2,j}})\\ (c) & corank(A,I)_{\widehat{G_{2,j}}}=\#\mathcal{E}_{cut,j}. \end{array} \tag{19.2.12}$$

These equalities hold in the following situations: either (i) $\Gamma^2_{\mathcal{C},j}$ is almost unicolored, or after determining the graph $\widehat{G}$ via the Collapsing Main Algorithm (14.2), $\widehat{G}$ turns out to be such that either (ii) $c(\widehat{G_{2,j}})=0$, or (iii) $corank(A,I)_{\widehat{G_{2,j}}}=\#\mathcal{E}_{cut,j}$ holds.

(II) The polynomial $P^{\#}(t)$ divides the polynomial $P_{\mathfrak{h}(|\widehat{G}|)}(t)$.
Moreover, the following statements are equivalent:

$$\begin{array}{ll} (a) & P^{\#}(t)=P_{\mathfrak{h}(|\widehat{G}|)}(t)\\ (b) & \#_1^2M_{\Phi,ver}=c(\widehat{G})\\ (c) & corank(A,I)_{\widehat{G}}=\#\mathcal{A}(G). \end{array} \tag{19.2.13}$$

These equalities hold in the following situations: either (i) $\Gamma_{\mathcal{C}}$ is almost unicolored, or after determining the graph $\widehat{G}$, it is such that either (ii) $c(\widehat{G})=0$ or (iii) $corank(A,I)_{\widehat{G}}=\#\mathcal{A}(G)$.
But, even if (19.2.13) does not hold, one has

$$P^{\#}(t)=P_{\mathfrak{h}(|\widehat{G}|)}(t) \quad \textit{up to a multiplicative factor of type } (t-1)^N \tag{19.2.14}$$

whenever (19.2.12) holds for all j.

This implies:

Theorem 19.2.15. *Assume that (19.2.12) holds for all j, or (19.2.13) holds. Then*

$$P_{H_1(\partial F),M}(t)=\frac{(t-1)^{2+corank(A)_{\widehat{G}}-\#\mathcal{A}(G)}}{P_{\mathfrak{h}(|\widehat{G}|)}(t)}\cdot\prod_{w\in\mathcal{W}(\Gamma_{\mathcal{C}})}(t^{(m_w,n_w)}-1)^{2g_w+\delta_w-2}$$

In particular

$$rank\,H_1(\partial F)_1=2g(\Gamma_{\mathcal{C}})+c(\Gamma_{\mathcal{C}})+corank(A)_{\widehat{G}}, \tag{19.2.16}$$

$$rank\,H_1(\partial F)_{\neq 1}=2g(\widehat{G})+c(\widehat{G})-2g(\Gamma_{\mathcal{C}})-c(\Gamma_{\mathcal{C}}). \tag{19.2.17}$$

More generally, in any situation (even if the above assumptions are not satisfied), there exists a polynomial Q with $Q(1)\neq 0$, which divides both $P_{\mathfrak{h}(|\widehat{G}|)}$ and $\prod_{w\in\mathcal{W}(\Gamma_{\mathcal{C}})}(t^{(m_w,n_w)}-1)^{2g_w+\delta_w-2}$, such that

$$P_{H_1(\partial F),M}(t)=\frac{(t-1)^N}{Q(t)}\cdot\prod_{w\in\mathcal{W}(\Gamma_{\mathcal{C}})}(t^{(m_w,n_w)}-1)^{2g_w+\delta_w-2},$$

where $N=2+corank(A)_{\widehat{G}}-\#\mathcal{A}(G)-c(\widehat{G})+\deg(Q)$.

COROLLARY 19.2.18. *Assume that (19.2.12) holds for all* j, *or (19.2.13) holds. Then the statement of (19.2.10) is valid provided that we replace* G *by* $\widehat{G}$.

§ 20. The proof of the characteristic polynomial formulae.

20.1. Counting Jordan blocks of size 2.

The proof is based on a specific construction. The presentation is written for the graph G (later modified to fit $\widehat{G}$), but it can be reformulated for $G_{2,j}$ too.

20.1.1. $m_{\Phi,ver}$ **as a quasi–periodic action.** We wish to understand the geometric monodromy $m_{\Phi,ver}:F_\Phi\to F_\Phi$. For this discussion our model is the topology of fibred links, as it is described in section 13 of [**18**]. (Although, in [loc.cit.] the machinery is based on splice diagrams, section 23 of [**18**] gives the necessary hints for plumbing graphs as well.)

Nevertheless, our situation is more complicated. First, in the present situation we will have several local types/contributions — in fact, three; two of them do not appear in the classical complex analytic case [**18**]. Second, that basic property which is satisfied by analytic germs defined on normal surface singularities, namely that a 'variation operator' has a uniform twist, in our situation is not true (it is ruined by the new local contributions).

Consider the graph $\Gamma_{\mathcal{C}}$ from § 7. For simplicity we will write $\mathcal{E}$, $\mathcal{W}$, etc. for $\mathcal{E}(\Gamma_{\mathcal{C}})$, $\mathcal{W}(\Gamma_{\mathcal{C}})$, etc. It is the dual graph of the curve configuration $\mathcal{C}\subset V^{emb}$, where $r:V^{emb}\to U$ is a representative of an embedded resolution of $(V_f\cup V_g,0)\subset(\mathbb{C}^3,0)$. Then, by (8.5.2), for any tubular neighbourhood $T(\mathcal{C})\subset V^{emb}$ of $\mathcal{C}$, one has an inclusion $(\Phi\circ r)^{-1}(c_0,d_0)$ for $(c_0,d_0)\in \mathsf{W}_{\eta,M}$. For simplicity, we write $\widetilde{F}_\Phi$ for the (diffeomorphically) lifted fiber $(\Phi\circ r)^{-1}(c_0,d_0)$ of Φ.

Moreover, consider the decomposition (8.5.3) of $\widetilde{F}_\Phi$ too. More precisely, for any intersection point $p\in C_v\cap C_u$ (or, self–intersection point of C_v if $v=u$), which corresponds to the edge $e\in\mathcal{E}$ of $\Gamma_{\mathcal{C}}$, let $T(e)$ (respectively $T^\circ(e)$) be a small closed ball centered at p (respectively its interior). Then, for (c_0,d_0) sufficiently close to the origin, $\widetilde{F}_\Phi\cap T(e)$ is a union of annuli. Moreover, $\widetilde{F}_\Phi\setminus\cup_e T^\circ(e)$ is a union $\cup_{v\in\mathcal{V}}\widetilde{F}_v$, where $\widetilde{F}_v$ is in a small tubular neighbourhood of C_v $(v\in\mathcal{V})$.

If v is an arrowhead supported by an edge e, then the inclusion $\widetilde{F}_v\cap\partial T(e)\subset\widetilde{F}_v$ admits a strong deformation retract. Hence the pieces $\{\widetilde{F}_v\}_{v\in\mathcal{A}}$ (and the separating annuli $\{\widetilde{F}_\Phi\cap T(e)\}_{e\in\mathcal{E}\setminus\mathcal{E}_{\mathcal{W}}}$) can be neglected. Thus, we will consider only

$$\widetilde{F}^*_\Phi:=\widetilde{F}_\Phi\setminus(\bigcup_{e\in\mathcal{E}\setminus\mathcal{E}_{\mathcal{W}}}T(e)\cup\bigcup_{v\in\mathcal{A}}\widetilde{F}_v\ ).$$

In particular, $\widetilde{F}^*_\Phi$ is separated by the annuli $\{\widetilde{F}_\Phi\cap T(e)\}_{e\in\mathcal{E}_{\mathcal{W}}}$ in surfaces $\{\widetilde{F}_w\}_{w\in\mathcal{W}}$, and each $\widetilde{F}_w$ is the total space of a covering, where the base space is $C_w\setminus\cup_e T(e)$ and the fiber is isomorphic to $\mathcal{P}_w:=\mathcal{P}$ from the Key Example (16.1.3).

Moreover, one might choose the horizontal/vertical monodromies of $\widetilde{F}^*_\Phi$ in such a way that they will preserve this decomposition, and their action on $\widetilde{F}_w$ will be induced by the permutations $\sigma_{w,hor}:=\sigma_{hor}$, respectively $\sigma_{w,ver}:=\sigma_{ver}$ acting on $\mathcal{P}_w$ (cf. (16.1.3)). This shows that $m_{\Phi,ver}$ is isotopic to an action $\widetilde{m}_{\Phi,ver}$, which preserves the above decomposition, and its restriction on each $\widetilde{F}_w$ is finite. Let q be a common multiple of the orders of $\{\sigma_{w,ver}\}_{w\in\mathcal{W}}$. Then $\widetilde{m}^q_{\Phi,ver}$ is the identity on each $\widetilde{F}_w$, and acts as a 'twist map' on each separating annulus. In the topological characterization of $\widetilde{m}_{\Phi,ver}$, this twist is crucial.

DEFINITION 20.1.2. [**18**, § 13] *Let* $h : A \to A$ *be a homeomorphism of the oriented annulus* $A = S^1 \times [0,1]$ *with* $h|\partial A = id$*. The (algebraic) twist of* h *is defined as the intersection number*

$$\operatorname{twist}(h) := (x, \operatorname{var}_h(x)),$$

where $x \in H_1(A, \partial A, \mathbb{Z})$ *is a generator, and* $\operatorname{var}_h : H_1(A, \partial A, \mathbb{Z}) \to H_1(A, \mathbb{Z})$ *is defined by* $\operatorname{var}_h([c]) = [h(c) - c]$*, for any relative cycle* c*.*

More generally, if B *is a disjoint union of annuli and* $h : B \to B$ *is a homeomorphism with* $h^q|\partial B = id$ *for some integer* $q > 0$*, define, for any component* A *of* B*,*

$$\operatorname{twist}(h; A) := \frac{1}{q} \operatorname{twist}(h^q|A).$$

Notice that $\operatorname{twist}(h; A)$, defined in this way, is independent of the choice of q.

EXAMPLE 20.1.3. In the ‘classical’ situation one considers an analytic family of curves (over a small disc), with central fiber a normal crossing divisor and generic fiber smooth. The generic fiber is cut by separating annuli, which sit in the neighbourhood of the normal crossing intersection point of the central fiber. Around such a point, in local equations $(u, v) \in (\mathbb{C}^2, 0)$, the family is given by the fibers of $f(u, v) = u^a v^b$ for two positive integers a and b, and the union of annuli is the fiber $f^{-1}(\epsilon)$ intersected with a small ball with center at the origin (and ϵ is small with respect to the radius of this ball). It consists of $\gcd(a, b)$ annuli. The (Milnor) monodromy action h is induced by $[0, 2\pi] \ni t \mapsto f^{-1}(\epsilon e^{it})$. In order to make the computation, one must choose h in such a way that its restriction on the boundary ‘near’ the x–axis is finite of order a, and similarly, on the boundary components ‘near’ the y–axis is finite of order b. Then, one can show (see e.g. [**18**, page 164]) that the twist, for each connected component A, is

$$\operatorname{twist}(h; A) = -\frac{\gcd(a, b)}{ab}.$$

20.1.4. In fact, in most of the arguments, what is really important is not the value of the twist itself, but its *sign*. We say that we have *uniform twist*, if for all the annuli the signs of all the twists are the same.

EXAMPLE 20.1.5. In our present situation of (20.1.1), we are interested in the twist of the separating annulus associated with the edges $e \in \mathcal{E}_{\mathcal{W}}$. Depending on the fact that the edge is of type 1 or 2, we have to consider two different situations. For both cases we will consider the local equations from (7.2).

If e is a 1–edge, then the fiber (union of annuli) and the (vertical) monodromy action is given by

$$u^m v^n w^l = c, \quad v^\nu w^\lambda = de^{it} \text{ (with } (c, d) \text{ constant, and } t \in [0, 2\pi]).$$

If e is a 2–edge, then the fiber (union of annuli) and the (vertical) monodromy action is given by

$$u^m v^{m'} w^n = c, \quad w^\nu = de^{it} \text{ (with } (c, d) \text{ constant, and } t \in [0, 2\pi]).$$

We invite the interested reader to compute the corresponding twists exactly in both cases; in the present proof we need only the following statement.

LEMMA 20.1.6. *Fix an edge* $e \in \mathcal{E}_{\mathcal{W}}$*, set* $B := \widetilde{F}_\Phi \cap T(e)$*, and let* A *be one of the connected components of* B*.*

(a) If e *is a 1–edge, then* $\operatorname{twist}(h; A) < 0$*.*

(b) If e *is a non–vanishing 2–edge, then* $\operatorname{twist}(h; A) > 0$*.*

(c) If e *is a vanishing 2–edge, then* $\operatorname{twist}(h; A) = 0$*.*

Proof. The first case behaves as a 'covering of degree m' of the classical case $v^\nu w^\lambda = e^{it}$ ($t \in [0, 2\pi]$), see (20.1.3). The monodromy of the second case behaves as the inverse of the monodromy of the classical monodromy operator: $u^m v^{m'} = e^{-nit/\nu}$ ($t \in [0, 2\pi]$). Finally, assume that $n = 0$. Then the restriction of the vertical monodromy to ∂B has order ν, hence one can take $q = \nu$. But h^ν extends with identity on the whole B. The details are left to the reader. □

20.1.7. Now we continue the proof of (19.2.2). The structure of the 2–Jordan blocks of $M_{\Phi,ver}$ is codified in the following commutative diagram (cf. [**18**, (14.2)]):

$$\begin{tikzcd}
H_1(\widetilde{F}^*_\Phi) \arrow[r, "i"] \arrow[dd, "M^q_{\Phi,ver} - I"] & H_1(\widetilde{F}^*_\Phi, \widetilde{F}_{\mathcal{W}}) \arrow[r] \arrow[dd, "T"] \arrow[dr, "\text{exc}"] & H_0(\widetilde{F}_{\mathcal{W}}) \arrow[r] & H_0(\widetilde{F}^*_\Phi) \arrow[r] & 0 \\
 & & H_1(B, \partial B) \arrow[dl, "\text{var}"] & & \\
H_1(\widetilde{F}^*_\Phi) & H_1(B) \arrow[l, "j"'] & & &
\end{tikzcd}$$

Above we use the following notations: $\widetilde{F}_{\mathcal{W}} := \cup_{w \in \mathcal{W}} \widetilde{F}_w$, $B := \cup_{e \in \mathcal{E}_{\mathcal{W}}} (\widetilde{F}^*_\Phi \cap T(e))$, q is a positive integer as in (20.1.1), hence $M^q_{\Phi,ver}$ is unipotent, var is the variation map (associated with $\tilde{m}^q_{\Phi,ver}$), exc is the excision isomorphism, and finally T is the composite var $\circ$ exc. The horizontal lines are homological exact sequences.

Since B is the disjoint union of the separating annuli, var is a diagonal map. On the diagonal, each entry corresponds to an annulus A, and it equals the integer $q \cdot \text{twist}(m_{\Phi,ver}; A)$ determined in (20.1.6).

Obviously, the number of *all* 2–Jordan blocks of $M_{\Phi,ver}$ is $\dim \operatorname{im}(M^q_{\Phi,ver} - I)$. On the other hand, by the commutativity of the diagram,

$$\operatorname{im}(M^q_{\Phi,ver} - I) \simeq j\,T(\operatorname{im}(i)) \simeq \operatorname{im}(i)/\ker(j\,T|\operatorname{im}(i)). \tag{20.1.8}$$

The point in this is that $\operatorname{im}(M^q_{\Phi,ver} - I)$ *appears as a factor space of* $\operatorname{im}(i)$.

20.1.9. In some cases $\operatorname{im}(M^q_{\Phi,ver} - I)$ can be determined exactly.

Assume that $\Gamma_{\mathcal{C}}$ has no vanishing 2–edges, i.e. the case (20.1.6)(c) does not occur. Then all the diagonal entries of var are non–zero, hence both var and T are isomorphisms. The next lemma basically follows from [**18**, page 113]:

Lemma 20.1.10. *Assume that* $\Gamma_{\mathcal{C}}$ *is unicolored (cf. (19.2.1)). Then the restriction of* $j \circ T$ *on* $\operatorname{im}(i)$ *is injective.*

Proof. For any $y, z \in H_1(\widetilde{F}_\Phi, \widetilde{F}_{\mathcal{W}})$, we consider the intersection number (y, Tz), denoted by $\langle y, z \rangle$. Since T is diagonal, and all the entries on the diagonal have the same sign, the form $\langle y, z \rangle$ is definite. Assume that $j\,Ti(x) = 0$. Then $0 = (x, j\,Ti(x)) = (i(x), Ti(x)) = \langle i(x), i(x) \rangle$, hence $i(x) = 0$. □

Therefore, if G is unicolored then the number of all 2–Jordan blocks of $M_{\Phi,ver}$ is $\dim$ *$im(i)$.*

20.2. Characters. The corresponding $\mathbb{Z}^2$–characters of $\operatorname{im}(i)$ can be determined by the following exact sequence (as part of the above diagram):

$$0 \longrightarrow \operatorname{im}(i) \longrightarrow H_1(\widetilde{F}^*_\Phi, \widetilde{F}_{\mathcal{W}}) \xrightarrow{\tilde{\partial}} H_0(\widetilde{F}_{\mathcal{W}}) \longrightarrow H_0(\widetilde{F}^*_\Phi) \longrightarrow 0,$$

and the action of the vertical/horizontal monodromies on this sequence. In this proof we need only those blocks of $M_{\Phi,ver}$ which have eigenvalue 1.

The action of the algebraic *vertical monodromy* on each term of this sequence is finite (because it is induced by a permutation of the connected components of

the spaces $\widetilde{F}_{\mathcal{W}}$ and $(B,\partial B)$). The corresponding 1–eigenspaces form the following exact sequence:
(20.2.1)

$$0\longrightarrow \operatorname{im}(i)_{ver,1}\longrightarrow H_1(\widetilde{F}^*_\Phi,\widetilde{F}_{\mathcal{W}})_{ver,1}\xrightarrow{\tilde{\partial}} H_0(\widetilde{F}_{\mathcal{W}})_{ver,1}\longrightarrow H_0(\widetilde{F}^*_\Phi)_{ver,1}\longrightarrow 0.$$

This sequence will be compared with another sequence which computes the simplicial homology of the connected 1–complex $|G|$. Namely, one considers the free vector space $\mathbb{C}^{\#\mathcal{E}_{\mathcal{W}}(G)}$, respectively $\mathbb{C}^{\#\mathcal{W}}(G)$, generated by the edges $\mathcal{E}_{\mathcal{W}}(G)$ and vertices $\mathcal{W}(G)$ of G, and let ∂' be the boundary operator. Then one has the exact sequence

$$0\longrightarrow H_1(|G|)\longrightarrow \mathbb{C}^{\#\mathcal{E}_{\mathcal{W}}(G)}\xrightarrow{\partial'}\mathbb{C}^{\#\mathcal{W}(G)}\longrightarrow H_0(|G|)\longrightarrow 0. \tag{20.2.2}$$

LEMMA 20.2.3. *The two exact sequences (20.2.1) and (20.2.2) are isomorphic. Moreover, the horizontal monodromy acting on (20.2.1) can be identified with the action on (20.2.2) induced by the cyclic action of the covering $G\to\Gamma_{\mathcal{C}}$. (The cyclic action of a cyclic covering $G\to\Gamma$ is induced by the positive generator of $\mathbb{Z}$, cf. (6.1.2).)*

PROOF. It is enough to identify the second and the third terms together with the connecting morphisms, and their compatibility with the monodromy action. (In fact, the identification of the last terms are trivial: $H_0(\widetilde{F}^*_\Phi)_{ver,1}=H_0(\widetilde{F}_\Phi)_{ver,1}=H_0(|G|)=\mathbb{C}$ is clear since $\widetilde{F}_\Phi$ and $|G|$ are connected.) The identification follows from the proof of the main algorithm.

Recall, that in the previous subsections, we constructed a decomposition of $\widetilde{F}^*_\Phi$, the lifted fiber $(\Phi\circ r)^{-1}(c_0,d_0)$. Let us repeat the very same construction for $(\Phi\circ r)^{-1}(\partial D_{c_0})$, where D_{c_0} is the disc $\{(c,d):c=c_0\}$ as in section §4, or in the proof of (13.3.3). Let $Tot(\widetilde{F}_{\mathcal{W}})$ be the space we get instead of $\widetilde{F}_{\mathcal{W}}$, which, in fact, is the total space of a fibration over S^1 with fiber $\widetilde{F}_{\mathcal{W}}$ and monodromy the vertical monodromy. Since the geometric vertical monodromy permutes the components of $\widetilde{F}_{\mathcal{W}}$, the algebraic vertical monodromy $M_{H_0(\widetilde{F}_{\mathcal{W}}),ver}$ acts finitely on $H_0(\widetilde{F}_{\mathcal{W}})$, and the $coker(M_{H_0(\widetilde{F}_{\mathcal{W}}),ver}-I)$ can be identified with $H_0(\widetilde{F}_{\mathcal{W}})_{ver,1}$. Hence, by the Wang exact sequence of the above fibration, we get that $H_0(\widetilde{F}_{\mathcal{W}})_{ver,1}=H_0(Tot(\widetilde{F}_{\mathcal{W}}))$. On the other hand, in the proof of (13.3.3) (complemented also with the second part of (4.2.1)), $\Phi^{-1}(\partial D_{c_0})\cap B_\epsilon$ appears as a part of $\partial\mathcal{S}_k$. Therefore, $Tot(\widetilde{F}_{\mathcal{W}})$ appears as a part of $\partial\widetilde{\mathcal{S}}_k$, that part which sits in the neighbourhood of the regular part of the compact components of $\mathcal{C}$. Hence, by (13.6.1) and (13.8.1), $H_0(Tot(\widetilde{F}_{\mathcal{W}}))$ is freely generated by the collection of curves sitting in the normalization $\mathcal{S}^{norm}_k$ of $\widetilde{\mathcal{S}}_k$ above the compact components of $\mathcal{C}$. This is codified exactly by the non–arrowhead vertices of G.

For the second terms, first notice that by the isomorphism $\text{exc}:H_1(\widetilde{F}^*_\Phi,\widetilde{F}_{\mathcal{W}})\to H_1(B,\partial B)$, the rank of $H_1(\widetilde{F}^*_\Phi,\widetilde{F}_{\mathcal{W}})$ counts the separating annuli of $\widetilde{F}^*_\Phi$. Now, we can repeat the entire construction and argument above for $\mathcal{E}_{\mathcal{W}}$ instead of $\mathcal{W}$. Indeed, $H_1(\widetilde{F}^*_\Phi,\widetilde{F}_{\mathcal{W}})_{ver,1}$ counts the separating tori (not considering those corresponding to the binding of the open book) of $(\Phi\circ r)^{-1}(\partial D_{c_0})$, and this, by the proof of the main algorithm, is codified exactly by $\mathcal{W}$. The details are left to the reader.

Since all the maps and identifications are natural and compatible with the action of the corresponding horizontal monodromies, the morphisms $\tilde{\partial}$ and ∂' and the actions of the horizontal monodromies are all identified. $\square$

Now, we are ready to finish the proof of (19.2.2). By the above discussion, $\#^2_1M_{\Phi,ver}$ is equal to the dimension of $I:=\operatorname{im}(i)_{ver,1}/\ker(j\,T|\operatorname{im}(i))_{ver,1}$, which is smaller than $\dim(i)_1=\dim H_1(|G|)=c(G)$. Moreover, $P^{\#}$ is the characteristic polynomial of the horizontal monodromy acting on I, which clearly divides the characteristic polynomial of the horizontal monodromy acting on $H_1(|G|)$, which is $P_{\mathfrak{h}(|G|)}$. If $c(G)=0$, or if $c(G)=\#_1^2 M_{\Phi,ver}$ (i.e., if *corank*$(A,I)=\#\mathcal{A}$, cf. (18.1.5)), or if $\Gamma_{\mathcal{C}}$ is unicolored (cf. (20.1.10)), then $P^{\#}=P_{\mathfrak{h}(|G|)}$.

20.2.4. The local case, valid for any j, follows by similar arguments if one replaces $\Gamma_{\mathcal{C}}$ by $\Gamma^2_{\mathcal{C},j}$. The last sentence follows from (17.2.9), or the sentence following it.

20.3. The proof of (19.2.11). The case of vanishing 2–edges revisited. Assume that $\Gamma_{\mathcal{C}}$ has a vanishing 2–edge $e\in\mathcal{E}_{\mathcal{W}}$, i.e the situation of (20.1.6)(c) occurs. Let $h:=\tilde{m}_{\phi,ver}$ be as in (20.1.1), and fix q such that the restriction of h^q on $\widetilde{F}_{\mathcal{W}}$ is the identity. The proof of (20.1.6)(c) shows that h^q can be extended by the identity map to $\widetilde{F}^*_{\Phi}\cap T(e)$ too. In particular, in such a situation it is better to replace the space $\widetilde{F}_{\mathcal{W}}$ from the diagram (20.1.7) by $\widetilde{F}'_{\mathcal{W}}$, defined as the union of $\widetilde{F}_{\mathcal{W}}$ with *all* separating annuli $\widetilde{F}^*_{\Phi}\cap T(e)$ corresponding to the vanishing 2–edges from $\mathcal{E}_{\mathcal{W}}$. Moreover, we define B' as the union of the other separating annuli. Then one gets a new diagram (involving the spaces $\widetilde{F}^*_{\Phi}$, $\widetilde{F}'_{\mathcal{W}}$, B', and morphisms i' and T') such that in the new 'collapsing' situation T' becomes *an isomorphism.* Then all the arguments above (complemented with the corresponding facts from section § 14 about the 'Collapsing Main Algorithm') can be repeated, and the second version (19.2.11) follows too.

Example 20.3.1. If (f,g) is as in (9.1), then we have only vanishing 2–edges, hence $\widetilde{F}'_{\mathcal{W}}=\widetilde{F}_{\Phi}$. Therefore, in the new diagram $H_1(\widetilde{F}^*_{\Phi},\widetilde{F}'_{\mathcal{W}})=0$. In fact, since $\nu=1$ for all vertices, we can even take $q=1$ (use e.g. (16.1.3)), hence in this case $m_{\phi,ver}$ is isotopic to the identity. (This can also be proved by a direct argument, see section § § 25).

§ 21. The mixed Hodge structure of $H_1(\partial F)$.

21.1. We believe that a substantial part of the numerical identities and inequalities obtained in the previous sections are closely related with general properties of mixed Hodge structures (in the sequel abbreviated by MHS) supported by different (co)homology groups involved in the constructions. (For general results, terminology and properties of MHS, see e.g. [**16**], or [**64, 65, 66**].)

Although the proof of the existence of the mixed Hodge structure on $H_1(\partial F)$ and the analysis of its properties exceed the aims of the present work, we decided to dedicate a few paragraphs to this subject too: we wish to formulate some of the expectations and to shed light on the obtained results from this point of view as well. Moreover, we wish to stimulate further research in this direction.

21.1.1. **Conjecture.** $H_1(F)$ carries a natural mixed Hodge structure, whose weight filtration $W_\bullet$ is defined over $\mathbb{Q}$,

$$0=W_{-3}\subset W_{-2}\subset W_{-1}\subset W_0=H_1(\partial F,\mathbb{Q}),$$

and for any graph G provided by the Main Algorithm one has:

$$\dim Gr^W_i H_1(\partial F)=\begin{cases} corank(A)_G & \text{if } i=-2,\\ 2g(G) & \text{if } i=-1,\\ c(G) & \text{if } i=0.\end{cases} \tag{21.1.2}$$

Obviously, there is a corresponding dual cohomological statement:

21.1.3. **Conjecture.** $H^1(F)$ carries a natural mixed Hodge structure, whose weight filtration $W_\bullet$ is defined over $\mathbb{Q}$,

$$0=W_{-1}\subset W_0\subset W_1\subset W_2=H^1(\partial F,\mathbb{Q}),$$

and for any graph G provided by the Main Algorithm one has:

$$\text{(21.1.4)} \qquad \dim Gr_i^W H^1(\partial F) = \begin{cases} corank(A)_G & \text{if } i=2, \\ 2g(G) & \text{if } i=1, \\ c(G) & \text{if } i=0. \end{cases}$$

Similarly, $H^2(F)$ carries a natural mixed Hodge structure, whose weight filtration $W_\bullet$ is defined over $\mathbb{Q}$,

$$0 = W_1 \subset W_2 \subset W_3 \subset W_4 = H^2(\partial F, \mathbb{Q}),$$

and for any graph G provided by the Main Algorithm one has:

$$\text{(21.1.5)} \qquad \dim Gr_i^W H^2(\partial F) = \begin{cases} corank(A)_G & \text{if } i=2, \\ 2g(G) & \text{if } i=3, \\ c(G) & \text{if } i=4. \end{cases}$$

REMARK 21.1.6.

(1) By 'natural' we mean that geometric maps induce MHS–morphisms. E.g., the monomorphism $H^1(F) \hookrightarrow H^1(\partial F)$ is *strictly compatible* with both weight and Hodge filtrations; namely, $W_i(H^1(F)) = H^1(F) \cap W_1(H^1(\partial F))$ for any i (and there is a similar statement for the Hodge filtration too).

Moreover, we expect that the cup product $H^1(\partial F) \otimes H^1(\partial F) \mapsto H^2(\partial F)$ is compatible with the MHS, e.g.

$$\text{(21.1.7)} \qquad W_i(H^1(\partial F)) \cup W_j(H^1(\partial F)) \subset W_{i+j}(H^2(\partial F)).$$

E.g., if A_G is non–degenerate, then the cup–product $H^1(Y) \otimes H^1(Y) \to H^2(Y)$ is trivial (reproving the result of Sullivan [**70**], see also (29.2)). Moreover, (21.1.7) can be compared with the list of inclusions of (19.2.10)(b) provided that $(A_G)_{\lambda\neq 1}$ is non–degenerate. (But, in any situation, one might write down similar inclusions.)

(2) The above Conjectures would have the following consequence: the numerical invariants $corank(A)_G$, $g(G)$ and $c(G)$ associated with the graph G obtained from the Main Algorithm are independent of the choice of the resolution r (or, of the graph $\Gamma_{\mathcal{C}}$ used in the algorithm). Therefore, we emphasize again, if one wishes to keep in G^m all the information regarding the MHS of ∂F, one has to use only those operations of the reduced plumbing calculus which preserve these numbers, namely, one has to exclude the oriented handle absorption R5.

(3) Conjecture (21.1.3) can be compared (and is compatible) with results regarding the MHS of links of normal surface singularities. (These type of results can be obtained from general purity results regarding the local cohomology of complex analytic spaces, or, for this particular case, one can also consult e.g. [**21**].) Namely, if K is such a link, then the weights of $H^1(K)$ are < 2, while the weighs of $H^2(K)$ are > 2.

(4) In the case of hypersurface singularities, the weight filtration of the vanishing cohomology (i.e., of $H^*(F)$) is related with the 'monodromy weight filtration' associated with the nilpotent part of the monodromy operators (although one has to treat the two generalized eigenspaces $H^*(F)_{\lambda=1}$ and $H^*(F)_{\lambda\neq 1}$ with different weight–conventions). In the present situation the corresponding fact is not so transparent. (We expect that one has to consider a more complicated direct sum decomposition determined by certain monodromy and variation operators, like in [**61**], and on each block the weight–filtration is determined by these operators.)

21.1.8. In § 24 (the case of homogeneous singularities) and in (25.3) (the case of cylinders) we provide evidences for the above Conjecture.

CHAPTER IX

The case of homogeneous singularities.

§ 22. The general case.

22.1. Assume that f is homogeneous of degree $d \geq 2$. In order to determine a possible $\Gamma_{\mathcal{C}}$, we take for g a generic linear function. We will adopt the notations of section § 10, where the graph $\Gamma_{\mathcal{C}}$ is constructed. Clearly

$$\#\mathcal{A}(\Gamma_{\mathcal{C}}) = \#\mathcal{A}(G) = d.$$

Moreover, $d_j = 1$ for any j, hence

$$M'_{j,hor} = M^{\Phi}_{j,hor} \text{ and } M'_{j,ver} = M^{\Phi}_{j,ver}. \tag{22.1.1}$$

We start our discussion with the list of some specific properties of the geometry of homogeneous singularities (regarding the graphs $\Gamma_{\mathcal{C}}$, G, or the ICIS Φ). Then we will combine this new information with the general properties established in the previous sections.

22.2. The first specific feature. The horizontal/vertical monodromies. Since f and g are homogeneous, by [**63**], we get

$$\begin{cases} M'_{j,ver} = (M'_{j,hor})^{-d} \\ M_{\Phi,ver} = (M_{\Phi,hor})^{-d}. \end{cases}$$

In particular, for any of the pairs $(M'_{j,ver}, M'_{j,hor})$ or $(M_{\Phi,ver}, M_{\Phi,hor})$, the number of 2–Jordan blocks of the vertical operator coincides with the number of 2–Jordan blocks of the horizontal one. Moreover, the horizontal monodromies determine the corresponding $\mathbb{Z}^2$–representations.

22.3. The second specific feature. The graphs $G_{2,j}$. A 'short–cut' for G. Consider the graph $\Gamma_{\mathcal{C}}$ of section § 10. In the Main Algorithm (12.3) applied for this $\Gamma_{\mathcal{C}}$, one puts exactly one vertex in G, say $\widetilde{v}_\lambda$, above a vertex v_λ of $\Gamma_{\mathcal{C}}$. If we delete all these vertices from G, we get the union of the graphs $G_{2,j}$, cf. (12.5.3). The point is that

> *if we delete all the arrows and multiplicities of $G_{2,j}$ we get a possible resolution graph of the d–suspension of the transversal singularity Σ_j with opposite orientation.*

More precisely, if $f'_j(u,v) = f|_{(S_x,x)}$ ($x \in \Sigma_j \setminus \{0\}$, cf. (3.2)) is the local equation of the transversal type plane curve singularity, then its d–suspension is the isolated hypersurface singularity $(\{w^d = f'_j(u,v)\}, 0)$. Then its link with reversed orientation admits $G_{2,j}$ (with the above simplifications) as a possible plumbing graph.

This follows from a comparison of the present Main Algorithm (12.3) and the algorithm which provides the graph of suspension singularities, see e.g. [**44**]. Similarly, it follows from the combination of (4.3.1)(2) and (22.2) too. (Compare also with (22.4).)

In particular, the graph G consists of the disjoint union of graphs of these suspensions (with opposite orientation) and $|\Lambda|$ new vertices $\widetilde{v}_\lambda$ (decorated by $[g_\lambda]$), altogether supporting d arrowheads. The edges connecting these new vertices to the graphs $G_{2,j}$ are $\ominus$–edges and reflect the combinatorics of the 'identification map' c (i.e. the incidence of the singular points on the components of C, see (10.1)). The arrowheads are distributed as follows: each $\widetilde{v}_\lambda$ supports d_λ arrowheads, all of them connected by a $+$–edges. The gluing property of the two pieces (i.e. of $\partial_1 F$ and $\partial_2 F$) is codified in the Euler numbers of the vertices $\widetilde{v}_\lambda$ in G. This is determined by (5.1.2), once we carry in the construction the multiplicity system of g: in the suspension graphs one has the multiplicity system of the germ $w : (\{w^d = f'_j(u,v)\},0) \to (\mathbb{C},0)$, and each $\widetilde{v}_\lambda$ and arrowhead has multiplicity (1). This provides a very convenient 'short–cut' to obtain G.

Example 22.3.1. It is well–known that there exists a rational cuspidal projective curve C of degree $d = 5$ with two local irreducible singularities with local equations $u^3 + v^4 = 0$ and $u^2 + v^7 = 0$ (see e.g. [**40**]). Then the above procedure provides two suspension singularities, both of Pham–Brieskorn type. Their equations are $u^3 + v^4 + w^5 = 0$ and $u^2 + v^7 + w^5 = 0$. (We made the choice of C carefully: we wished to get pairwise relative prime exponents in each singularity, in order to 'minimize' $|H_1(\partial F,\mathbb{Z})|$, cf. (22.8).) The embedded resolution graphs of the coordinate function w restricted on these suspension singularities (providing the arrow and multiplicities) are the following:

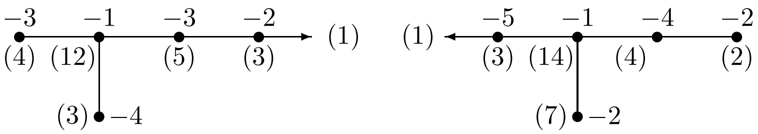

Reversing the orientations we get the following graphs, which coincide with the graphs $G_{2,j}$ $(j = 1, 2)$:

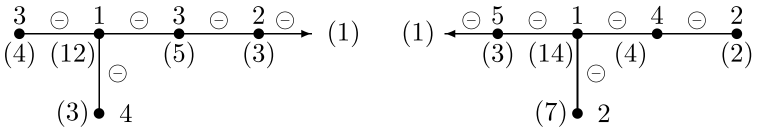

In order to get G, we have to insert one more vertex $\widetilde{v}$ (corresponding to C) with multiplicity (1) and genus decoration zero, and $d = 5$ arrowheads, all with multiplicity (1), connected with $+$–edges to $\widetilde{v}$:

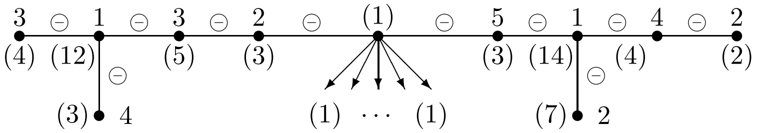

The missing Euler number e of $\widetilde{v}$ is computed via (5.1.2), namely $e+5-3-3 = 0$, hence $e = 1$. Deleting all the multiplicities gives the graph

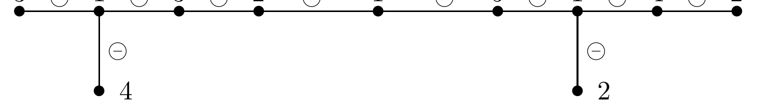

By plumbing calculus, one can blow down twice 1–curves, and also one may delete the $\ominus$'s. The result is a possible graph of ∂F. (This is not the 'normal form' of [**49**], the interested reader may transform it easily to get a graph with all Euler numbers negative. But even if we pass to the normal form, the intersection matrix will not be negative definite, its index will be $(-12, +1)$.)

Notice that ∂F is a rational homology sphere. In fact, it is easy to verify that $H_1(\partial F, \mathbb{Z}) = \mathbb{Z}_5$.

As a consequence of the above discussion, we get:

COROLLARY 22.3.2. *If C is a rational unicuspidal projective plane curve (i.e. C has only one singular point which is locally irreducible), and its local singularity has only one Puiseux pair, then ∂F can be represented by a plumbing graph which is either star–shaped or a string.*

This will be exemplified more in subsection (22.10).
Another consequence is the following

COROLLARY 22.3.3. *$corank(A, I)_G = \#\mathcal{A}(G)$. In particular, the characteristic polynomial of the monodromy acting on $H_1(\partial F, \mathbb{Z})$ is determined by (19.2.7), $\#_1^2 M_{\Phi,ver} = c(G)$, and $rank\, H_1(\partial F)_{\neq 1} = 2g(G)+c(G)-2g(\Gamma_\mathcal{C})-c(\Gamma_\mathcal{C})$. Moreover, the equivalent statements of (19.2.3) are also satisfied, in particular $\#_j^2 M'_{j,ver} = c(G_{2,j})$.*

PROOF. Since each $\widetilde{v}_\lambda$ supports at least one arrowhead, the rank of (A, I) is maximal if all the ranks of the intersection matrices associated with $G_{2,j}$ are maximal. But these matrices are definite, hence non–degenerate. For the last two identities see (19.2.4) and (19.2.9). □

After stating the third specific feature, and determining *corank*(A) as well, we will return to the characteristic polynomial formula.

22.4. The third specific feature. The *d*–covering. Let $C \subset \mathbb{P}^2$ as before. It is well–known that there is a regular d–covering $F = \{f = 1\} \to \mathbb{P}^2 \setminus C$ given by $(x, y, z) \mapsto [x : y : z]$. Let T be a small tubular neighbourhood of C, and let ∂T be its boundary. In the next discussion it is more convenient to orient ∂T not as the boundary of T, but as the boundary of $\mathbb{P}^2 \setminus T^\circ$. Then the above covering induces a regular d–covering

$$\partial F \to \partial T.$$

Moreover, the $\mathbb{Z}_d$–Galois action on ∂F coincides with (a representative) of the Milnor monodromy action on ∂F. Using either this, or just the homogeneity of f, we get that *the monodromy action is finite of order d.*

EXAMPLE 22.4.1. Let us exemplify this covering on a simple case. Assume that C has degree 3 and has a cusp singularity. Then a possible plumbing representation for ∂T (oriented as the boundary of T) is the graph (i) below.

(i)

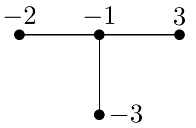

(ii)

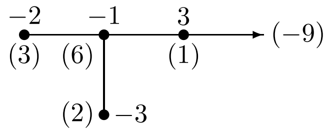

Then the $\mathbb{Z}_3$–cyclic covering of ∂T can be computed as the $\mathbb{Z}_3$–covering of the divisor marked in (ii) by a similar algorithm as described in [**44**] for cyclic coverings. This provides the graph (iii) below (as the graph covering of the graph (i)). This is a possible plumbing graph of ∂F with opposite orientation. Changing the orientation and after (reduced) calculus, we get the graph (iv). This is the graph that we get by the Main Algorithm as well (after modified by reduced calculus).

The monodromy action permutes the three -2–curves.

(iii)

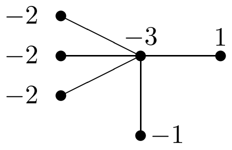

(iv)

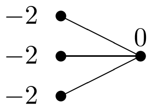

22.4.2. The 3–manifold ∂T was studied intensively by many authors (D.C. Cohen, A. Suciu, E. Hironaka, see [**14, 15, 24**] and the references therein). Hence, once the representation $\pi_1(\partial T)\to\mathbb{Z}_d$ associated with the covering is identified, one can try to recover all data about ∂F from that of ∂T (some of it can be done easily, some of it by rather hard work).

The geometry of the covering sometimes provides certain numerical invariants easily. E.g., in the next paragraphs we will show a computation which provides the rank of the 1–eigenspace $\dim H_1(\partial F)_1$ (associated with the monodromy action).

22.4.3. **The rank of $H_1(\partial F)_1$ and $corank(A)_G$.** By the above discussion we get $H_1(\partial F)_1=H_1(\partial T)$. On the other hand, $H_1(\partial T)$ can be computed easily, since ∂T is also a plumbed 3–manifold (cf. (18.2.8)(c)). One can determine a possible plumbing graph for ∂T as follows. Start with the curve C, blow up the infinitely near points of its singularities (as in section § 10), and transform the combinatorics of the resulting curve configuration into a graph. In this way we get as a plumbing graph the graph $\Gamma_{\mathcal{C}}$ with some natural modifications: we have to keep the genus decorations, delete the arrowheads and the weight decorations of type $(m;n,\nu)$, and have to insert the Euler numbers. These can be determined as follows: start with the intersection matrix of the components of C. This, by Bézout's theorem, is the $\Lambda\times\Lambda$ matrix A_C with entries $(d_\lambda d_\xi)_{\lambda,\xi}$. This intersection matrix is modified by blow ups to get the intersection matrix $A_{\Gamma_{\mathcal{C}}}$ of the plumbing graph of ∂T. Hence, similarly as in (18.1.2)), one has:

$$\dim H_1(\partial F)_1=\dim H_1(\partial T)=2g(\Gamma_{\mathcal{C}})+c(\Gamma_{\mathcal{C}})+corank(A)_{\Gamma_{\mathcal{C}}}. \tag{22.4.4}$$

Using the notations of section § 10, we compute each summand. $g(\Gamma_{\mathcal{C}})=\sum_\lambda g_\lambda$ is clear. Since each Γ_j is a tree, one also gets

$$c(\Gamma_{\mathcal{C}})=\sum_j(\,|I_j|-1\,)-(\,|\Lambda|-1\,).$$

Finally, by blowing up, the corank of an intersection matrix stays stable, hence $corank(A)_{\Gamma_{\mathcal{C}}}=corank(A_C)=corank((d_\lambda d_\xi)_{\lambda,\xi})$, i.e.:

$$corank(A)_{\Gamma_{\mathcal{C}}}=|\Lambda|-1. \tag{22.4.5}$$

Therefore we get the identities (where $b_1(C)$ denotes the first Betti number of C):

$$\dim H_1(\partial F)_1=2g(\Gamma_{\mathcal{C}})+\sum_j(\,|I_j|-1\,)=b_1(C)+|\Lambda|-1. \tag{22.4.6}$$

This has the following immediate consequence:

Corollary 22.4.7. *$corank(A)_G=|\Lambda|-1$. Hence, in general, A_G is degenerate.*

Proof. $corank(A)_G=corank(A)_{\Gamma_{\mathcal{C}}}$ by (19.2.8) and (22.4.4). Then use (22.4.5). □

Now we start our list of applications.

22.5. Application. The characteristic polynomial of ∂F. Using (19.2.7) and (22.4.7) we get:

COROLLARY 22.5.1. *If f is homogeneous, then the characteristic polynomial of the (Milnor) monodromy acting on $H_1(\partial F)$ is*

$$\frac{(t-1)^{|\Lambda|-d}\cdot\prod_{w\in\mathcal{W}(\Gamma_{\mathcal{C}})}(t^{(m_w,d)}-1)^{2g_w+\delta_w-2}\cdot(t^{\mathfrak{n}_w}-1)}{\prod_{e\in\mathcal{E}_w(\Gamma_{\mathcal{C}})}(t^{\mathfrak{n}_e}-1)}. \tag{22.5.2}$$

(For the integers $\mathfrak{n}_w$ and $\mathfrak{n}_e$ see (12.3), with the additional remark that all the second entries of the vertex–decorations are equal to d.)

Notice that this is a formula given entirely in terms of $\Gamma_{\mathcal{C}}$. If $c(G)=0$, then via (19.1.2) it simplifies to:

$$(t-1)^{1+|\Lambda|-d}\cdot\prod_{w\in\mathcal{W}(\Gamma_{\mathcal{C}})}(t^{(m_w,d)}-1)^{2g_w+\delta_w-2}. \tag{22.5.3}$$

Since the monodromy has finite order, the complex algebraic monodromy is determined completely by its characteristic polynomial. By (22.3.3) and (16.4.4), the complex monodromy is trivial if and only if $c(G)=c(\Gamma_{\mathcal{C}})$ and $g(G)=g(\Gamma_{\mathcal{C}})$.

22.5.4. Now, we provide an (almost) independent description of the characteristic polynomial, completely in terms of the projective curve C. Indeed, the divisor $Div=\sum k_\lambda(\lambda)\in\mathbb{Z}[S^1]$ of the characteristic polynomial can also be determined as follows.

Clearly, by (22.4), the multiplicity k_1 of the eigenvalue $\lambda=1$ is $b_1(C)+|\Lambda|-1$.

On the other hand, for $\lambda\neq 1$, (17.2) and (22.1.1) provides the following identity in terms of the local horizontal/Milnor algebraic monodromies of the transversal types (i.e. in terms of the monodromy operators of the local singularities of C):

$$k_\lambda=\sum_j\sum_{\lambda^d=1}\#\{\text{Jordan block of } M'_{j,hor} \text{ with eigenvalue } \lambda\}\quad(\lambda\neq 1).$$

In order to see this, we apply (22.2), and the Wang homological exact sequence for $F'_j\to\partial_{2,j}\to S^1$, cf. (18.1.4).

Indeed, if B is a 1–Jordan block of $M'_{j,hor}$ with eigenvalue λ, and $\lambda^d=1$, then this creates a 1–block in $M'_{j,ver}$ with eigenvalue 1, and the corresponding 1–dimensional eigenspace survives in $coker(M'_{j,ver}-1)$.

If B is a 2–Jordan block of $M'_{j,hor}$ with eigenvalue λ, and $\lambda^d=1$, then this creates a 2–block in $M'_{j,ver}$ with eigenvalue 1, and in $coker(M'_{j,ver}-1)$ only a 1–dimensional space survives, and $M'_{j,hor}$ acts on it by multiplication by λ.

This and the last identity of (22.3.3) imply:

$$\sum_j\sum_{\lambda^d=1,\ \lambda\neq 1}\#\{\text{Jordan block of } M'_{j,hor} \text{ with eigenvalue } \lambda\}$$
$$=2g(G)+c(G)-2g(\Gamma_{\mathcal{C}})-c(\Gamma_{\mathcal{C}}).$$

EXAMPLE 22.5.5. Assume that C is irreducible, and it has a unique singular point (C,P) which is locally equisingular to $\{(u^2+v^3)(u^3+v^2)=0\}$. For the embedded resolution graph of (C,P) see (9.1.1). In order to get $\Gamma_{\mathcal{C}}$ one has to add one more vertex, which will have genus decoration $[g]$, where $2g=(d-1)(d-2)-12$, and it will support d arrows. The reader is invited to complete the picture of $\Gamma_{\mathcal{C}}$.

By (22.5.2), we get that the characteristic polynomial of the monodromy operator acting on $H_1(\partial F)$ is

$$\frac{(t-1)^{(d-1)(d-2)-10}}{t^{(d,2)}-1}\cdot\Big(\frac{t^{(d,10)}-1}{t^{(d,5)}-1}\Big)^2.$$

In all the cases, the multiplicity of the eigenvalue 1 is $k_1 = (d-1)(d-2) - 11 = (d-1)(d-2) - \mu(f')$. If d is odd, then there are no other eigenvalues, hence the complex monodromy on $H_1(\partial F, \mathbb{C})$ is trivial.

If d is even then other eigenvalues appear too. If $5 \nmid d$ then only one, namely -1, otherwise their divisor is the divisor of $(t^5+1)^2/(t+1)$.

This result can be compared with (22.5.4). For this use that the algebraic monodromy of the local transversal singularity has characteristic polynomial $(t^5+1)^2(t-1)$, and exactly one 2–Jordan block, which has eigenvalue -1.

The graph G^m for $d = 10$ is the following (for this d all the Hirzebruch–Jung strings in the main algorithm are trivial):

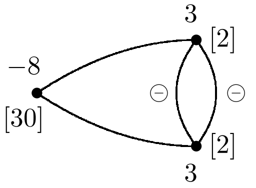

In this case $\dim H_1(\partial F) = 70$, $\dim H_1(\partial F)_1 = 61$, A_G is non–degenerate with $|\det(A_G)| = 50$.

EXAMPLE 22.5.6. The characteristic polynomial of the example (12.5.11) is $(t-1)^{d^2-3d+1}$, hence the complex monodromy on $H_1(\partial F, \mathbb{C})$ is trivial.

22.6. Applications. The determination of the six (complex) operators $M'_{j,hor}$, $M'_{j,hor}$, $M^{\Phi}_{j,hor}$, $M^{\Phi}_{j,ver}$, $M_{\Phi,hor}$ and $M_{\phi,ver}$.

In this subsection we show that the local horizontal/Milnor monodromy operators $\{M'_{j,hor}\}_j$ (of the transversal types), together with the integers d and $c(G)$ determine completely the $\mathbb{Z}^2$–representations generated by the commuting pairs $(M'_{j,hor}, M'_{j,ver})$, $(M^{\Phi}_{j,hor}, M^{\Phi}_{j,ver})$, respectively $(M_{\Phi,hor}, M_{\Phi,ver})$.

Indeed, the first two pairs agree (cf. (22.1.1)), hence by (22.2) it is enough to determine $M_{\Phi,hor}$. Moreover, for eigenvalues $\lambda \neq 1$, the following generalized eigenspaces (together with the corresponding horizontal actions) coincide:

$$H_1(F_\Phi)_{M_{\Phi,hor},\lambda\neq 1} = \oplus_j H_1(F_\Phi \cap T_j)_{M^{\Phi}_{j,hor},\lambda\neq 1} = \oplus_j H_1(F'_j)_{M'_{j,hor},\lambda\neq 1}. \tag{22.6.1}$$

Next, we determine the action of $M_{\Phi,hor}$ on the generalized 1–eigenspace $H_1(F_\Phi)_1$ of $M_{\Phi,hor}$. The rank of $H_1(F_\Phi)_1$ can be determined in several ways.

First, one can consider the rank of the total space $H_1(F_\Phi)$, which is $(d-1)^2$. Indeed, F_Φ is the Milnor number of an ICIS (f, g), where f is homogeneous of degree d and l is generic linear, hence their Milnor number is the Milnor number of a homogeneous plane curve singularity of degree d. Since we already determined the $(\lambda \neq 1)$–generalized eigenspaces the rank of $H_1(F_\Phi)_1$ follows too.

There is another formula based on (16.2.10)(a), which provides

$$rank\, H_1(F_\Phi)_1 = 2g(\Gamma_{\mathcal{C}}) + 2c(\Gamma_{\mathcal{C}}) + d - 1 = d - |\Lambda| + b_1(C) + \sum_j (|I_j| - 1).$$

In particular, since we have only one and two–dimensional Jordan blocks:

$$\#_1^1 M_{\Phi,hor} + 2\#_1^2 M_{\Phi,hor} = rank\, H_1(F_\Phi)_1.$$

On the other hand, by (22.2) and (22.6.1) we have

$$\#_1^2 M_{\Phi,ver} = \#_1^2 M_{\Phi,hor} + \sum_j \sum_{\lambda^d = 1 \neq \lambda} \#_\lambda^2 M'_{j,hor}.$$

Since by (22.3.3) the left hand side is $c(G)$, we get

$$\#_1^2 M_{\Phi,hor} = c(G) - \sum_j \sum_{\lambda^d=1\neq\lambda} \#_\lambda^2 M'_{j,hor}.$$

EXAMPLE 22.6.2. Assume that we are in the situation of (22.5.5) with $d = 10$. Then both local operators $M'_{1,hor}$ and $M'_{1,ver}$ have one 2–Jordan block, the first with eigenvalue -1, the other with 1. This is compatible with the fact that $c(G_{2,1}) = 1$.

Since the order of any eigenvalue of $M_{\Phi,hor}$ divides 10, we get that $M_{\Phi,ver}$ is unipotent. By (22.3.3), the number of 2–Jordan blocks of $M_{\Phi,ver}$ is $c(G) = 2$. Hence $M_{\Phi,hor}$ has two 2–Jordan blocks as well. By (22.6.1), there is only one with eigenvalue $\neq 1$, namely with eigenvalue -1. Hence the remaining block has eigenvalue 1.

22.7. When is ∂F a rational homology sphere? By (22.5.4) we get the following characterization:

COROLLARY 22.7.1. *∂F is a rational homology sphere if and only if C is an irreducible, rational cuspidal curve (i.e. all its singularities are locally irreducible), and there is no eigenvalue λ of the local singularities (C, P_j) with $\lambda^d = 1$.*

This situation can indeed appear, see e.g. (22.3.1), or many examples of the present work.

We wish to emphasize that the classification of rational cuspidal projective curves is an open problem. (For a partial classification with d small see e.g. [**40**], or [**8**] and the references therein.) It would be very interesting and important to continue the program of the present section: some restrictions about the structure of ∂F might provide new data in the classification problem as well.

22.8. When is ∂F an integral homology sphere? The answer to this question is simple: Never (provided that $d \geq 2$)! This follows from the following proposition:

PROPOSITION 22.8.1. *Assume that f is homogeneous of degree d. Then there exists an element $h \in H_1(\partial F, \mathbb{Z})$ whose order is (infinity or) a multiple of d. If $H_1(\partial F, \mathbb{Z})$ is finite, one can choose such an h fixed by the monodromy action.*

PROOF. By (22.7) we may assume that C is irreducible, rational and cuspidal. Consider the following diagram (for notations, see (22.4)):

$$\begin{tikzcd}
\pi_1(\partial F) \arrow[r, "i"] \arrow[d, "q"] & \pi_1(\partial T) \arrow[r, "p"] \arrow[d, "r"] & \mathbb{Z}_d \\
H_1(\partial F, \mathbb{Z}) \arrow[r] & H_1(\partial T, \mathbb{Z}) \arrow[r, equal] & \mathbb{Z}_{d^2}
\end{tikzcd}$$

Here the first line is exact provided by the homotopy exact sequence of the covering, i is injective, and q, r and p are surjective. Let $\gamma \in \pi_1(\partial T)$ be the class of a small loop around C. Then $p(\gamma^d) = 0$, hence $\gamma^d \in \pi_1(\partial F)$.

On the other hand, $H_1(\partial T, \mathbb{Z}) = \mathbb{Z}_{d^2}$, and it is generated by $[\gamma]$. This follows from the fact (see (22.4.3) and the proof of (18.1.2)) that $H_1(\partial T, \mathbb{Z}) = coker(A)_{\Gamma_C}$, but in this case A has only one entry, namely d^2.

Hence $r(\gamma^d)$ has order d in $H_1(\partial T, \mathbb{Z})$. In particular, the order of $q(\gamma^d) \in H_1(\partial F, \mathbb{Z})$ is a multiple of d. Since the monodromy action in $\pi_1(\partial F)$ is conjugation by γ, the second part also follows. $\square$

The above bound is sharp: there are examples when $H_1(\partial F, \mathbb{Z}) = \mathbb{Z}_d$; see e.g. (22.3.1). The above result also shows that the monodromy action (over $\mathbb{Z}$) is trivial whenever $H_1(\partial F, \mathbb{Z}) = \mathbb{Z}_d$.

The fact that for f homogeneous ∂F cannot be an integral homology sphere was for the first time noticed by Siersma in **[61]**, page 466, where he used a different argument.

22.9. Examples. Cases with d small. In this section we will treat all the possible examples with $d = 2$ and $d = 3$, and we present some examples with $d = 4$. The statements are direct applications of the Main Algorithm and the above discussions regarding the monodromy. (One of our goals in this 'classification list' is to provide an idea about the variety of the possible 3–manifolds obtained in this way, and to check if the same 3–manifold can be realized from essentially two different situations.)

22.9.1. ($\mathbf{d = 2}$) There is only one case: C is a union of two lines. A possible graph G^m is $0\,\bullet$; hence $\partial F = S^1 \times S^2$. The monodromy is trivial.

22.9.2. ($\mathbf{d = 3}$) There are six cases:

(3a) C is irreducible with a cusp. See (22.4.1), or (22.10.1)(a) with $d = 3$ for the graph G^m of ∂F. In this case $H_1(\partial F, \mathbb{Z}) = \mathbb{Z}_6 \oplus \mathbb{Z}_2$, hence the complex monodromy is trivial. The integral homology has the following special form (specific to the homology of any Seifert 3–manifold):

$$H_1(\partial F, \mathbb{Z}) = \langle\, x_1, x_2, x_3, h \mid 2x_1 = 2x_2 = 2x_3 = h,\ x_1 + x_2 + x_3 = 0 \,\rangle.$$

h has order 3 and it is preserved by the integral monodromy, while the elements x_1, x_2, x_3 are cyclically permuted (in order to prove this, use e.g. (22.4.1)).

(3b) C is irreducible with a node. A possible graph of ∂F is

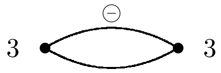

The rank of $H_1(\partial F)$ is 1, and the complex monodromy is trivial.

(3c) C is the union of a line and an irreducible conic, intersecting each other transversely. A possible graph for ∂F is $3\,\bullet\,[1]$, and the complex monodromy is trivial.

(3d) C is the union of an irreducible conic and one of its tangent lines. $\partial F = S^2 \times S^1$ and the monodromy is trivial.

(3e) C is the union of three lines in general position: $\partial F = S^1 \times S^1 \times S^1$ and the monodromy is trivial.

(3f) C is the union of three lines intersecting each other in one point: then by *reduced* calculus we get for ∂F the graph G^m:

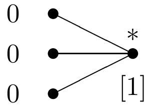

(the decoration * is irrelevant)

In fact, if we apply the *splitting operation* (not permitted by reduced calculus), we obtain that $\partial F = \#_4 S^2 \times S^1$.

The characteristic polynomial of the monodromy is $(t^3 - 1)(t - 1)$.

22.9.3. ($\mathbf{d = 4}$) We will start with the cases when C **is irreducible, rational and cuspidal** (i.e. all local singularities are locally irreducible). There are four cases:

(4a) C has three A_2 singular points. A possible equation for f (and $\Gamma_{\mathcal{C}}$) is given in (10.1.4). ∂F is a rational homology sphere with graph:

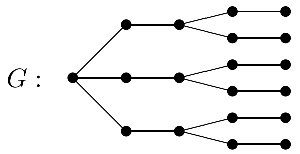

(with all the Euler numbers 2)

(In this case, neither G, nor G with the opposite orientation can be represented by a negative definite graph.)

(4b) C has two singular points with local equations $u^2+v^3=0$ and $u^2+v^5=0$. This case has an unexpected surprise in store: having two singular points we expect that the graph will have two nodes. This is indeed the case for the graph G, the immediate result of the main algorithm. Nevertheless, via (reduced) plumbing calculus the chain connecting the two nodes disappears (by a 0–chain absorption). Finally, we get that ∂F is a Seifert manifold with graph:

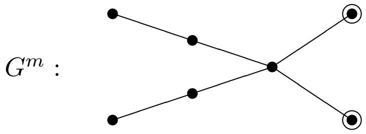

● is decorated by 2

◉ is decorated by 5

The orbifold Euler number is $4/15>0$, and the order of $H_1(\partial F,\mathbb{Z})$ is 60.

(4c) C has one singular point with local equation $u^3+v^4=0$. ∂F is a rational homology sphere, its graph is given in (22.10.2)(a) (with $d=4$). It is worth mentioning that there are two projectively non–equivalent curves of degree four with this local data, namely $x^4-x^3y+y^3z=0$ and $x^4-y^3z=0$.

(4d) C has one singular point with local equation $u^2+v^7=0$. In this case, rather surprisingly, ∂F is the lens space of type $L(28,15)$ (i.e. the graph is a string with decorations: -2, -8, -2).

For an example of **irreducible non–rational** C, see (12.5.11) together with (22.5.6). For **reducible** C we give three more examples:

(4a') Let C be the union of two conics intersecting each other transversely. The characteristic polynomial is $(t-1)^4$, the complex monodromy is trivial, and the graph of ∂F is:

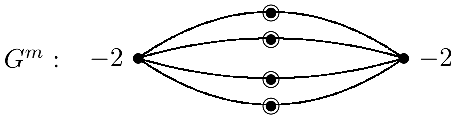

◉ is decorated by -4

(4b') Let $C=$ be the union of a smooth irreducible conic and two different tangent lines. The characteristic polynomial is $(t^2+1)^2(t-1)^3$. The graph G^m is $0\bullet[3]$.

(4c') Let C be the union of two smooth conics intersecting tangentially in two singular points of type A_3 (e.g. the equation of f is $x^2y^2+z^4$). Then the graph G^m is $4\bullet[3]$. The characteristic polynomial is $(t^2+1)^2(t-1)^2$.

22.9.4. It is also instructive to see the case when C is given by $(x^3-y^2z)(y^3-x^2z)=0$. C has two components, and they intersect each other in 6 points. One of them, say (C,P), has local equation $(u^3-v^2)(v^3-u^2)=0$ (cf. (9.1.1)), the others are nodes. Some of the cycles of G are generated by these intersections, and one more by a 2–Jordan block of (C,P): $c(\Gamma_{\mathcal{C}})=5$ and $c(G)=6$.

22.10. Examples. The case of rational unicuspidal curves with one Puiseux pair.

The present subsection is motivated by two facts.

First, by such curves we produce plumbed 3–manifolds with start–shaped graphs, cf. (22.3.2), some of which are irreducible with Seifert fiber–structure, some of which are not irreducible. Seifert 3–manifolds play a special role in the world of 3–manifolds. Therefore, it is an important to classify all Seifert manifolds realized as ∂F, where F is a Milnor fiber as above. Even if we restrict ourselves to the homogeneous case, the problem looks surprisingly hard: although all unicuspidal rational curves with one Puiseux pair produce star–shaped graphs, in (22.9)(4b) we have found a curve C with two cusps, which still produces a Seifert manifold. Since the classification of the cuspidal rational curves is not finished, the above question looks hard. On the other hand, notice that Seifert manifolds can also be produced by other type of germs as well, e.g. by some weighted homogeneous germs as in (12.5.12) or (26.1.8), but not all weighted homogeneous germs provide Seifert manifolds.

In this subsection we will list those star–shaped graphs which are produced by unicuspidal curves with one Puiseux pair.

It is also worth mentioning, that the normalization of V_f (for any f where C is rational) has a very simple resolution graph: only one vertex with genus zero and Euler number $-d$. This graph can be compared with those obtained for ∂F listed below.

For the second motivation (of more analytic nature), see (22.10.5).

22.10.1. Assume that C is rational and unicuspidal of degree $d\geq 3$, and the equisingularity type of its singularity is given by the local equation $u^a+v^b=0$. The possible triples (d,a,b) are classified in [**7**].

In order to state this result, consider the Fibonacci numbers $\{\varphi_j\}_{j\geq 0}$ defined by $\varphi_0=0$, $\varphi_1=1$, and $\varphi_{j+2}=\varphi_{j+1}+\varphi_j$ for $j\geq 0$.

Then (d,a,b) $(1<a<b)$ is realized by a curve with the above properties if and only if it appears in the following list:

(a) $(a,b)=(d-1,d)$;
(b) $(a,b)=(d/2,2d-1)$, where d is even;
(c) $(a,b)=(\varphi_{j-2}^2,\varphi_j^2)$ and $d=\varphi_{j-1}^2+1=\varphi_{j-2}\varphi_j$, where j is odd and ≥ 5;
(d) $(a,b)=(\varphi_{j-2},\varphi_{j+2})$ and $d=\varphi_j$, where j is odd and ≥ 5;
(e) $(a,b)=(\varphi_4,\varphi_8+1)=(3,22)$ and $d=\varphi_6=8$;
(f) $(a,b)=(2\varphi_4,2\varphi_8+1)=(6,43)$ and $d=2\varphi_6=16$.

(a) is realized e.g. by the curve $\{x^d=zy^{d-1}\}$, (b) by $\{zy-x^2)^{d/2}=xy^{d-1}$. (c) and (d) appear in Kashiwara's list [**26**], while (e) and (f) were found by Orevkov in [**51**].

22.10.2. Now we list the graphs G^m for ∂F. The computations are straightforward, perhaps except the cases (c) and (d); for these ones we provide more details.

- **Case (a)**

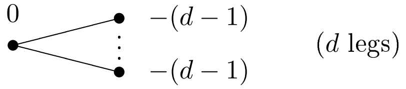

- **Case (b)**

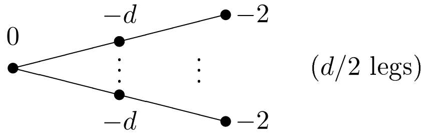

In the examples (a) and (b) the above 'normal forms' are *not* negative definite, hence the graphs cannot be transformed by plumbing calculus into a negative definite graph (without changing the orientation).

- **Case (c)** Let Γ be the minimal resolution graph of the Brieskorn isolated hypersurface singularity $\{u^a + v^b + w^d = 0\}$, where $(a, b, d) = (\varphi_{j-2}^2, \varphi_j^2, \varphi_{j-2}\varphi_j)$. This is a star–shaped graph, it can be determined in a standard way, e.g. by the cyclic covering algorithm of [**44**], or by the procedure described in [**52**]. Let $-\Gamma$ be Γ with opposite orientation (the sign of each Euler number is changed, and the edges are endowed with $\ominus$ —, however this last edge decoration modification can be omitted since Γ is a tree), and let v be its central vertex (which has genus decoration $g = (a-1)(b-1)/2$). Then (22.3) for G^m provides the graph:

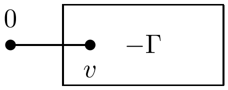

E.g., if $j = 5$, i.e. $(a, b, d) = (2^2, 5^2, 10)$, then the central fiber of G^m has genus [2] (and its Euler number is irrelevant), the graph has 8 legs, all of which are of length one. Five of the end–curves are decorated by 2, two of them by 5, and one by 0.

Notice that the 3–manifold ∂F is reducible: the irreducible components can be seen if we apply the 'splitting operation' to the unique 0–vertex. E.g.. in the above case of $j = 5$, we get 4 copies of $\overset{0}{\bullet}$, 2 copies of $\overset{5}{\bullet}$, and 5 copies of $\overset{2}{\bullet}$.

- **Case (d)** The graph G^m of ∂F is $\overset{d}{\bullet}$. This follows from the very special arithmetical properties of the Fibonacci numbers. In order to see this, we need to use the identities (for j odd)

$$\varphi_{j-2} \cdot \varphi_{j+2} = \varphi_j^2 + 1, \qquad \varphi_{j-2} + \varphi_{j+2} = 3\varphi_j. \tag{22.10.3}$$

Similarly as in the previous case, and following (22.3), we have to first determine the (minimal) resolution graph Γ of the Brieskorn singularity with coefficients (a, b, d). Notice that in this case these integers are pairwise relatively prime, hence the decorations of the three legs are determined by the (Hirzebruch–Jung) continued fraction expansions of the rational numbers ab/d, ad/b and bd/a (for more details, see e.g. [**18**, §22]). The point is that in our situation the identities (22.10.3) have the following congruences

$$\varphi_{j-2}\varphi_{j+2} \equiv 1 \ (mod\ \varphi_j) \qquad \varphi_{j\pm 2}\varphi_j \equiv -3 \ (mod\ \varphi_{j\mp 2}), \tag{22.10.4}$$

and $\varphi_{j\pm 2}$ is not divisible by 3. Hence, by a computation, Γ has the following shape: the central fiber has decoration -2 (and genus 0), one of the legs consists of $\varphi_j - 1$ (-2)–vertices, another has three vertices with decorations -2, -2, $-\lceil \varphi_{j\pm 2}/3 \rceil$ (where the first -2 vertex is connected to the central vertex), and a third leg has two vertices with decorations -3 and $-\lceil \varphi_{j\mp 2}/3 \rceil$, where the -3 vertex is connected to the central vertex.

By the procedure (22.3) we have to change the orientation and add one more vertex to the end-curve of the -2–string, which will be decorated by 1. Hence this new extended string can be contracted completely. After this contraction the central curve becomes a 1–curve. This generates 3 more blow–downs and a 0–chain absorption.

As an interesting phenomenon: the graph of the normalization of V_f is $\overset{-d}{\bullet}$. Hence the boundary of the Milnor fiber coincides with the link of the normalization with opposite orientation.

- **Case (e)**

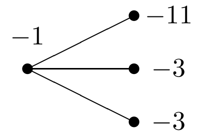

- **Case (f)**

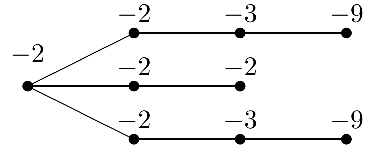

The normal forms in (e) and (f) are *negative definite*, a property which rather rarely happens. In particular, in both cases, ∂F is diffeomorphic (under a diffeomorphism which preserves orientation) with the link of a(n) (elliptic, not complete intersection) normal surface singularity.

22.10.5. Looking at the shapes and decorations of the above graphs, one can group them in four categories (a)–(b), (c), (d) and (e)–(f). This is compatible with some other groupings based on some analytic/combinatorial invariants of these curves, see [**7, 8**].

E.g., if $\pi : X \to \mathbb{P}^2$ is the minimal embedded resolution of $C \subset \mathbb{P}^2$, and $\bar{C}$ denotes the strict transform of C, then $\bar{C}^2 = d^2 - ab = 3d - a - b - 1$. In the above six cases this value is the following: it is positive for (a) and (b), it is zero for (c), it is -1 for (d), and -2 for (e) and (f).

Perhaps, the most striking 'coincidence' is that the cases (e)–(f) are the only cases when the logarithmic Kodaira dimension of $\mathbb{P}^2 \setminus C$ is 2 (for the first four cases it is $-\infty$), while from the point of view of the present discussion (e)–(f) are the only cases when ∂F is an irreducible Seifert 3–manifold, representable by a negative definite graph (which is not a lens space).

This suggests that the topology of ∂F probably carries a prestigious amount of analytic information about f.

§ 23. Line arrangements.

23.1. Assume that C is a projective line arrangement. We will use the notations of (10.2). Recall that $\#\mathcal{A}(\Gamma_{\mathcal{C}}) = \#\mathcal{A}(G) = d$, and *corank*$(A)_G = d-1$, cf. (22.4.7). Moreover, additionally we have $g(\Gamma_{\mathcal{C}}) = 0$, and the following identities:

23.1.1. The covering data of G over $\Gamma_{\mathcal{C}}$ is trivial, hence

$$c(G) = c(\Gamma_{\mathcal{C}}) = \sum_{j\in\Pi}(m_j - 1) - (d-1).$$

By (16.4.3),

$$2g(G) = \sum_{j\in\Pi}(m_j - 2)\big(\gcd(m_j, d) - 1\big).$$

23.1.2. **(Characteristic polynomial)** Since $\mathfrak{n}_w = \mathfrak{n}_e = 1$ for $w \in \mathcal{W}(\Gamma_{\mathcal{C}})$ and $e \in \mathcal{E}_{\mathcal{W}}(\Gamma_{\mathcal{C}})$, (22.5.1) via a computation transforms into

THEOREM 23.1.3. *Let $\{L_\lambda\}_{\lambda\in\Lambda}$ be an arrangement with $d = |\Lambda|$ lines and with singular points Π. Then the characteristic polynomial of the monodromy acting on $H_1(\partial F)$ is*

$$(t-1)^{|\Pi|} \cdot \prod_{j\in\Pi} (t^{(m_j,d)} - 1)^{m_j-2}.$$

23.1.4. **(Jordan blocks of $M_{\Phi,hor}$ and $M_{\Phi,ver}$)** Since $M'_{j,hor}$ is semisimple, from (22.6) we get

$$\#^2_\lambda M_{\Phi,hor} = \#^2_\lambda M_{\Phi,ver} = 0 \text{ for } \lambda \neq 1, \text{ and}$$

$$\#^2_1 M_{\Phi,hor} = \#^2_1 M_{\Phi,ver} = c(\Gamma_{\mathcal{C}}).$$

23.2. Examples.

EXAMPLE 23.2.1. **The generic arrangement.** Consider the generic arrangement: all the intersection points of the d lines are transversal. In this case there are $|\Pi| = d(d-1)/2$ intersection points, all with $m_j = 2$. Therefore, the characteristic polynomial is just $(t-1)^{|\Pi|}$.

A possible graph for ∂F can be constructed as follows.

Consider the complete graph $\mathfrak{G}$ with d vertices (i.e. any two different vertices are connected by an edge). Decorate all these vertices by -1. Put on any edge e of $\mathfrak{G}$ a new vertex with decoration $-d$. In this way, the edge e is 'cut' into two edges, decorate one of them by $\ominus$ (and do this with all the edges of $\mathfrak{G}$).

Notice that any (-1)–vertex is adjacent with $d-1$ vertices (all decorated by $-d$). Hence, if $d \leq 3$, this graph is not minimal, but otherwise in this way we get the 'normal form'. The graph has $(d-1)(d-2)/2$ cycles and $corank(A) = d-1$.

EXAMPLE 23.2.2. **The $\mathbf{A}_3$ arrangement.** Consider the arrangement from (10.2.1). The characteristic polynomial is $(t^3-1)^4 \cdot (t-1)^7$. The graph can be deduced easily from $\Gamma_{\mathcal{C}}$ (which is presented in (10.2.1)). There are 4 vertices with $g = 1$, 6 cycles and $corank(A)_G = d-1 = 5$.

EXAMPLE 23.2.3. **The pencil.** Assume that all the lines contain a fixed point. (E.g., $f = x^d + y^d$.) Then the characteristic polynomial is $(t-1)(t^d-1)^{d-2}$, and G^m is

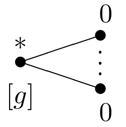

d legs and $g = (d-1)(d-2)/2$

In fact, $\partial F = \#_{(d-1)^2} S^2 \times S^1$.

EXAMPLE 23.2.4. Assume that $f = z(x^{d-1} + y^{d-1})$. Then the characteristic polynomial is $(t-1)^{2d-3}$, and G^m is

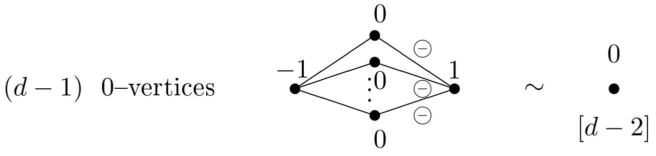

In particular, for any oriented surface S, the product $S \times S^1$ can be realized as ∂F.

23.3. The torsion of the integral homology $H_1(\partial F,\mathbb{Z})$. In general, even for homogeneous f, $H_1(\partial F,\mathbb{Z})$ might have nontrivial torsion. One may ask whether in the case of arrangements some non–trivial torsion elements exist. The interest in such a question is motivated by a conjecture which predicts that for arrangements $H_1(F,\mathbb{Z})$ has no torsion. Hence it is natural to attack this conjecture via the epimorphism $H_1(\partial F,\mathbb{Z})\to H_1(F,\mathbb{Z})$.

EXAMPLE 23.3.1. Assume that f is the generic arrangement with $d=4$. Then the torsion part of $H_1(\partial F,\mathbb{Z})$ is $\mathbb{Z}_4$.

Indeed, by (18.1.3), the torsion part of $H_1(\partial F,\mathbb{Z})$ is exactly the torsion part of $coker(A)_G$. Since the intersection matrix A is determined explicitly in (23.2.1), a computation provides the result.

In fact, for generic arrangements and larger d, the torsion part of $H_1(\partial F,\mathbb{Z})$ is even bigger. One can prove easily that $A\otimes\mathbb{Z}_d$ has corank $\geq (d^2-3d+4)/2$, which is considerably larger than $corank(A)=d-1$.

§ 24. The weight filtration of the mixed Hodge structure.

24.1. In this subsection we prove that if f is homogeneous then $H^*(\partial F)$ carries a natural Mixed Hodge structure, which satisfies Conjecture (21.1.3).

Indeed, assume that f is homogeneous of degree d. Let $C=\{f=0\}\subset\mathbb{P}^2$ be the projective curve as above. Recall that $H_1(\mathbb{P}^2\setminus C,\mathbb{Z})=\mathbb{Z}^{|\Lambda|}/(d_1,\ldots,d_{|\Lambda|})$. Therefore, the representation

$$\pi_1(\mathbb{P}^2\setminus C,*)\xrightarrow{ab}H_1(\mathbb{P}^2\setminus C,\mathbb{Z})\xrightarrow{\sigma}\mathbb{Z}_d,$$

where ab is the Hurewicz epimorphism and $\sigma([a_1,\ldots,a_{|\Lambda|}])=\sum a_\lambda$, is well–defined, is onto, and it provides a cyclic covering $\pi:Y\to\mathbb{P}^2$, branched along C. Moreover, $F:=\pi^{-1}(\mathbb{P}^2\setminus C)$ is a smooth affine variety which can be identified with the (open) Milnor fiber of f, cf. (22.4).

The singularities of Y are isolated and are sitting above the singular points of C: if $\{f_j(u,v)=0\}$ is the local equation of a singular point of C, then its cyclic covering $\{w^d=f_j(u,v)\}$ is the local equation of the corresponding singular point in Y above it. Let $r:\widetilde{Y}\to Y$ be the minimal good resolution of the singularities of Y and set $\widetilde{\pi}:=\pi\circ r:\widetilde{Y}\to\mathbb{P}^2$. Then $\widetilde{Y}$ is smooth and $F=\widetilde{Y}\setminus\widetilde{\pi}^{-1}(C)$ is the complement of the normal crossing curve configuration $\widetilde{\pi}^{-1}(C)$. Moreover, the dual graph associated with this curve configuration is exactly $-G$, where G is the graph provided by the Main Algorithm, cf. (22.3). Therefore, for any sufficiently small tubular neighbourhood T of $\widetilde{\pi}^{-1}(C)$, $\partial F=-\partial T$, cf. (22.4), and the natural mixed Hodge structure of $H_1(\partial T)$ transports by this isomorphism into a natural mixed Hodge structure of $H_1(\partial F)$. This combined with (18.2.8)(c) (or with [**20**, (6.9)]) shows that this mixed Hodge structure satisfies Conjecture (21.1.1), hence its dual structure in cohomology satisfies Conjecture (21.1.3).

REMARK 24.1.1. As we already mentioned, the oriented handle absorption modifies the integers $c(G^m)$, $g(G^m)$ and $corank(A)_{G^m}$, and this can happen even in the homogeneous case. E.g., if $f=z(xy+z^2)$, cf. (22.9)(3c), one might use the operation (cf. (18.1.7)):

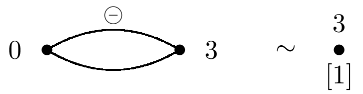

$c(G^m)$, $2g(G^m)$ and $corank(A)_{G^m}$ read from the left hand side graph provide the ranks $Gr^W_\bullet H_1(\partial F)$, while the right hand side graph does not have this property. (In particular, the topological methods from (28.1) or (28.2) are perfectly good to determine the oriented 3–manifold ∂F, or even the characteristic polynomial of its algebraic Milnor monodromy, but they are not sufficiently fine to recover the weight filtration of the mixed Hodge structure of $H_1(\partial F)$.)

EXAMPLE 24.1.2. **The weight filtration of the MHS of $H_1(\partial F)$ is not a topological invariant.**

Consider the homogeneous function $f = xy(xy+z^2)$ of degree $d=4$. Its graph G under 'strictly reduced calculus' (cf. (5.1.9)) (i.e. under reduced calculus excluding R5) can be transformed into

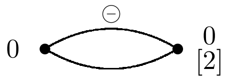

In particular, $c(G)=1$, $2g(G)=4$ and $corank(A)_G = 2$, and these numbers equal the ranks of $Gr^W_\bullet H_1(\partial F)$.

Next, consider the homogeneous function $f = z(x^4+y^4)$ of degree $d=5$. For its graphs G see (23.2.4); hence $c(G)=3$, $2g(G)=0$ and $corank(A)_G = 4$.

Note that both graphs, using R3 and R5, can be transformed into 0 • [3] , hence ∂F is (orientation preserving) diffeomorphic with the product of S^1 with a surface of genus 3. In particular, the C^∞ type of ∂F does not determine the weight filtration of $H_1(\partial F)$. (This phenomenon might happen with the links of isolated singularities of higher dimension as well, see [**67**].)

Additionally, the two characteristic polynomials of the algebraic monodromies acting on $H_1(\partial F)$ associated with the above two examples are $(t^2+1)^2(t-1)^3$ and $(t-1)^7$ respectively. Hence, from ∂F one cannot, in general, read the characteristic polynomial. (Note that the multiplicity of f can neither be read!)

EXAMPLE 24.1.3. In fact, the Milnor fibers of the above two functions treated in (24.1.2) are also different. Indeed, let S_g denote the oriented closed surface of genus g. Then for $f = xy(xy+z^2)$ the Milnor fiber is diffeomorphic to $[0,1]\times S^1 \times (S_1 \setminus 2 \text{ points})$ (cf. (28.1)), while for $f = z(x^4+y^4)$, the Milnor fiber is $[0,1]\times S^1\times (S_0 \setminus 4 \text{ points})$ (cf. § 26). (Although these spaces are not homeomorphic, in fact, they are homotopic.)

24.2. The weight filtration on $H_1(\partial F)$ is compatible with the eigenspace decomposition of the algebraic monodromy action. Indeed, from the computations of section § 22 and (19.2.10)(a), for the generalized eigenspaces one has:

(24.2.1)
$$\dim Gr^W_i(H_1(\partial F)_{\lambda=1}) = \begin{cases} corank(A)_G = corank(A)_{\Gamma_\mathcal{C}} = |\Lambda|-1 & \text{if } i=-2,\\ 2g(\Gamma_\mathcal{C}) & \text{if } i=-1,\\ c(\Gamma_\mathcal{C}) & \text{if } i=0,\end{cases}$$

and

$$\dim Gr^W_i(H_1(\partial F)_{\lambda\neq 1}) = \begin{cases} 0 & \text{if } i=-2,\\ 2g(G)-2g(\Gamma_\mathcal{C}) & \text{if } i=-1,\\ c(G)-c(\Gamma_\mathcal{C}) & \text{if } i=0.\end{cases} \tag{24.2.2}$$

Recall that the algebraic monodromy action is finite, hence the weight filtration on the subspaces $H_1(\partial F)_{\lambda=1}$ and $H_1(\partial F)_{\lambda\neq 1}$ *cannot* be the monodromy weight filtration associated with the monodromy action.

CHAPTER X

More examples.

§ 25. Cylinders of plane curve singularities: $f = f'(x, y)$

25.1. Using the Main Algorithm. The graph G. Assume that $f(x, y, z) = f'(x, y)$, as in (9.1). Assume that f' has r local irreducible components, let μ be its Milnor number.

If we take $g(x, y, z) = z$ then the graph $\Gamma_{\mathcal{C}}$ is determined in (9.1). Let

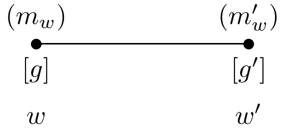

be an edge e of the minimal embedded resolution graph Γ' of f'. Then using the recipe of (9.1), the transformation step from (12.1.2), and the algorithm (12.3), this edge will be replaced in G by $\mathfrak{n}_e = (m_{w_1}, m_{w_2})$ edges with the next decorations (compare also with (14.1.1)):

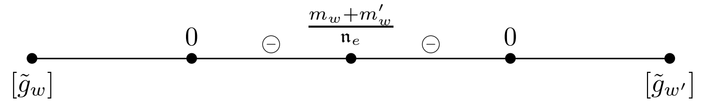

Above w one has $\mathfrak{n}_w$ vertices in G, where $\mathfrak{n}_w$ is the greatest common divisor of m_w and all the multiplicities of the adjacent vertices of w in Γ'. Their genus decoration $\tilde{g}_w$ is given by

$$\mathfrak{n}_w(2 - 2\tilde{g}_w) = (2 - \delta_w)m_w + \sum_{e \text{ adjacent to } w} \mathfrak{n}_e.$$

There is a similar picture for edges supporting arrowheads. Notice that $\#\mathcal{A}(G) = r$.

In general, G is not a tree, the number $c(G)$ of its cycles is given by

$$1 - c(G) = \sum_{w \in \mathcal{W}(\Gamma')} \mathfrak{n}_w - \sum_{e \in \mathcal{E}_w(\Gamma')} \mathfrak{n}_e. \tag{25.1.1}$$

After executing all the 0–chain absorptions we get

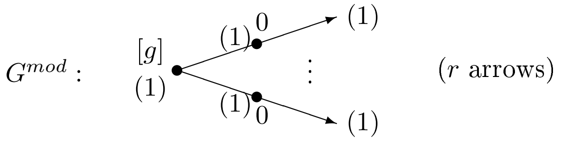

Above the Euler number of the central vertex is missing, since it is irrelevant. The genus g is determined as a sum provided by the 0–chain absorption formula: $2g = 2c(G) + 2\sum_{w \in \mathcal{W}(\Gamma')} \mathfrak{n}_w \tilde{g}_w$, which via the above identities is equal to $2 - r - \sum_w (2 - \delta_w)m_w$. Hence, by A'Campo's formula for μ, we get

$$g = (\mu + 1 - r)/2.$$

25.1.2. Clearly, the fiber F_Φ is the same as the Milnor fiber F' of f'. The vertical monodromy of F_Φ is isotopic to the identity (this follows either from (20.3.1), or by the observation that $\Delta_\Phi = \{c = 0\}$). Therefore, from (16.4.6) we get

$$\mu = 2g(G) + 2c(G) + r - 1. \tag{25.1.3}$$

From the above diagram of G^{mod}, by (18.1.2) we get dim $H_1(\partial F) = 2g(G^{mod}) + c(G^{mod}) + corank(A)_{G^{mod}} = (\mu + 1 - r) + 0 + (r - 1) = \mu$. Hence, again by (18.1.2) applied for G, we have

$$\mu = 2g(G) + c(G) + corank(A)_G. \tag{25.1.4}$$

Then, from (25.1.3), (25.1.4) and (18.1.5) we obtain

$$\begin{cases} corank(A)_G = c(G) + r - 1, \\ corank(A, I)_G = c(G) + r. \end{cases} \tag{25.1.5}$$

This shows that the upper bounds from (18.2.1) can be realized.

In fact, $c(G)$ has an intrinsic meaning (hence, by (25.1.5) $corank(A, I)_G$ and $corank(A)_G$ too): the expression (25.1.1) combined with [**18**, (14.1)], or with [**44**, (3.20)], gives that

(25.1.6) $c(G) =$ the number of 2–Jordan blocks of the monodromy of f'.

25.1.7. **The Collapsing Algorithm. The graph $\widehat{G}$.** In fact, if we delete the arrow-heads and multiplicities of G^{mod} from the previous subsection, we get $\widehat{G}$ (cf. § 14) with $c(\widehat{G}) = 0$ and $corank(A)_{\widehat{G}} = r - 1$:

$\widehat{G}$:

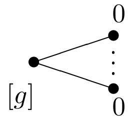

(r legs and $g = (\mu + 1 - r)/2$)

By 'splitting operation' (R6 in the plumbing calculus of [**49**, (2.1)]), we get another possible (non-connected) plumbing graph for ∂F: the disjoint union of μ vertices (without any edges), all of them decorated with Euler number and genus zero. In other words:

$$\partial F = \#_\mu S^2 \times S^1.$$

Although this fact can be deduced by other methods too (see e.g. subsection (25.2)), the graph of G associated with the open book decomposition of $g = z$ (or any graph G computed in this way associated with any germ g) is a novelty of the present method. (Obviously, for different germs g, one might get different open book decompositions of ∂F, all of them determined by the above algorithm.)

25.1.8. **The characteristic polynomial.** Since $M_{\Phi,ver} = id$, the characteristic polynomial $P_{H_1(\partial F)}$ of the Milnor monodromy acting on $H_1(\partial F)$ can be computed from (16.2.10)(a). It turns out that this expression coincides with the expression of the characteristic polynomial of the monodromy of the isolated plane curve singularity f' provided by A'Campo.

25.2. Comparing with a different geometric construction. Let F' be the Milnor fiber of f'. In the above situation it is easy to see (since $\Delta_\Phi = \{c = 0\}$) that $F = F' \times D$, where D is a disc. In particular, we also have the following geometric description for ∂F:

$$\partial F = F' \times S^1 \ \cup_{\partial F' \times S^1} \ \partial F' \times D. \tag{25.2.1}$$

Using the Mayer–Vietoris exact sequence of this decomposition, one gets that $H_1(\partial F, \mathbb{Z}) = H_1(F', \mathbb{Z})$. Since the monodromy acts on this sequence, we also obtain that the monodromy on $H_1(\partial F, \mathbb{Z})$ is the same as the monodromy of the plane curve singularity f' acting on $H_1(F',\mathbb{Z})$. In particular, in this way we get the Jordan block structure of the monodromy acting on $H_1(\partial F,\mathbb{Z})$ too.

This shows that, in general, the *algebraic monodromy acting on* $H_1(\partial F)$ *is not finite* (take e.g. for f' the germ from (9.1.1)).

25.3. The mixed Hodge structure on $H_1(\partial F)$. We expect that (once on $H_1(\partial F)$ one defines a natural mixed Hodge structure), the natural inclusion $F'\subset\partial F$ of (25.2), which induces isomorphisms $H_1(F')\to H_1(\partial F)$ and $H^1(\partial F)\to H^1(F')$, will induce, in fact, isomorphisms of mixed Hodge structures. Here we prefer to treat the (more traditional) cohomological case.

The mixed Hodge structure of $H^1(F')$ is Steenbrink's MHS defined on the vanishing cohomology of the plane curve singularity f' [**65, 66**]. Its weight filtration is compatible with the generalized eigenspace decompositions. According to the general theory, $H^1(F')_{\lambda=1}$ is pure of weight 2, and it has rank $r-1$. On the other hand, $H^1(F')_{\lambda\neq 1}$, in general, has weights 0, 1 and 2, and the weight filtration is the monodromy weight of the algebraic monodromy. In particular, the ranks of $Gr^W_0(H^1(F')_{\lambda\neq1})$ and $Gr^W_2(H^1(F')_{\lambda\neq1})$ are equal, and they agree with the number of 2–Jordan blocks of the monodromy (recall that the monodromy has no 2–blocks with eigenvalue one). Hence, this rank is exactly $c(G)$ by (25.1.6). In particular, the rank of $Gr^W_0(H^1(F'))$ is $c(G)$, while the rank of $Gr^W_2(H^1(F'))$ is $c(G)+r-1=corank(A)_G$, cf. (25.1.5). Hence, by dimension computation, we get that the remaining $Gr^W_1(H^1(F'))$ has rank $2g(G)$. This supports Conjecture (21.1.3).

This information about the ranks of $Gr^W_\bullet(H^1(F'))$ cannot be read from $\widehat{G}$; $\widehat{G}$ contains information about r and μ only.

§ 26. f of type $zf'(x,y)$.

In this section we assume that $f(x,y,z)=zf'(x,y)$, where f' is an isolated plane curve singularity.

26.1. A geometric representation of F and ∂F. Similarly as in the case of cylinders (or, in the case of 'composed singularities' [**41**]), consider the ICIS $\bar\Phi:(\mathbb{C}^3,0)\to(\mathbb{C}^2,0)$ given by $\bar\Phi=(f'(x,y),z)$. By similar notations as in § 4, the Milnor fiber F of f is

$$F=B^3_\epsilon\cap\bar\Phi^{-1}(\{cd=t\}\cap D^2_\eta),$$

where $0<t\ll\eta\ll\epsilon$. For any $\eta>0$ consider the disc $D_\eta:=\{c:\,|c|\leq\eta\}$. Then, by isotopy, the above representation of F can be transformed into

$$F=B^3_\epsilon\cap\bar\Phi^{-1}(D_\eta\times\{t\}\setminus D^\circ_{\eta'}\times\{t\}),$$

for some $0<\eta'\ll\eta$. From this one can eliminate the variable z, namely, if B^2_ϵ is the ϵ–ball in the (x,y)–plane, then

$$F=B^2_\epsilon\cap(f')^{-1}(D_\eta\setminus D^\circ_{\eta'}). \tag{26.1.1}$$

One also verifies that the monodromy on F is (isotopic to) the identity (it is the rotation by 2π of the disc D_η). This provides a geometric picture for ∂F as well, and proves that its monodromy action is trivial.

26.1.2. From (26.1.1) one can read the following plumbing representation for ∂F. In order to understand the geometry behind the statement, let us analyze different constituent parts of ∂F. Notice that $B^2_\epsilon\cap(f')^{-1}(\partial D_\eta)$ can be identified with the complement of the link of f' in S^3. Similarly, $B^2_\epsilon\cap(f')^{-1}(\partial D_{\eta'})$ is the same, but with opposite orientation. Moreover, they are glued together along their boundaries in a natural way.

Notice also that projecting $D_\eta \setminus D_{\eta'}$ to $S^1 = \partial D_\eta$, and composing with f' we get a map $\partial F \to S^1$ which is a locally trivial fibration. Hence, ∂F fibers over S^1.

26.1.3. Therefore, the plumbing graph can be constructed as follows.

Take the (minimal) embedded resolution graph of $(\mathbb{C}^2, V_{f'})$. This has r arrows, where r is the number of irreducible components of f'. Keep all the Euler numbers and delete all the multiplicity decorations. Let the schematic form of the result be the next 'box':

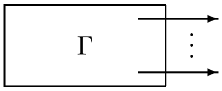

Then a possible plumbing graph for ∂F is:

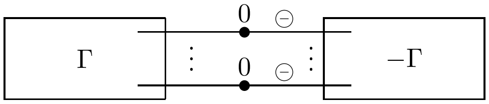

Here, in $-\Gamma$, we change the sign of all Euler numbers and edge–decorations. (put $\ominus$ on edges).

Notice that any 3–manifold M obtained in this way is orientation preserving diffeomorphic with the manifold obtained by changing its orientation: $M \approx -M$.

The statement about the above shape of the graph can be tested by the examples listed in (9.2) as well.

EXAMPLE 26.1.4. The first (and simplest) example already was considered in (23.2.4), when $f' = x^{d-1} + y^{d-1}$. Its graph produced by the Main Algorithm is the first diagram of (23.2.4) supporting (together with the characteristic polynomial computation) the above statements.

EXAMPLE 26.1.5. Assume that $f = z(x^2 + y^3)$ and take g to be a generic linear form. The graph $\Gamma_{\mathcal{C}}$ is given in (9.2.1). Running the algorithm and reduced calculus, a possible G^m is

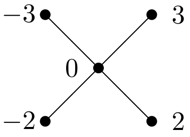

which is compatible with the predicted form from (26.1.3).

REMARK 26.1.6. This family might also serve as a testing family for some of the characteristic polynomial formulae (16.2.10) (regarding the vertical monodromies $M'_{j,ver}$, which, in fact, are much harder to test).

Indeed, if $f = zf'$ and g is a generic linear function, then $s = 1$, $\Sigma = \Sigma_1 = \{x = y = 0\}$, hence $d_1 = 1$. Moreover, the Milnor fiber F'_1 of the transversal type can be identified with the Milnor fiber of f' (in two variables). Since $\{f'e^{i\alpha} = \delta\} = \{f' = \delta e^{-i\alpha}\}$, we get that the the vertical monodromy of F'_1 coincides with the inverse of Milnor monodromy acting on the Milnor fiber of f'. Hence, the characteristic polynomial of $M'_{1,ver}$ (determined by (16.2.10)(c)) should coincide with the characteristic polynomial of f' provided by the classical A'Campo formula. The interested reader is invited to verify this on all the available graphs $\Gamma_{\mathcal{C}}$.

26.1.7. It is amazing in this computation that, although the graph $\Gamma_{\mathcal{C}}$ shows no symmetry, after running the algorithm and calculus the output graph has the symmetry (up to orientation) predicted in (26.1.3). The same is happening in the example (26.1.4), the starting graph $\Gamma_{\mathcal{C}}$ is not symmetric, in fact the two corresponding parts are rather different, codifying two different geometric situations, nevertheless after calculus we get the two parts represented by Γ and $-\Gamma$.

To construct a resolution r which produces Γ is rather natural (see e.g. the the case of cylinders), but to get a resolution r which (or part of it) produces $-\Gamma$ in a natural way, is very tricky. But, in fact, this is what $\Gamma_{\mathcal{C}}$ does: a part of it produces Γ, another part of it produces $-\Gamma$. This anti–duality is still a mystery for the authors. This shows how hard it is to recognize and follow global geometrical properties by manipulating (local) equations/resolutions.

Remark 26.1.8. Notice that if $f' = x^a + y^b$, then in the graph of (26.1.3) all the 0–vertices can be eliminated by 0–chain or handle absorption, hence we get a star–shaped graph (with four legs and central vertex with genus $\gcd(a,b)-1$). In particular, ∂F has a Seifert structure.

§ 27. The $T_{*,*,*}$–family.

27.1. The series $T_{a,\infty,\infty}$. We start our list of examples with the series associated with $T_{\infty,\infty,\infty}$, where $T_{\infty,\infty,\infty}$ denotes the germ $f = xyz$. This germ was already clarified (either as an arrangement or by the algorithm of § 26); next we will consider the series $T_{a,\infty,\infty}$ with one–parameter $a \geq 2$ given by $f = z^a + xyz$. For g we take the generic linear function.

The case $a = 2$ can be rewritten as $z^2 = x^2y^2$ and its graph $\Gamma_{\mathcal{C}}$ is given in (9.3.2)(CASE 1). The case $a = 3$ is treated in (22.9)(3c), the general $a > 3$ in (9.4). The Main Algorithm provides for the boundary of the Milnor fibre ∂F the graph

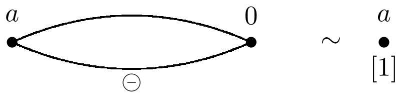

27.2. The series $T_{a,2,\infty}$. Running the Main Algorithm (and calculus) for the graphs of (9.4.2) (see also (9.3.3)), we get for ∂F the plumbing graph:

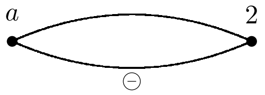

We expect that ∂F for $T_{a,b,\infty}$ ($f = x^a + y^b + xyz$) is given by the plumbing graph:

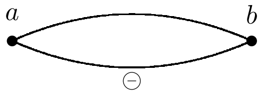

§ 28. f of type $\tilde{f}(x^a y^b, z)$. Suspensions.

28.1. f of type $\tilde{f}(xy, z)$. First, we sketch a geometric construction which provides ∂F and its monodromy, provided that $f(x,y,z) = \tilde{f}(xy,z)$, where $\tilde{f}$ is an isolated plane curve singularity in variables (u,z).

We will use the following notations: $\tilde{F} = \{\tilde{f} = \eta\}$ is the Milnor fiber and $\tilde{\mu}$ the Milnor number of $\tilde{f}$. Define I as zero if u is a component of $\tilde{f}$, otherwise I denotes the intersection multiplicity $(\tilde{f}, u)_0$ at the origin. Set $\Delta := \tilde{F} \cap \{u = 0\}$; then clearly $\#\Delta = I$.

Next, consider the Morse singularity $h:(\mathbb{C}^2,0)\to(\mathbb{C},0)$, $h(x,y)=xy$. Then the Milnor fiber F of f can be reproduced via the projection $\bar\Phi:(\mathbb{C}^3,0)\to(\mathbb{C}^2,0)$ given by $(x,y,z)\mapsto(h(x,y),z)=(u,z)$. Indeed, $\bar\Phi$ maps F onto $\tilde F$. The fibers of $\bar\Phi$ are as follows: above generic points of $\tilde F$ we have the Milnor fiber $F_h=S^1\times[0,1]$ of h, while over the special points $P\in\Delta$ we have the contractible central fiber $D\vee D$ of h.

Hence, ∂F decomposes into two parts, one of them is $(S^1\sqcup S^1)\times\tilde F$, while the other is $\bar\Phi^{-1}(\partial\tilde F)$, which is a locally trivial fiber bundle over $\partial\tilde F$ with fiber $F_h=S^1\times[0,1]$. The monodromy of this bundle is given by the variation map of $\bar\Phi$, hence it is the composition of I Dehn twists (corresponding to the variation maps around the Morse points P_i). Therefore, if we define the 'double of $\tilde F$' as $d\tilde F:=\tilde F\sqcup_{\partial\tilde F}(-\tilde F)$, then ∂F is an S^1–bundle over $d\tilde F$: two trivial copies of $S^1\times\tilde F$ are glued along $\bar\phi^{-1}(\partial\tilde F)$ so that the Euler number of the resulting S^1–bundle is I.

Notice that the genus of $d\tilde F$ is exactly $\tilde\mu$, hence:

$$\partial F \textit{ is given by the plumbing graph} \qquad \overset{I}{\underset{[\tilde\mu]}{\bullet}}$$

In particular, any S^1–bundle with arbitrary genus and non–negative Euler number can be realized as ∂F (and any such bundle might have many realizations by rather different singularities).

EXAMPLE 28.1.1. If $f=z^a+xyz$ as in (27.1), then $\tilde F=\{z^a+uz=\eta\}$ $(0<\eta\ll 1)$ and $\Delta=\{u=0,\ z^a=\eta\}$. Then $\tilde F$, via the projection $(u,z)\mapsto z$, is diffeomorphic with the annulus $A:=\{x:\eta_1\leq|z|\leq\eta_2\}$, where $\eta_1<\sqrt[a]{\eta}<\eta_2$, and by this identification its special points from Δ are $\cup_{i=1}^a P_i=\{z^a=\eta\}$. Notice that $d\tilde F$ is a torus. Moreover, the monodromy is the rotation of A, hence it is isotopic to the identity. In particular, we get (a fact compatible with (27.1)):

$$\partial F \textit{ is the torus bundle} \quad \overset{a}{\underset{[1]}{\bullet}} \quad \textit{with trivial monodromy.}$$

28.1.2. More generally, in the situation of (28.1), the monodromy on ∂F is induced by the monodromy of $\tilde f$, hence if $P_{\partial F}$ (resp. $P_{\tilde f}$) denotes the characteristic polynomial of the algebraic monodromy acting on $H_1(\partial F)$ (resp. $H_1(\tilde F)$), then

(28.1.3)
$$P_{\partial F}(t)=\big(P_{\tilde f}(t)\big)^2\cdot(t-1)^{1-sign(I)}$$

where $sign(I)$ is 1 for $I>0$ and zero for $I=0$.

28.1.4. The above result can be applied for $f=xyz$, $f=z(z^2+xy)$, $f=xy(z^2+xy)$ and $f=z^a+x^ky^k$, cases which can be compared with (22.9)(3e), (3c), (4b') or (4c'). Moreover, (28.1.3) can also be compared with the formula (19.2.7) valid for the characteristic polynomial. But, definitely, the interested reader might take an arbitrary germ $\tilde f$ to test the result. It is interesting to note that even if $\tilde f$ has many Puiseux pairs (hence its embedded resolution graph has many rupture vertices), ∂F is still Seifert, in fact, it is an S^1–bundle.

28.1.5. The above construction provides the structure of the Milnor fiber F as well: one may extract from it important information, such as the Euler characteristic, zeta–function of the monodromy, etc.

28.2. f of type $\tilde f(x^ay^b,z)$. Assume now that a and b are two positive relative prime integers. Then, the discussion of (28.1) can be modified as follows. Fix any isolated plane curve singularity $\tilde f(u,z)$, and replace h by $u=h(x,y):=x^ay^b$ in order to get $f := \tilde{f} \circ \bar{\Phi}$. Then all the arguments of (28.1) remain valid with the following modification.

The difference is that in the case $h = xy$, $\bar{\Phi}$ restricted on ∂F is a trivial fibration above any small neighbourhood of any point of Δ. In the new situation of $h = x^a y^b$, above a small neighbourhood of a point P of Δ, $\bar{\Phi}|_{\partial F}$ is *not* a fibration; in fact, in ∂F two special S^1–fibers appear above P. One of them has the same local neighbourhood (Seifert structure) as $\{x = 0\}$ in $S^3 = \{|x|^2 + |y|^2 = 1\}$ with S^1–fibers/orbits cut out by the family $x^a y^b$ =constant; the other has local behaviour as $\{y = 0\}$ in the same space. These two local Seifert neighbourhoods in S^3 are well–understood, they are guided by the continued fractions of a/b, respectively b/a.

Therefore, we get the following result:

Proposition 28.2.1. *Let $\tilde{f}(u, z)$ be an isolated plane curve singularity, and a and b two positive relative prime integers. Then ∂F associated with $f = \tilde{f}(x^a y^b, z)$ is a Seifert 3–manifold whose (minimal) star–shaped plumbing graph can be constructed as follows:*

(i) The central vertex has genus $\tilde{\mu}$ (=the Milnor number of $\tilde{f}$) and Euler number I (where I is zero if $u|\tilde{f}$, otherwise $I = (\tilde{f}, u)_0$).

(ii) Let $a/b = [p_0, p_1, \dots, p_s]$, respectively $b/a = [q_0, q_1, \dots, q_t]$ be the Hirzebruch continued fraction expansions of a/b and b/a with $p_0, q_0 \geq 1$, $p_i \geq 2$ for $i \geq 1$ and $p_j \geq 2$ for $j \geq 1$. Then the graph has $2I$ legs (with all vertices having genus–decoration zero). I strings have length s, the vertices are decorated by Euler numbers $p_1, \dots, p_s$ such that the vertex decorated by p_s is glued to the central vertex; while the other I legs are strings decorated by Euler numbers $q_1, \dots, q_t$, and the q_t–vertex is glued to the central vertex.

If $b = 1$ then the first set of I legs is empty, if $a = 1$ then the second set of I legs is empty. (If $a = b = 1$ we recover (28.1), in which case the graph has no legs.)

(iii) The orbifold Euler number of the Seifert 3–manifold is $\frac{I}{ab} \geq 0$.

(iv) The characteristic polynomial of monodromy action on $H_1(\partial F)$ is

$$P_{\partial F}(t) = \big(P_{\tilde{f}}(t)\big)^2 \cdot (t-1)^{1-sign(I)}.$$

Proof. We need to prove only *(iii)*. For this use the fact that for any a and b one has:

$$\frac{[p_1, \dots, p_{s-1}]}{[p_1, \dots, p_s]} + \frac{[q_1, \dots, q_{t-1}]}{[q_1, \dots, q_t]} = 1 - \frac{1}{ab}.$$

□

Example 28.2.2. If we take $\tilde{f} = z^n + u^d$, then $f = z^n + x^{da} y^{db}$, $\tilde{\mu} = (n-1)(d-1)$ and $I = n$. In this way we recover the main result of [**35**].

See also (12.5.12) for an explicit example determined via $\Gamma_{\mathcal{C}}$.

The reader can also verify that the graphs $\Gamma_{\mathcal{C}}$ from (9.3) produce compatible answers via the main algorithm.

Remark 28.2.3. In (28.2.1), if the total number of legs is less than two and $\tilde{\mu} = 0$, then we get a lens space. In particular the graph (a posteriori) will have no central vertex. E.g., take $z^2 = xy^2$. Then $\tilde{f} = z^2 - u$, hence $I = 2$ and $\tilde{\mu} = 0$. Thus we have to glue to a vertex (with Euler number 2) two other vertices, both decorated by 2. Hence, ∂F is the lens space $L(4, 1)$, which can also be represented by a unique vertex decorated by -4; cf. (12.5.9).

CHAPTER XI

Peculiar structures on ∂F. Open problems.

§ 29. Contact structures. Triple product. Resonance varieties

29.1. Contact structures. Recently, there is an intense activity in the theory of contact structures of 3–manifolds. A central place is occupied by links of normal surface singularities: by the classification of their (tight) contact structures and the classification of the corresponding Stein fillings. In the case of normal/isolated surface singularities, the analytic structure of the singularity induces a *canonical* contact structure on the link. Moreover, all the Milnor open books (i.e. open book decompositions associated with analytic map–germs) support (in the sense of Giroux, cf. [**23**]) exactly this contact structure (for details, see [**11**]). In fact, [**11**] also proves that this canonical contact structure can be recovered from the topology of the link, and can be topologically identified among all the contact structures. If the singularity is smoothable, then all the Milnor fibers (smoothings) appear as natural Stein fillings of the canonical contact structure (together with the resolution of the singularity).

One may ask the validity of similar properties in the present situation, i.e. about ∂F associated with a non-isolated singularity f. Although in this case the link is not smooth, hence from the point of view of theory of 3–manifolds it is not interesting, we can concentrate on the boundary of the Milnor fiber. We can ask about the classification of its (tight) contact structures. Moreover, the Milnor fiber, as a Stein manifold with boundary, induces a contact structure on ∂F. A crucial question is to characterize and identify this structure among all the contact structures. (Notice also that all the open book decompositions of ∂F cut out by germs g considered in this article (namely the pair (f,g) is an ICIS) support the very same contact structure induced by F (cf. [**10**]).)

The point we wish to emphasize is that the new geometric situation (considering non–isolated f instead of isolated singularities) introduces a new set of *3–manifolds*, a new set of *contact structures* together with a new set of *Stein fillings* realizable by singularity theory. Their classification is of major interest.

We would like to stress that if a 3–manifold appears as ∂F for some non–isolated f as in the present work, and also as a singularity link (i.e. if it can be represented by a connected negative definite plumbing graph), the contact structure induced by the Milnor fiber F (let us call it 'Milnor–fiber contact structure'), and the canonical contact structure (as singularity link) are, in general, non–isotopic.

The simplest proof of this statement is by comparison of the Chern classes of the corresponding structures in $H_1(\partial F,\mathbb{Z}) = H^2(\partial F,\mathbb{Z})$ (already noticed in [**10**]). The Chern class of the Milnor–fiber contact structure is zero, since F is (stably) parameterizable. On the other hand, the Chern class of the canonical contact structure is the class of the canonical cycle in $H_1(\partial F,\mathbb{Z})$. In particular, this class is zero if and only if the singularity/link is numerical Gorenstein (see e.g. [**43**] for the terminology). In particular, if ∂F can be realized by a negative definite graph which is not numerical Gorenstein, then the two contact structures are different.

This is happening in the case of all lens spaces which are not A_n–singularity links, and also in (22.10), cases (e)-(f).

29.2. Triple product. For any oriented 3–manifold Y, the cohomology *ring* $H^*(Y,\mathbb{Z})$ of Y carries rather subtle information. This can be reformulated in the *triple product*, induced by the cup product $\mu_Y \in \Lambda^3 H'$ given by $\mu_Y(a,b,c) = \langle a\cup b\cup c, [Y]\rangle$ for $a,b,c\in H^1(Y,\mathbb{Z})$ (and H' is the dual of $H^1(Y,\mathbb{Z})$).

Sullivan in [**70**] proved that for any pair (H,μ) (where H is a finitely generated free abelian group, and $\mu\in\Lambda^3H'$), there exists a 3–manifold Y with $H^1(Y)=H$ and $\mu_Y=\mu$. Moreover, for any singularity link, μ is trivial. In fact, by the proof of Sullivan, if Y can be represented by a plumbing graph with non–degenerate intersection form, then the cup–product $H^1(Y)\otimes H^1(Y)\to H^2(Y)$ is trivial.

In our situation, however, $Y=\partial F$ might have non-trivial μ_Y; see e.g. the example of $S^1\times S^1\times S^1$ realized by $f=xyz$. It would be very interesting to determine the triple product for all the 3–manifolds appearing as ∂F, and connect it with other singularity invariants. For partial results see (19.2.10) and (19.2.18).

29.3. Resonance varieties. The dth *resonance variety* of a space X is the set $\mathcal{R}_d(X)$ of cohomology classes $\lambda\in H^1(X,\mathbb{C})$ for which there is a subspace $W\subset H^1(X,\mathbb{C})$, of dimension $d+1$, such that $\lambda\cup W=0$. The resonance varieties of arrangements were introduced by Falk in [**22**], and since then they play a central role in several parts of mathematics. Their relationship with characteristic varieties is crucial.

Since the cup–product on $H^1(\partial F)$ might be non–trivial, and rather subtle, it would be again of major interest to determine the resonance varieties of ∂F and connect them with other singularity invariants.

29.4. Relation with the homology of the Milnor fiber. From the cohomology long exact sequence of the pair $(F,\partial F)$, one gets a monomorphism

$$H^1(F,\mathbb{Z})\hookrightarrow H^1(\partial F,\mathbb{Z}),$$

which is compatible with the monodromy action. In particular, we get an upper bound $b_1(F)\leq \mathit{rank}\, H^1(\partial F)$ for the first Betti number $b_1(F)$ of F. In fact, the characteristic polynomial of the monodromy acting on $H^1(F)$ should divide the characteristic polynomial of $H^1(\partial F)$, which is expressed combinatorially in (23.1.2).

This is important, since, in general, the behaviour of $b_1(F)$ can be rather involved, mysterious. Even in the case of arrangements, it is not known whether $b_1(F)$ can be deduced from the combinatorics of the arrangement or not; this is an open conjecture, see (30.1.8) from the list of open problems § 30. In this situation, however, by our algorithm, ∂F is deduced from the combinatorics of the arrangement, hence we get a combinatorial upper bound for $H_1(F)$ as well.

In fact, one can determine an even better bound. Notice that $a\cup b\cup c=0$ for any $a,b,c\in H^1(F)$. Therefore, $H^1(F)$ should sit in such a subspace of $H^1(\partial F)$ on which the restriction of the triple product vanishes.

(For homogeneous singularities, § 24 combined with known facts regarding the mixed Hodge structure of $H^1(F)$ might produce even stronger restrictions. Recall that in the homogeneous case, $H^1(F)_{\lambda\neq 1}$ is pure of weight 1, while $H^1(F)_{\lambda=1}$ is pure of weight 2.)

29.4.1. The Milnor fiber might help in the classification of the possible boundaries as well. E.g.:

PROPOSITION 29.4.2. *Let* $f:(\mathbb{C}^3,0)\to(\mathbb{C},0)$ *be a hypersurface singularity with Milnor fiber* F.

(a) If F is a rational ball (i.e. the rational homology of F and of a point coincide) then f is smooth.

(b) If the boundary ∂F of the Milnor fiber is S^3 then f is smooth.

PROOF. (a) follows from A'Campo's theorem [**2**]. Part (b) follows from (a) and a theorem of Eliashberg, which says that the *only* Stein filling of S^3 is the ball [**19**]. □

The result can be compared with the famous conjecture of Lê and Oka, which claims that if the *link* of f is homeomorphic to S^3, then V_f is an equisingular family of irreducible plane curves.

§ 30. Open Problems.

30.1. We start with some general questions/open problems, or natural tasks for further study:

30.1.1. Determine/characterize all oriented plumbed 3–manifolds which might appear as ∂F for some non–isolated hypersurface singularity f. (Recall that the classification of all normal surface singularity links which might appear as hypersurface singularity, or complete intersection, or Gorenstein singularity links is also open.)

30.1.2. Classify all lens spaces realized as ∂F. Classify all Seifert manifolds realized as ∂F.

30.1.3. Find a ∂F (with f a non–isolated singularity) which is an integral homology sphere (cf. also with Question 3.21 of [**60**]).

30.1.4. Determine the Jordan block–structure of the algebraic monodromy acting on $H_1(\partial F)$.

30.1.5. Develop the mixed Hodge structure of $H^1(\partial F)$. Prove Conjecture (21.1.1) from § 21. (For the case of homogeneous germs and cylinders, see § 24 and (25.3).)

30.1.6. Determine the graph G° for which $c(G^\circ)$ is minimal among all $c(G^m)$, $G^m \sim G$. Has G° any intrinsic significance? Has $c(G^\circ)$ any intrinsic significance? (Is e.g. $c(G^\circ)$ independent of g ? When is this minimum realized by $\widehat{G}$?)

30.1.7. Determine completely the wedge product of $H^*(\partial F)$. Determine the triple product and the resonance varieties, cf. § 29.

30.1.8. Can $H^1(F)$ be determined from ∂F (at least in particular cases, say, for arrangements)? Or, from G of $\Gamma_{\mathcal{C}}$ used here? Understand the monomorphism from (29.4) better. (Recall, that it is a famous conjecture for arrangements that $b_1(F)$ is determined combinatorially.)

30.1.9. In the case of arrangements, can the combinatorics of the arrangement be recovered from ∂F? (We conjecture that yes.)

30.1.10. Classify/characterize all the 'Milnor–fiber contact structures' induced on 3–manifolds realized as ∂F, cf. (29.1). Are there natural families when one can classify all the Stein fillings of the Milnor–fiber (or all the) contact structures ? Find examples when the Milnor–fiber contact structure (besides the Milnor fiber) has other Stein filling as well.

30.1.11. Compute the Seiberg–Witten invariants, or more generally, the Heegaard–Floer homologies (or generalized versions of the lattice homologies) for those 3–manifolds ∂F which are rational homology spheres. How are they related with the signature of F?

30.1.12. Clarify the open question (13.7.1) (i.e. determine the resolution of the real analytic variety $\{(u,v,w)\in(\mathbb{C}^3,0)\,:\,u^m v^{m'} w^n = |w|^k\}^+$).

30.1.13. Establish the relationship between the present work (which determines the boundary ∂F) and **[48]**, which determines the links $K(f,g)_k$ of the Iomdin series $f+g^k$ ($k\gg 0$). In what sense is ∂F the 'limit' of $\{K(f,g)_k\}_k$?

30.1.14. We believe/conjecture that there exists some kind of a rigidity property restricting the pairs $(\partial_1 F, \partial_2 F)$ (cf. (4.3)) which might together form a possible ∂F. (I.e., the normalization has some effect on the possible types of transversal singularities, and vice-versa.) Understand the precise meaning of the conjecture, formulate it concretely, and prove it.

30.1.15. Determine ∂F for any quasi–ordinary singularity f in terms of the characteristic pairs of f.

More questions related mostly to the technicalities used in the proofs and results:

30.1.16. Develop the 'calculus' of decorated graphs such as $\Gamma_{\mathcal{C}}$, cf. (7.2.2).

30.1.17. Analyze the possible relations connecting the decorations of $\Gamma_{\mathcal{C}}$. (E.g., provide an independent proof of the fact that the expressions (16.2.10)(c) are independent of g.)

30.1.18. Find closed formulae for $corank(A)$ and $corank(A,I)$. In what situations can we expect the validity of the relation $corank(A,I)_{\widehat{G}} = c(\widehat{G}) + \#\mathcal{A}(G)$ (or similar formula for G° instead of $\widehat{G}$) ?

30.1.19. Is it true that $\#_1^2 M_{\Phi,ver} = c(\widehat{G})$? Or for G° instead of $\widehat{G}$?

30.1.20. Is the technical lemma (20.1.10) true in general ?

30.1.21. Discuss the case of *all* eigenvalues of the vertical monodromy $M_{\Phi,ver}$.

Bibliography

[1] A'Campo, N.: La fonction zêta d'une monodromie, *Comment. Math. Helv.* **50** (1975), 233-248.

[2] A'Campo, N.: Le nombre de Lefschetz d'une monodromie, *Indag. Math.* **35** (1973), 113-118.

[3] Artal–Bartolo, E.: Forme de Seifert des singularités de surface, *C. R. Acad. Sci. Paris* **t. 313**, Série I (1991), 689-692.

[4] Ban, C., McEwan, L.J. and Némethi, A.: The embedded resolution of $f(x,y)+z^2:(\mathbb{C}^3,0)\to(\mathbb{C},0)$, *Studia Sc. Math. Hungarica* **38** (2001), 51–71.

[5] Barth, W., Peters, C. and Van de Ven, A.: *Compact complex surfaces*, Ergebnisse der Mathematik und ihrer Grenzgebiete, 3. Folge, Band 4, A Series of Modern Surveys in Mathematics, Springer-Verlag 1984.

[6] Blank, S. and Laudenbach, F.: Isotopie des formes fermées en dimension 3, *Inv. Math.* **54** (1979), 103-177.

[7] de Bobadilla, J.F., Luengo, I., Melle-Hernández, A. and Némethi, A.: Classification of rational unicuspidal projective curves whose singularities have one Puiseux pair, Proceedings of Sao Carlos Workshop 2004 *Real and Complex Singularities*, Series *Trends in Mathematics*, Birkhäuser 2007, 31-46.

[8] de Bobadilla, J.F., Luengo, I., Melle-Hernández, A. and Némethi, A.: On rational cuspidal projective plane curves, *Proc. London Math. Soc.* (3) **92** (2006), 99-138.

[9] Bochnak, J., Coste, M., Roy, M-F.: Real algebraic geometry. *Ergebnisse der Mathematik und ihrer Grenzgebiete (3)*, **36**; Springer-Verlag, Berlin, 1998.

[10] Caubel, C.: Contact structures and non-isolated singularities, *Singularity theory*, World Sci. Publ., Hackensack, NJ, 2007, 475-485.

[11] Caubel, C., Némethi, A. and Popescu–Pampu, P.: Milnor open books and Milnor fillable contact 3-manifolds, *Topology* **45**(3) (2006), 673-689.

[12] Brieskorn, E.: Die Monodromie der isolierten Singularitäten von Hyperflächen, *Manuscripta Math.* **2** (1970), 103-161.

[13] Clemens, H.: Picard–Lefschetz theorem for families of non–singular algebraic varieties acquiring ordinary singularities, *Trans. Amer. Math. Soc.* **136** (1969), 93-108.

[14] Cohen, D.C., Suciu, A.I.: The boundary manifold of complex line arrangements, *Geometry and Topology Monographs* **13** (2008), 105-146.

[15] Cohen, D.C., Suciu, A.I.: Boundary manifolds of projective hypersurfaces, *Advances in Mathematics* **206**(2) (2006), 538-566.

[16] Deligne, P.: Theorie de Hodge, II and III, *Publ. Math. IHES* **40** (1971), 5-58 and **44** (1074), 5-77.

[17] Durfee, A.H.: The signature of smoothings of complex surface singularities, *Math. Ann.* **232**, no. 1 (1978), 85-98.

[18] Eisenbud, D. and Neumann, W.: Three–dimensional link theory and invariants of plane curve singularities, *Annals of Math. Studies*, **110**, Princeton University Press, 1985.

[19] Eliashberg, Y.: Filling by holomorphic discs and its applications, *London Math. Soc. Lecture Notes Series* **151** (1991), 45–67.

[20] El Zein, F. and Némethi, A.: On the Weight Filtration of the Homology of Algebraic Varieties: The Generalized Leray Cycles, *Ann. Scuola Norm. Sup. Pisa*, Cl. Sci. (5) **Vol. I** (2002), 869-903.

[21] Durfee, A.H.: Mixed Hodge structures on punctured neighborhoods, *Duke Math. J.* **50** (1983), 1017-1040.

[22] Falk, M.: Arrangements and cohomology, *Ann. Combin.* **1** (1997), 135-157.

[23] Giroux, E.: *Géométrie de contact: de la dimension trois vers les dimensions supérieures*, Proceedings of the ICM, Vol II, (Beijing 2002), 405-414, Higher Ed. Press, Beijing 2002.

[24] Hironaka, E.: Boundary manifolds of line arrangements, *Math. Ann.* **319** (2001), 17-32.

[25] Hirzebruch, F.: Über vierdimensionale Riemannsche Flaĉhen mehrdeutiger analytischer Functionen von zwei complexen Veränderlichen, *Math. Ann.* **126** (1953), 1-22.

[26] Kashiwara, H.: Fonctions rationelles de type $(0, 1)$ sur le plan projectif complexe, *Osaka J. of Math.* **24** (1987), 521-577.

[27] Kulikov, V.S.: Mixed Hodge Structures and Singularities, *Cambridge Tracts in Mathematics* **132**, Cambridge University Press 1998.

[28] Laufer, H.B.: Normal two–dimensional singularities, *Annals of Math. Studies* **71**, Princeton University Press 1971.

[29] Laufer, H.B.: On μ for surface singularities, *Proc. of Symp. in Pure Math.* **30** (1977), 45-49.

[30] Landman, A.: On Picard–Lefschetz transformation for algebraic manifolds acquiring general singularities, *Trans. Amer. Math. Math.* **181** (1973), 89-126.

[31] Looijenga, E. J. N.: *Isolated Singular Points on Complete Intersections*, London Math. Soc. Lecture Note Series 77, Cambridge University Press 1984.

[32] Looijenga, E., Wahl, J.: Quadratic functions and smoothing surface singularities, *Topology* **25**(3) (1986), 261-291.

[33] Michel, F., Pichon, A.: On the boundary of the Milnor fibre of nonisolated singularities, *Int. Math. Res. Not.* **43** (2003), 2305-2311.

[34] Michel, F., Pichon, A.: Erratum: "On the boundary of the Milnor fibre of nonisolated singularities" [Int. Math. Res. Not. 2003, no. 43, 2305-2311;], *Int. Math. Res. Not.* **6** (2004), 309-310.

[35] Michel, F., Pichon, A., Weber, C.: The boundary of the Milnor fiber of Hirzebruch surface singularities, *Singularity theory*, World Sci. Publ., 2007, 745-760.

[36] Lê Dûng Tráng: Calcul du nombre de cycles évanouissants d'une hypersurface complexe, *Ann. Inst. Fourier (Grenoble)* **23**(4) (1973), 261-270.

[37] Lê Dûng Tráng: Ensembles analytiques complexes avec lieu singulier de dimension un (d'aprčs I. N. Iomdine), Seminar on Singularities (Paris, 1976/1977), pp. 87-95, Publ. Math. Univ. Paris VII, 7, Univ. Paris VII, Paris, 1980.

[38] Milnor, J.: Singular points of complex hypersurfaces, *Annals of Math. Studies*, **61**, Princeton University Press, 1968.

[39] Mumford, D.: The topology of normal surface singularities of an algebraic surface and a criterion of simplicity, *IHES Publ. Math.* **9** (1961), 5-22.

[40] Namba, M.: Geometry of projective algebraic curves, *Monographs and Textbooks in Pure and Applied Math.* **88**, Marcel Dekker, New York 1984.

[41] Némethi, A.: The Milnor fiber and the zeta function of the singularities of type $P(f, g)$, *Compositio Math.* **79** (1991), 63-97.

[42] Némethi, A.: The signature of $f(x, y) + z^n$, *Proceedings of Real and Complex Singularities*, Liverpool (England), August 1996; London Math. Soc. Lecture Note Series **263** (1999), 131-149.

[43] Némethi, A.: Five lectures on normal surface singularities; lectures delivered at the Summer School in "Low dimensional topology", Budapest, Hungary 1998; *Proceedings of the Summer School*, Bolyai Society Mathematical Studies **8** (1999); *Low Dimensional Topology*, 269-351.

[44] Némethi, A.: Resolution graphs of some surface singularities, I. (cyclic coverings), *Contemporary Math.* **266** (2000), 89-128.

[45] Némethi, A.: Invariants f normal surface singularities, *Centemp. Math.* **354** (2004), 161-208.

[46] Némethi, A.: Lattice cohomology of normal surface singularities. *Publ. Res. Inst. Math. Sci.* **44** (2) (2008), 507-543.

[47] Némethi, A. and Popescu–Pampu, P.: On the Milnor fibers of cyclic quotient singularities, arXiv:MATH/0805.3449

[48] Némethi, A. and Szilárd, Á.: Resolution graphs of some surface singularities, II. (Generalized Iomdin series), *Contemporary Math.* **266** (2000), 129-164.

[49] Neumann, D.W.: A calculus for plumbing applied to the topology of complex surface singularities and degenerating complex curves, *Trans. of Amer. Math. Soc.* **268** (2) (1981), 299-344.

[50] I. Ono and K. Watanabe, On the singularity of $z^p + y^q + x^{pq} = 0$, *Sci. Rep. Tokyo Kyoika Daigaku Sect. A.* **12** (1974), 123-128.

[51] Orevkov, S. Yu.: On rational cuspidal curves, I. Sharp estimate for degree via multiplicity, *Math. Ann.* **324** (2002), 657-673.

[52] Orlik, P., Wagreich, Ph.: Isolated singularities of algebraic surfaces with $\mathbb{C}^*$ action, *Ann. of Math.*, **93**(2) (1971), 205-228.

[53] Pichon, A.: Three-dimensional manifolds which are the boundary of a normal singularity $z^k - f(x, y)$, *Math. Z.* **231**(4) (1999), 625-654.

[54] Pichon, A.: Variétés de Waldhausen et fibrations sur le cercle, *C. R. Acad. Sci. Paris Sér. I Math.* **324**(6) (1997), 655-658.

[55] Pichon, A.: Singularities of complex surfaces with equations $z^k - f(x, y) = 0$, *Internat. Math. Res. Notices* **5** (1997), 241-246.

[56] Pichon, A., Seade, J.: Fibred multilinks and singularities $f\overline{g}$, *Math. Ann.* **342**(3) (2008), 487-514.

[57] Pichon, A.; Seade, J.: Real singularities and open-book decompositions of the 3-sphere, *Ann. Fac. Sci. Toulouse Math. (6)*, **12**(2) (2003), 245-265.

[58] Seade, J.A.: A cobordism invariant for surface singularities. Singularities, Part 2 (Arcata, Calif., 1981), *Proc. Sympos. Pure Math.* **40**, 479-484; Amer. Math. Soc., Providence, R.I., 1983.

[59] Seade, J.A.: On the topology of isolated singularities in analytic spaces. *Progress in Mathematics*, **241**, Birkhäuser Verlag, Basel, 2006.

[60] Siersma, D.: The vanishing topology of non isolated singularities, *New developments in singularity theory (Cambridge, 2000)*, 447-472, Kluwer Acad. Publ., Dordrecht, 2001.

[61] Siersma, D.: Variation mappings of singularities with 1-dimensional critical locus, *Topology* **30** (1991), 445-469.

[62] Siersma, D.: The monodromy of series of hypersurface singularities, *Comment. Math. Helv.* **65** (1990), 181-197.

[63] Steenbrink, J.H.M.: The spectrum of hypersurface singularities, *Actes du Colloque de Theorie de Hodge (Luminy, 1987)*, Astérisque **179–180** (1989), 163-184.

[64] Steenbrink, J.: Limits of Hodge Structures, *Inv. Math.* **31** (1976), 229-257.

[65] Steenbrink, J.H.M.: Mixed Hodge structures of the vanishing cohomology, *Nordic Summer School/NAVF, Symp. in Math.* Oslo, August 5-25, 1976, 525-563.

[66] Steenbrink, J.H.M.: Mixed Hodge structures associated with isolated singularities, *Proc. of Symp. in Pure Math.* **40** (1983), Part 2, 513-536.

[67] Steenbrink, J.H.M. and Stevens, J.: Topological invariance of the weight filtration, *Indagationes Math.* **46** (1984).

[68] Stipsicz, A., Szabó, Z., Wahl, J.: Rational blowdowns and smoothings of surface singularities, *J. Topol.* **1**(2) (2008), 477-517.

[69] Sebastiani, M., Thom, R.: Un résultat sur la monodromie, *Invent. Math.* **13** (1971), 90-96.

[70] Sullivan, D.: On the intersection ring of compact three manifolds, *Topology* **14** (1975), 275-277.

[71] Teissier, B.: The hunting of invariants in the geometry of discriminants, *Real and complex singularities (Proc. Ninth Nordic Summer School/NAVF Sympos. Math., Oslo, 1976)*, pp. 565–678. Sijthoff and Noordhoff, Alphen aan den Rijn, 1977.

[72] Wagreich, Ph.: The structure of quasihomogeneous singularities, *Proc. of Symp. in Pure Math.* **40**(2) (1983), 593-611.

[73] Wahl, J.: Smoothings of normal surface singularities, *Topology* **20**(3) (1981), 219-246.

[74] Waldhausen, F.: On irreducible 3–manifolds that are sufficiently large, *Ann. of Math.* **87** (1968), 56-88.